ASSEMBLY AND TRAFFICKING OF NICOTINIC AND $5HT_3$ RECEPTORS

Anne Isabel Doward

April 2005

A thesis presented for the degree of Doctor of Philosophy to the University of London

Department of Pharmacology

University College London

London, WC1E 6BT

ProQuest LLC
789 East Eisenhower Parkway
P.O. Box 1346
Ann Arbor, MI 48106-1346

ABSTRACT

Nicotinic acetylcholine receptors (nAChRs) and 5-hydroxytryptamine type 3 receptors ($5HT_3Rs$) are pentameric ligand-gated ion channels which form both heteromeric and homomeric complexes. Aspects of the assembly and pharmacological properties of the α7 nAChR and $5HT_3R$ were examined through three independent studies.

The first study examined the mechanism by which the $5HT_{3B}$ subunit, when expressed alone, is retained within the endoplasmic reticulum (ER). The $5HT_3R$ forms both homomeric (composed of $5HT_{3A}$ subunits) and heteromeric (composed of $5HT_{3A}$ and $5HT_{3B}$ subunits) complexes. In contrast to $5HT_{3A}$, the $5HT_{3B}$ subunit cannot form a functional homomeric receptor. An ER retention motif (RAR) was identified in the $5HT_{3B}$ subunit, which appears to be masked by the $5HT_{3A}$ subunit. Evidence to support this conclusion was obtained from co-expression of the subunits, which resulted in the presence of $5HT_{3B}$ on the cell surface.

The α7 nAChR and $5HT_3R$ have similar N-terminal ligand binding domains and cross-reactivity of some ligands is observed. Both mouse $5HT_{3A}$ and α7 are potentiated by the aromatic moiety of 5-HT, 5-hydroxyindole (5-HI), whereas human $5HT_{3A}$ is not. In an attempt to define the 5-HI binding site, human/mouse $5HT_{3A}$ subunit chimeras were constructed. Studies using the chimeras suggest that the action of 5-HI may be mediated by both the N- and C-terminal domains of $5HT_{3A}$.

In the final study, the effects of the putative chaperone protein, RIC3, on α7 receptor expression were examined. The efficient functional expression of the α7 nAChR has been shown to be critically dependent on host-cell type, unlike the $5HT_3R$. RIC3 was shown to facilitate the efficient cell-surface expression of α7 in a mammalian cell line, where functional expression was not previously observed. The RIC3 protein has been identified as an α7-interacting protein which promotes the efficient assembly and folding of the subunit. RIC3 was also shown to promote $5HT_{3A}R$ assembly.

ACKNOWLEDGEMENTS

This work was funded by the Medical Research Council and Eli Lilly & Company Ltd (MRC CASE PhD Studentship).

My thanks to Dr Neil Millar, for the opportunity to work in his laboratory, and to the rest of the Millar group, both past and present, for entertaining me over the years. Special thanks to Dr Stuart Lansdell (Dr Spew) and Patricia Harkness. Many thanks to Tony Langford, the lab. manager, and Sam Ranasinghe for assistance with the FLIPR at University College London.

Many thanks to those at Eli Lilly & Company Ltd (Lilly Research Centre, Windlesham, Surrey, UK), in particular, Drs Emanuele Sher, Lisa Broad and Ruud Zwart. Thanks to Dr Ruud Zwart for electrophysiology carried out with the $m5HT_{3A(S)}$ subunit.

Thanks to Dr Christopher Connolly (University of Dundee) for providing the cDNAs and the collaboration resulting in Chapter 3 of this thesis.

Many thanks to my family and friends. Thanks to my parents for allowing me to move back home to write this; don't worry, my papers and I will be gone soon! Thanks to Dr Amanda Lam and last, but not least, thank you Steve.

CONTENTS

LIST OF FIGURES

CHAPTER 4

Effects of 5-hydroxyindole on the 5-HT induced responses of mouse and human $5HT_{3A}$ receptors

CHAPTER 5

Investigation of the effects of the RIC3 proteins on the α7 nAChR and $5HT_{3A}$R expressed in mammalian cells

LIST OF TABLES

CHAPTER 2

Materials and methods

ABBREVIATIONS

5-HT	5-hydroxytryptamine
$5HT_{3A}$	'A' subunit of the 5-hydroxytryptamine type 3 receptor
$5HT_{3B, C...}$	'B', 'C'... subunit of the 5-hydroxytryptamine type 3 receptor
$5HT_3R$	5-hydroxytryptamine type 3 receptor
α-BTX	alpha bungarotoxin
ACh	acetylcholine
AChBP	acetylcholine binding protein
amp	ampicillin
Arg	arginine
Asp	aspartic acid
ATP	adenosine triphosphate
BSA	bovine serum albumin
Ca^{2+}	calcium ion
CeRIC3	*Caenorhabditis elegans* RIC3
CIAP	calf intestinal alkaline phosphatase
CMV	cytomegalovirus
Cys	cysteine
DMEM	Dulbecco's modified eagle medium
DNA	deoxyribonucleic acid
dNTP	deoxynucleotide triphosphate
d-TC	*d*-tubocurarine
EC_{20}	20% effective concentration
EC_{50}	median effective concentration
E_{max}	maximum effective concentration
EDTA	ethylenediaminetetraacetic acid
ER	endoplasmic reticulum
FLIPR	Fluorescent Imaging Plate Reader
GABA	γ-aminobutyric acid
$GABA_AR$	γ-aminobutyric acid receptor, type A
Glu	glutamate
HA	haemagglutinin eptitope

HBSS	Hanks buffered/balanced salt solution
HEK293	human embryonic kidney fibroblast cell line
hRIC3	human RIC3
HRP	horseradish peroxidase
IgG	immunoglobulin G
Ile	isoleucine
IPTG	isopropyl-1-thio-β-D-galactopyranoside
kDa	kilodalton
LB broth	Luria-Bertani medium
Leu	leucine
M1	first putative transmembrane region
mAb	monoclonal antibody
*m*CPBG	*m*-chlorophenylbiguanide
MQ	Milli-Q water
myc	synthetic peptide of human c-myc protein
N1E-115	murine neuroblastoma cell line
nAChR	nicotinic acetylcholine receptor
n-BTX	neuronal bungarotoxin
NCB-20	mouse neuroblastoma/Chinese hamster embryonic brain cell hybrid
n_H	Hill coefficient
NMJ	neuromuscular junction
pAb	polyclonal antibody
Phe	phenylalanine
PBS	phosphate buffered saline
PCR	polymerase chain reaction
PEI	polyethylenimine
PFA	paraformaldehyde
PMSF	phenylmethylsulphonyl fluoride
pS	picosiemens
RIC3	resistant to inhibitors of cholinesterase
SDM	site directed mutagenesis
SDS-PAGE	sodium dodecyl sulphate – polyacrylamide gel electrophoresis
Ser	serine

SH-SY5Y	human neuroblastoma cell line
SV40	Simian virus
tet	tetracycline
Thr	threonine
TMB	3, 3', 5, 5'-tetramethylbenzidine (liquid substrate system)
Trp	tryptophan
tsA201	temperature sensitive cell line derivative of the HEK293 cell line
Tyr	tyrosine
Val	valine
VTA	ventral tegmental area
X-Gal	5-bromo-4-chloro-3-indoyl-β-D-galactopyranoside

CHAPTER 1

INTRODUCTION

The nicotinic acetylcholine receptors (nAChRs) and 5-hydroxytryptamine (serotonin) type 3 receptors ($5HT_3Rs$) are members of the superfamily of ligand-gated ion channels which also includes the γ-aminobutyric acid type A ($GABA_A$) and glycine receptors (Stroud *et al.*, 1990). These receptors are oligomeric proteins consisting of five membrane-spanning subunits. The nAChR and $5HT_3R$ conduct cations and mediate fast excitatory neurotransmission whilst the $GABA_A$ and glycine receptors conduct anions and mediate inhibitory neurotransmission. Neurotransmission occurs when a chemical signal, released by a nerve cell, binds to an ion channel receptor and is converted into an electrical signal via the opening of the ion channel, allowing the passage of ions into the cell.

1.1 THE NICOTINIC ACETYLCHOLINE RECEPTOR (nAChR)

Acetylcholine (ACh) acts on two different classes of receptor classified by their activation by the plant alkaloids nicotine (nicotinic) and muscarine (muscarinic). The nAChRs are further divided into two classes based on their location. The "muscle-type" nAChRs are expressed at the neuromuscular junction (NMJ), whilst the "neuronal" nAChRs are expressed throughout the central and peripheral nervous systems (Lukas *et al.*, 1999).

1.1.1 The nAChR from the *Torpedo* electric organ

The marine rays, *Torpedo marmorata* and *Torpedo californica* and the electric eel, *Electrophorus electricus* have electric organs which consist of stacks of modified muscle cells known as electrocytes. The membranes of these electrocytes are packed tightly with nAChRs which resemble the nAChR isolated from the vertebrate neuromuscular junction (Section 1.1.2). The electrocytes are flattened cells with nAChRs covering virtually the entire surface of one face. The arrangement of the electrocytes in stacks causes the voltage differences, across many cells to accumulate, resulting in a very large voltage that can be used to stun prey, upon nAChR activation.

The snake toxin, α-bungarotoxin (α-BTX) isolated from the venom of the Malayan many-banded krait, *Bungarus multicinctus* (Lee and Chang, 1966), can bind almost irreversibly to *Torpedo* electric organ nAChRs. Together with the rich source of receptor from *Torpedo*, α-BTX binding enabled purification of the nAChR (Changeux *et al.*, 1970).

The *Torpedo* electric organ nAChR is composed of four different membrane-spanning subunits (α, β, δ and γ) arranged as a pentamer with the stoichiometry $\alpha_2\beta\gamma\delta$ (Unwin, 1993). The native receptor exists as a single pentamer but is found predominantly in a "dimeric" form, where two pentamers are cross-linked by a disulphide bond (Hamilton *et al.*, 1979; DiPaola *et al.*, 1989). The subunits form a ring around a central pore which forms the ion channel. In the resting state the channel is impermeable to ions (Unwin, 1993). Upon ligand binding and nAChR activation, a conformational change is induced causing the channel pore to open to allow the passage of ions through the plasma membrane (Miyazawa *et al.*, 1999; Miyazawa *et al.*, 2003).

1.1.2 The nAChR of the vertebrate neuromuscular junction

To isolate vertebrate homologues of the *Torpedo* nAChR subunits, mammalian cDNA libraries were screened with probes constructed from the nucleotide sequences of the *Torpedo* subunits. Mammalian α1, β1, γ and δ subunits were identified as well as a novel subunit, ε, resembling the γ subunit (Nef *et al.*, 1984; LaPolla *et al.*, 1984; Takai *et al.*, 1985). Differences in gating and conduction between foetal and adult forms of the muscle nAChR can be accounted for by the developmentally regulated switch from the γ-subunit which is expressed in the foetus ($\alpha 1_2\beta 1\gamma\delta$), to the closely related ε-subunit ($\alpha 1_2\beta 1\varepsilon\delta$) which is expressed in adults (Mishina *et al.*, 1986). The vertebrate neuromuscular nAChRs are situated postsynaptically within the membrane of the muscle endplate, and are involved in signalling between motor neurons and the muscle effector cells.

1.1.3 The neuronal nAChRs

Nicotinic receptors are also present throughout the central and peripheral nervous sytems (Greene *et al.*, 1973; Hunt and Schmidt, 1978; McGehee and Role, 1995). Molecular cloning suggests classification into two families of neuronal nAChR subunits, termed α and β. To date, twelve neuronal-type subunits, designated α2-α10 and β2-β4 have been identified and cloned (Sargent, 1993; McGehee and Role, 1995; Elgoyhen *et al.*, 2001). The α8 subunit has been identified only in chick (Schoepfer *et al.*, 1990; Sargent, 1993). The α subunits are classified by a pair of adjacent cysteine residues that are present in the extracellular N-terminal region, at positions equivalent to Cys192 and Cys193 of the *Torpedo* electric organ nAChR α subunit, and are thought to contribute to the ligand binding site (Kao *et al.*, 1984; Kao and Karlin, 1986; Galzi *et al.*, 1991a). These cysteine residues are conserved in the α subunits of the muscle-type and *Torpedo* electric organ nAChRs. The non-α subunits (β subunits) do not contain this cysteine pair (Lukas *et al.*, 1999).

Neuronal nAChRs exhibit considerable subunit diversity. Whilst most nAChRs are assembled from two or more different subunit subtypes (and are therefore known as heteromeric nAChRs), there is evidence for the formation of receptors containing only one subunit subtype (homomeric nAChRs) (Millar, 2003). Heteromeric nAChRs consist of a combination of both α and β subunits and can be stimulated by the application of nicotine, but are insensitive to the antagonist α-BTX (McGehee and Role, 1995; Itier and Bertrand, 2001). When expressed in *Xenopus* oocytes the α2, α3 and α4 subunits are capable of forming functional receptors upon co-expression of the β2 or β4 subunits (Boulter *et al.*, 1987; Deneris *et al.*, 1988; Sargent *et al.*, 1993). The α5 subunit only forms a functional receptor when co-expressed with at least two different subunit subtypes (Boulter *et al.*, 1990; Couturier *et al.*, 1990a; Millar, 2003). The β3 subunit requires co-expression with at least one other β subunit subtype for functional expression (Forsayeth and Kobrin, 1997; Boorman *et al.*, 2000; Kuryatov *et al.*, 2000). The α6 subunit can be functionally expressed with β2 and β4 (Fucile *et al.*, 1998), but more robust expression is observed when it is co-expressed with more than one type of α or β subunit (Fucile *et al.*, 1998; Kuryatov *et al.*, 2000).

The α7, α8 and α9 subunits are capable of forming homomeric receptors which are sensitive to α-BTX (Couturier *et al.*, 1990b; Séguéla *et al.*, 1993; Elgoyhen *et al.*, 1994; Gerzanich *et al.*, 1994; Gotti *et al.*, 1994). Initially, studies suggested that the pharmacological properties of α7 were unaffected by co-expression of the α3, α5, β2, β3 and β4 nAChR subunits (Couturier *et al.*, 1990b; Séguéla *et al.*, 1993), but more recent data has suggested that α7 may co-assemble with other subunits such as β2, β3 or α5 *in vivo* (Yu and Role, 1998a; Yu and Role 1998b; Palma *et al.*, 1999; Khiroug *et al.*, 2002). Native α7 and α8 in chick form heteromeric receptors (Keyser *et al.*, 1993; Gotti *et al.*, 1994; Gotti *et al.*, 1997). When expressed in *Xenopus* oocytes, α10 does not form a functional receptor either alone or in combination with any of the neuronal β subunits. However, when α10 is co-expressed with α9 a functional heteromeric receptor is formed (Elgoyhen *et al.*, 2001; Sgard *et al.*, 2002).

1.2 THE 5-HYDROXYTRYPTAMINE TYPE 3 RECEPTOR ($5HT_3R$)

The actions of 5-hydroxytryptamine (5-HT; serotonin) are mediated by a number of receptor classes ($5HT_{1-7}$). The 5-hydroxytryptamine type 3 receptor ($5HT_3R$) is the only ligand-gated ion channel of the 5-HT receptor family, the other members are G-protein coupled metabotropic receptors and mediate slow responses via second messenger signalling pathways (Hoyer and Martin, 1997). Three subunits of the $5HT_3R$ have been identified: $5HT_{3A}$, $5HT_{3B}$ and $5HT_{3C}$ (Maricq *et al.*, 1991; Miyake *et al.*, 1995; Belelli *et al.*, 1995; Davies *et al.*, 1999; Dubin *et al.*, 1999; Dubin *et al.*, 2001). Recently, two $5HT_3R$-like genes, $5HT_{3D}$ and $5HT_{3E}$, have been identified (Niesler *et al.*, 2003; Karnovsky *et al.*, 2003).

The first $5HT_3R$ subunit to be identified was $5HT_{3A}$, which was cloned from the mouse neuroblastoma/Chinese hamster embryonic brain cell hybrid (NCB-20) by Maricq *et al.* (1991). Subsequently, $5HT_{3A}$ sequences were identified in a number of other species including rat (Johnson and Heinemann, 1992), human (Belelli *et al.*, 1995; Miyake *et al.*, 1995), guinea pig (Lankiewicz *et al.*, 1998) and ferret (Mochizuki *et al.*, 2000).

An alternatively spliced variant of $5HT_{3A}$ has been identified in the murine neuroblastoma cell line, N1E-115 (Hope *et al.*, 1993). This shorter variant, $5HT_{3A(S)}$, differs from the originally identified $5HT_{3A}$ by a deletion of six amino acids in the putative large intracellular loop between transmembrane domains three and four. The $5HT_{3A(S)}$ subunit has been identified in other species such as rat (Miquel *et al.*, 1995; Isenberg *et al.*, 1993), guinea pig (Lankiewicz *et al.*, 2000) and human (Miyake *et al.*, 1995; Belleli *et al.*, 1995). The $5HT_{3A(S)}$ subunit appears to be the only functional $5HT_{3A}$ subunit expressed in human. The $5HT_{3A(S)}$ subunit appears to predominate in both mouse neuronal tissue and murine derived cell lines (Werner *et al.*, 1994). There is little difference in pharmacological properties between the splice variants (Downie *et al.*, 1994; Niemeyer and Lummis, 1998). There is evidence that they are differentially regulated during development (Miquel *et al.*, 1995) and that intracellular regulatory kinases can discriminate between them (Hubbard *et al.*, 2000).

Most of the $5HT_{3A}$ receptor subunits described thus far are capable of forming functional homomeric receptors. However, two human $5HT_{3A}$ splice variants (a truncated form and a long form) which are incapable of forming functional homomers have been described (Brüss *et al.*, 2000). The truncated human $5HT_{3A}$ subunit contains a major part of the N-terminal region, including the ligand binding domain, followed by an altered and truncated C-terminal domain containing a single putative transmembrane domain (Brüss *et al.*, 2000). The long form of the human $5HT_{3A}$ subunit has an additional 32 amino acids in the M2-M3 extracellular loop (Brüss *et al.*, 2000).

The second $5HT_3R$ subunit to be identified was $5HT_{3B}$ (Davies *et al.*, 1999; Dubin *et al.*, 1999; Hanna *et al.*, 2000). The discovery of this subunit helped to explain the previously observed functional differences between recombinant and native $5HT_3Rs$. Homomeric $5HT_{3A}Rs$ exhibit a very low single channel conductance (sub-picosiemens (pS)) (Davies *et al.*, 1999) unlike those of native receptors (Kelley *et al.*, 2003). Heteromeric receptors, composed of $5HT_{3A}$ and $5HT_{3B}$, have a much larger single channel conductance (9-17 pS) which is more similar to that of native $5HT_3Rs$. The $5HT_{3B}$ subunit shares approximately 45% amino acid sequence identity with $5HT_{3A}$. When expressed alone, $5HT_{3B}$ can not form a functional

homomeric receptor (Davies *et al.*, 1999; Dubin *et al.*, 1999; Hanna *et al.*, 2000; Boyd *et al.*, 2002). When $5HT_{3B}$ is co-expressed with $5HT_{3A}$, a functional heteromeric receptor is formed where the $5HT_{3B}$ subunit modifies receptor kinetics, voltage dependence, pharmacology and ion permeability of $5HT_{3A}$ (Dubin *et al.*, 1999; Brady *et al.*, 2001).

A third human $5HT_3R$ subunit has been identified, $5HT_{3C}$ (Dubin *et al.*, 2001), which has approximately 39% sequence identity with $5HT_{3A}$. When co-expressed with $5HT_{3A}$, the $5HT_{3C}$ subunit is reported to decrease the responses of $5HT_{3A}$ to 5-HT (Dubin *et al.*, 2001). Recently, additional novel putative human $5HT_3R$ subunits have been identified, $5HT_{3D}$ and $5HT_{3E}$ (Niesler *et al.*, 2003), but to date have not been characterised in detail. Other $5HT_3R$-like genes, homologous to the $5HT_{3C}$ subunit gene, have been identified in other species additional to human (Karnovsky *et al.*, 2003).

1.3 RECEPTOR STRUCTURE

1.3.1 Subunit structure

The nAChR and $5HT_3R$ subunits contain an amino- (N-) terminal signal peptide which is cleaved to form the mature protein. The receptor subunits have a large hydrophilic extracellular N-terminal domain, four putative transmembrane domains, M1-M4, (Noda, 1983; Sargent, 1993; Maricq *et al.*, 1991), and a short extracellular carboxy (C)-terminal domain (Mukerji *et al.*, 1996). The extracellular N-terminal domain forms the ligand binding site (Eiselé *et al.*, 1993) and contains sites for asparagine (N)-linked glycosylation (Nomoto *et al.*, 1986; McKernan, 1992; Quirk and Siegel, 2000). The large intracellular loop in between M3 and M4 contains several sites for phosphorylation (Huganir and Greengard, 1990; Lankiewicz *et al.*, 2000) (Figure 1.1A).

Analysis of the putative $5HT_{3D}$ subunit sequence suggests that it encodes a protein that differs from the other $5HT_3R$ subunits, in that it has no signal peptide, a very

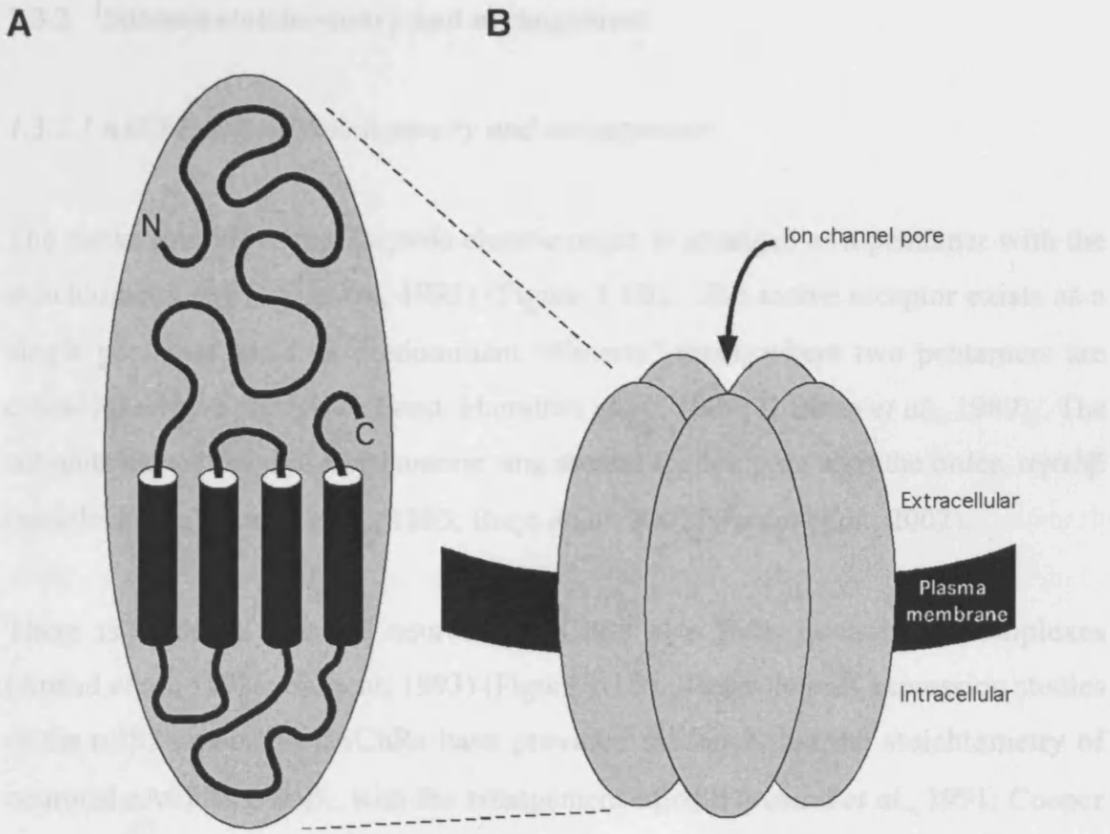

Figure 1.1 *Predicted topology of the nAChR and $5HT_3R$ subunits and schematic representation of assembled subunits as a pentameric receptor.* **A**, The receptor subunits have a large hydrophilic extracellular N-terminal domain which contains potential sites for N-linked glycosylation and is proposed to form the ligand binding site. The N-terminal domain is followed by four putative transmembrane domains (M1-M4) and a short extracellular C-terminal domain. There is a large intracellular loop in between M3 and M4 which contains several sites for phosphorylation. **B**, The nAChRs and $5HT_3Rs$ contain five subunits arranged around a central ion channel pore. Receptors may be assembled from a single subunit type (homomeric) or from more than one type of subunit (heteromeric). Adapted from Millar, 2003.

short N-terminal extracellular domain lacking the ligand binding site, and an intracellular C-terminal (Niesler *et al.*, 2003).

1.3.2 Subunit stoichiometry and arrangement

1.3.2.1 nAChR subunit stoichiometry and arrangement

The native nAChR of the *Torpedo* electric organ is arranged as a pentamer with the stoichiometry $\alpha_2\beta\gamma\delta$ (Unwin, 1993) (Figure 1.1B). The native receptor exists as a single pentamer and in a predominant "dimeric" form, where two pentamers are cross-linked by a disulphide bond (Hamilton *et al.*, 1979; DiPaola *et al.*, 1989). The subunits are arranged in a pentameric ring around the ion pore with the order, $\alpha\gamma\alpha\delta\beta$ (anticlockwise) (Karlin *et al.*, 1983; Brejc *et al.*, 2001; Unwin *et al.*, 2002).

There is evidence that the neuronal nAChRs also form pentameric complexes (Anand *et al.*, 1993a; Sargent, 1993) (Figure 1.1B). Heterologous expression studies of the $\alpha4\beta2$ and $\alpha3\beta4$ nAChRs have provided evidence that the stoichiometry of neuronal nAChRs is $\alpha_2\beta_3$, with the arrangement $\alpha\beta\alpha\beta\beta$ (Anand *et al.*, 1991; Cooper *et al.*, 1991; Boorman *et al.*, 2000). The expression of different ratios of $\alpha4$ and $\beta2$ subunits in *Xenopus* oocytes has provided evidence for the existence of nAChRs with alternative stoichiometries (Zwart and Vijverberg, 1998; Nelson *et al.*, 2003). The stoichiometry and arrangement of the neuronal nAChRs is complicated by subtypes containing more than one type of α or β subunit (Millar, 2003).

1.3.2.2 $5HT_3R$ subunit stoichiometry and arrangement

The $5HT_3R$ is thought to consist of five subunits arranged around a central ion channel pore (Boess *et al.*, 1995) (Figure 1.1B). The $5HT_3$ subunits form homomeric receptors, containing $5HT_{3A}$ subunits, or heteromeric receptors, containing both $5HT_{3A}$ and $5HT_{3B}$ subunits. The stoichiometry and arrangement of the subunits of the heteromeric $5HT_3Rs$ have not yet been determined, but studies in *Xenopus* oocytes have provided evidence for the existence of receptors with different stoichiometries (Dubin *et al.*, 1999). When different ratios of $5HT_{3A}$ to $5HT_{3B}$

cRNA are injected into oocytes, differences in agonist potency are observed (Dubin *et al.*, 1999) suggesting the presence of a heterogenous receptor population. To date, the contribution of the more recently identified subunits, $5HT_{3C}$, $5HT_{3D}$, and $5HT_{3E}$, to the $5HT_3R$ pentamers has not yet been reported.

1.3.3 The ligand binding site

The ligand binding sites of both the nAChR and $5HT_3R$ are found in the N-terminal extracellular domain of the receptor subunits. Many biochemical and mutagenesis studies suggest that the binding site is located in the extracellular domain and further evidence has been provided by the construction of a chimeric receptor subunit comprising the N-terminal region of the α7 nAChR up to M1, fused to the remainder of $5HT_{3A}$ (α7/$5HT_{3A}$). The α7/$5HT_{3A}$ chimeric subunit forms a homomeric receptor and displays the pharmacological properties of α7, but the ion channel properties of $5HT_{3A}$ (Eiselé *et al.*, 1993).

A soluble protein, acetylcholine-binding protein (AChBP), has been identified in the snail *Lymnea stagnalis* (Brejc *et al.*, 2001). AChBP forms a homopentameric structure which closely resembles the ligand binding domain of nAChR α-subunit. The determination of the structure of the AChBP, has aided in characterisation of the nAChRs and $5HT_3R$ binding sites (Brejc *et al.*, 2001; see Section 1.3.5.1).

1.3.3.1 The ligand binding site of the nAChR

The acetylcholine (ACh) binding sites of the *Torpedo* electric organ and muscle nAChR were localised to the interface between the α subunit and the adjacent non-α subunit by affinity labelling studies (Galzi e*t al.*, 1991a; Changeux *et al.*, 1998; Taylor *et al.*, 2000). The muscle nAChR contains two ligand binding sites at the interfaces between the α subunit and either the γ or δ subunit (Pedersen and Cohen, 1990). The binding sites are not identical and show different pharmacological properties (Blount and Merlie, 1989), suggesting that residues from both subunits at the interface contribute to ligand binding (Reynolds and Karlin, 1978; Pedersen and Cohen, 1990).

The heteromeric neuronal nAChRs with an $\alpha_2\beta_3$ stoichiometry contain two ligand binding sites at the interfaces between the α and non-α (β) subunits (Changeux *et al.*, 1998). The homomeric neuronal nAChRs composed of five α subunits contain five putative ligand binding sites at the α-α subunit interfaces (Palma *et al.*, 1996).

Six loops, termed A-F, have been identified in nAChR subunits and are proposed to be important in the formation of the ACh-binding site (Galzi *et al.*, 1990; Fu and Sine, 1994; Corringer *et al.*, 1995; Martin *et al.*, 1996; Prince and Sine, 1996; Brejc *et al.*, 2001). The α subunit possesses the principal components of the binding site (loops A, B and C). The complementary component of the ligand binding site (loops D, E and F) is provided by the subunit adjacent to the α subunit, forming the ligand binding interface (Figure 1.2).

Several residues involved in ligand binding within loops A-F have been identified by affinity labelling and site-directed mutagenesis. The Cys192 and Cys193 residues of loop C of the *Torpedo* electric organ nAChR α subunit were labelled with 4-(*N*-maleimido)benzyltri[^{3}H]-methyl ammonium ([^{3}H]-MBTA), which competes for the binding site (Kao *et al.*, 1984). Labelling with *p*-(*N*,*N*-dimethyl)aminobenzenediazonium fluoroborate (DDF) also identified Cys192 and Cys193 as well as α-Trp86 and α-Tyr93 (in loop A), α-Trp149 (in loop B) and α-Tyr190 and α-Tyr-198 (in loop C) (Galzi *et al.*, 1991b; Galzi and Changeux, 1995). Nicotine and *d*-tubocurarine identified γ-Trp55 and δ-Trp57 in loop D (Chiara *et al.*, 1998). Residues γ-Tyr111 and δ-Arg113 (in loop E) were weakly, but specifically labelled by *d*-tubocurarine (Chiara *et al.*, 1998; Chiara *et al.*, 1999). Mutation of δ-Asp180 (in loop F) to asparagine resulted in a reduced affinity for ACh, suggesting a role for this residue in ligand binding (Martin *et al.*, 1996).

The residues identified in loops A-C are conserved in all of the α subunits, except α5 (Couturier *et al.*, 1990b). The residues identified in loop D are conserved in the neuronal β2, β4, α7 and α8 subunits. The α7 nAChR therefore possesses both the principal and complementary components of the ligand binding site (Corringer *et al.*, 2000). Mutation of the conserved tyrosine and tryptophan residues in α7 alters the

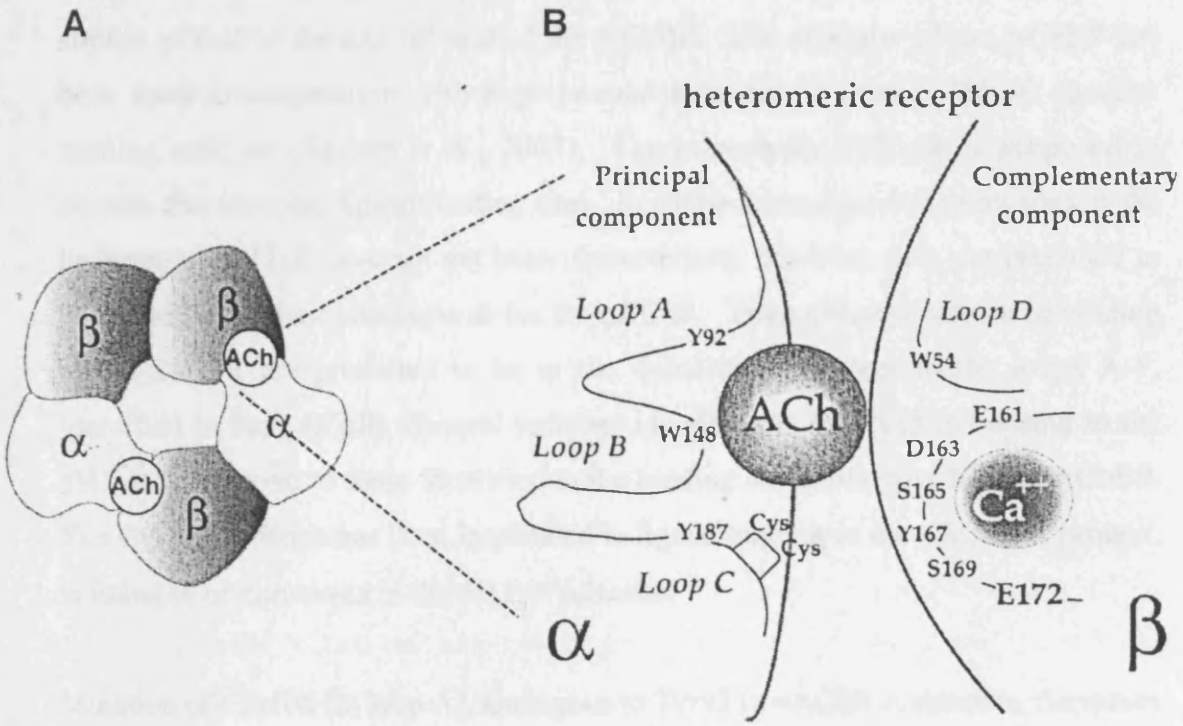

Figure 1.2 *Model of the nAChR ligand binding domain.* **A**, Pentameric complex of neuronal nAChR α and β subunits. The ACh-binding site is located at the interface between the α subunit and the adjacent β subunit. **B**, Representation of the principal component (α subunit) of the ligand binding site with its three loops, A, B and C and two of the loops (D and E) from the complementary component (β subunit). Each loop is modelled with the principal amino acids identified in the chick α7 subunit. Adapted from Itier and Bertrand, 2001.

affinity of the receptor for agonists and competitive antagonists, demonstrating their involvement in ligand binding (Galzi *et al.*, 1991b; Corringer *et al.*, 2000).

1.3.3.2 The ligand binding site of the $5HT_3R$

The extracellular N-terminal ligand binding domain of the $5HT_3R$ is proposed to be similar to that of the nAChR and of the AChBP. The structure of the AChBP has been used in conjunction with experimental evidence to predict $5HT_3R$ agonist-binding residues (Reeves *et al.*, 2003). The homomeric $5HT_{3A}R$ is proposed to contain five identical ligand binding sites. In contrast, the ligand binding sites of the heteromeric $5HT_3R$ have not yet been characterised, however, they are predicted to be formed at subunit interfaces as for the nAChR. The residues involved in binding to the $5HT_3R$ are predicted to be in the domains equivalent to the loops A-F, identified in the nAChR. Several residues identified as involved in binding to the $5HT_3R$ correspond to those identified in the binding site of the nAChR and AChBP. The Cys loop, which has been implicated in ligand binding in the nAChR α subunit, is found to be conserved in the $5HT_3R$ subunits.

Mutation of Glu106 (in loop A), analogous to Tyr93 in nAChR α subunits, decreases the affinity of the $5HT_3R$ for 5-HT and several antagonists, suggesting this residue to be important in ligand binding (Boess *et al.*, 1997). Mutation of Phe107 (in loop A) also alters the binding characteristics of the $5HT_3R$ (Steward *et al.*, 2000). Mutation of the $5HT_{3A}$ subunit tryptophan residues, Trp95, Trp102, Trp121 (loop A; analogous to Trp86 in the nAChR α subunit) and Trp214, results in receptors incapable of binding radioligand (Spier and Lummis, 2000). Trp95 and Trp121 are conserved in all nAChR subunits and Trp102 and Trp214 are conserved in most nAChR subunits (North, 1995). Mutation of Trp183 (loop B) results in a decrease in ligand binding affinity (Spier and Lummis, 2000). This residue is homologous to Trp149 in loop B of the nAChR α subunit which is implicated in ligand binding. Trp195 is also implicated in $5HT_3R$ ligand binding (Spier and Lummis, 2000). The loop C region of the $5HT_3R$ is involved in the binding of *m*-chlorophenylbiguanide (*m*CPBG) (Mochizuki *et al.*, 1999a) and d-TC (Hope *et al.*, 1999). Trp90 (equivalent to Trp53 in AChBP, and Trp54 in the nAChR α subunit), Arg92

(equivalent to Gln55 in AChBP) and Tyr194 in loop D are proposed to play a role in ligand binding (Yan *et al.*, 1999; Spier and Lummis, 2000). Tyr141, Tyr143 (equivalent to Arg104 in AChBP) and Tyr153 in loop E are also involved in $5HT_3R$ ligand binding (Price and Lummis, 2004). Most of the residues identified as playing a role in ligand binding to the $5HT_3R$ are aromatic, the electron-rich side chains of which may interact with the positively charged ammonium group of $5HT_3R$ ligands. The structure of the ligand binding domain of the $5HT_3R$ appears similar to that of the nAChR and AChBP.

1.3.4 The ion channel

1.3.4.1 The ion channel of the nAChR

The neuromuscular junction nAChRs are permeable to monovalent cations, but are relatively impermeable to divalent cations (see Itier and Bertrand, 2001). The neuronal nAChRs are permeable to both divalent and monovalent cations, showing a significant permeability to calcium (Sargent, 1993; McGehee and Role, 1995). When expressed in *Xenopus* oocytes, the homomeric α7 nAChR displays a ratio of calcium permeability to sodium permeability (P_{Ca}/P_{Na}) of approximately 20 (McGehee and Role, 1995). Heteromeric neuronal nAChRs display a P_{Ca}/P_{Na} in the range of 0.5-2.5 (McGehee and Role, 1995; Changeux *et al.*, 1998).

The nAChR subunits assemble to form a ring around a central ion channel pore. The structure of the ion channel of the muscle-type nAChR was initially studied by photo-affinity labelling using non-competitive open channel blockers, such as chlorpromazine. Chlorpromazine was found to label residues in the putative transmembrane domain 2 (M2) of each of the five receptor subunits suggesting that this region formed the lining of the ion channel (Giraudat *et al.*, 1986; Hucho *et al.*, 1986; Revah *et al.*, 1990; Stroud *et al.*, 1990). M2 has an α-helical structure with several serine and threonine residues in positions which point towards the lumen of the ion channel (Unwin, 1993; Miyazawa *et al.*, 2003). Chlorpromazine labels Thr244, Ser248, Leu251, Val255 and Glu262 of M2 of the α subunit (Giraudat *et al.*, 1986; Hucho *et al.*, 1986; Revah *et al.*, 1990). These residues are conserved within

the other subunits resulting in rings of residues with similar charge, side chain size or hydrophobicity within the lumen of the ion channel (Figure 1.3).

The rings of residues within the pore are predominantly non-polar and therefore present a relatively inert surface to diffusing ions (Miyazawa *et al.*, 2003). There are two rings of negatively charged residues (at α-Glu259 and α-Glu280) which may influence transport by attracting cations (Miyazawa *et al.*, 2003). A third ring of negatively charged residues is at α-Glu241, which is at the inner mouth of the pore and may also attract cations (Miyazawa *et al.*, 2003). Mutation of Glu237 to alanine at the cytoplasmic end of M2 in the α7 subunit causes a 1000-fold decrease in calcium permeability, but does not alter permeability to monovalent cations (Galzi *et al.*, 1992; Bertrand *et al.*, 1993). Replacement of amino acids in the chick α7 subunit with corresponding residues from $GABA_A$ or glycine receptor subunits results in the conversion of ion selectivity from cationic to anionic (Galzi *et al.*, 1992; Corringer *et al.*, 1999).

A ring of conserved leucine residues is present near the centre of the membrane and may form the channel gate (Miyazawa *et al.*, 1999; Miyazawa *et al.*, 2003). In the α7 nAChR subunit, Leu247 is predicted to be near the channel selectivity filter. Mutation of Leu247 to polar serine or threonine residues alters the ion channel properties (Revah *et al.*, 1991; Palma *et al.*, 1996). The mutation converts the receptor from a high affinity desensitised state into a state that conducts ions, confirming the role of Leu247 in forming the channel gate (Miyazawa *et al.*, 2003).

1.3.4.2 The ion channel of the $5HT_3R$

The ion channel of the $5HT_3R$ is proposed to be a relatively non-selective cation channel (Yang, 1990; Yang *et al.*, 1992; Jackson and Yakel, 1995; Glitsch *et al.*, 1996; Mochizuki *et al.*, 1999b). Initially, the $5HT_3R$ was considered to be impermeable to calcium (Eiselé *et al.*, 1993; Gilon and Yakel, 1995; Glitsch *et al.*, 1996), but studies using intracellular calcium indicators have clearly demonstrated calcium entry through the mouse $5HT_3R$ (Hargreaves *et al.*, 1994; Nichols and Mollard, 1996). Recombinant heteromeric $5HT_3$ receptors are much less permeable

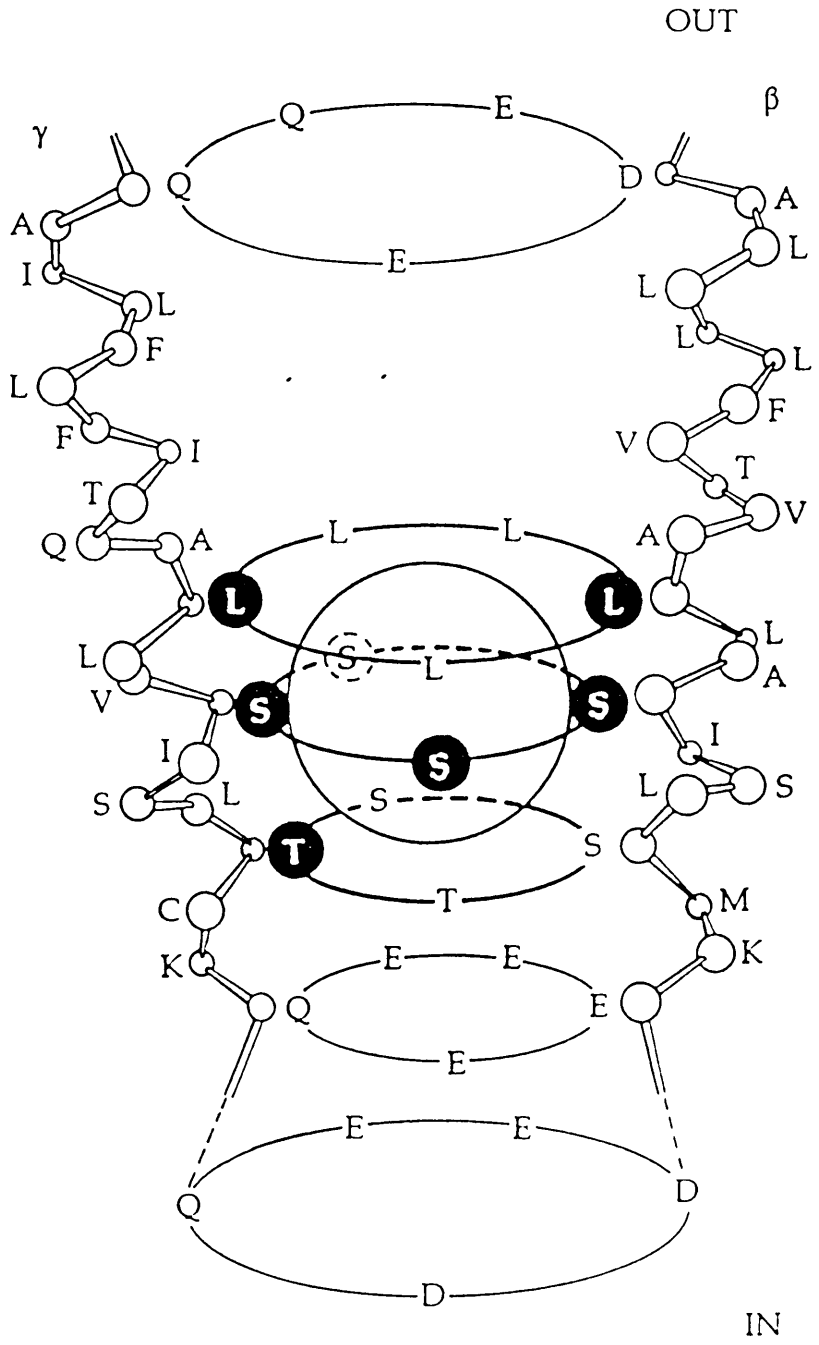

Figure 1.3 *A model of the high affinity binding site for the open channel blocker, chlorpromazine.* The M2 α-helices of the β and γ subunits which line the ion channel pore are illustrated. The filled circles represent three rings of amino acids which are photolabelled by [^{3}H]-chlorpromazine. The sphere represents chlorpromazine. Rings of negatively charged residues are located at either end of the channel pore and are implicated in ion transport. Adapted from Revah *et al.*, 1990.

to calcium than homomeric $5HT_{3A}$ receptors (Brown *et al.*, 1998; Davies *et al.*, 1999). Unlike $5HT_{3A}$ and the nAChR subunits, the $5HT_{3B}$ subunit lacks the classical three rings of negatively charged residues which are thought to promote cation permeation (Imoto *et al.*, 1988; Dubin *et al.*, 1999).

The structure of the $5HT_3R$ ion channel pore is proposed to be similar, but not identical to that of the nAChR (Reeves *et al.*, 2001). Like the nAChR, the M2 domain of the $5HT_3R$ is suggested to be α-helical and to line the ion channel pore (Reeves *et al.*, 2001). A ring of conserved leucine residues (at Leu287) is proposed to function in channel gating. Mutation of Leu287 to polar residues results in a decrease in the rate of desensitisation (Yakel *et al.*, 1993). Similar to the α7 nAChR, substitution of residues in M2 of the $5HT_{3A}$ subunit with the corresponding residues from $GABA_A$ or glycine receptors (V291T, E276A and introduction of a proline residue before residue 276) results in a conversion of ion selectivity from cationic to anionic (Gunthorpe and Lummis, 2001). Mutation of Ile294 in M2 of $5HT_{3A}$ to alanine ablates calcium permeability (Reeves and Lummis, 2000), in a similar way to mutation at the homologous position in the α7 nAChR (see Section 1.3.4.1; Bertrand *et al.*, 1993), providing further evidence of structural and functional conservation between these receptors.

1.3.5 The 3-dimensional structure

1.3.5.1 The 3-dimensional structure of the nAChR

The structure of the *Torpedo* electric organ nAChR, and how the structure changes upon activation, have been examined by electron microscopy (Toyoshima and Unwin, 1990; Unwin, 1993; Miyazawa *et al.*, 2003; Unwin, 2003; Unwin, 2005) (Figure 1.4). The high density and regular arrangement of *Torpedo* electric organ nAChRs have facilitated these studies. Isolated postsynaptic membranes convert readily into tubular crystals with receptors organised as they are *in vivo* (Brisson and Unwin, 1984).

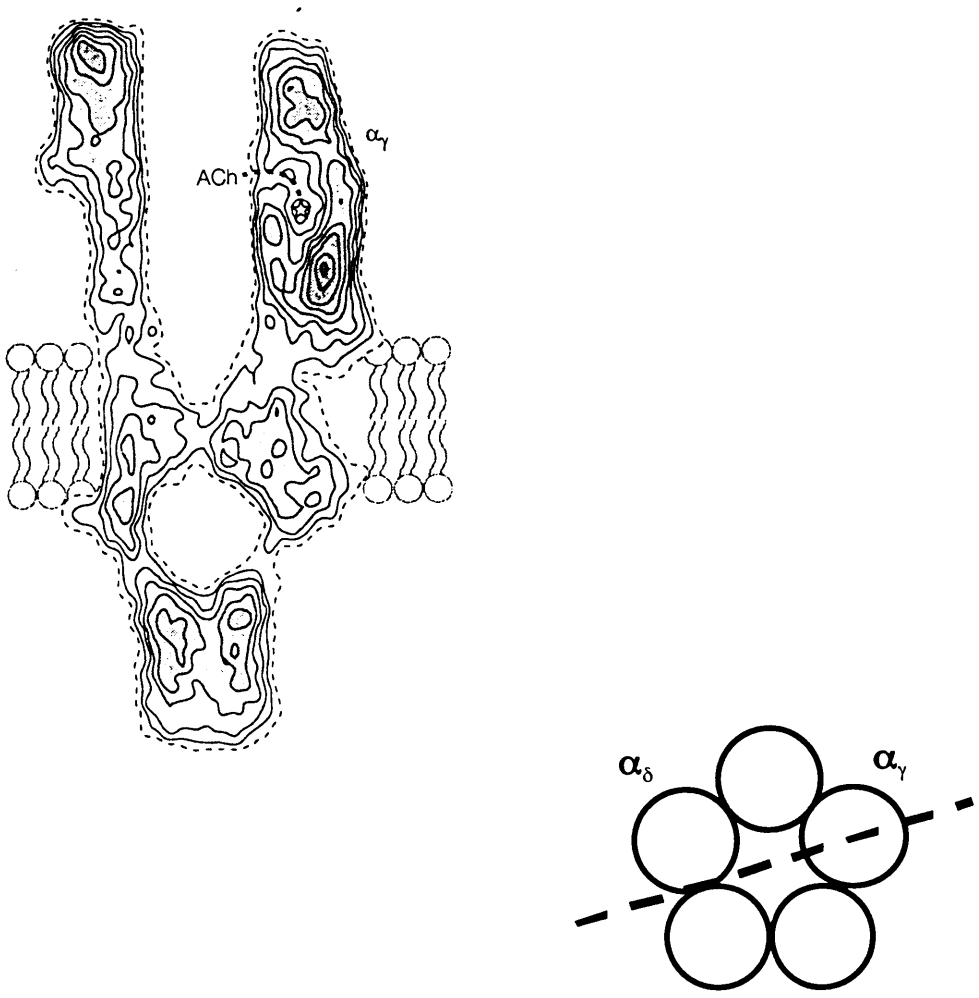

Figure 1.4 *3-Dimensional structure of the nAChR.* A cross-section through the 4.6 Å resolution structure of the *Torpedo* electric organ nAChR determined by electron microscopy. The dashed line indicates the pathway to the binding site. Adapted from Miyazawa *et al.*, 1999 and Karlin, 2002.

The most recent structure of the *Torpedo* electric organ nAChR is at a resolution of 4 Å (Miyazawa *et al.*, 2003; Unwin, 2005). The total length of the receptor is about 160 Å, with a pseudo-5-fold symmetry of subunits identified as rods arranged around a narrow central pore which spans the membrane (Toyoshima and Unwin, 1990; Unwin, 1993; Unwin, 2005). The receptor extends approximately 65 Å above the extracellular surface of the membrane and approximately 15 Å below the intracellular surface of the membrane. The intracellular portion of the receptor has an associated density below it, which is partly formed by rapsyn, a 43 kDa protein involved in clustering of the muscle-type nAChR (Sealock, 1982; Moransard *et al.*, 2003). The putative ACh-binding sites are cavities in the α subunits approximately 40 Å above the surface of the cell membrane (Unwin, 2005). The ion channel is a wide opening of 25 Å in the extracellular domain which narrows as it passes through the membrane before widening at the intracellular domain (Itier and Bertrand, 2001). The channel gate is approximately 15 Å from the cytoplasmic surface of the membrane (Unwin, 1993; Miyazawa *et al.*, 1999).

The four subunits of the *Torpedo* electric organ nAChR (α, β, δ, γ) are of a similar size and share the same structure. The extracellular N-terminal ligand-binding domain of each subunit is composed of two sets of β-sheets, packed into a β-sandwich, and are joined by a disulphide bond which forms the characteristic Cys-loop. The extracellular domain also contains several of the loop regions involved in ligand binding (loops A-C). The membrane spanning region of the subunits is composed of four α-helices (M1-M4) and the M1-M2 and M2-M3 loops. The intracellular domain of the subunits is composed mainly of the M3-M4 loop which, apart from a single α-helix, has a disordered structure.

The wall lining of the ion channel pore is formed by the M2 transmembrane domain (Unwin, 1993), and M1, M3 and M4 form a lipid-facing scaffold. The M2 helix is kinked near the middle of the membrane where it comes closest to the pore, tilting radially outwards on either side, and is proposed to form the channel gate (Unwin, 1993; Miyazawa *et al.*, 1999). Binding of ACh causes a rotational movement of the inner structure of the α subunits in the ligand binding domain. These movements are transduced, via the M2-M3 loop, to the M2 helices lining the pore. The movement in

M2 pulls apart the weak interactions between the side chains of the residues in M2, breaking apart the gate, resulting in the opening of the channel pore (Unwin *et al.*, 2002; Miyazawa *et al.*, 2003; Unwin, 2003; Unwin, 2005).

Determination of the structure of the homologous pentameric ACh-binding protein (AChBP), at a resolution of 2.7 Å, has helped to elucidate the structure of the N-terminal ligand binding domain of the nAChR (Brejc *et al.*, 2001; Smit *et al.*, 2001; Sixma *et al.*, 2003). AChBP is involved in the modulation of synaptic transmission through binding ACh. AChBP forms a homopentameric structure which closely resembles the ligand binding domain of nAChR. It does not possess transmembrane or intracellular domains, but is capable of binding nicotinic ligands. Like the nAChR, the binding sites of AChBP are found at the subunit interfaces and are composed of residues found in the loops A-F (Brejc *et al.*, 2001). Models of the nAChR binding domain have been generated based on the structure of the AChBP (Le Novère *et al.*, 2002; Schapira *et al.*, 2002).

1.3.5.2 The 3-dimensional structure of the $5HT_3R$

To date, there have been few reported studies aimed at determining the 3-dimensional structure of the $5HT_3R$. Electron microscopy of purified $5HT_{3A}$ homomeric receptors reveals that the receptors form a pentameric 'doughnut' shape (Boess *et al.*, 1995), with similar dimensions to the nAChR (Unwin, 1993). Use of the substituted cysteine accessibility method (SCAM) has confirmed that the M2 domain of the $5HT_{3A}$ subunit is α-helical (Cruz *et al.*, 2001; Reeves *et al.*, 2001). As the $5HT_3R$ shares structural and functional similarities with the nAChR, much of the structural analysis performed on the nAChR (Unwin, 1993; Miyazawa *et al.*, 1999; 2003; Unwin, 2005) and the AChBP (Brejc *et al.*, 2001) can be extrapolated to the $5HT_3R$ (see Section 1.3.5.1). Recently, the structure of the extracellular domain of the $5HT_3R$ has been modelled on the AChBP (Reeves *et al.*, 2003), but further experimental characterisation of the models is required to determine their accuracy.

1.4 RECEPTOR ASSEMBLY

The formation of functional ligand-gated ion channels such as the nAChR and $5HT_3R$ is a complex and poorly understood process. The receptor subunits must fold with the correct membrane topology and associate with other subunits to form pentamers of the correct stoichiometry and arrangement, in the endoplasmic reticulum (ER) before export through the Golgi apparatus to the plasma membrane (Green and Millar, 1995). This maturation process is slow and relatively inefficient (Merlie and Lindstrom, 1983). Receptor subunits also undergo several post-translational modifications, within the ER, before functional expression is achieved. It has been suggested that the formation of pentameric complexes is a strict requirement for exit from the ER, but there is evidence for the occurrence of further folding events after exit from the ER (Green and Wanamaker, 1998; Green, 1999). Subunits that do not fold and assemble correctly are retained within the ER and degraded (Smith *et al.*, 1987; Claudio *et al.*, 1989; Verrall and Hall, 1992; Blount and Merlie, 1990).

1.4.1 Assembly models of the nAChR

The muscle-type nAChR is the most well characterised of the ligand-gated ion channels, in terms of its assembly. There are very few reports investigating the assembly mechanisms of the neuronal nAChRs or the $5HT_3R$. There are currently two models that describe the assembly of the *Torpedo* electric organ/muscle-type nAChR. In the "heterodimer" model (Blount and Merlie, 1991; Gu *et al.*, 1991) the α subunit associates with γ or δ subunits forming $\alpha\gamma$ or $\alpha\delta$ heterodimers. The heterodimers assemble with β subunits to form $\alpha_2\beta\gamma\delta$ pentamers. In the second model, the "sequential" model (Green and Claudio, 1993; Green and Wanamaker, 1997; Green and Wanamaker, 1998), the α, β and γ subunits assemble rapidly into trimers. Post-translational folding of the α subunit occurs when it is assembled as a trimer, leading to the formation of an α-bungarotoxin binding site. The δ subunit assembles with the trimer to form the $\alpha\beta\gamma\delta$ tetramer and an ACh binding site is formed. Finally, the second α subunit assembles creating the $\alpha_2\beta\gamma\delta$ pentamer, and a second ACh binding site is formed.

1.4.2 Chaperones and folding enzymes in the ER

Chaperone proteins recognise and stabilise intermediates during protein folding and oligomerisation (Keller *et al.*, 1996). Association with chaperones is the most commonly observed primary mechanism of quality control in protein folding. The ER contains many chaperone proteins and folding factors which are essential for the successful folding and maturation of proteins.

One of the best characterised ER chaperones is the immunoglobulin-binding protein (BiP). BiP associates with newly synthesised muscle-type nAChR subunits and some αγ and αδ complexes, but not with mature pentameric nAChRs. BiP is suggested to play a role in the conformational maturation and folding of nAChRs (Blount and Merlie, 1991; Paulson *et al.*, 1991). BiP also associates with misfolded subunits, which are susceptible to degradation (Forsayeth *et al.*, 1992). Another chaperone protein, calnexin, associates with newly synthesised, partially glycosylated proteins including α and β muscle-type nAChR subunits (Gelman *et al.*, 1995; Keller *et al.*, 1996; Keller and Taylor, 1999). Calnexin is thought to have a role in the folding of the subunits into an assembly-competent conformation. Co-transfection of calnexin with muscle-type nAChR subunits, in COS and HEK293 cells, enhances folding, assembly and cell surface expression of the receptors (Chang *et al.*, 1997). Association with calnexin mediates retention in the ER of the interacting protein (Ellgaard *et al.*, 1999). BiP and calnexin both associate with the $5HT_3R$ subunits, suggesting that they play a role in the assembly of the $5HT_3R$ and in the degradation of misfolded subunits (Boyd *et al.*, 2002).

The 14-3-3 family of proteins are intracellular proteins with diverse functions. The 14-3-3η member of this family acts as a chaperone protein through interactions with the neuronal nAChR α4 subunit (Jeanclos *et al.*, 2001). Phosphorylation of the α4 subunit by cyclic AMP-dependent kinase (PKA), followed by association of 14-3-3η increases the stability of the α4 subunit and α4β2 nAChR (Jeanclos *et al.*, 2001).

The ER contains a number of other factors which play roles in the folding and assembly process. For example, the enzyme protein disulphide isomerase (PDI) is

involved in the formation and rearrangement of disulphide bonds during folding. Cyclophilin A, which may act as a chaperone or as a folding enzyme (peptidyl prolyl isomerase), has been suggested to be required for the functional expression of homo-oligomeric nAChRs and the $5HT_3R$ (Helekar and Patrick, 1997).

1.4.3 Post-translational modifications

Multi-subunit ion channels undergo many post-translational processes such as disulphide bond formation, signal sequence cleavage, glycosylation, phosphorylation and fatty acylation, such as palmitoylation, which occur in the ER and Golgi apparatus throughout the folding and assembly of subunits and complexes. Some of the post-translational modifications to the nAChR and $5HT_3R$ are described below.

1.4.3.1 Post-translational modifications of the nAChR

Phosphorylation modulates the functional properties of many cellular proteins. The intracellular loop region between M3 and M4 of the nAChR contains potential sites for phosphorylation. Tyrosine kinase can phosphorylate the β, γ and δ subunits of the *Torpedo* electric organ nAChR (Huganir *et al.*, 1984). Whereas, cyclic AMP (cAMP)-dependent kinase (PKA) phosphorylates the γ and δ subunits (Huganir and Greengard, 1983). The major functional effect of phosphorylation is the regulation of the rate of receptor desensitisation (Huganir and Greengard, 1990). Protein kinase C (PKC) phosphorylates the α and δ subunits (Huganir *et al.*, 1984) which causes an increase in the rate of nAChR desensitisation and affects channel conductance (Eusebi *et al.*, 1987). Forskolin, which activates adenylyl cyclase and subsequently PKA, causes desensitisation of muscle nAChRs, without affecting channel conductance, and also causes nAChR upregulation. There is a cAMP-dependent protein kinase consensus sequence in the α4 subunit and a potential PKC site in the β4 subunit in between M3 and M4. The intracellular domain of α7 is a substrate of PKA (Moss *et al.*, 1996).

The extracellular N-terminal domain of the nAChR contains several putative sites for asparagine (N)-linked glycosylation (Boulter, 1986; Nomoto *et al.*, 1986; Goldman

et al., 1987). The role of N-linked glycosylation is poorly understood, but may provide protein stability and control receptor assembly, whilst also introducing lectin binding sites. The N-linked glycosylation of the $\alpha_2\beta\gamma\delta$ nAChR, expressed in *Xenopus* oocytes, appears to be necessary for the correct folding and expression of functional receptors (Gehle *et al.*, 1997).

Palmitoylation of the α7 nAChR has recently been identified as a factor important in its expression (Drisdel *et al.*, 2004). In cell lines such as HEK293, which are incapable of expressing functional, α-BTX-binding α7 nAChRs, receptors are not significantly palmitoylated (Drisdel *et al.*, 2004). However, in cell lines such as PC12, where α7 is functionally expressed, the receptors are shown to be palmitoylated (Drisdel *et al.*, 2004). Palmitoylation of membrane proteins has been shown to be important in trafficking of proteins to the plasma membrane (reviewed in Smotrys and Linder, 2004).

1.4.3.2 Post-translational modifications of the $5HT_3R$

The $5HT_{3A}R$ subunit contains a number of consensus sites for phosphorylation (Maricq *et al.*, 1991). The $5HT_{3B}$ subunit contains four potential phosphorylation sites in the intracellular loop between M3 and M4 (Dubin *et al.*, 1999). Serine 414 of $5HT_{3A}$ is found to be phosphorylated *in vivo* by PKA (Lankiewicz *et al.*, 2000). Phosphorylation may play a role in receptor conductance levels and desensitisation (van Hooft and Vijverberg, 1995; Hubbard *et al.*, 2000). Phosphorylation by casein kinase II enhances $5HT_3R$ currents when expressed in rodent NG108-15 cells (Jones and Yakel, 2003).

The $5HT_{3A}$ and $5HT_{3B}$ subunits have several potential N-linked glycosylation sites, which have been shown to be important in receptor stability and assembly (McKernan, 1992; Boyd *et al.*, 2002). The N-linked glycosylation sites of the mouse $5HT_{3A}R$ have roles in receptor regulation (Quirk *et al.*, 2004). One site (N109) is necessary for receptor assembly, whereas N174 and N190 have roles in plasma membrane targeting and ligand binding (Quirk and Siegel, 2000; Quirk *et al.*, 2004).

1.4.4 Retention motifs

Control of protein transport from the ER, and retention of incompletely assembled proteins and of ER resident proteins such as chaperones involve several mechanisms. Many of the ER resident proteins contain motifs such as KDEL or KKXX which serve as ER retention/retrieval signals (Teasdale and Jackson, 1996). Membrane proteins themselves can contain ER retention/retrieval signals, as recent studies on a number of receptors have illustrated (Zerangue *et al.*, 1999; Bichet *et al.*, 2000; Margeta-Mitrovic *et al.*, 2000). The masking of these motifs by assembly with other subunits, interactions with other proteins or phosphorylation may regulate the forward trafficking of such proteins (Zerangue *et al.*, 1999; Bichet *et al.*, 2000; Margeta-Mitrovic *et al.*, 2000). The identification of an ER retention motif in the $5HT_{3B}$ subunit is described in Chapter 3.

An ER retention motif (PL(Y/F)(F/Y)XXN) has been identified within the M1 domain of the muscle-type nAChR subunits (Wang *et al.*, 2002; Mei and Xiong, 2003). The motif is found to be conserved in all muscle-type nAChR subunits as well as neuronal subunits (α2-α6 and β2-β4). The motif is not conserved in the α7-α9 nAChR subunits. In unassembled subunits the motif is exposed and promotes degradation, but in pentameric assemblies the motif is buried allowing exit from the ER (Wang *et al.*, 2002).

1.4.5 Interacting proteins

The identification of proteins that interact with the nAChR and $5HT_3R$ subunits and complexes may provide insight into the mechanisms involved in aspects of their folding, assembly and functional expression. To date, except for the chaperone proteins described in Section 1.4.2, relatively few specific nAChR- or $5HT_3R$-interacting proteins have been identified.

Rapsyn (or 43K), a 43 kDa protein, causes clustering of nAChRs at the postsynaptic membrane of the neuromuscular junction and in the *Torpedo* electric organ (Sealock, 1982; Froehner, 1991; Phillips *et al.*, 1991a; Phillips *et al.*, 1991b; Moransard *et al.*,

2003). The mechanism by which rapsyn functions is unclear. Muscle nAChRs are suggested to assemble with rapsyn and then cluster via a tyrosine kinase-dependent pathway which is induced by agrin (Qu *et al.*, 1996; Moransard *et al.*, 2003). Rapsyn is not thought to associate with neuronal nAChRs. The lynx1 protein, which is similar to the snake venom neurotoxins, co-localises with neuronal nAChRs and enhances ACh-evoked currents (Miwa *et al.*, 1999; Ibanez-Tallon *et al.*, 2002). The calcium sensor protein, Visinin-like protein 1 (VILIP), has also been identified as a nAChR regulatory protein which directly affects the function of the neuronal nAChRs (Lin *et al.*, 2002). PDZ-containing proteins of the PSD-95 family have also been shown to associate with neuronal nAChRs (Conroy *et al.*, 2003).

The recently identified family of RIC3 proteins has been shown to be important in the maturation of a number of nAChR subtypes (Halevi *et al.*, 2002; Halevi *et al.*, 2003). Co-expression of *C. elegans* RIC3 (CeRIC3) and its human homologue, hRIC3, in *Xenopus* oocytes enhances the activity of the *C. elegans* DEG-3/DES-2 and rat and human α7 nAChRs (Halevi *et al.*, 2002; Halevi *et al.*, 2003). The hRIC3 protein is reported to exert effects on the $5HT_3R$ (Halevi *et al.*, 2003). The co-expression of hRIC3 with the α7 nAChR in a mammalian cell line has recently been shown to facilitate functional expression of the receptor (Williams *et al.*, 2005). The function of the RIC3 proteins is investigated in Chapter 5.

1.5 DISTRIBUTION OF THE nAChR AND $5HT_3R$

1.5.1 Native neuronal nAChRs

The neuronal nAChRs can be broadly divided into two main classes, those that are sensitive to α-BTX, and those that are insensitive to α-BTX. In mammalian brain, the α-BTX sensitive nAChRs correspond to α7-containing nAChRs (Séguéla *et al.*, 1993). In mammalian brain, one α-BTX insensitive nAChR contains α4 and β2 subunits, and binds the nicotinic ligands, ACh, nicotine and cytisine with high affinity (Whiting *et al.*, 1987a; Zoli *et al.*, 1998). In the ganglia, the major α-BTX-insensitive nAChR contains α3 and β4 subunits (Flores *et al.*, 1996). The α4, β2 and

α7 subunits are the most widely expressed in brain, whereas the other subunits' expression is more limited (Drago *et al.*, 2003).

1.5.1.1 α-BTX-insensitive nAChRs of the central nervous system

The majority of high affinity nAChRs in the brain comprise the α4β2 subtype (Whiting *et al.*, 1987a; Flores *et al.*, 1992; Zoli *et al.*, 1998). The expression of α4 mRNA is high in the cerebellum and cortex, whilst the expression of β2 is fairly widely distributed throughout human brain (Paterson and Nordberg, 2000). An antibody to β2 (mAb270) immunoprecipitates more than 90% of the high affinity [^{3}H]-nicotine binding sites from solubilised chick brain extracts (Whiting and Lindstrom, 1986; Nef *et al.*, 1988; Schoepfer *et al.*, 1988). The α4 subunit is also co-immunoprecipitated with mAb270 (Whiting *et al.*, 1987b; Whiting *et al.*, 1987c; Nef *et al.*, 1988).

Knockout mice, in which a nAChR gene is silenced, have been used to investigate the endogenous role of nAChRs, and the effects of their ligands in the central nervous system (Cordero-Erausquin *et al.*, 2000, Drago *et al.*, 2003). Deletion of the β2 subunit results in the loss of high affinity nicotine binding sites (Picciotto *et al.*, 1995). Knockout of the α4 subunit results in the loss of [^{3}H]-nicotine and [^{3}H]-epibatidine binding sites which are observed in the cortex and hippocampus of wild-type mice (Marubio and Changeux, 2000). These studies provide further evidence for α4β2 as the major nAChR subtype in brain.

The α2 mRNA has a limited expression pattern. Moderate expression of α2 is observed in the interpenduncular nucleus of the brainstem (Wada *et al.*, 1989). Low levels of α3 are observed in most cortical regions and the hippocampus (Paterson and Nordberg, 2000; Drago *et al.*, 2003). The α5 subunit mRNA has been detected in a number of localised sites and also in the cortex at a lower level (Drago *et al.*, 2003). The α6 subunit is expressed at high levels in limited brain areas such as the substantia nigra and is often observed with β3 subunits (Le Novère *et al.*, 1999). The β3 subunit is also expressed in other areas such as the thalamus (Drago *et al.*, 2003). The β4 subunit is widely expressed in areas including the cerebellum and striatum

(Forsayeth and Kobrin, 1997). The co-localisation of the β4 and α3 subunits suggests that they may be co-assembled (Flores *et al.*, 1996).

1.5.1.2 α-BTX-insensitive nAChRs of the ganglia

Chick ciliary ganglia and neonatal rat sympathetic ganglia have been studied widely and have been shown to express the α3 α5, β2 and β4 subunits (Corriveau and Berg, 1993; Mandelzys *et al.*, 1994; Zoli *et al.*, 1995). The α7 subunit, which forms α-BTX-sensitive nAChRs is also expressed. The α4 subunit is expressed in adult rats (Rust *et al.*, 1994), but is not observed in chick ciliary ganglia. Embryonic chick ciliary neurons express at least four different nAChR subtypes (Conroy *et al.*, 1992; Vernallis *et al.*, 1993; Conroy and Berg, 1995; Pugh *et al.*, 1995).

1.5.1.3 α-BTX-sensitive nAChRs of the brain and ganglia

The α-BTX-sensitive nAChRs are predominantly homomeric α7 nAChRs. The α7 subunit is detected, at a high level, in the hippocampus, hypothalamus, amygdala, olfactory areas and brainstem of the human brain. Lower levels of α7 expression are detected in the cortex, cerebellum and thalamus (Dominguez del Toro *et al.*, 1997; Paterson and Nordberg, 2000; Drago *et al.*, 2003). The expression of α7 mRNA is observed widely within peripheral ganglia (Rust *et al.*, 1994). In chick brain, three classes of α-BTX-sensitive nAChRs exist. The majority are α7 homomers; the others comprise α7α8 heteromers and α8 homomers (Gotti *et al.*, 1994).

In rat brain, [^{125}I]-α-BTX binding sites closely parallel α7 mRNA expression (Séguéla *et al.*, 1993). Knockout of the α7 subunit gene results in the loss of [^{125}I]-α-BTX binding sites, but the level of [^{3}H]-nicotine binding sites remains unchanged compared to wild-type animals (Orr-Urtreger *et al.*, 1997). In α4 or β2 knockout mice, levels of [^{125}I]-α-BTX binding sites are unaffected (Zoli *et al.*, 1998; Marubio *et al.*, 1999).

1.5.1.4 α9 and α10 distribution

The α9 and α10 subunits are not easily classified as either muscle-type or neuronal nAChRs (Elgoyhen *et al.*, 2001). Their expression is largely restricted to the hair cells of the inner ear and neither subunit is found in the central nervous system (Elgoyhen *et al.*, 1994; Elgoyhen *et al.*, 2001; Lustig *et al.*, 2001).

1.5.2 Distribution of the $5HT_3R$

The $5HT_3Rs$ are expressed throughout the central and peripheral nervous systems (Barnes and Sharp, 1999). Radioligand binding studies, using compounds such as the $5HT_3R$ antagonist [^{3}H]-GR65630, have been used to map $5HT_3R$ distribution (Marazziti *et al.*, 2001). In the peripheral nervous system, $5HT_3Rs$ are mainly localised to the enteric nervous system and ganglionic neurons. In the brain, the highest density of binding sites is in the area postrema, followed by the nucleus tractus solitarus, trigeminal nucleus, dorsal vagal complex and substantia gelatinosa (Marazziti *et al.*, 2001). $5HT_3R$ expression in other areas of the brain is low, with the highest levels in the hippocampus, amygdala and superficial layers of the cortex (Barnes and Sharp, 1999). In situ hybridisation studies indicate that $5HT_{3A}$ transcripts are distributed similarly to the pattern of $5HT_3R$ radioligand binding sites. $5HT_{3A}$ mRNA is found in the brain (cortex, brainstem, midbrain), spinal cord and heart (Maricq *et al.*, 1991). $5HT_{3B}$ mRNA is co-expressed with the $5HT_{3A}$ subunit in the human brain in the cerebral cortex, amygdala, caudate nucleus, thalamus and hippocampus (Davies *et al.*, 1999; Dubin *et al.*, 1999). In rat, $5HT_{3B}$ subunit expression appears to be restricted to the peripheral nervous system (Morales and Wang, 2002). However, weak signals for $5HT_{3B}$ mRNA have been detected in whole brain extracts (Sudweeks *et al.*, 2002). Taken together, these data and that from other studies suggest that the $5HT_{3B}$ subunit is not a major determinant of receptor function in the central nervous system (van Hooft and Yakel, 2003). Using reverse transcriptase-polymerase chain reaction in situ hybridisation (RT-PCR ISH), a very sensitive technique which can detect a single molecule of mRNA, both $5HT_{3A}$ and $5HT_{3B}$ mRNA were detected in a small population of cells in spleen, tonsil, small and large intestine, uterus, prostate, ovary and placenta (Dubin *et al.*, 1999).

Little is known about the cells expressing these subunit mRNAs. The recently identified putative $5HT_{3D}$ subunit was found to be expressed in the kidney, colon and liver, whilst $5HT_{3C}$ and $5HT_{3E}$ were found to be more widely expressed in many tissues including brain (Niesler *et al.*, 2003). Interspecies differences in $5HT_3R$ distribution exist.

1.6 HETEROLOGOUS EXPRESSION OF RECEPTORS

The oocytes of *Xenopus laevis* (South African clawed frog) have been used widely as a heterologous expression system for the characterisation of nAChRs and $5HT_3Rs$. The reconstitution of functional recombinant nAChRs in *Xenopus* oocytes has been demonstrated by injection of mRNA encoding the nAChR subunits of the *Torpedo* electric organ (Sumikawa *et al.*, 1981). Cell surface receptors were expressed with properties resembling those of native receptors (Barnard *et al.*, 1982).

The *Xenopus* oocyte can be injected with known combinations of receptor subunit mRNAs or cDNAs and the resulting receptors can be compared to native receptors. Heterologous expression of receptor subunits in mammalian cell lines has also proved useful, and may provide an environment which more closely resembles the receptors' native environment, compared to that provided by *Xenopus* oocytes (Sivilotti *et al.*, 2000). The transient and stable expression of receptor subunits is possible in mammalian cell lines.

1.6.1 Native versus recombinant expression of nAChRs

The heterologous expression of nAChRs is an extremely useful tool for the characterisation of nAChRs. Properties of receptors often resemble those of native receptors, but differences have been observed. Properties of receptors may vary between different heterologous expression systems and with the use of different techniques. The environment of the host cell may affect the properties of the receptor being expressed. When expressed natively, the *Torpedo* electric organ nAChR occurs predominantly in a dimeric form, whereas expression in oocytes results in single pentameric receptors (Sumikawa *et al.*, 1981; DiPaola *et al.*, 1989).

The pharmacological properties of the chick α7 nAChR expressed in oocytes correlate well with, but are not identical to, the α-BTX sensitive nAChRs observed natively in chick (Anand *et al.*, 1993a; Anand *et al.*, 1993b; Gotti *et al.*, 1994; Gotti *et al.*, 1997). Recombinant α7 homomeric receptors have a fifty-fold higher affinity for cytisine than the α7-containing nAChRs of embryonic chick brain (Anand *et al.*, 1993b). In different expression systems, differences exist in the single channel conductance of the α7 nAChR. In a mammalian cell line, BOSC23, two conductance states are observed for α7, whereas in oocytes a single conductance state is observed (Revah *et al.*, 1991; Bertrand *et al.*, 1992; Ragozzino *et al.*, 1997).

The different properties of the recombinant homomeric α7 nAChRs compared to those of the native suggested that, *in vivo*, α7 may co-assemble with other subunits (Anand *et al.*, 1993b; Yu and Role, 1998; Palma *et al.*, 1999; Khiroug *et al.*, 2002; Virginio *et al.*, 2002). The α7 and β2 subunits have been observed to co-precipitate when transiently transfected into a mammalian cell line and are shown to produce functional α7β2 receptors in *Xenopus* oocytes with properties differing from α7 homomers (Khiroug *et al.*, 2002).

1.6.2 Native versus recombinant expression of $5HT_3$Rs

The heterologous expression of $5HT_3$Rs has been useful in the characterisation of the $5HT_3$Rs. Electrophysiological investigations revealed a striking difference in single channel conductance between heterologously expressed and native $5HT_3$Rs (Maricq *et al.*, 1991; Hussy *et al.*, 1994; Brown *et al.*, 1998). In various native tissues, the conductance of the $5HT_3$R ion channel is between 9 and 17 pS (Derkach *et al.*, 1989; Hussy *et al.*, 1994). The $5HT_3$R expressed in, for example, the NCB-20 or N1E-115 cell line, or heterologous expression of the $5HT_{3A}$ subunit, results in a receptor with a sub-pS conductance (Peters *et al.*, 1992; Hussy *et al.*, 1994). The cloning of the $5HT_{3B}$ subunit helped to account for the observed functional differences between native and recombinant receptors. Heterologous co-expression of the $5HT_{3A}$ and $5HT_{3B}$ subunits resulted in receptors with properties more similar to those of native $5HT_3$Rs (Davies *et al.*, 1999; Dubin *et al.*, 1999; Hanna *et al.*, 2000). Native receptors do also exist in a low conductance homomeric ($5HT_{3A}$) form, for example,

in rodent superior cervical ganglion neurons the expression of both low and high (heteromeric; $5HT_{3A}/5HT_{3B}$) conductance receptors is observed (Yang *et al.*, 1992; Hussy *et al.*, 1994).

In neuroblastoma cell lines, such as N1E-115, in which the $5HT_3R$ single channel conductance is similar to that observed for $5HT_{3A}$ homomers, the expression of both $5HT_{3A}$ and $5HT_{3B}$ mRNA is observed, suggesting that the $5HT_{3B}$ subunit does not contribute significantly to the properties of $5HT_3Rs$ of neuroblastoma cells (Hanna *et al.*, 2000; Stewart *et al.*, 2003). The functional recombinant expression of $5HT_{3A}$ homomers has been demonstrated in dorsal root ganglion neurons (Smith *et al.*, 1997) and cortical neurons (Boyd *et al.*, 2002).

1.6.3 Influence of the host cell environment

The expression of recombinant nAChRs, such as the homomeric α7 and α8 receptors, has been observed to be critically dependent upon the nature of the host cell (Blumenthal *et al.*, 1997; Cooper and Millar, 1997; Cooper and Millar, 1998; Sweileh *et al.*, 2000; Drisdel *et al.*, 2004), whereas expression of the closely related $5HT_3R$ is not. Correctly folded and assembled cell surface nAChRs are only detected in a few cell lines, for example, the human neuroblastoma SH-SY5Y cell line (Cooper and Millar, 1997; Cooper and Millar, 1998). In several other cell lines, such as human embryonic kidney HEK293 cells, α7 subunit protein can be detected, but receptors are not expressed on the cell surface (Cooper and Millar, 1997; Cooper and Millar, 1998). The expression of the α7 subunit can vary between different populations of cells. For example, three isolates of the PC12 cell line revealed differences in the ability to express functional α7 nAChRs (Blumenthal *et al.*, 1997). Taken together, the results suggest the requirement of an additional factor, which is only present in certain cell types, for the correct folding, assembly and localisation of the α7 nAChR (Cooper and Millar, 1997; Dineley and Patrick, 2000; Sweileh *et al.*, 2000).

In contrast to α7, the $5HT_3R$ efficiently forms functional receptors in several cell lines, for example, HEK293 cells (Hope *et al.*, 1996). The inefficient expression of

α7, and several other nicotinic subunits, can be enhanced through the construction of subunit chimeras in which the C-terminal region of the nicotinic subunit is replaced with the corresponding region of the $5HT_{3A}$ subunit (Eiselé *et al.*, 1993; Cooper and Millar, 1998; Cooper *et al.*, 1999; Rakhilin *et al.*, 1999; Harkness and Millar, 2002). A chimera consisting of the N-terminal region of α7 fused to the C-terminal region of $5HT_{3A}$ is efficiently expressed on the cell surface in cell types which inefficiently fold wild-type α7 (Eiselé *et al.*, 1993; Cooper and Millar, 1998).

1.7 PHYSIOLOGICAL FUNCTION AND DYSFUNCTION

1.7.1 nAChR function and dysfunction in the central nervous system

The distribution of nicotinic receptors throughout the central nervous system has been well defined, whilst the physiological functions of nAChRs are still unclear. Nicotinic receptors have been implicated in a variety of brain functions, including cognitive functions, such as attention, learning and memory formation, sensory perception and reward (Gotti *et al.*, 1997; Jones *et al.*, 1999).

1.7.1.1 The role of presynaptic nAChRs

In the central nervous system, the primary role of presynaptic nAChRs is proposed to be in the modulation of synaptic transmission through the regulation of neurotransmitter release (Wonnacott, 1997; Role and Berg, 1996; Levin and Simon, 1998). The release of most of the classical neurotransmitters, including dopamine, noradrenaline, GABA and glutamate, has been shown to be affected by presynaptic nAChRs. High affinity nicotine binding sites are found on the terminals of dopamine neurones in the striatum (Wonnacott, 1997; Wonnacott *et al.*, 2000). These receptors are thought to be a heterogenous population of α4β2 and α3-containing receptors (Wonnacott, 1997).

The presynaptic nAChRs may also function as 'autoreceptors' on ACh-containing nerve terminals, modulating the release of ACh via a feedback mechanism. Release

of ACh from a nerve terminal may cause stimulation of the autoreceptors, which then mobilise ACh from a reserve store to be available upon demand (Wonnacott, 1997).

An additional role for presynaptic nAChRs is in development. Nicotinic receptors are observed on growth cones, where they respond to ACh, which is spontaneously released by the growth cone, and may participate in the regulation of neurite outgrowth (Role and Berg, 1996; Wonnacott, 1997). When the neurite reaches a postsynaptic target, the release of ACh increases and signals for the growth to end, resulting in synapse formation and stabilisation (Wonnacott, 1997). The receptors mediating this action appear to be of the $\alpha 7$ subtype, their high calcium permeability playing a role in calcium-dependent activation of signalling pathways.

1.7.1.2 The role of postsynaptic nAChRs

Postsynaptic nAChRs mediate nicotinic transmission in autonomic ganglia, within the spinal cord (at the Renshaw cell-motoneuron synapse), and at efferent synapses of the cochlea hair cells (Role and Berg, 1996). Determining the role of postsynaptic nAChRs in the brain has proved much more elusive than in the peripheral nervous system. The most clearly demonstrated role identified is in the fast ACh-mediated synaptic transmission in the hippocampus and in the sensory cortex (Jones *et al.*, 1999). The lack of definitive evidence for postsynaptic receptor function in the brain suggest that they participate in functions other than direct synaptic transmission (Role and Berg, 1996).

1.7.1.3 The role of nAChRs in tobacco dependence

A well established physiological role of the neuronal nAChRs is their mediation of nicotine-induced tobacco addiction. Tobacco smoking in humans and nicotine self-administration in animals are associated with an increase in dopamine release that follows the action of nicotine upon mesencephalic dopaminergic neurones (see Lena and Changeux, 1998). Nicotine exploits the intrinsic reward pathways of the nervous system that mediate the reinforcing effects of natural rewards such as food, by increasing dopamine-mediated activity (Jones *et al.*, 1999). The increase in dopamine-mediated activity is primarily via nAChRs in the ventral tegmental area

(VTA) of the midbrain (Nisell *et al.*, 1994). The reward system includes the mesolimbic dopaminergic pathways which originate from the dopaminergic neurons of the VTA and project to the nucleus accumbens and prefrontal cortex. Nicotine alters the activity of the VTA to enhance dopamine release in the nucleus accumbens (Raggenbass and Bertrand, 2002). To date, three cell types in the VTA have been observed to express nAChRs: dopaminergic neurons, GABAergic neurons, and glutamatergic presynaptic terminals which synapse onto dopaminergic neurons (Mansvelder and McGehee, 2002). The principal excitatory input to VTA neurons, which ultimately increase dopamine release in the nucleus accumbens, are the glutamatergic terminals (Mansvelder and McGehee, 2000). The glutamatergic terminal nAChRs are α7-containing, and block with MLA prevents nicotine-induced increases in dopamine release. The principal inhibitory inputs to VTA neurons are GABAergic, including local interneurons as well as projections from the nucleus accumbens. The majority of the nAChRs on the GABAergic neurons are proposed to contain α4 and β2 subunits (Mansvelder and McGehee, 2000; Mansvelder and McGehee, 2002). Dopamine release from the VTA projections depends on the balance of excitatory and inhibitory inputs, and the intrinsic activity of the dopaminergic neurons. Nicotine-induced dopamine release in the nucleus accumbens does not occur in β2 knockout mice. Also, β2 knockout mice do not self-administer nicotine, suggesting the β2 subunit to be involved in nicotine addiction (Picciotto *et al.*, 1998).

In rats, chronic exposure to nicotine results in an upregulation of high affinity [^{3}H]-nicotine binding sites in the brain which correspond to α4β2. A similar upregulation of [^{3}H]-nicotine binding sites is observed in postmortem brains of chronic smokers (Benwell *et al.*, 1988). The upregulation of receptors varies with cell-type and receptor subtype and the receptors increase in number through increased assembly (Olale *et al.*, 1997). Although the nAChRs increase in number upon chronic nicotine treatment, a net decrease in nAChR function is observed. This decrease in function may explain the tolerance for nicotine of tobacco smokers. The nicotine-upregulated receptors accumulate in a desensitised and inactive state (Peng *et al.*, 1997).

1.7.1.4 nAChR Pathology

Nicotinic receptors are implicated in several neurological disorders. In neurodegenerative diseases such as Alzheimer's disease, Parkinson's disease and Lewy-body disease, a decrease in high affinity nicotine binding sites is observed (Paterson and Nordberg, 2000; Picciotto and Zoli, 2002).

Alzheimer's disease (AD) is characterised by a progressive deterioration of higher cognitive functions, such as the loss of memory. In addition to a number of neuropathological features, AD is characterised by the loss of cholinergic innervation of the cerebral cortex and hippocampus. Binding studies performed on postmortem brain tissue have indicated that the major subtype of nAChRs lost in AD is $\alpha4\beta2$. The mRNA levels of $\alpha4$ and $\beta2$ are also observed to decrease with age in the frontal cortex, and levels of $\beta2$ are reduced in the hippocampus. The level of $\alpha3$ subunit mRNA is also reduced with age, but no significant difference between mRNA levels in AD brain and age matched controls is observed (Terzano *et al.*, 1998). A significant correlation between reduced [^{3}H]-epibatidine sites and reduced levels of the presynaptic marker, synaptophysin, in the frontal cortex of AD brains has been demonstrated, suggesting that the majority of nAChRs lost are presynaptic.

Autosomal dominant nocturnal frontal lobe epilepsy (ADNFLE) is a partial epilepsy which can result from a missense mutation in the $\alpha4$ subunit gene. A highly conserved serine at position 247 of the M2 channel lining domain of the subunit is replaced with a phenylalanine (S247F), resulting in impaired channel function (Weiland *et al.*, 1996; Kuryatov *et al.*, 1997). When $\alpha4$(S247F) is co-expressed with $\beta2$ in *Xenopus* oocytes, a receptor with reduced calcium permeability, channel opening and recovery from desensitisation, compared to wild-type $\alpha4\beta2$, is produced (Weiland *et al.*, 1996). A second mutation involving the insertion of a leucine after position 259 in the M2 domain of the $\alpha4$ subunit also causes ADNFLE. Epilepsy results from an excess of neuronal activation, so mutations causing a reduction in nAChR function are surprising. An explanation may be provided if the mutant receptors are located presynaptically on inhibitory nerve terminals.

1.7.2 $5HT_3R$ function and dysfunction in the central and peripheral nervous systems

1.7.2.1 Presynaptic and postsynaptic $5HT_3R$ function

The stimulation of $5HT_3R$ affects cardiac, intestinal and lung functions and induces nausea and vomiting. The $5HT_3Rs$ are proposed to play roles in anxiety and cognition. Generally, the $5HT_3Rs$ are thought to be involved in the presynaptic modulation of neurotransmitter release in the central nervous system, although their precise role in this function is unclear (Lambert *et al.*, 1995; Barnes and Sharp, 1999; van Hooft and Vijverberg, 2000). Presynaptic $5HT_3Rs$ are reported to be involved in the modulation of release of neurotransmitters such as dopamine, cholecystokinin (CCK), 5-HT and GABA in a number of brain regions. Postsynaptic $5HT_3Rs$ present on GABAergic interneurons have been observed to mediate fast synaptic transmission in the central nervous system (Sugita *et al.*, 1992; Roerig *et al.*, 1997). Most of the initial evidence for the presence of functional $5HT_3Rs$ in the brain was from reports of the behavioural effects of $5HT_3R$ ligands (mostly $5HT_3R$ antagonists). The use of $5HT_{3A}$ knockout mice has not contributed much information concerning the function of $5HT_3Rs$ (Barnes and Sharp, 1999).

A significant proportion of $5HT_3Rs$ in the amygdala are located on serotonergic terminals. Chemical lesion of the serotonergic system causes a decrease in the number of these receptors, whereas the number of receptors in the hippocampus or cerebral cortex are unaffected. However, experiments investigating $5HT_3R$-mediated 5-HT release in the amygdala have not been performed. A $5HT_3R$-mediated enhancement of 5-HT release in the hippocampus has been reported.

Evidence has been provided from *in vivo* studies for the involvement of $5HT_3Rs$ in the release of dopamine in the nucleus accumbens (Imperato and Angelucci, 1989), but the exact location of these receptors has not been determined.

The majority of cortical and hippocampal $5HT_3Rs$ are located on CCK-containing GABAergic interneurons and so it is likely that activation of these receptors leads to the release of both GABA and CCK. In synaptosome preparations from the cortex,

5-HT is observed to enhance CCK release and this effect is antagonised by $5HT_3R$ antagonists (van Hooft and Vijverberg, 2000). However, $5HT_3R$ antagonists have no effect on CCK release in *in vivo* studies (van Hooft and Vijverberg, 2000). There is little direct evidence for the role of presynaptic $5HT_3Rs$ in GABA release.

1.7.2.2 $5HT_3Rs$ as therapeutic targets

Animal studies using $5HT_3R$ antagonists have suggested that they might be clinically useful in a number of areas including anxiety, cognitive dysfunction and psychosis, in addition to their anti-emetic use. However, no clinical studies have yet clearly demonstrated the effectiveness of $5HT_3R$ antagonists in the treatment of central nervous system disorders (Greenshaw and Silverstone, 1997).

The $5HT_3R$ antagonists, ondansetron and granisetron, are commonly used anti-emetics for the treatment of chemotherapy- and radiation-induced emesis (Jones and Blackburn, 2002). In animal studies, it was shown that chemotherapeutic agents caused the release of vast quantities of 5-HT in the gut. This 5-HT then activated $5HT_3Rs$ in the gut and in the dorsal vagal complex in the brainstem, resulting in emesis. Further animal studies demonstrated that this response was blocked by $5HT_3R$ antagonists.

1.8 CO-ASSEMBLY AND CROSS-PHARMACOLOGY OF THE nAChR AND $5HT_3R$

The nAChRs and $5HT_3Rs$ are structurally and functionally related proteins. Their structures are similar enough to enable construction of viable chimeras, such as those containing the extracellular N-terminal ligand binding domain of a nAChR (e.g. $\alpha7$, $\alpha4$ or $\beta2$), fused to the C-terminal region of $5HT_{3A}$ (Eiselé *et al.*, 1993; Cooper *et al.*, 1999; Harkness and Millar, 2001; Harkness and Millar, 2002).

The co-assembly of recombinant $5HT_{3A}$ and nicotinic subunits has also been reported. Heterologous expression of the $5HT_{3A}$ and $\alpha4$ nAChR subunits resulted in

co-assembly of the subunits, generating a 5-HT-activated channel with enhanced calcium permeability compared to the homomeric $5HT_{3A}$ channel (van Hooft *et al.*, 1998). A further report suggested that the α4 nAChR subunit, in α4 and $5HT_{3A}$ heteromeric complexes, contributes to the lining of the ion channel pore (Kriegler *et al.*, 1999). The co-assembly of the $5HT_{3A}$ subunit with the β2 nAChR subunit was also reported (Harkness and Millar, 2001). The functional significance of this co-assembly remains unclear. Co-expression of α4 and $5HT_{3A}$ in a mammalian cell line did not result in efficient cell surface expression of $\alpha4/5HT_{3A}$ heteromeric complexes (Harkness and Millar, 2001). Immunoprecipitation studies on porcine brain demonstrated that native $5HT_3$Rs do not contain nAChR subunits (Fletcher *et al.*, 1998). The $5HT_3$R co-localises with the α4 nAChR subunit on striatal nerve terminals, however, it is proposed that the receptors do not physically interact, but that interactions occur between their signalling pathways (Nayak *et al.*, 2000).

Some pharmacological cross-reactivity is observed between the nAChRs and $5HT_3$Rs. For example, the endogenous $5HT_3$R agonist, 5-HT, causes block of nAChRs (Palma *et al.*, 1996; Fucile *et al.*, 2002). The nicotinic agonists, nicotine and ACh are competitive $5HT_3$R antagonists (Gurley and Lanthorn, 1998). The $5HT_3$R antagonist tropisetron is reported to act as a partial agonist at the α7 nAChR expressed in *Xenopus* oocytes (Macor *et al.*, 2001). Some overlap in pharmacological properties is observed, for example, PSAB-OFP which is a selective α7 nAChR agonist, is also a potent agonist of the $5HT_3$R (Broad *et al.*, 2002). The aromatic moiety of 5-HT, 5-hydroxyindole (5-HI), potentiates the responses of both the α7 nAChR and $5HT_3$Rs (van Hooft *et al.*, 1997; Gurley *et al.*, 2000; Zwart *et al.*, 2002).

1.9 AIM OF STUDY

The nAChRs and $5HT_3$Rs are widely expressed throughout the central and peripheral nervous systems and are involved in a number of functional processes. The aim of this study was to gain a better understanding of the structural and functional properties of these receptors. A variety of molecular and cell biological techniques

have been used to investigate the mechanisms involved in the folding, assembly, trafficking and function of these receptors. A better understanding of these mechanisms should help to elucidate the mechanisms involved in the functional expression of native receptors. The nAChRs and $5HT_3Rs$ are implicated in a number of physiological processes as well as several neurological disorders. Characterisation of these receptors is essential to further define their roles in the brain and other organs, and to realise their potential as therapeutic targets.

CHAPTER 2

MATERIALS AND METHODS

2.1 PLASMID CONSTRUCTS AND SUBCLONING

2.1.1 Competent cells

2.1.1.1 Preparation of competent Escherichia coli strain XL1-blue

Luria-Bertani (LB) medium (20 ml) was inoculated with *Escherichia coli* (*E. coli*) strain XL1-blue from a frozen glycerol stock, and grown at 37°C with shaking at 225 rpm overnight. The culture was transferred to 500 ml of SOB (20 g/l bacto-tryptone, 5 g/l bacto-yeast extract, 0.5g/l NaCl, 2.5 mM KCl, 10 mM $MgCl_2$) and incubated at 37°C with shaking at 225 rpm until an optical density at 550 nm of 0.5-0.55 was reached. The culture was centrifuged at 2500 rpm for 15 minutes at 4°C in a Beckman J2-M1 centrifuge, the supernatant discarded and the pellet resuspended in 20 ml of ice-cold RF1 (100 mM RbCl, 50 mM $MnCl_2.4H_2O$, 30 mM potassium acetate, 10 mM $CaCl_2.2H_2O$, 15 % w/v glycerol, pH adjusted to 5.8 with 0.2 M acetic acid, filter sterilised (0.22 μm)) and incubated on ice for 15 minutes. The cells were centrifuged at 2500 rpm for 9 minutes at 4°C, the supernatant discarded and the pellet resuspended in 3.5 ml of ice-cold RF2 (10 mM RbCl, 10 mM MOPS, 75 mM $CaCl_2.2H_2O$, 15 % w/v glycerol, pH adjusted to 6.8 with 0.2 M acetic acid, filter sterilised (0.22 μM)). Cells were incubated on ice for 15 minutes and aliquoted on a dry ice and ethanol bath. Cells were stored at -80°C.

2.1.1.2 Other E. coli strains

For most applications the XL1-blue strain of *E.coli* was used. However, if the plasmid required restriction enzyme digestion with *BclI* whose activity is blocked by *dam* methylation then the GM2163 (*dam*$^-$) strain was used.

The MC1061/P3 strain was used for plasmids such as pCDM8 which carry the *SupF* gene. These cells contain a P3 episome which carries amber mutations in the ampicillin and tetracycline resistance genes. The *SupF* gene enables the amber/termination codon to be passed over and therefore confers ampicillin and

tetracycline resistance to transformed cells. All strains were made competent, essentially as above.

2.1.2 Transformation into *E. coli*

Bacterial transformations were performed using frozen stocks of competent *E. coli* cells as described above. DNA (1-30 ng) or 2-5 µl of ligation mixture was gently mixed with 50 µl of competent *E. coli* cells in a Falcon 352005 polypropylene tube and incubated on ice for 30 minutes. The cells were heat shocked for 90 seconds in a 42°C water-bath. 500 µl of SOC (SOB plus 20 mM glucose) was added and the cells incubated at 37°C with shaking at 225 rpm for 1 hour. An aliquot (20-500 µl) was plated on to a LB-agar plate, containing the appropriate antibiotic for the plasmid used, and grown overnight at 37°C.

2.1.3 Preparation of plasmid DNA

2.1.3.1 Small scale preparation of plasmid DNA: Extraction by alkaline lysis method

A single colony was transferred to 2 ml of LB containing the appropriate antibiotic for the plasmid used and grown for 6-14 hours at 37°C with shaking at 225 rpm. Cells (1.5 ml) were centrifuged at 12,000*g* for 30 seconds and the resulting cell pellet resuspended in 100 µl ice-cold solution I (50 mM glucose, 25 mM Tris.HCl, 10 mM EDTA) by vigorous vortexing. Solution II (200 µl) (0.2 NaOH, 1 % SDS) was added and mixed by inversion. Ice-cold solution III (150 µl) (100 ml contains: 60 ml 5 M potassium acetate, 11.5 ml glacial acetic acid, 28.5 ml H_2O) was added and mixed by vortexing in an inverted position and tubes were then stored on ice for 3-5 minutes. The mixture was centrifuged at 12,000*g* for 5 minutes at 4°C and the supernatant transferred to a fresh tube. An equal volume of phenol/chloroform was added, mixed and the preparation centrifuged and the supernatant removed to a fresh tube. The DNA was precipitated with two volumes of 100 % ethanol at room temperature and allowed to stand for 2 minutes before being centrifuged at 12,000*g* for 5 minutes. The supernatant was removed and the pellet washed with 70 %

ethanol allowed to air dry before being resuspended in 20-50 µl of milli-Q (MQ) water containing 50 µg/ml RNAse A.

2.1.3.2 Large scale preparation of plasmid DNA

A plasmid purification kit from Qiagen (Qiagen Plasmid Maxi Kit), based on a modified alkaline lysis procedure, was used according to the manufacturers instructions. A single colony or a stab from a glycerol stock was grown overnight in 250 ml of LB medium plus appropriate antibiotic at 37°C with shaking at 225 rpm. The cells were harvested by centrifugation at 6,000*g* for 10 minutes at 4°C. The cell pellet was resuspended in 10 ml of ice-cold buffer P1 (50 mM Tris.Cl (pH 8.0), 10 mM EDTA, 100 µg/ml RNase A) by vortexing and pipetting up and down until no cell clumps remained. Buffer P2 (10 ml) (lysis buffer: 200 mM NaOH, 1 % SDS) was added and mixed by inverting gently 5 times and incubated at room temperature for 5 minutes. Buffer P3 (10 ml) (neutralisation buffer: 3 M potassium acetate (pH 5.5)) was added and mixed immediately by gently inverting and incubated on ice for 20 minutes before centrifugation at ≥20,000*g* for 30 minutes at 4°C. The resulting supernatant was applied to a Qiagen tip (equilibrated with 10 ml buffer QBT (750 mM NaCl, 50 mM MOPS, 15 % isopropanol, 0.15 % Triton X-100)) and allowed to empty by gravity flow. The Qiagen tip was washed twice with 30 ml of buffer QC (1 M NaCl, 50 mM MOPS, 15 % isopropanol) and eluted with 15 ml buffer QF (1.25 M NaCl, 50 mM Tris.HCl (pH 8.5), 15 % isopropanol) into a glass 30 ml tube. The DNA was precipitated by addition of 0.7 volumes of room-temperature isopropanol and centrifugation at 15,000*g* for 30 minutes at 4°C. The supernatant was carefully decanted and the pellet washed with 5 ml of room-temperature 70 % ethanol. The pellet was air-dried for 5-10 minutes and resuspended in 1 ml of TE buffer (10 mM Tris.Cl, 1 mM EDTA), pH 8.0.

2.1.3.3 Determination of yield

DNA concentration and purity were determined by measurement of absorbance at 260 nm (A_{260}) and 280 nm (A_{280}) in a BIORAD SmartSpec™ 3000 spectrophotometer. An A_{260}: A_{280} value of 1.6-2.0 indicates a pure DNA preparation.

Ratios significantly less indicate protein contamination and ratios above 2.0 indicate salt impurities.

2.1.4 Polymerase chain reaction

Polymerase chain reaction (PCR) thermocycling was performed in a Peltier Thermal Cycler, PTC-225 (MJ Research). Typical reactions were carried out in a 20 µl volume and contained 10-500 ng DNA, 0.25 µM of each of forward and reverse primer, 2.5 µM dNTPs, 1X *Pfu* or KOD reaction buffer plus 2.5 mM $MgSO_4$ if using KOD and 2.5 U *Pfu* or KOD DNA polymerase made up to the final volume with MQ water. *Pfu* and KOD have a higher proof reading ability than *Taq* DNA polymerase as they possess 3'-5' exonuclease activity as well as 5'-3' DNA polymerase activity (*Taq* only has 5'-3' exonuclease activity), and so DNA synthesis fidelity is increased. *Taq* polymerase was used for standard diagnostic PCR. Reactions using *Taq* included *Taq* buffer and 2.5 mM $MgCl_2$.

2.1.5 Restriction enzyme digestion

Typically, reactions were carried out in a 20 µl reaction volume. Plasmid DNA (1-3 g) was digested with 5-10 U of restriction enzyme in an appropriate buffer for 1 hour at an incubation temperature for optimal enzyme activity (usually 37°C). For digests using two enzymes with incompatible buffers the first digestion was carried out in a 20 µl volume for 1 hour. This digestion reaction was diluted with MQ water to 60 µl, the second buffer added to a 1X concentration and digestion continued for 1 hour.

2.1.6 Dephosphorylation of DNA

If subcloning involved digestion with a single enzyme, 5'-phosphate groups were removed using calf intestinal alkaline phosphatase (CIP) to prevent religation of the plasmid vector. Typically, reactions were carried out in a 90 µl volume which included 40 µl of a restriction digest reaction mixed with 1X CIP buffer and 2-3 U CIP. This reaction was incubated for 30 minutes at 37°C when another 2-3 U of CIP was added and incubated for a further 30 minutes.

2.1.7 Agarose gel electrophoresis

Electrophoresis through agarose gel allows the separation, visualisation and purification of plasmid DNA and DNA fragments. For most purposes, 1 % agarose gels were used. Electrophoresis-grade agarose was melted in TAE (Tris-acetate: 0.04 M Tris-acetate, 0.001 M EDTA) and 0.3 μg/ml ethidium bromide added. DNA samples were run alongside 1 μg *Hin*dIII digested Lamda (λ) DNA standard markers, and PCR markers if appropriate, to enable estimation of the size of the DNA bands. Samples and markers were loaded in 1X blue/orange loading dye.

If DNA fragments were required for subcloning they were separated on low melting point agarose gels. DNA bands were excised from the gel and purified using the Wizard™ DNA clean up system (Promega) according to the manufacturers instructions. Briefly, gel slices were melted in a hot block, resuspended in 1 ml Wizard™ DNA Clean-Up resin and forced through a mini-column using a 2 ml syringe. DNA bound to the column was washed with 2 ml isopropanol and the excess removed by centrifugation at 13,000 rpm for 2 minutes. DNA was eluted in 30-50 μl pre-warmed (65°C) MQ water by centrifugation at 13,000 rpm for 1 minute.

2.1.8 DNA ligations

Ligation reactions were carried out in a 10 μl volume containing 1 μl of vector, 3-7 μl of insert (depending on Wizard™ purification yield), 0.5 U T4 DNA Ligase and 1 μl 10X T4 DNA ligase buffer. Reactions were incubated overnight at 14°C. To assess levels of vector re-ligation reactions containing no insert were performed.

2.1.9 Plasmid constructs and cDNA libraries

Rat α7 nAChR subunit cDNA was obtained from Dr Jim Patrick, Baylor College of Medicine, Houston. Human α7 and chick α8 nAChR subunit cDNAs (Schoepfer *et al.*, 1990, Peng *et al.*, 1994) were provided by Dr Jon Lindstrom (University of Pennsylvania, PA., USA). Mouse $5HT_{3A(L)}$ in the mammalian expression vector pCDM6x1 was from David Julius, University of California (Maricq *et al.*, 1991) and

was subcloned into pRK5 using the *XbaI* site in this laboratory by Dr Elizabeth Baker. Mouse $5HT_{3A(S)}$ was a gift to Eli Lilly & Company from Dr Sarah Lummis, University of Cambridge. Human $5HT_{3A}$ in pcDNA3 from Eli Lilly was used in studies directly related to Eli Lilly. Human $5HT_{3A}$ and $5HT_{3B}$, in pCDM8, from Ewen Kirkness, Institute for Genomic Research, Rockville, Maryland were used in all other work. CeRIC3 was from Millet Treinin, Hebrew University, Israel and was subcloned into the mammalian expression vectors pRK5 and pcDNA3 in this laboratory by Dr Stuart Lansdell. The SH-SY5Y cDNA library was constructed in this laboratory by Dr Sandra Cooper. Dr Chris Connolly, University of Dundee, provided HA and myc tagged human $5HT_{3A}$ and $5HT_{3B}$ as well as the following truncated/mutant subunit cDNAs: HA tagged human $5HT_{3B}$ truncated at residue 267 and at TM1 and TM2 termed $5HT_{3B}$(267), $5HT_{3B}$(TM1) and $5HT_{3B}$(TM2) respectively, HA tagged human $5HT_{3A}$(CRAR), myc tagged $5HT_{3B}$(SGER) and $5HT_{3B}$(SGER)-myc truncated at residue 270 ($5HT_{3B}$(SGER)270) and at TM2 ($5HT_{3B}$(SGER)TM2).

2.1.10 Expression vectors

Expression Vector	Promoter	Inducible/ Constitutive	Poly-A Signal	Selection
pcDNA3	CMV	Constitutive	SV40	amp
pcDNA3.1	CMV	Constitutive	SV40	amp
pRK5	CMV/SP6	Constitutive	SV40	amp
pcDM8/6XL	CMV/SP6	Constitutive	SV40	*SupF (amp/tet)

Table 2.1 *Summary of the plasmid expression vectors used in this study.*
Abbreviations: amp, ampicillin; tet, tetracycline; CMV, cytomegalovirus; poly-A, polyadenylation; SV40, Simian virus.
*SupF: Plasmids expressing the SupF gene require growth in a bacterial strain, such as MC1061, that contains the P3 episome. The P3 episome contains amp and tet selectable markers containing amber mutations which are corrected by SupF.

2.2 CONSTRUCTION OF CHIMERIC cDNA

Chimeric subunit cDNAs between human $5HT_{3A}$ ($h5HT_{3A}$) and mouse $5HT_{3A}$ ($m5HT_{3A}$) were constructed (Figure 2.1). The long splice variant of the $m5HT_{3A}$ ($m5HT_{3A(L)}$) was used. A chimeric subunit cDNA was constructed containing the extracellular N-terminal domain of the $h5HT_{3A}$ subunit fused to the transmembrane and intracellular domains of the $m5HT_{3A}R$ subunit, termed human/mouse (h/m) $5HT_{3A}$ chimera. A second, similar chimeric subunit cDNA contained the extracellular N-terminal domain of the $m5HT_{3A}R$ subunit fused to the transmembrane and intracellular domains of the $h5HT_{3A}R$ subunit, termed mouse/human (m/h) $5HT_{3A}$ chimera.

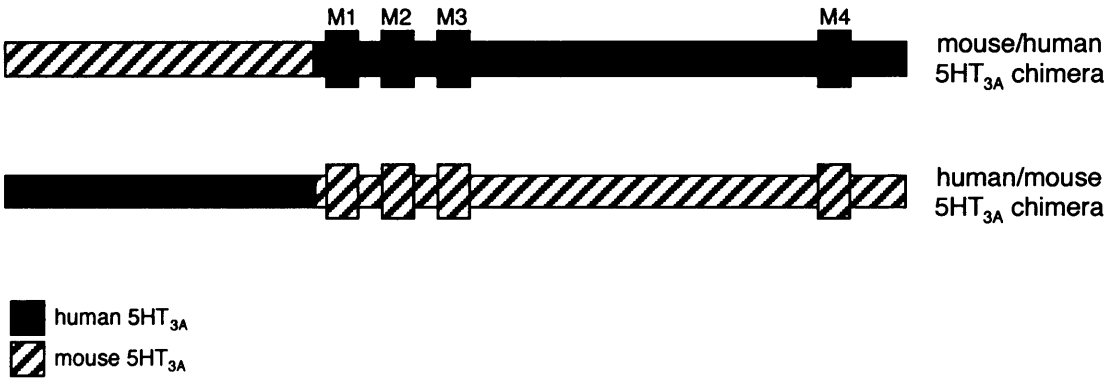

Figure 2.1 *Chimeric $5HT_{3A}$ subunits.* The mouse/human $5HT_{3A}$ chimera consisted of the extracellular N-terminal domain of the mouse $5HT_{3A}$ subunit fused to the transmembrane and intracellular domains of the human $5HT_{3A}$ subunit. The human/mouse $5HT_{3A}$ chimera consisted of the extracellular domain of the human $5HT_{3A}$ subunit fused to the transmembrane and intracellular domains of the mouse $5HT_{3A}$ subunit. (M1-M4=transmembrane domains)

The $m/h5HT_{3A}$ chimera in the pRK5 expression vector was constructed from $h5HT_{3A}$ in pcDNA3.1 and $m5HT_{3A}$ in pRK5 (Figure 2.2A). Mutations were introduced by site directed mutagenesis in $h5HT_{3A}$ to create a *Bam*HI site to enable subcloning using

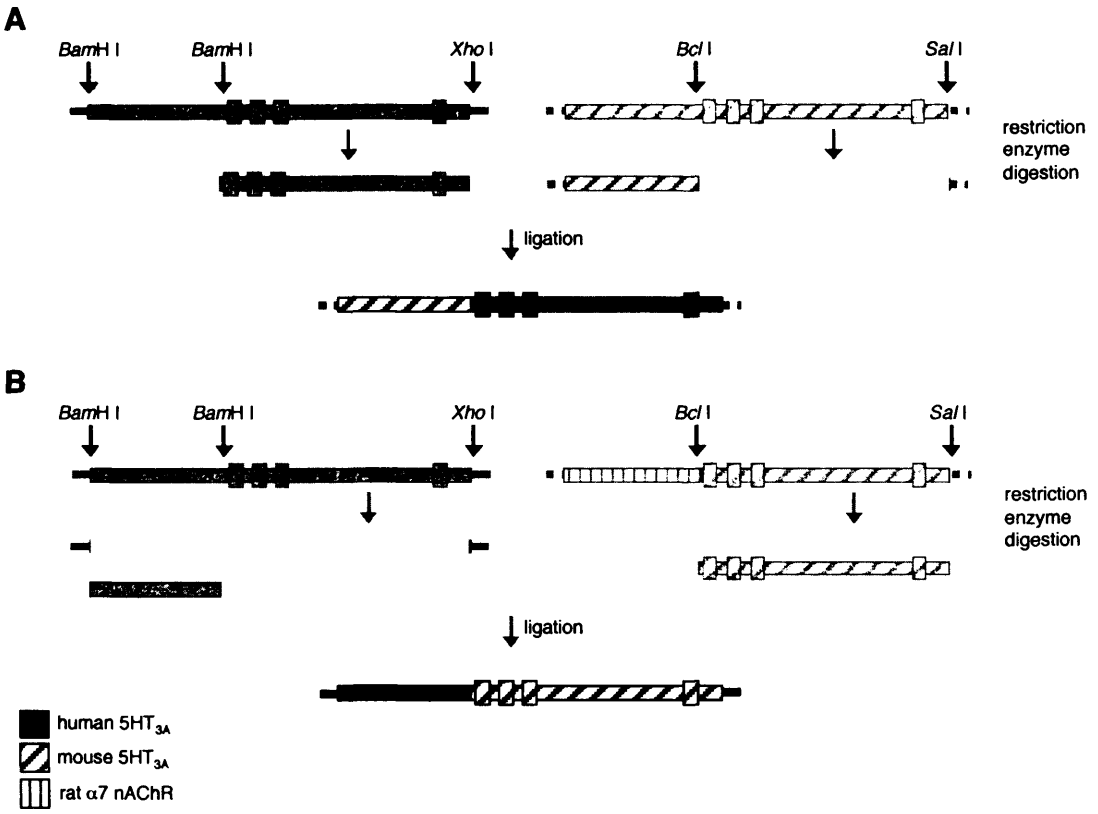

Figure 2.2 *Construction of chimeric $5HT_{3A}$ subunits.* **A**, The mouse/human $5HT_{3A}$ chimera: Mutations were introduced by SDM to create a *Bam*HI site in the human subunit. The mutated subunit was digested with *Bam*HI and *Xho*I to excise the C-terminal portion. The mouse subunit was digested with *Bcl*I and *Sal*I to create a cloning cassette containing the N-terminal portion of the subunit. The human fragment and the mouse fragment and vector were ligated resulting in the m/h$5HT_{3A}$ chimera. **B**, The human/mouse $5HT_{3A}$ chimera: The mutated human subunit, containing a *Bam*HI site, was digested with *Bam*HI to excise the N-terminal portion. The mutated subunit was also digested with *Bam*HI and *Xho*I together to create a cloning cassette. The rat $\alpha7^{(V201)}$/mouse $5HT_{3A}$ chimera was digested with *Bcl*I and *Sal*I to excise the C-terminal mouse $5HT_{3A}$ portion. The resulting two fragments and vector cassette were ligated to produce the chimeric subunit.

the complementary *Bcl*I site present at the equivalent position in the m5HT$_{3A}$R subunit. Mouse 5HT$_{3A}$ in pRK5 was digested with *Bcl*I and *Sal*I to remove the C-terminal domain of m5HT$_{3A}$ (amino acids 1–246). Human 5HT$_{3A}$ in pcDNA3.1 was digested with *Bam*HI and *Xho*I to excise the C-terminal domain which was then cloned into the *Bcl*I/*Sal*I digested mouse 5HT$_{3A}$ in pRK5 generating the m/h5HT$_{3A}$ chimera in pRK5. Digestion with *Bcl*I and *Bam*HI and also *Sal*I and *Xho*I produces fragments with ends compatible for ligation, but ligation does not result in regeneration of the restriction enzyme sites.

The h/m5HT$_{3A}$ chimera in pcDNA3.1 was constructed from rat $\alpha7^{(V201)}$/mouse 5HT$_{3A}$ chimera in pRK5 and human 5HT$_{3A}$ in pcDNA3.1 with a *Bam*HI site introduced by SDM, as described above (Figure 2.2B). The wild-type mouse 5HT$_{3A}$ was not used as the presence of an additional *Bcl*I site in the N-terminal domain was discovered. The rat $\alpha7^{(V201)}$/mouse 5HT$_{3A}$ chimera in pZeoSV was constructed by Dr Sandra Cooper (Cooper and Millar, 1997) and subcloned into pRK5 in this laboratory by Dr Elizabeth Baker. Human 5HT$_{3A}$ was digested with *Bam*HI to generate a fragment containing the N-terminal domain of the subunit (amino acids 1-238). Human 5HT$_{3A}$ was also digested with *Bam*HI and *Xho*I to excise the h5HT$_{3A}$ cDNA, and generate an empty vector suitable for subcloning. The rat $\alpha7^{(V201)}$/mouse 5HT$_{3A}$ chimera was digested with *Bcl*I and *Sal*I to excise the C-terminal domain of the m5HT$_{3A}$ fragment. The two fragments and vector were ligated together and the h/m5HT$_{3A}$ chimera in pcDNA3.1 chimera generated.

The fidelity of the chimeric constructs was verified by sequencing. The h/m5HT$_{3A}$ chimera was found to be incapable of ligand binding. The reason for this lack of binding was identified and resolved (see Chapter 4, Section 4.3.2).

2.3 CLONING OF HUMAN RIC3 HOMOLOGUE

Human *ric3* (*hric3*) was cloned from a human neuroblastoma cell line (SH-SY5Y) cDNA library by PCR. Oligonucleotide primers were designed to the 5' and 3' untranslated regions of the *hric3* sequence identified in the human genome sequence

database. The primers incorporated restriction enzyme sites to facilitate sub-cloning. The primers are detailed below.

OL650 (+): 5' CGTCTGCACCTGCGAATTCCGTGAGCAGTC**ATG**G 3'
OL651 (-): 5' CTTGGGACTTGAGTAATGGATCCTTCAGACTGGC 3'

(+) = forward primer; (-) = reverse primer; **ATG** = start codon
GAATTC = *Eco*RI site; GGATCC = *Bam*HI site

PCR was performed and resulted in the amplification of a fragment of about 1200 base pairs (bp) which corresponded to the size of *hric3*. A second fragment of about 600 bp was also amplified which corresponded to the size of a partial *hric3* clone which had previously been identified in this laboratory. PCR fragments were treated with *Taq* polymerase, cloned into the TA cloning vector (pCR2.1; Invitrogen) and sequenced. Correct *hric3* PCR clones were sub-cloned into the expression vectors pRK5 and pcDNA3.

2.4 CONSTRUCTION OF FLAG-EPITOPE TAGGED RIC3 PROTEINS

To facilitate biochemical analyses, CeRIC3 and hRIC3 were modified by the introduction of a FLAG epitope tag. The FLAG tag is a short hydrophilic peptide (DYKDDDDK) (Hopp *et al.*, 1988). The topology of the proteins was assumed to be as predicted by Halevi *et al.*, 2002 and Halevi *et al.*, 2003 (Figure 2.3). The FLAG tag was introduced in the C-terminal domain of CeRIC3, CeRIC3^{FLAG-A} (Figure 2.4). The FLAG tag was introduced at three different positions in hRIC3: in the C-terminal region (hRIC3^{FLAG-A}), in between the two transmembrane domains (hRIC3^{FLAG-B}) and close to the N-terminal (hRIC3^{FLAG-C}) (Figure 2.4). The fidelity of all constructs was confirmed by nucleotide sequencing.

2.4.1 Introduction of the FLAG tag to the C-terminal region of CeRIC3

The Quikchange^{TM} Site-Directed Mutagenesis Kit (Stratagene) (see Section 2.6) was used to introduce mutations creating a unique *Bst*EII site at the position where the tag was to be inserted (after amino acid 373 (R)).

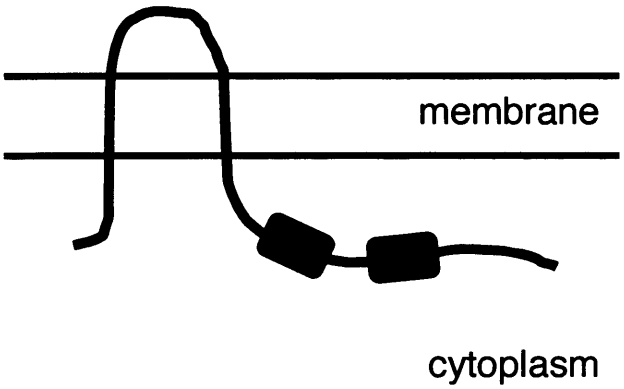

Figure 2.3 *Structure and topology of the RIC3 proteins* (predicted by Halevi *et al.* 2002; Halevi *et al.*, 2003). Structure predictions suggested that the RIC3 proteins have two hydrophobic, putative transmembrane domains separated by a proline-rich domain, followed by at least one coiled-coil region (CC), with their N- and C-termini being cytoplasmic.

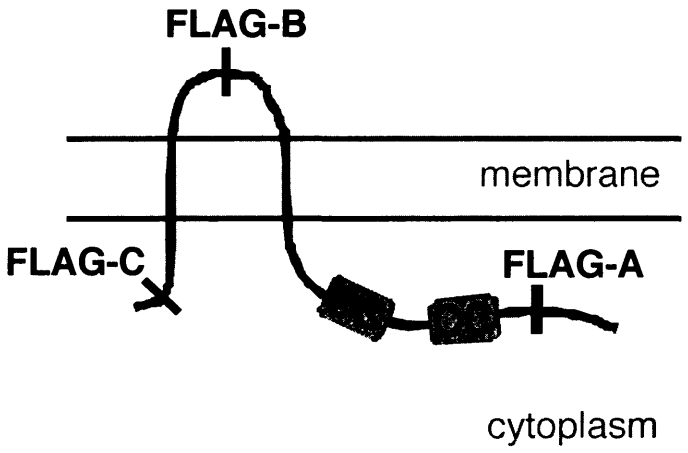

Figure 2.4 *Positions of the FLAG tags introduced into the RIC3 proteins* (based on the topology predicted by Halevi *et al.*, 2002; Halevi *et al.*, 2003). The FLAG epitope tag was introduced into the C-terminal regions of CeRIC3 and hRIC3 (FLAG-A). The FLAG tag was also introduced in hRIC3 between the two predicted transmembrane domains (FLAG-B) and close to the N-terminal (FLAG-C).

CeRIC3 sequence (bp 1111-1130):

5' -CGAAGGCGGAGACCTAAAAA- 3'

3' -GCTTCCGCCTCTGGATTTTT- 5'

R R R R P K K

Primers to introduce *Bst*EII site:

OL654 (+): 5' GATAAAAATGTGCGAAGGCGGTTACCTAAAAAGACTTGA 3'

OL655 (-): 5' TCAAGTCTTTTTAGGTAACCGCCTTCGCACATTTTTATC 3'

(+) = forward primer; (-) = reverse primer; *Bst*EII: GGTTACC. Amino acids to be mutated are shown in bold.

The FLAG tag was introduced into CeRIC3 at the *Bst*EII site by ligation of oligonucleotide primers which incorporated the FLAG tag and possessed complementary ends for subcloning into the *Bst*EII site.

OL545 (+): 5' GTTACCTGACTACAAGGACGACGATGACAAGTG 3'

OL546 (-): 5' GTAACCACTTGTCATCGTCGTCCTTGTAGTCAG 3'

FLAG tag; part of BstEII site

The primers were mixed at an equimolar ratio and annealed by heating to 80°C for 20 minutes in a hot block and allowed to cool slowly. The annealed primers were ligated with *Bst*EII digested CeRIC3 DNA to produce the tagged construct, CeRIC3^{FLAG-A}.

2.4.2 Introduction of the FLAG tag to the C-terminal region of hRIC3

Oligonucleotides incorporating the FLAG tag with ends complementary to the *Bst*EII site (OL545 and OL546; see Section 2.4.1) were used to insert the FLAG tag at an endogenous *Bst*EII site (bp 703-709) in the C-terminal region of hRIC3. The FLAG tag was introduced into hRIC3 after amino acid 223 (G), as described in Section 2.4.1 for CeRIC3, generating hRIC3^{FLAG-A}.

2.4.3 Introduction of the FLAG tag to the region between the two transmembrane domains of hRIC3

A FLAG epitope tag was introduced in the putative loop region between the two predicted transmembrane domains of hRIC3, after amino acid 58 (S), by site-directed mutagenesis. Complementary oligonucleotide primers incorporating the coding sequence for the FLAG tag were used:

OL700 (+):

5' CAGGCACACTCAGACTACAAGGACGACGATGACAAGGATGGCCAGACT 3'

OL701 (-):

5' AGTCTGGCCATCCTTGTCATCGTCGTCCTTGTAGTCTGAGTGTGCCTG 3'

(+) and (-) indicate a forward and reverse oligonucleotide primer, respectively; FLAG tag

2.4.4 Introduction of the FLAG tag to the N-terminal region of hRIC3

A FLAG epitope tag was inserted in the N-terminal region of hRIC3 after amino acid 2 (A) by site-directed mutagenesis using complementary oligonucleotide primers incorporating the coding sequence for the FLAG tag:

OL725 (+):

5' GCAGTCATGGCGGACTACAAGGACGACGATGACAAGTACTCCACAGTG 3'

OL726 (-):

5' CACTGTGGAGTACTTGTCATCGTCGTCCTTGTAGTCCGCCATGACTGC 3'

(+) and (-) indicate a forward and reverse oligonucleotide primer, respectively; FLAG tag

2.5 NUCLEOTIDE SEQUENCING

Fluorescence-based cycle sequencing was carried out using ABI Prism® BigDye™ Terminator Cycle Sequencing Ready Reaction Kit versions 1.0 and 1.1 (ABI Applied Biosystems, Applera UK) according to the manufacturer's instructions. Briefly, 200-

500 ng template DNA and 3.2 pmol specific primer were mixed with 8 µl Terminator Ready Reaction Mix (containing dye-labelled ddNTP terminators, unlabelled dNTPs, AmpliTaq DNA polymerase, $MgCl_2$ and buffer) in a reaction volume of 20 µl. Thermocycling of the reactions involved denaturation at 96°C for 30 seconds, annealing at 50°C for 15 seconds and extension at 60°C for 4 minutes for 25 cycles. Reactions were ethanol/sodium acetate precipitated by addition of 2 µl sodium acetate, pH 5.2 and 50 µl 99% ethanol per reaction, incubation on ice for 15 minutes and centrifugation at 13,000 rpm for 15 minutes. Pellets were washed with 500 µl 70% ethanol, air-dried and resuspended in 10 µl formamide. Samples were sequenced using an ABI Prism® 3100-*Avant* Genetic Analyzer (ABI Applied Biosystems). Reactions were run on a 50 cm capillary array using POP 6 polymer (ABI Applied Biosystems). Data was extracted using 3100-*Avant* Data Collection Software Version 1.0 (ABI Applied Biosystems).

2.6 SITE-DIRECTED MUTAGENESIS

The QuikChange™ Site-Directed Mutagenesis Kit (Stratagene) was used to create mutations in cDNA sequences according to the manufacturers instructions. Two complimentary oligonucleotide primers containing the desired mutation, flanked by unmodified nucleotide sequence were designed. Primers were between 25 and 45 bases in length, with the desired mutation in the middle, had a melting temperature (T_m) greater than or equal to 78°C, a minimum GC content of 40 % and terminated in one or more G or C bases. Primers were purified by polyacrylamide gel electrophoresis.

Setting up the SDM PCR reactions

Reactions were carried out in a 50 µl volume containing: 1X reaction buffer, 50 ng template DNA, 125 ng of each forward and reverse oligonucleotide primers, 1 µl dNTP mix and 1 µl *Pfu*Turbo DNA polymerase (2.5 U/µl).

Thermocycling the reactions

Reactions were heated to 95°C for 30 seconds, then 12-18 (dependent on type of mutation desired) thermocycling steps were performed that included denaturation at

95°C for 30 seconds, annealing at 55°C for 1 minute and extension at 68°C for 2 minutes/kb of plasmid length. Reactions were cooled on ice.

Digestion of the products

Reactions were digested with 1 µl *Dpn*I (10 U/µl) at 37°C for one hour.

Transformation into XL1-Blue supercompetent cells

Digested DNA (1 µl) was mixed with 50 µl XL1-blue supercompetent cells in a pre-chilled Falcon 2059 polypropylene tube and incubated on ice for 30 minutes. Transformation was carried out via heat shock at 42°C for 45 seconds, followed by incubation in 500 µl NZY^+ broth (10 g/l NZ amine (casein hydrosylate), 5 g/l yeast extract, 5 g/l NaCl, pH 7.5 with NaOH, 12.5 ml/l 1M $MgCl_2$ and 12.5 ml/l $MgSO_4$ and 10 ml/l of 2M glucose) for one hour at 37°C with shaking at 225 rpm. Transformation mix (250 µl) was plated onto LB agar plates containing 50 µg/ml ampicillin, prepared with 20 µl 10% (w/v) 5-bromo-4-chloro-3-indolyl-β-D-galactopyranoside (X-Gal) and 20 µl 100 mM isopropyl-1-thio-β-D-galactopyranoside (IPTG) and incubated at 37°C for at least 16 hours.

2.7 CELL CULTURE AND TRANSFECTION

2.7.1 Cell lines

The tsA201 cell line was obtained from Dr William Green, University of Chicago, IL, USA. The tsA201 cell line is a transformed human embryonic kidney HEK293 cell line which stably expresses an SV40 temperature-sensitive T antigen. HEK293 cells were obtained from Eli Lilly. HEK293 cell lines stably expressing either the mouse $5HT_{3A(S)}$ or human $5HT_{3A}$ receptor subunit were a gift to Eli Lilly from Dr Sarah Lummis, University of Cambridge.

2.7.2 Cell culture

HEK293 and tsA201 cells were cultured in Dulbecco's modified Eagle's medium (DMEM) with Glutamax-1™ , supplemented with 10% heat inactivated fetal calf

serum, 100 units/ml penicillin and 100 μg/ml streptomycin and maintained in a humidified incubator containing 5 % CO_2 at 37°C.

2.7.3 Transient transfection

HEK293 and tsA201 cells were transiently transfected using Effectene™ Transfection Reagent (Qiagen) according to the manufacturer's instructions. Effectene is a non-liposomal lipid formulation which is used in conjunction with a DNA-condensing enhancer solution in an optimised buffer. Cells were trypsinised and re-plated 6 hours before transfection to reach approximately 70% confluency. For transfection of a 10 cm dish, 0.6 μg DNA was added to a sterile microfuge tube and 120 μl Buffer EC, added. Enhancer solution (4.8 μl), which condenses the DNA, was added and incubated for 5 minutes followed by 13 μl Effectene, which coats the condensed DNA with cationic lipids. After 10 minutes incubation, 600 μl growth medium was added and the mixture added dropwise to cells in 3 ml medium. After approximately 17 hours, 6 ml growth medium was added. For cells cultured on 13 and 19 mm coverslips, 0.05 and 1 μg DNA, respectively, were transfected. The DNA:Enhancer:Effectene ratios were maintained as above. Cells were used 40-46 hours post-transfection. All transfections were performed using Effectene unless otherwise stated.

HEK293 cells were transiently transfected at Eli Lilly with FuGENE 6 transfection reagent according to the manufacturer's instructions. One day before transfection, cells were plated at a density to yield 60-80% confluency on the day of transfection. FuGENE was added to an aliquot of serum-free medium and incubated for 5 minutes. This transfection mix was added to DNA aliquots, mixed and incubated at room temperature for a further 15 minutes before being added dropwise to the cells. For FLIPR experiments the cells were incubated at 37°C for 48 hours and then replated on to poly-L-lysine pre-coated black-walled 96-well plates.

2.8 RADIOLIGAND BINDING

2.8.1 Binding studies using [^{3}H]-GR65630

For binding studies with [^{3}H]-GR65630, a $5HT_3R$-specific radioligand, on cell membrane preparations, transfected cells on 10 cm dishes were washed with phosphate-buffered saline (PBS), then resuspended and assayed in 10 mM potassium phosphate buffer (pH 7.2) containing the protease inhibitors leupeptin and aprotinin (2 μg/ml) and pepstatin (1 μg/ml). Cells were incubated with radioligand (12.5 nM [^{3}H]-GR65630) plus 100 μl of 10 % BSA in a total volume of 400 μl for 2 hours at 4°C. Non-specific binding was determined by addition of 12.5 mM 5-HT. Radioligand binding was assayed by filtration onto 0.5 % polyethylenimine presoaked GF/B glass fibre filters (Whatman) followed by rapid washing with cold 10 mM phosphate buffer using a Brandel cell harvester (Model M-36, Semaat, UK). Radioactivity was measured by scintillation counting.

2.8.2 Binding studies using [^{125}I]-α-bungarotoxin

To study cell-surface α7 receptors, intact cells were incubated with 10 nM [^{125}I]-α-bungarotoxin. Transfected cells were washed twice with PBS and gently resuspended in Hank's Buffered Saline Solution (HBSS) containing 1 % bovine serum albumin (HBSS/BSA). Cells were incubated with radioligand, in HBSS/BSA, for 2 hours at room temperature. Non-specific binding was determined by addition of 1 mM carbachol and 1 mM nicotine in HBSS/BSA. Samples were harvested as above using GF/A glass fibre filters. Filters were washed 6 times with PBS and assayed in a Wallac 1261 gamma-counter. To study 'total' receptors, using membrane preparations, cells were resuspended and harvested in 10 mM potassium phosphate buffer.

2.8.3 Determination of protein concentration

The protein concentration of cell membrane preparations was determined using a BioRad *DC* protein assay kit according to the manufacturer's instructions. Briefly,

20 µl of cell membrane preparation or BSA standard sample were added to a semi-microcuvette and mixed with 100 µl Reagent A (alkaline copper tartarate solution). Reagent B (800 µl; a dilute folin reagent) was added, mixed and incubated at room temperature for 15 minutes. A colour change is observed following reduction of the folin reagent by the copper-treated protein. Protein concentration was determined by spectrophotometric measurement at 750 nm and comparison against a standard curve constructed using BSA at concentrations of 0.2, 0.4, 0.6, 0.8, 1.0, 1.2 and 1.5 mg/ml.

2.9 ANTIBODIES

Antibody	Species Immunised	Specificity	Source
mAbHA-7 (anti-HA)	mouse	HA peptide*	Sigma
9E10 (anti-myc)	mouse	myc peptide*[2]	mAb, purified from myc1-9E10 hybridoma cell line (ECACC 85102202)
anti-FLAG	mouse	FLAG peptide*[3]	Sigma
pAb120	rabbit	extracellular region of $5HT_{3A}$	Dr S. Lummis*[4] Spier *et al.*, 1999
pAb$5HT_3$	rabbit	intracellular loop region of $5HT_{3A}$	Dr R. McKernan*[5] Turton *et al.*, 1993
mAb319	rat	intracellular loop region of α7	Sigma Schoepfer *et al.*, 1990
mAbOAR1a mAbOAR11b	mouse	extracellular conformational epitopes (α7)	Dr H. Betz Betz *et al.*, 1984
Goat α-mouse IgG peroxidase	mouse		Pierce
Goat α-rabbit IgG peroxidase	rabbit		Pierce

Table 2.2 *Summary of antibodies used in this study*

* HA peptide: 9 amino acid synthetic peptide (YPYDVPDYA) corresponding to residues 98-106 of the human influenza virus haemagglutinin (Kolodziej and Young, 1991).

*[2] Myc peptide: 10 amino acid synthetic peptide (EQKLISEEDL) corresponding to residues 408-432 of the human c-myc protein.

*[3] FLAG peptide: (DYKDDDDK) (Hopp *et al.*, 1988).

*[4]Dr S. Lummis (University of Cambridge).

*[5]Dr R. McKernan (Merck Sharp and Dohme Research Laboratories, Harlow).

2.10 METABOLIC LABELLING AND IMMUNOPRECIPITATION

Cells (tsA201) grown on 10 cm dishes were transiently transfected with receptor subunit cDNA overnight, washed and incubated for 20 minutes in L-methionine (Met) and L-cysteine (Cys) free medium to starve cells of methionine and cysteine. Cells were labelled with 150 μCi [^{35}S]-Pro-mix (mixture of [^{35}S]-Met and [^{35}S]-Cys), in 4 ml Met/Cys-free medium for 3 hours at 37°C. The label was 'chased' by addition of 6 ml DMEM containing Met and Cys for 2 hours at 37°C. Cells were washed twice and harvested into 1 ml ice-cold PBS. Cells were pelleted in a benchtop centrifuge at 6000 rpm for 5 minutes at 4°C and resuspended in 500 μl ice-cold low salt lysis buffer (150 mM NaCl, 50 mM Tris/Cl, pH 8.0, 5 mM EDTA, 1 % Triton X-100) containing protease inhibitors (0.2 mM phenylmethylsulphonyl fluoride (PMSF), 2 mM *N*-ethylmaleimide (NEM) and 2 μg/ml each of pepstatin, leupeptin, aprotinin). Solubilised samples were pre-cleared by incubation with 40 μl Protein G-sepharose beads, pre-equilibrated in low salt lysis buffer containing protease inhibitors, and were rotated overnight at 4°C. Protein G-sepharose beads and non-solubilised material was pelleted by centrifugation at 13,000 rpm for 30 minutes at 4°C in a benchtop centrifuge. The supernatant was transferred to a fresh tube and incubated with an appropriate antibody for 2-4 hours, rotating at 4°C. The antibody-receptor complexes were immunoprecipitated by incubation with 20 μl of protein G-sepharose beads for 2-3 hours, rotating at 4°C. Samples were centrifuged at 13,000 rpm for 5 minutes pelleting beads carrying antibody-receptor complexes. The beads were washed in 750 μl high salt (500 mM NaCl) lysis buffer, followed by

medium (300 mM NaCl) and low salt lysis buffer washes. Beads were resuspended in 20 µl sodium dodecyl sulphate (SDS)-loading dye (50 mM Tris/Cl pH 6.8, 200 mM dithiothreitol (DTT), 2% SDS, 0.2 % bromophenol blue, 10 % glycerol) and centrifuged at 13,000 rpm for 2 minutes. Supernatants were loaded and separated on a 7.5% SDS-polyacrylamide gel. The gel was fixed for 30 minutes in 30% methanol, 10% glacial acetic acid and incubated in Amplify™ for 30 minutes. The gel was dried and exposed to Kodak X-OMAT photographic film at –80°C in a cassette containing intensifying screens.

2.11 ENZYME-LINKED ANTIBODY BINDING ASSAY

2.11.1 Assaying cell-surface receptors

Cells were plated onto glass coverslips coated with poly-L-lysine (10 µg/ml) and collagen, and transiently transfected. Cells were washed with HBSS supplemented with 25 µM $MgCl_2$ and 25 µM $CaCl_2$ ($HBSS^{++}$) and non-specific binding blocked by incubation for 15 minutes with $HBSS^{++}$ containing 2 % BSA and 25 mM lysine (BLOCK). Cells were incubated with primary antibody in BLOCK with 5 % fetal calf serum added in a humidified chamber for 1 hour. Cells were washed 5 times in HBSS and fixed for 15 minutes using 3 % paraformaldehyde. Cells were incubated with a secondary antibody conjugated to horse-radish peroxidase (HRP) in BLOCK plus 5 % fetal calf serum in a humidified chamber for 1 hour. Cells were washed 5 times followed by incubation in 750 µl of a liquid HRP substrate, 3,3',5,5'-tetramethylbenzidine (TMB) to quantify labelled receptors. The supernatant was removed to a cuvette and colour change measured spectrophotometrically at 655 nm.

2.11.2 Assaying permeabilised cells

The assay described above was modified to obtain a measure of total receptor expression. Cells were washed with $HBSS^{++}$, fixed and then permeabilised in $HBSS^{++}$ containing 0.1 % Triton X-100 and the assay carried out essentially as for

cell-surface antibody binding. All solutions contained in addition 0.1 % Triton X-100 including the first two wash steps.

2.12 INTRACELLULAR CALCIUM MEASUREMENT BY FLIPR

Transfected cells were replated onto black-walled 96-well plates (Marathon Laboratories, London) coated with poly-L-lysine, approximately 18-20 hours post transfection. Approximately 24 hours later cell medium was removed and the cells incubated in 50-100 µl of 1 µM Fluo-4 acetoxymethyl ester in HBSS with 0.02 % Pluronic® F-127 for 30-60 minutes at room temperature. Cells were rinsed 1-2 times, 140-160 µl of HBSS added and the cells assayed using the Fluorometric Imaging Plate Reader system (FLIPR) (Molecular Devices, Winnersh) (Schroeder and Neagle, 1996). Cells were excited by light of 488 nm wavelength from a 4 W argon-ion laser and the emitted fluorescence passed through a 510 to 570 nm bandpass interference filter before detection with a cooled 'charge coupled device' (CCD) camera (Princeton Instruments). Drug dilutions were prepared in a separate 96-well plate. Parameters for drug addition to the cell plate were programmed on the computer and delivery was automated through a 96-tip head pipettor. Generally, drugs were added in 20-40 µl volumes and mixed twice by automatic pipetting. 5-HI was dissolved in DMSO and pre-applied manually or co-applied with 5-HT automatically. Data was exported and is presented as peak response (maximum fluorescence – minimum fluorescence) unless otherwise stated.

2.13 OOCYTE RECORDINGS

Adult female *Xenopus laevis* frogs were obtained from Blades Biological (Edenbridge) and housed at Oxford Brookes University (Dr I. Bermudez, Oxford). *Xenopus* oocytes were defolliculated manually after treatment with collagenase type I (4 mg/ml in Ca^{2+}-free Barth's solution) for 1.5 hours at room temperature. Plasmids containing receptor coding sequences suspended in distilled water were injected into the nuclei of stages V and VI oocytes within 4 hours of harvesting, using a Drummond variable volume microinjector (Broomall, PA, USA). After injection the oocytes were incubated at 18 °C in a modified Barth's solution

containing (mM) (NaCl, 88; KCl, 1; $NaHCO_3$, 2.4; $Ca(NO_3)_2$, 0.3; $CaCl_2$, 0.41; $MgSO_4$, 0.82; HEPES, 15, and 50 mg/l neomycin (pH 7.6 with NaOH; osmolarity 235 mosM)). Experiments were performed after 3-5 days of incubation.

Oocytes were placed in a recording chamber and continuously perfused with a saline solution containing (mM): NaCl, 115; KCl, 2.5; $CaCl_2$, 1.8, and HEPES, 10 (pH 7.3 with NaOH; osmolarity 235 mosM) at a rate of ~ 10 ml/min. The perfusion chamber had an internal diameter of 3 mm. On some occasions, $BaCl_2$ replaced $CaCl_2$ in the saline solution in order to minimise the possible contribution of secondary Ca^{2+}-activated Cl^- currents. Dilutions of agonists in external saline were prepared immediately before the experiments and applied by switching between control and drug-containing saline using an eight-channel bath perfusion system (BPS-8; ALA Scientific, Westbury, NY, USA). The eight channels were controlled by pinch valves. 5-HI was dissolved in DMSO, whilst 5-HT was dissolved in water.

Oocytes were impaled by two microelectrodes filled with 3 M KCl and voltage clamped using a Geneclamp 500B amplifier (Axon Instruments) according to the method described by Stühmer (1998). The external saline was clamped at ground potential by means of a virtual ground circuit using an Ag/AgCl reference electrode and a Pt/Ir current passing electrode. The membrane potential was held at -60 mV. Membrane currents were low-pass filtered (four-pole low pass Bessel filter, -3 dB at 0.3 kHz), digitised (1000 samples/s), and stored on disk for off-line computer analysis. All experiments were performed at room temperature.

Ion current amplitudes were measured and normalised to the amplitude of control responses induced by the near-maximum effective concentration of 100 μM 5-HT for $5HT_3$ receptors. Control responses were evoked alternately, in order to adjust for small variations in response amplitude over time. Concentration-response curves were fitted to the data obtained in separate experiments and mean ± standard deviation of estimated parameters were calculated for n oocytes. Agonist curves were fitted according to the equation: $I/I_{max}=1/\{1+(EC_{50}/[agonist])n_H\}$. Curve fitting was performed using GraphPad prism.

2.14 STATISTICAL ANALYSIS

Most of the data analysed statistically was in small samples ($n \leq 30$) and unpaired. Firstly, a frequency histogram was produced to assess the distribution of the data. If the data appeared approximately normal, a Students *t* test, a modification of the '*z*' test for small samples, was used. Before performing the *t* test, the Fisher's test (*F* test) was performed to ensure that the variances of the two samples were not grossly different from each other. The ratio between the two variances, with the smaller as the divisor, was calculated.

$$F = \text{variance}_1 / \text{variance}_2$$

The derived value was then looked up in tables of *F* with $[n_1-1]$ degrees of freedom on the horizontal axis and $[n_2-1]$ on the vertical axis, where n_1 is from the sample with the larger variance. If *F* was not significant then a Students *t* test was used as described below. If *F* was significant then a non-parametric test should be used.

t test:

$$t = |\text{mean}_1 - \text{mean}_2| / \sqrt{[(SE_1)^2 + (SE_2)^2]}$$

where SE = standard error. The *t* value was then looked up in a table of *t* values with the appropriate degrees of freedom (ν) to determine the significance of any difference between sample means.

$$\nu = (n_1-1) + (n_2-1)$$

2.15 MATERIALS

Chemicals and Reagents

All biochemicals were from BDH unless otherwise specified. Agarose, LMP-agarose and Lamda *Hin*dIII DNA markers were from Gibco. Polyacrylamide for SDS gels was from Amresco. Amplify™ and rainbow molecular weight markers were from Amersham. Carbamylcholine chloride (carbachol), 5-hydroxytryptamine, 5-hydroxyindole, EDTA, yeast extract and 3,3',5,5'-tetramethylbenzidine (TMB) were from Sigma. Protein G-sepharose beads were from Calbiochem. Liquid scintillation cocktail was from Beckman. All restriction enzymes and reaction buffers were from Promega unless otherwise specified. PCR markers, *Taq* polymerase, blue/orange loading dye and calf intestinal alkaline phosphatase (CIP) were also from Promega. *Pfu* was from Stratagene. KOD was from Novagen. T4 DNA ligase kit was from Roche. Effectene™ transfection reagent was from Qiagen. Fluo-4 acetoxymethyl ester and Pluronic® F-127 were from Molecular Probes.

Radioligand Studies

[^{125}I]-α-bungarotoxin, [^{35}S]-Pro-mix and [^{14}C]-methylated protein markers were from Amersham. [^{3}H]-GR65630 was from PerkinElmer. GF/A and GF/B glass fibre filters were from Whatman. Liquid scintillation cocktail and Fast Turn Cap Poly Q Vials were from Beckman. BioRad *DC* protein assay kit was from BioRad. Semi-microcuvettes were from Sarstedt.

Cell Culture

All tissue culture media and additives were obtained from Gibco unless otherwise specified. Fetal bovine serum was from Sigma. Effectene transfection reagent was from Qiagen. FuGENE 6 transfection reagent was from Roche.

E. coli, strain XL-1 blue, were from Stratagene. *E. coli*, strain MC1061/P3, were from Invitrogen.

Disposables

Tissue culture dishes (6 and 10 cm diameter) were from Corning. Tissue culture plates (96, 24 and 12 well) and tissue culture flasks (75 cm^2) were from Nunclon. Serological pipettes (10 and 25 ml) and Falcon tubes (15 ml) were from Sarstedt. Centrifuge tubes (50 ml) were from Nunc. Stericup filtration systems (0.22 μm) were from Millipore. Black-walled 96 well plates were from Marathon Laboratories.

RESULTS

CHAPTER 3

Identification of an endoplasmic reticulum retention signal in the 5-hydroxytryptamine type 3 receptor subunit, $5HT_{3B}$

3.1 Introduction

Two subunits of the 5-hydroxytryptamine type 3 receptor ($5HT_3R$) have been used in this study, $5HT_{3A}$ (Maricq *et al.*, 1991) and $5HT_{3B}$ (Davies *et al.*, 1999; Dubin *et al.*, 1999). The $5HT_{3A}$ subunit is capable of forming functional homomeric receptors in heterologous expression systems. In contrast, the $5HT_{3B}$ subunit is not able to form functional homomeric receptors. However, the $5HT_{3B}$ subunit appears to be able to co-assemble with $5HT_{3A}$ to generate heteromeric receptors (Davies *et al.*, 1999; Dubin *et al.*, 1999; Hanna *et al.*, 2000; Boyd *et al.*, 2002). When expressed alone in heterologous expression systems, such as the human embryonic kidney cell line (HEK293), the $5HT_{3B}$ subunit is retained within the endoplasmic reticulum (ER) (Boyd *et al.*, 2002). However, upon co-expression of $5HT_{3A}$ and $5HT_{3B}$, $5HT_{3B}$ is expressed on the cell surface in a functional heteromeric receptor complex (Boyd *et al.*, 2002).

The release of proteins from the ER is an important quality control checkpoint for their cell surface expression. Proteins may be held in the ER by chaperone proteins, such as Immunoglobulin binding protein (BiP) and calnexin (Haas and Wabl, 1983; Pelham, 1989; Helenius and Aebi, 2001; Schrag *et al.*, 2003), until they have folded and assembled correctly resulting in release. These chaperone proteins contain certain sequences/motifs which cause them to remain within the ER. They may interact with incompletely or incorrectly assembled proteins and prevent their export. Recently, a number of ER retention/retrieval motifs have been identified in cell surface expressed proteins. These motifs are thought to be exposed when the proteins are incompletely or incorrectly folded or assembled, thereby resulting in their retention within the ER. The aim of this project was to investigate the mechanisms involved in the ER retention of the $5HT_{3B}$ subunit.

3.2 Epitope tagged $5HT_{3A}$ and $5HT_{3B}$ constructs

Human $5HT_3$ subunit cDNAs tagged with the myc (EQKLISEEDL) or HA (YPYDVPDYA) epitopes were provided by Dr Christopher Connolly, University of Dundee (Boyd *et al.*, 2002). These subunit constructs contain epitope tags inserted between amino acids 5 and 6 of the mature polypeptides and have been shown to be

functionally silent (Boyd *et al.*, 2002). All further $5HT_3R$ cDNAs described in this chapter were constructed and provided by Dr C. Connolly (see Chapter 2 (Materials and Methods), section 2.1.9 for more detail).

3.3 Expression and co-expression of $5HT_{3A}$ and $5HT_{3B}$ in mammalian cells

3.3.1 Radioligand binding assay

To study the heterologous expression of the $5HT_3R$ subunits in mammalian cells, human $5HT_{3A}$ and $5HT_{3B}$ subunit cDNAs were introduced into tsA201 cells, a subclone of the human embryonic kidney cell line, HEK293, by transient transfection. Radioligand binding was performed on cell membrane preparations using a saturating concentration of the $5HT_3R$ specific antagonist [^{3}H]-GR65630. Specific binding was determined by subtracting 'non-specific' binding, performed in the presence of 12.5 mM 5-HT, from 'total' binding, performed in the absence of 5-HT. Specific binding was observed for cells expressing $5HT_{3A}$ (Figure 3.1). However, cells expressing $5HT_{3B}$ did not show any specific binding (Figure 3.1). Co-expression of $5HT_{3B}$ with $5HT_{3A}$ appeared to decrease the level of [^{3}H]-GR65630 binding (Figure 3.1).

3.3.2 Functional studies using a FLIPR

The ability of the $5HT_3$ subunits to generate functional $5HT_3Rs$ in tsA201 cells was examined. Cells were transiently transfected and assayed using a Fluorometric Imaging Plate Reader system (FLIPR). Cells, grown on 96-well plates, were loaded with the Ca^{2+}-sensitive dye, fluo-4, and responses to the $5HT_3R$ agonist chlorophenylbiguanide (CPBG; 1 μM) recorded. Ionomycin was added approximately two minutes after agonist addition to give a measure of total intracellular calcium. In cells expressing $5HT_{3A}$ alone responses to CPBG, recorded as elevations in intracellular calcium, were observed (Figure 3.2A). Untransfected cells gave no response to CPBG. Cells expressing $5HT_{3B}$ alone gave no response to CPBG (Figure 3.2B).

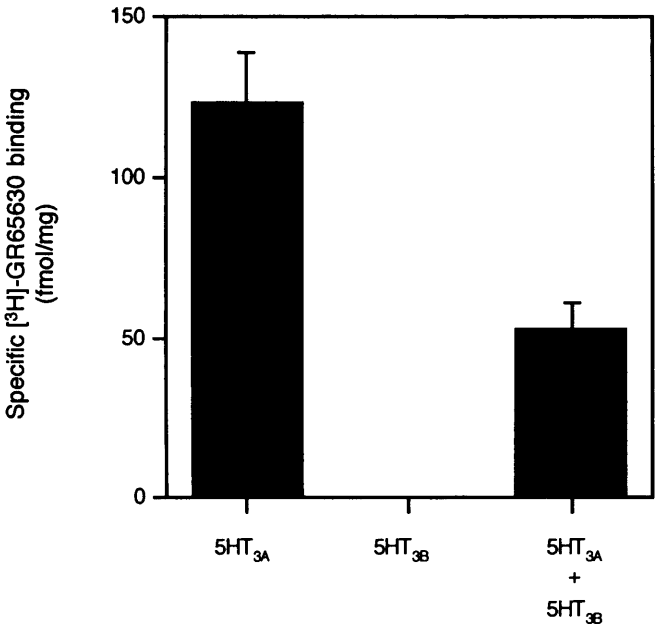

Figure 3.1 *Specific [^{3}H]-GR65630 binding to cell membrane preparations of tsA201 cells expressing 5HT$_3$R subunits.* Cells were transiently transfected with the 5HT$_{3A}$ or 5HT$_{3B}$ subunit alone and together, and binding performed using 12.5 nM [^{3}H]-GR65630. A high level of specific binding was observed in cells expressing 5HT$_{3A}$. No specific binding was observed in cells expressing 5HT$_{3B}$. Co-expression of 5HT$_{3B}$ with 5HT$_{3A}$ decreased the level of binding. Data are means, ± standard error, from at least 4 independent experiments performed in triplicate.

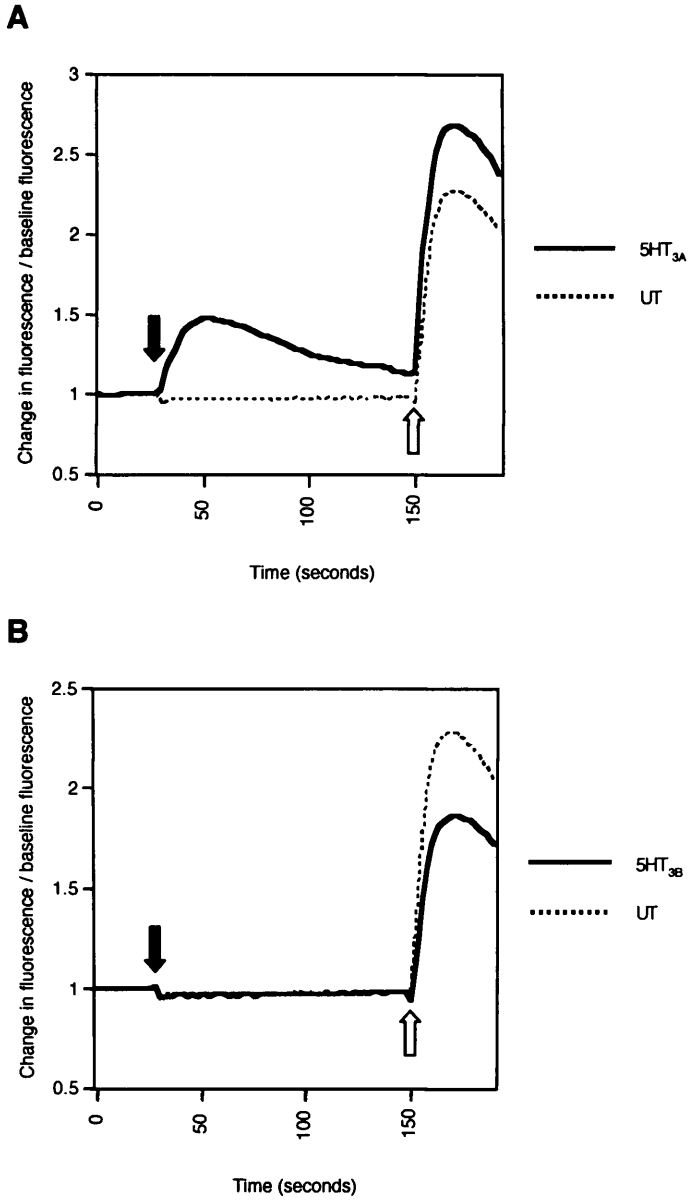

Figure 3.2 *Functional assay of $5HT_{3A}$ and $5HT_{3B}$ expressed in tsA201 cells using a FLIPR.* Cells transiently transfected with $5HT_{3A}$ (A) or $5HT_{3B}$ (B) and untransfected (UT) cells were assayed using a FLIPR. Cells were loaded with Fluo-4 and responses to 1 μM CPBG (filled arrow) recorded. Ionomycin was added (unfilled arrow) at the end of experiments to give a measure of total intracellular Ca^{2+}. Responses, recorded as elevations in intracellular Ca^{2+}, to CPBG were observed in cells expressing $5HT_{3A}$. Cells expressing $5HT_{3B}$ did not produce functional responses to CPBG. Traces are averages from 4 wells representative of more than 4 independent experiments.

3.3.3 Cell surface expression of homomeric and heteromeric $5HT_3R$

To study the subcellular distribution of the $5HT_3R$ subunits, intact and permeabilised tsA201 cells transiently transfected with tagged subunits were analysed using an enzyme-linked antibody binding assay (Section 2.11). The assay involves detection of the tagged subunit protein with a primary antibody to the epitope tag. The primary antibody is then detected by a secondary antibody conjugated to horseradish peroxidase (HRP). A liquid HRP substrate is added which is converted from colourless to a blue colour by HRP. Receptor expression is quantified by measuring the absorbance of the coloured product spectrophotometrically.

Cells expressing $5HT_{3A}$-myc or $5HT_{3B}$-myc and untransfected cells were labelled with the anti-myc antibody, 9E10. Clear evidence of the cell surface expression of $5HT_{3A}$-myc was observed (Figure 3.3A). In contrast, no cell surface expression of $5HT_{3B}$-myc could be detected, (Figure 3.3A). However, performing the assay on permeabilised cells revealed that the $5HT_{3B}$-myc protein was expressed, and at a level similar to that of $5HT_{3A}$-myc, (Figure 3.3A).

The effect of co-expressing $5HT_{3A}$ with $5HT_{3B}$ was examined. Cells were transfected with $5HT_{3B}$-HA alone or with $5HT_{3A}$-myc and labelled with mAbHA-7 (anti-HA). When expressed alone, $5HT_{3B}$-HA was not detected on the cell surface. However, upon co-expression with $5HT_{3A}$-myc, $5HT_{3B}$-HA was found to be expressed on the cell surface at a level similar to $5HT_{3A}$ alone (Figure 3.3B).

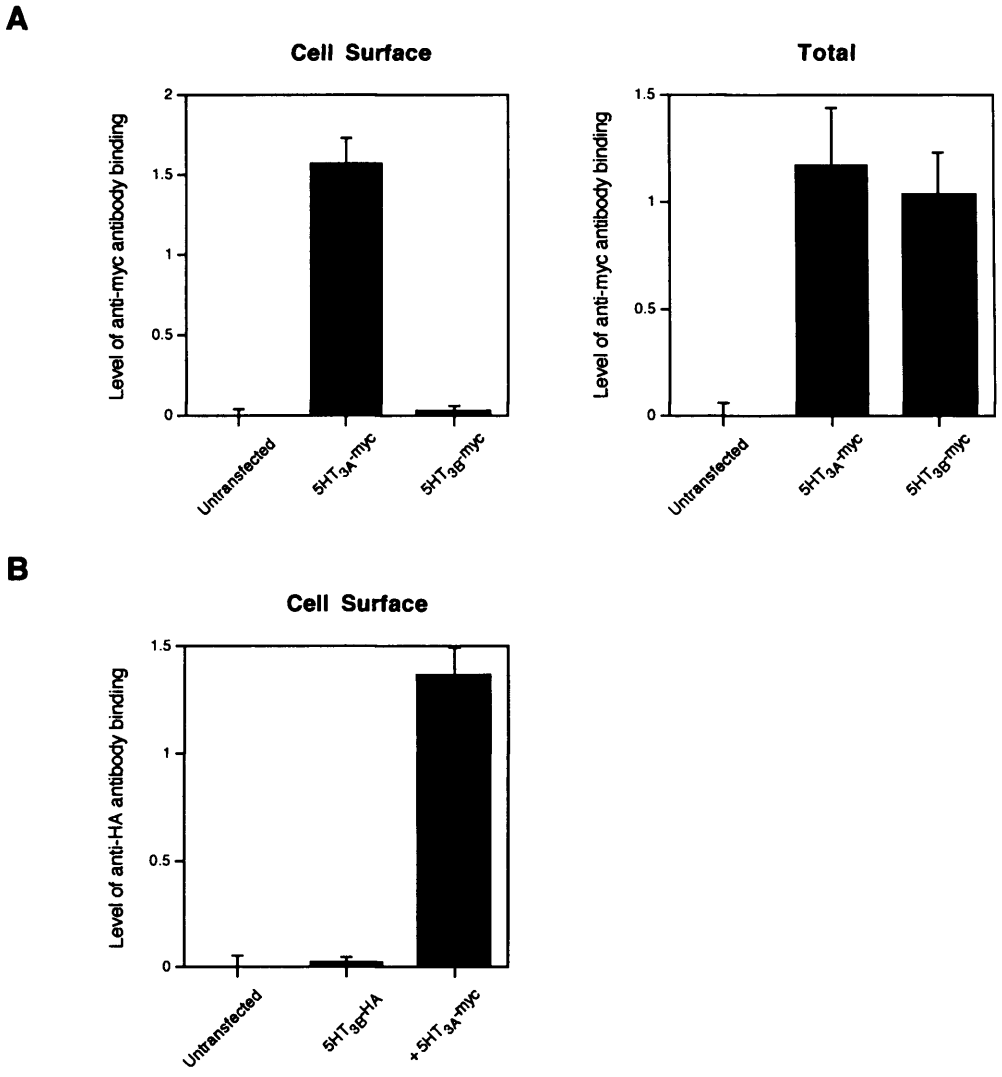

Figure 3.3 *Expression of 5HT$_3$R subunits in transfected tsA201 cells.* Cells grown on coverslips were transiently transfected with various tagged 5HT$_3$R subunits. **A**, Cells were labelled with 9E10 (anti-myc antibody) either as intact cell monolayers (Cell Surface) or after permeabilisation (Total). A high level of specific cell surface 9E10 binding was observed upon expression of 5HT$_{3A}$-myc. No cell surface 9E10 binding was observed upon expression of 5HT$_{3B}$-myc. Upon permeabilisation a high level of specific binding was observed for both 5HT$_{3A}$-myc and 5HT$_{3B}$-myc. **B**, Intact cell monolayers were labelled with mAbHA-7 (anti-HA). 5HT$_{3B}$-HA expressed alone was not detectable, however, upon co-expression with 5-HT$_{3A}$-myc a high level of surface expression was measured. Data is mean absorbance at 655 nm, ± standard error, from at least 4 independent experiments performed in triplicate. The background signal from untransfected cells has been subtracted.

3.4 Expression of truncated $5HT_{3B}$ subunits

To investigate the mechanisms involved in the retention of the $5HT_{3B}$ subunit and in an attempt to identify regions responsible, chimeric subunits were constructed using regions of $5HT_{3A}$ and $5HT_{3B}$ and were analysed using immunofluorescence by Dr C. Connolly (Boyd *et al.*, 2003). These results implicated the C-terminal of $5HT_{3B}$ in ER retention. To determine whether retention signals were present in $5HT_{3B}$ a number of truncated $5HT_{3B}$ subunits were constructed. The rationale for this approach was that progressive removal of C-terminal portions would eventually remove any retention signals present.

The cell surface expression of a number of the truncated $5HT_{3B}$ subunits was examined through the use of an enzyme-linked antibody binding assay. Cells were transfected with HA-tagged $5HT_{3A}$, $5HT_{3B}$, $5HT_{3B}$ truncated just after transmembrane domain 1 ($5HT_{3B}$(TM1)), $5HT_{3B}$ truncated at residue 267, in between M1 and M2, ($5HT_{3B}$(267)) or $5HT_{3B}$ truncated just after M2 ($5HT_{3B}$(TM2)). Intact cell monolayers and permeabilised cells were labelled with mAbHA-7 (anti-HA). Labelling of intact cells revealed the presence of $5HT_{3B}$(TM1) and also $5HT_{3B}$(267) on the cell surface. However $5HT_{3B}$(TM2) was not found to be expressed on the cell surface (Figure 3.4; Cell Surface). Labelling of permeabilised cells revealed similar total levels of expression for all constructs (Figure 3.4; Total). These results indicated a role for the region between M1 and M2 in the ER retention of the $5HT_{3B}$ subunit.

The amino acid sequences of $5HT_{3A}$ and $5HT_{3B}$ between M1 and M2 were aligned (Figure 3.5). Alignment of these sequences revealed that the subunits differ by only 3 residues in this region. $5HT_{3B}$ contains an RXR motif (RAR). The RXR motif has previously been reported to play a role in the ER retention of a number of other receptors (Zerangue *et al.*, 1999; Margeta-Mitrovic *et al.*, 2000; Scott *et al.*, 2001; Shikano and Li, 2003).

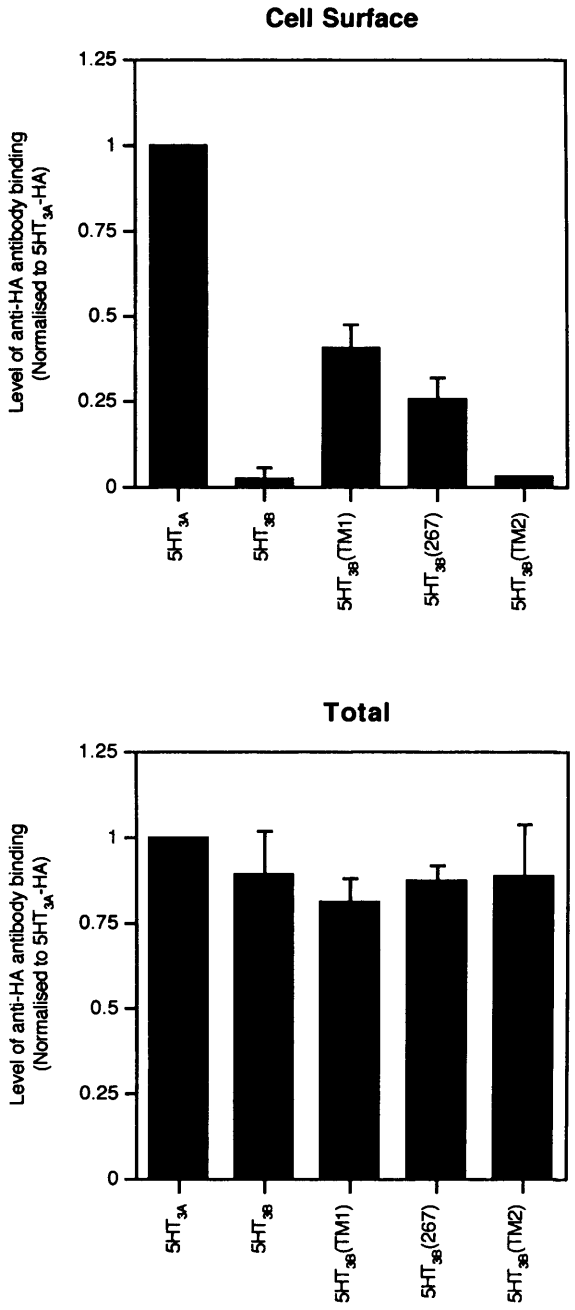

Figure 3.4 *Expression of truncated 5HT$_3$B subunits in transfected tsA201 cells.* Cells grown on coverslips were transiently transfected with HA-tagged 5HT$_3$R subunits. Cells were labelled with mAbHA-7 (anti-HA) either as intact cell monolayers (Cell Surface) or after permeabilisation (Total). Data is mean (normalised to level of antibody binding for 5HT$_{3A}$-HA), ± standard error, from at least 3 independent experiments performed in triplicate. The background signal from untransfected cells has been subtracted.

Figure 3.5 *Alignment of $5HT_{3A}$ and $5HT_{3B}$ between transmembrane domains 1 and 2.* Comparison of the homologous regions of $5HT_{3A}$ and $5HT_{3B}$ between transmembrane domains M1 and M2 revealed that the subunits differ by three residues. The residues in $5HT_{3B}$ incorporate the RAR motif.

3.5 Expression of $5HT_{3A}$(CRAR) and $5HT_{3B}$(SGER)

To investigate the effects of the RAR motif, a mutant $5HT_{3A}$ subunit containing CRAR, in place of SGER was generated (construct $5HT_{3A}$(CRAR)). The subcellular distribution of $5HT_{3A}$(CRAR)-HA was examined using an enzyme-linked antibody binding assay. Cells were transiently transfected with HA-tagged $5HT_{3A}$(CRAR) alone and co-transfected with $5HT_{3A}$-myc or $5HT_{3B}$-myc. Levels of mAbHA-7 binding were quantified for both intact and permeabilised cells. When expressed alone, $5HT_{3A}$(CRAR)-HA was not detected on the cell surface at a significant level (Figure 3.6). This finding provided evidence for the role of RAR as an ER retention signal. Co-expression of $5HT_{3A}$ with $5HT_{3A}$(CRAR)-HA resulted in cell surface expression of the subunit (Figure 3.6). This result indicated that the mutant subunit could fold and assemble correctly when co-expressed with $5HT_{3A}$, similar to the effect of co-expression of $5HT_{3A}$ with $5HT_{3B}$. Co-expression of $5HT_{3B}$ with $5HT_{3A}$(CRAR)-HA did not result in cell surface expression of the $5HT_{3A}$(CRAR)-HA subunit (Figure 3.6). Performing the assay on permeabilised cells revealed that the total levels of expression for all subunits tested were approximately the same (Figure 3.6).

To assess the role of the RAR motif in $5HT_{3B}$, a mutant $5HT_{3B}$ subunit was generated containing SGER, from $5HT_{3A}$, in place of CRAR (construct $5HT_{3B}$(SGER)). The

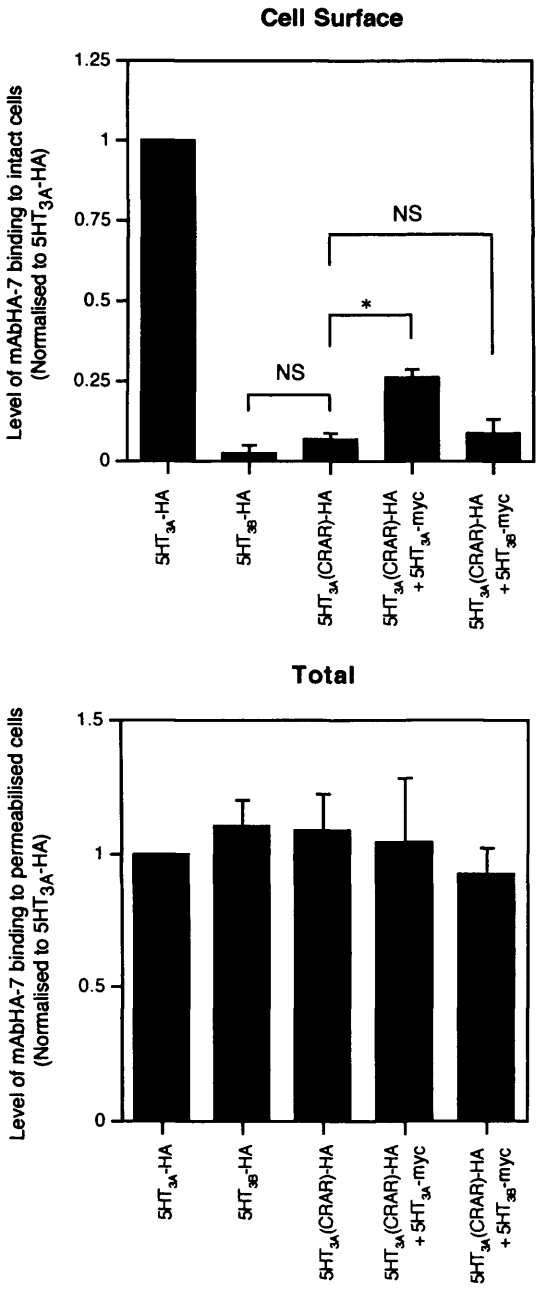

Figure 3.6 *Expression of 5HT$_{3A}$(CRAR) in transfected tsA201 cells.* Cells grown on coverslips were transiently transfected with the mutant 5HT$_{3A}$(CRAR)-HA subunit (alone and with 5HT$_{3A}$ or 5HT$_{3B}$) and levels of cell surface and total expression compared to 5HT$_{3A}$ and 5HT$_{3B}$ expressed alone. Cells were labelled with mAbHA-7 (anti-HA) either as intact cell monolayers (Cell Surface) or after permeabilisation (Total). Data is mean (normalised to level of antibody binding to 5HT$_{3A}$-HA), ± standard error, from at least 4 independent experiments performed in triplicate. The background signal from untransfected cells has been subtracted. Significance determined by Student's *t* test (*$p<0.05$; NS=not significant).

subcellular distribution of the $5HT_{3B}$(SGER) construct was examined using an enzyme-linked antibody binding assay. Cells were transiently transfected with myc-tagged $5HT_{3B}$(SGER) alone and co-transfected with $5HT_{3A}$-HA or $5HT_{3B}$-HA and levels of 9E10 (anti-myc) binding quantified for both intact and permeabilised cells. When expressed alone, $5HT_{3B}$(SGER)-myc was not detected on the cell surface (Figure 3.7). Like wild-type $5HT_{3B}$, when $5HT_{3B}$(SGER)-myc was co-expressed with $5HT_{3A}$ it was found to be expressed on the cell surface. When $5HT_{3B}$(SGER)-myc was co-expressed with $5HT_{3B}$ it was not expressed on the cell surface (Figure 3.7). Levels of 9E10 binding in permeabilised cells were similar for all combinations of constructs (Figure 3.7).

3.6 Expression of truncated $5HT_{3B}$(SGER) constructs

The failure of $5HT_{3B}$(SGER) to reach the cell surface when expressed alone suggested the presence of additional retention signals in the $5HT_{3B}$ subunit. To investigate this, truncated constructs based on $5HT_{3B}$(SGER) were generated. $5HT_{3B}$(SGER) was truncated after residue 270 (immediately following SGER), termed $5HT_{3B}$(SGER)270, and also just after M2, termed $5HT_{3B}$(SGER)TM2. The subcellular localisation of these subunits was investigated using an enzyme-linked antibody binding assay. Both truncated constructs were detected on the cell surface at a significant level (Figure 3.8). Wild-type $5HT_{3B}$ truncated at M2 is not expressed on the cell surface (see Section 3.4, Figure 3.4). Performing the assay on permeabilised cells revealed that total levels of expression were similar for all constructs (Figure 3.8). These results confirm the ability of RAR to act as an ER retention signal in the $5HT_{3B}$ subunit, and suggest that there are further retention signals beyond M2.

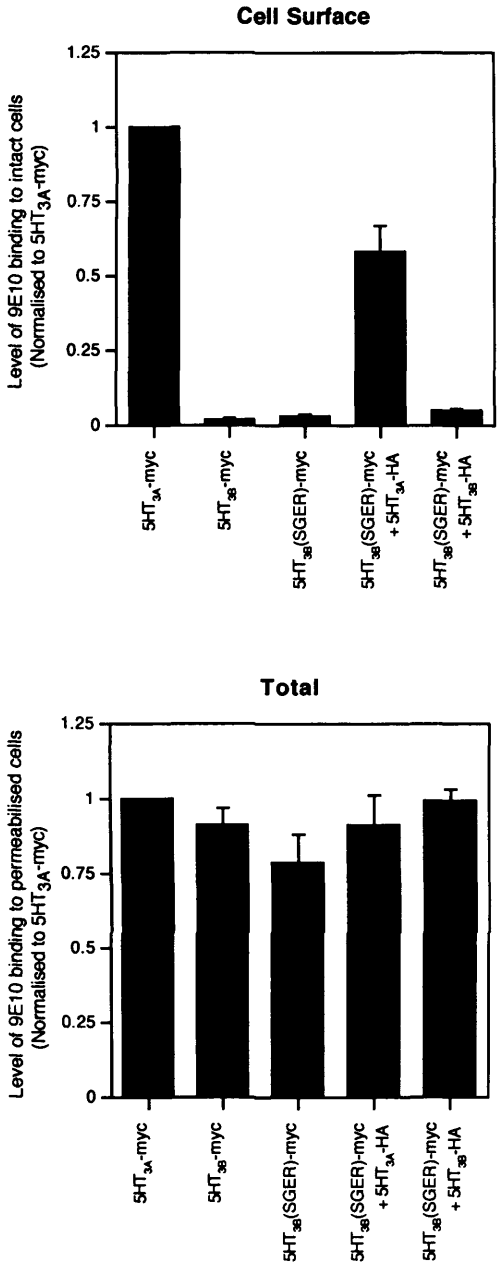

Figure 3.7 *Expression of 5HT$_{3B}$(SGER) in transfected tsA201 cells.* Cells grown on coverslips were transiently transfected with the mutant 5HT$_{3B}$(SGER) subunit (alone and with 5HT$_{3A}$ or 5HT$_{3B}$) and levels of cell surface and total expression compared to 5HT$_{3A}$ and 5HT$_{3B}$ expressed alone. Cells were labelled with 9E10 (anti-myc) either as intact cell monolayers (Cell Surface) or after permeabilisation (Total). Data is mean (normalised to level of antibody binding to 5HT$_{3A}$-myc), ± standard error, from at least 4 independent experiments performed in triplicate. The background signal from untransfected cells has been subtracted.

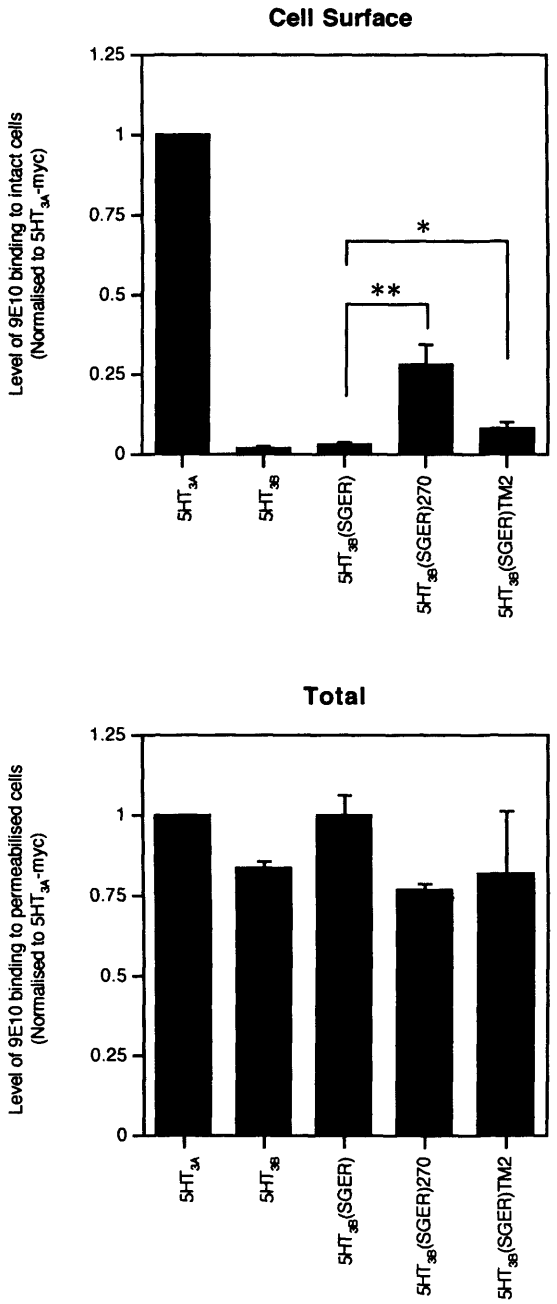

Figure 3.8 *Expression of truncated 5HT$_{3B}$(SGER) subunits in transfected tsA201 cells.* Cells grown on coverslips were transiently transfected with myc-tagged 5HT$_3$R subunits. Cells were labelled with 9E10 either as intact cell monolayers (Cell Surface) or after permeabilisation (Total). Data is mean (normalised to level of antibody binding to 5HT$_{3A}$-myc), ± standard error, from at least 3 independent experiments performed in triplicate. The background signal from untransfected cells has been subtracted. Significance determined by Student's *t* test (*p<0.05; **p<0.01).

3.7 Discussion

The $5HT_{3A}$ (Maricq *et al.*, 1991; Belelli *et al.*, 1995; Miyake *et al.*, 1995) and $5HT_{3B}$ (Davies *et al.*, 1999; Dubin *et al.*, 1999) subunits were examined in this study. The $5HT_{3A}$ subunit is capable of forming functional homomeric receptors in heterologous expression systems which exhibit a very low single channel conductance (sub-picosiemens (pS)) (Brown *et al.*, 1998), unlike those of native receptors (Hussy *et al.*, 1994). The discrepancies in conductance between recombinant heterologous and native receptors suggested the possible existence of other $5HT_3R$ subunits (Fletcher and Barnes, 1998). The cloning of the $5HT_{3B}$ subunit (Davies *et al.*, 1999) helped to explain these differences. A heteromeric receptor composed of $5HT_{3A}$ and $5HT_{3B}$ has a much larger single channel conductance (9-17 pS). When recombinant $5HT_{3B}$ is expressed in heterologous expression systems, such as *Xenopus* oocytes or the HEK293 cell line, it is observed to modify the receptor kinetics, voltage dependence, pharmacology and ion permeability of $5HT_{3A}$ (Dubin *et al.*, 1999). Heteromeric receptors have a lower affinity for 5-HT than homomeric receptors (Davies *et al.*, 1999; Dubin *et al.*, 1999; Hanna *et al.*, 2000; Boyd *et al.*, 2002). Homomeric receptors have a higher permeability to Ca^{2+} relative to monovalent cations than heteromeric receptors (Davies *et al.*, 1999). Unlike $5HT_{3A}$, $5HT_{3B}$ is not capable of forming a functional homomeric receptor (Davies *et al.*, 1999; Dubin *et al.*, 1999; Hanna *et al.*, 2000; Spier and Lummis, 2000). When expressed alone, $5HT_{3B}$ is retained within the ER unless co-expressed with $5HT_{3A}$ (Boyd *et al.*, 2002). The inability of $5HT_{3B}$ to reach the cell surface when expressed alone in a heterologous expression system has been confirmed in this study. Transient transfection of $5HT_{3B}$ in mammalian tsA201 cells followed by cell surface antibody labelling revealed that $5HT_{3B}$ was not expressed on the cell surface. However, performing the assay on permeabilised cells indicated that the protein was expressed. The ability of $5HT_{3A}$ to enable $5HT_{3B}$ to reach the cell surface was shown by antibody labelling of cell surface $5HT_{3B}$ subunits when co-transfected with $5HT_{3A}$. When expressed alone in tsA201 cells and assayed using a FLIPR, $5HT_{3B}$ did not show functional responses to the $5HT_3R$ agonist, CPBG, providing further evidence that this subunit does not form functional homomeric receptors.

When expressed alone, $5HT_{3B}$ did not form a ligand binding site in tsA201 cells and membrane preparations from these cells did not bind the $5HT_3R$ specific antagonist [^{3}H]-GR65630. It was previously reported that $5HT_{3B}$ expressed alone in tsA201 cells or *Xenopus* oocytes could not bind the selective $5HT_3R$ antagonist [^{3}H]-granisetron (Boyd *et al.*, 2002). There are several possible explanations for the lack of specific binding to the $5HT_{3B}$ subunit. The binding site, which is thought to be contained in the N-terminal region, may not be fully formed in the ER, and, as described previously, $5HT_{3B}$ is ER-retained unless $5HT_{3A}$ is present. However, studies performed with the nAChR, a member of the ligand-gated ion channel (LGIC) family that is structurally related to the $5HT_3R$, have shown that the ligand binding domain is formed in the ER (Mitra *et al.*, 2001). It has also been reported that some $5HT_{3A}$ receptors retained in the ER can bind [^{3}H]-granisetron (Green *et al.*, 1995) suggesting that the $5HT_3R$ ligand binding site may also be formed in the ER. A second possibility for the lack of binding to $5HT_{3B}$ may be that the subunit cannot form a ligand binding site by itself. The $5HT_{3B}$ subunit might only be able to contribute to the ligand binding sites in heteromeric receptor complexes with $5HT_{3A}$. Drawing analogies with other members of the LGIC family it is likely that ligand binding sites are formed at different subunit interfaces. Ligand binding sites of the $5HT_3R$ may be present at the $5HT_{3A}/5HT_{3B}$ subunit interface or at the $5HT_{3A}/5HT_{3A}$ subunit interface. Formation of the nAChR binding site is thought to require the contribution of a 'principal' binding site from one subunit and a 'complementary' binding site from another subunit (Changeux *et al.*, 1992; Karlin and Akabas, 1995). As $5HT_{3B}$ cannot form a binding site by itself it may lack the principal binding site, but contain a complementary binding site. It is evident that $5HT_{3B}$ does contribute to ligand binding, as the pharmacological properties of heteromeric receptors differ from those of the homomeric $5HT_{3A}R$ (Dubin *et al.*, 1999). The $5HT_{3A}$ subunit must possess and contribute the principal ligand recognition and binding site (Boess *et al.*, 1997; Hope *et al.*, 1999; Spier and Lummis, 2000; Steward *et al.*, 2000).

The cell surface expression of multimeric protein complexes such as the $5HT_3R$ requires the proper folding, assembly and trafficking of the constituent subunits. Protein expression is tightly regulated by mechanisms such as ER retention, to prevent cell surface expression of monomers and incompletely or incorrectly assembled complexes. The ER retention of the $5HT_{3B}$ subunit was investigated in

this study. ER retention is an important quality control checkpoint; protein subunits must be correctly folded and assembled in order to exit. Studies of nicotinic receptor assembly suggest that exit from the ER is an important checkpoint for controlling receptor stoichiometry (Blount *et al.*, 1990). ER resident chaperone proteins such as immunoglobulin binding protein (BiP) and calnexin interact with incompletely folded proteins, and through the ER localisation motifs within them, prevent ER exit. Both $5HT_{3A}$ and $5HT_{3B}$ are reported to interact with BiP and calnexin (Boyd *et al.*, 2002). In particular, $5HT_{3A}$ and $5HT_{3B}$ subunits which are not fully glycosylated, and are therefore unsuitable for cell surface expression, are shown to interact with BiP and calnexin (Boyd *et al.*, 2002). Previous studies imply that $5HT_{3B}$ requires assembly with $5HT_{3A}$ to exit from the ER (Boyd *et al.*, 2002).

Membrane proteins themselves can contain ER retention/retrieval signals, as recent studies on a number of receptors have illustrated (Zerangue *et al.*, 1999; Bichet *et al.*, 2000; Margeta-Mitrovic *et al.*, 2000). The masking of these motifs by assembly with another subunit, interactions with other proteins or phosphorylation may regulate the forward trafficking of such proteins (Zerangue *et al.*, 1999; Bichet *et al.*, 2000; Margeta-Mitrovic *et al.*, 2000).

To investigate the mechanisms involved in the retention of the $5HT_{3B}$ subunit and in an attempt to identify regions responsible, chimeric subunits between $5HT_{3A}$ and $5HT_{3B}$ were constructed and analysed using immunofluorescence by Dr C. Connolly, University of Dundee (Boyd *et al.*, 2003). One chimera, composed of $5HT_{3A}$ up to and including M1 fused to the remainder of $5HT_{3B}$ ($5HT_{3A\text{-}3B}$), was found not to be capable of cell-surface expression (Boyd *et al.*, 2003). However, a second chimera composed of $5HT_{3B}$ up to M3 fused to the remainder of $5HT_{3A}$ ($5HT_{3B\text{-}3A}$), was found to be expressed on the cell surface (Boyd *et al.*, 2003). These findings demonstrate the presence of an inhibitory element involved in ER retention of the $5HT_{3B}$ subunit beyond M1 of $5HT_{3B}$.

To determine whether retention signals were present in $5HT_{3B}$ a number of truncated $5HT_{3B}$ subunits were constructed. The rationale for this approach was that removal of C-terminal portions would eventually remove any retention signals and thereby result in cell surface expression. Analysis of the cellular localisation of the truncated

$5HT_{3B}$ subunits implied involvement of the region between M1 and M2 in the retention of $5HT_{3B}$. Alignment of the sequences in this region led to the identification of a potential RXR motif in $5HT_{3B}$, RAR, which had previously been identified as an ER retention motif in a number of other receptors (Zerangue *et al.*, 1999; Margeta-Mitrovic *et al.*, 2000; Standley *et al.*, 2000; Scott *et al.*, 2001).

Introduction of this potential ER retention motif from $5HT_{3B}$ to the homologous position in $5HT_{3A}$ ($5HT_{3A}$(CRAR)), prevented cell surface expression, thereby providing evidence for its role in ER retention. Like $5HT_{3B}$, $5HT_{3A}$(CRAR) can reach the cell surface when co-expressed with $5HT_{3A}$, but not $5HT_{3B}$. The reciprocal mutation was generated in $5HT_{3B}$ replacing CRAR with the homologous amino acids from $5HT_{3A}$ creating $5HT_{3B}$(SGER). This mutant also did not reach the cell surface indicating the presence of additional retention signals downstream of M2.

To provide direct evidence for 'RAR' as a retention signal in $5HT_{3B}$, the $5HT_{3B}$(SGER) construct was truncated just after SGER (residue 270) and also just after M2. Both of these constructs were expressed on the cell surface. Together with the observation that wild-type $5HT_{3B}$ truncated at M2 is not expressed on the cell surface, this data suggests that the RAR motif is capable of causing the retention of the $5HT_{3B}$ subunit in the ER.

In an attempt to determine how the identified signal might be overcome, $5HT_{3A}$(CRAR) and $5HT_{3B}$(SGER) were co-expressed and their cellular distribution determined by immunofluorescence. Neither subunit reached the cell surface suggesting that there is no direct masking between the homologous domains, CRAR/SGER (Boyd *et al.*, 2003). Other regions are likely to be required for masking of the motif which are likely to be provided by another neighbouring subunit.

To determine whether direct subunit interactions in the M1-M2 region mask the ER retention signal, constructs consisting of M1-M2 were generated for both $5HT_{3A}$ and $5HT_{3B}$ (Boyd *et al.*, 2003). Co-expression of these with $5HT_{3B}$ did not result in its surface expression, suggesting that a direct interaction in this region alone does not mask the retention signal. The subunits were however shown to interact in this

region by co-immunoprecipitation following cross-linking. A number of other proteins were observed to co-immunoprecipitate with M1-M2 constructs, and may be potential novel interacting proteins (Boyd *et al.*, 2003).

The mechanism by which the RXR motif in $5HT_{3B}$ is masked, resulting in the cell surface expression of the $5HT_{3B}$ subunit is unclear. It has been shown that co-expression of $5HT_{3B}$ with $5HT_{3A}$ is necessary to allow exit of $5HT_{3B}$ from the ER suggesting that $5HT_{3A}$ is responsible for masking of the motif. From the data presented here, a region beyond M2 in $5HT_{3A}$ is predicted to mask the motif. Studies with the $5HT_{3A}$(CRAR) mutant suggest that the motif is masked by a neighbouring $5HT_{3A}$ subunit. Further studies reported by Boyd *et al.*, 2003 suggest that a region beyond M3, possibly the large intracellular loop between M3 and M4, may be responsible for masking the motif. This is based upon the observation that the $5HT_{3B\text{-}3A}$ chimera which, despite containing the RAR motif, is expressed on the cell surface. It may not be a direct interaction between $5HT_{3A}$ and $5HT_{3B}$ that masks the motif; it may be that interaction of the subunits induces a conformational change that buries the motif and thereby allows cell surface expression. It may also be possible that association of $5HT_{3A}$ and $5HT_{3B}$ leads to the recruitment of an additional factor/protein which may mask the motif.

The RXR motif has been identified in a number of other receptors, for example the ATP-sensitive potassium (K_{ATP}) channel (Zerangue *et al.*, 1999), the $GABA_B$ G protein-coupled receptor (Margeta-Mitrovic *et al.*, 2000) and the Kainate receptor (Jaskolski *et al.*, 2004). The masking of the motif by a number of different mechanisms leads to the cell surface expression of subunits in fully assembled receptor complexes. The mechanism by which the unmasked motif retains proteins has not yet been determined.

The RXR motif differs from the more well characterised ER retention/retrieval signals such as KKXX and KDEL (Teasdale and Jackson, 1996). Unlike the KKXX motif, for example, which only functions when situated three residues from the C-terminus, the RXR motif functions at the N- or C- terminus of membrane proteins as well as in intracellular regions, and no specific spacing is required (Zerangue *et al.*, 1999; Shikano and Li, 2003). The middle residue of the motif was reported to

preferentially be a large neutral or positively charged amino acid (Zerangue *et al.*, 1999) but other data contradicts this finding (Schutze *et al.*, 1994).

The RXR motif has been shown to be regulated by phosphorylation. Protein kinase C (PKC) and protein kinase A (PKA) phosphorylation of serine residues flanking an RXR motif in the NR1 subunit of the NMDA receptor have been shown to suppress ER retention (Scott *et al.*, 2001; Scott *et al.*, 2003). There are no potential phosphorylation sites close to the RAR motif in $5HT_{3B}$.

Another proposed mechanism by which the RXR motif may function is through interactions with intracellular proteins. A type I PDZ-binding domain in the NR1 subunit of the NMDA receptor is reported to suppress ER retention (Standley *et al.*, 2000; Scott *et al.*, 2001). Two isoforms of the 14-3-3 protein (ε and ζ) have been shown to interact specifically with the RXR motif in the K_{ATP} channel (Yuan *et al.*, 2003). The binding of 14-3-3 is proposed to mediate ER release (Yuan *et al.*, 2003). A few potential interacting proteins were identified by co-immunoprecipitation following cross-linking with the M1-M2 region of $5HT_{3B}$ (Boyd *et al.*, 2003).

The mechanism behind retention in the ER via the unmasked RXR motif is not known. The KKXX motif is thought to function through its interactions with the coatomer protein (COPI) complex (Teasdale and Jackson, 1996). Recent studies have reported an interaction between the COPI vesicle coat and RXR (Yuan *et al.*, 2003; Hermosilla *et al.*, 2004) and this may explain the ER localisation of proteins bearing this motif.

In summary, an ER retention motif of the RXR type has been identified in the $5HT_{3B}$ subunit which can be overcome by co-expression with the $5HT_{3A}$ subunit. The motif is sufficient to cause retention of the subunit, but is not the only factor involved in the ER retention of the subunit. Studies have implied the presence of additional mechanisms or retention signals in $5HT_{3B}$ involving regions beyond the M2 domain of the subunit.

3.8 Future directions

It would be particularly interesting to continue this work and determine how the identified ER retention motif functions. Whilst it is clear that co-expression with $5HT_{3A}$ results in masking of the identified motif, as cell surface expression is observed, it is not clear how the motif is masked. The $5HT_{3A}$ subunit may mask the motif through a direct interaction or may induce conformational changes resulting in masking indirectly. Determining how the RXR motif causes ER retention would also be interesting. Recent studies have shown that the RXR motif is capable of interacting with the COPI family of proteins (Yuan *et al.*, 2003; Hermosilla *et al.*, 2004) which may explain the ER localisation of proteins containing this motif.

Proteins that interact with the RXR motif could be identified using a system such as the yeast 2-hybrid system. Cross-linking and co-immunoprecipitation experiments using $5HT_{3A}$ and $5HT_{3B}$ 'M1-M2' constructs identified a few potential interacting proteins (Boyd *et al.*, 2003) which could be further characterised.

It would be interesting to determine why the $5HT_{3B\text{-}3A}$ chimera, which contains the RXR motif, is expressed on the cell surface whilst $5HT_{3A}$(CRAR) is not. The $5HT_{3B}$(SGER) mutant could be used to generate a series of truncated subunits and their cell surface expression assayed to identify the next N-terminal ER retention signal present in the $5HT_{3B}$ subunit.

Some of the work presented in this chapter has been published: Cell Surface Expression of 5-Hydroxytryptamine Type 3 Receptors is Controlled by an Endoplasmic Reticulum Retention Signal. G. W. Boyd, A. I. Doward, E. W. Kirkness, N. S. Millar and C. N. Connolly *Journal of Biological Chemistry* 2003, **278** (30), 27681-27687.

CHAPTER 4

Effects of 5-hydroxyindole on the 5-HT-induced responses of mouse and human $5HT_{3A}$ receptors

4.1 Introduction

5-hydroxyindole (5-HI), the aromatic moiety of 5-hydroxytryptamine (5-HT) (Figure 4.1), is known to potentiate the ion current of native mouse $5HT_3$ receptors ($m5HT_3R$) in N1E-115 neuroblastoma cells (Kooyman *et al.*, 1993; Kooyman *et al.*, 1994; van Hooft *et al.*, 1997). At low millimolar concentrations 5-HI is thought to potentiate currents and slow the ion current decay by binding to an allosteric site on the $5HT_3R$ which stabilises the open state. At higher millimolar concentrations (greater than 10 mM) 5-HI blocks the $5HT_3R$, and this effect is thought to be mediated by a competitive interaction with the agonist binding site (Kooyman *et al.*, 1994).

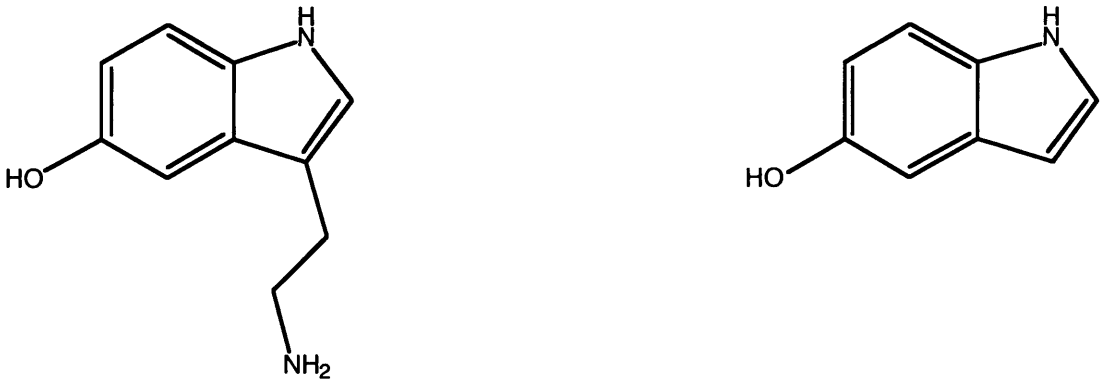

Figure 4.1 *Chemical structures of 5-hydroxytryptamine (5-HT; serotonin) and 5-hydroxyindole (5-HI).*

There is high sequence similarity in the N-terminal ligand-binding domain between the $5HT_{3A}$ subunit of different species, but differences in pharmacological properties are observed. For example, d-tubocurarine is 1800-fold more potent at mouse than human $5HT_3Rs$ (Hope *et al.*, 1999) and 2-Me-5-HT, a full agonist on human $5HT_3Rs$ acts only as a partial agonist on mouse $5HT_3R$ (Miyake *et al.*, 1995).

In addition to potentiating the mouse $5HT_3R$, 5-HI has been shown to potentiate homomeric $\alpha 7$ neuronal nicotinic acetylcholine receptors (nAChRs) (van Hooft *et*

al., 1997; Gurley *et al.*, 2000; Zwart *et al.*, 2002). There is approximately 33% sequence homology between the ligand binding domains of the $5HT_3R$ and α7 nAChR and cross-reactivity of agonists and antagonists has been reported (Machu *et al.*, 2001; Macor *et al.*, 2001; Broad *et al.*, 2002).

4.2 Preliminary studies performed at Eli Lilly

The work presented in this chapter is in collaboration with a research group based at Eli Lilly, Windlesham, UK. Studies carried out at Eli Lilly confirmed the potentiating effects of 5-HI on mouse $5HT_{3A}$ ($m5HT_{3A}$) receptors stably expressed in HEK293 cells using a Fluorometric Imaging Plate Reader (FLIPR) assay (unpublished result; see Section 4.5.1, Figure 4.6). However, HEK293 cells stably expressing the human $5HT_{3A}$ ($h5HT_{3A}$) subunit were not potentiated by 5-HI. The aim of this project was to investigate this difference between $5HT_{3A}R$ species variants and to determine the binding site of 5-HI. Defining the 5-HI binding site might be useful for rationalisation of drug design with the aim of generating α7 nAChR selective compounds/potentiators which might be useful in the treatment of neurological disorders (Lloyd and Williams, 2002; Maelicke and Albuquerque, 2000).

Unpublished studies, performed at Eli Lilly, using α7/$5HT_{3A}$ chimeric subunits suggested that the effects of 5-HI are mediated through the N-terminal extracellular domain of the receptor subunit. Epibatidine-induced responses in HEK293 cells stably expressing a human α7/mouse $5HT_{3A}$ chimera (α7 up to transmembrane region 1 joined to the C-terminal of mouse $5HT_{3A}$) are potentiated by 5-HI, as are (to a lesser extent) cells expressing a human α7/human $5HT_{3A}$ chimera suggesting that the extracellular N-terminal domain is responsible for mediating the effects of 5-HI.

4.3 Construction of chimeric $5HT_{3A}R$ subunits

In order to confirm whether 5-HI acts by binding to the N-terminal domain, chimeric subunits of mouse and human $5HT_{3A}R$ were constructed. A chimeric subunit cDNA was generated containing the extracellular N-terminal domain of $h5HT_{3A}$ fused to the

transmembrane and intracellular domains of m5HT$_{3A}$ (h/m5HT$_{3A}$ chimera) (Figure 4.2). A second, similar chimeric subunit cDNA containing the extracellular N-terminal domain of m5HT$_{3A}$ fused to the transmembrane and intracellular domains of h5HT$_{3A}$ (m/h5HT$_{3A}$ chimera) was also constructed (Figure 4.2). The long splice variant of mouse 5HT$_{3A}$ (m5HT$_{3A(L)}$) was used in construction of these chimeras. The construction of these chimeras is detailed in Chapter 2, Section 2.2. If 5-HI was acting via the N-terminal region it was predicted that agonist-induced responses of the m/h5HT$_{3A}$ chimera would be potentiated whilst the h/m5HT$_{3A}$ chimera would not. It was hoped that these chimeras would be the basis for constructing further chimeras to determine residues and regions of the receptors responsible for conferring 5-HI sensitivity.

4.4 Expression of 5HT$_{3A}$ chimeras in tsA201 cells

4.4.1 Radioligand binding studies

To confirm that the chimeric subunits were capable of forming correctly folded ligand binding sites, radioligand binding studies using the 5HT$_3$R specific radioligand [^{3}H]-GR65630 were performed, on membrane preparations of cells transiently transfected with the human, mouse or chimeric 5HT$_{3A}$Rs. Specific binding, determined by subtracting binding performed in the presence of a high concentration of 5-HT from that performed in its absence, was observed for the mouse, human and m/h and h/m5HT$_{3A}$ chimeras (Figure 4.3). Initially, no specific binding was detected for the h/m5HT$_{3A}$ chimera. Binding was also not detected with a h5HT$_{3A}$ subunit containing a *Bam*HI site which had been introduced to enable construction of the h/m5HT$_{3A}$ chimera. To investigate the reason for the lack of specific [^{3}H]-GR65630 binding, the amino acid sequences where the *Bam*HI site was introduced by site-directed mutagenesis in h5HT$_{3A}$ and the equivalent region in the h/m5HT$_{3A}$ chimera were examined. The mutagenesis had resulted in the substitution of a glycine (G) residue for a valine (V) residue which was found to be conserved

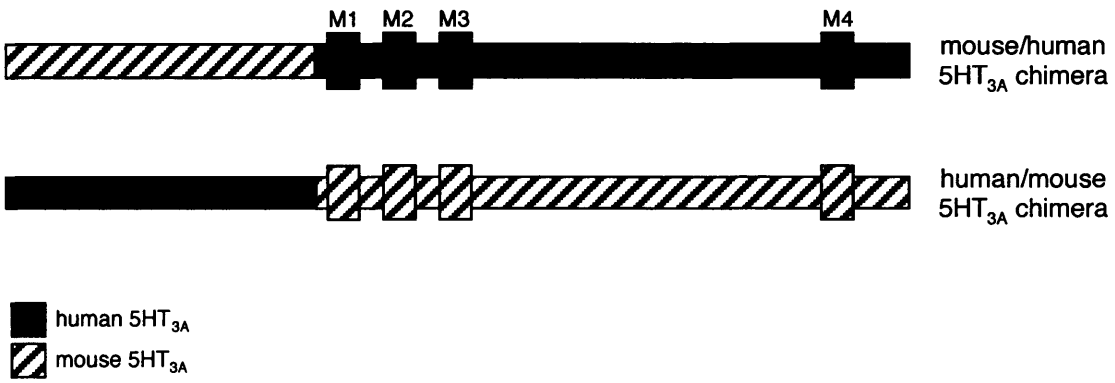

Figure 4.2 *Chimeric $5HT_{3A}$ subunits.* The mouse/human $5HT_{3A}$ chimera consisted of the extracellular N-terminal domain of the mouse $5HT_{3A}$ subunit fused to the transmembrane and intracellular domains of the human $5HT_{3A}$ subunit. The human/mouse $5HT_{3A}$ chimera consisted of the extracellular domain of the human $5HT_{3A}$ subunit fused to the transmembrane and intracellular domains of the mouse $5HT_{3A}$ subunit. (M1-M4=transmembrane domains)

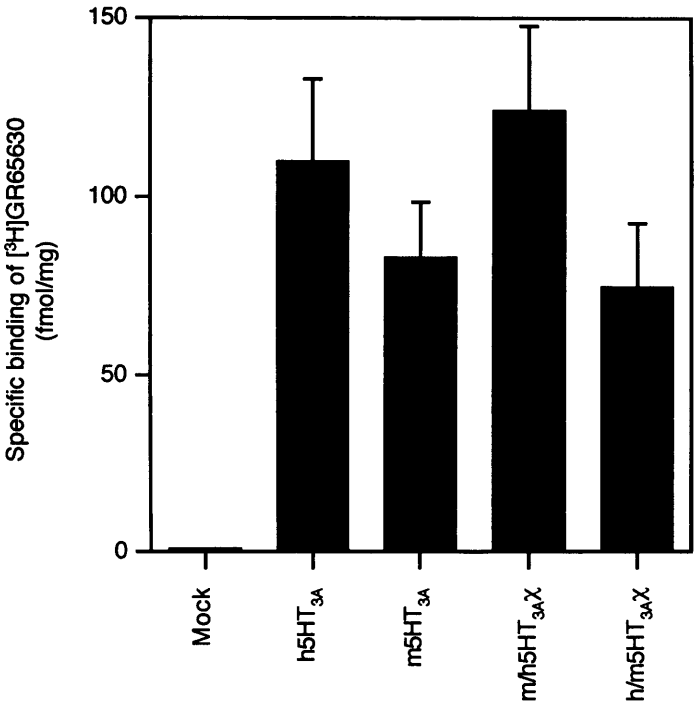

Figure 4.3 *Specific [^{3}H]-GR65630 binding to chimeric 5HT$_{3A}$Rs expressed in tsA201 cells.* Cells were transiently transfected with wild-type and chimeric 5HT$_{3A}$ subunits and binding performed on cell membrane preparations using 12.5 nM [^{3}H]-GR65630. For brevity, chimeras are referred to using the Greek letter, chi (χ). Specific binding data to cell membrane preparations are means, ± standard error, from 4 to 8 experiments performed in triplicate.

between species. An alignment of the amino acids in this region in the different constructs is shown below.

Mouse $5HT_{3A}$	F Y V I I R
Human $5HT_{3A}$	F Y V V I R
Human $5HT_{3A}$ (*Bam*HI)	F Y **G** I L R
Human (*Bam*HI)/mouse $5HT_{3A}$ chimera	F Y **G** I I R
Mouse/human $5HT_{3A}$ chimera	F Y V I L R
Corrected human/mouse $5HT_{3A}$ chimera	F Y V I I R

Using site-directed mutagenesis the glycine residue was replaced by the conserved valine residue in the h/m$5HT_{3A}$ chimera. Radioligand binding was performed with [^{3}H]-GR65630 and specific binding was observed for the h/m$5HT_{3A}$ chimera at a level not significantly different from mouse, human or m/h$5HT_{3A}$ chimera (Figure 4.3).

4.4.2 Metabolic labelling and immunoprecipitation

Cells (tsA201) were transiently transfected with the chimeric subunit cDNAs. Metabolic labelling and immunoprecipitation were performed on transfected cells to confirm expression of subunit protein. An antibody which recognises the extracellular domain of the mouse $5HT_{3A}$R (pAb120; Spier *et al.*, 1999), and an antibody which recognises a region within the intracellular loop of both the mouse and human $5HT_{3A}$R (pAb$5HT_3$; Turton *et al.*, 1993) were used to detect wild-type and chimeric subunits.

Specific bands were detected for both chimeras and wild type subunits when immunoprecipitated with pAb$5HT_3$. Specific bands were detected for the m$5HT_{3A}$R and m/h$5HT_{3A}$ chimera with pAb120 (Figure 4.4). The molecular weights of the chimeric subunits were predicted from their amino acid sequences using the Protein Information Resource at Georgetown University Medical Center (http://pir.georgetown.edu/pirwww/search/comp_mw.shtml). The wild type and

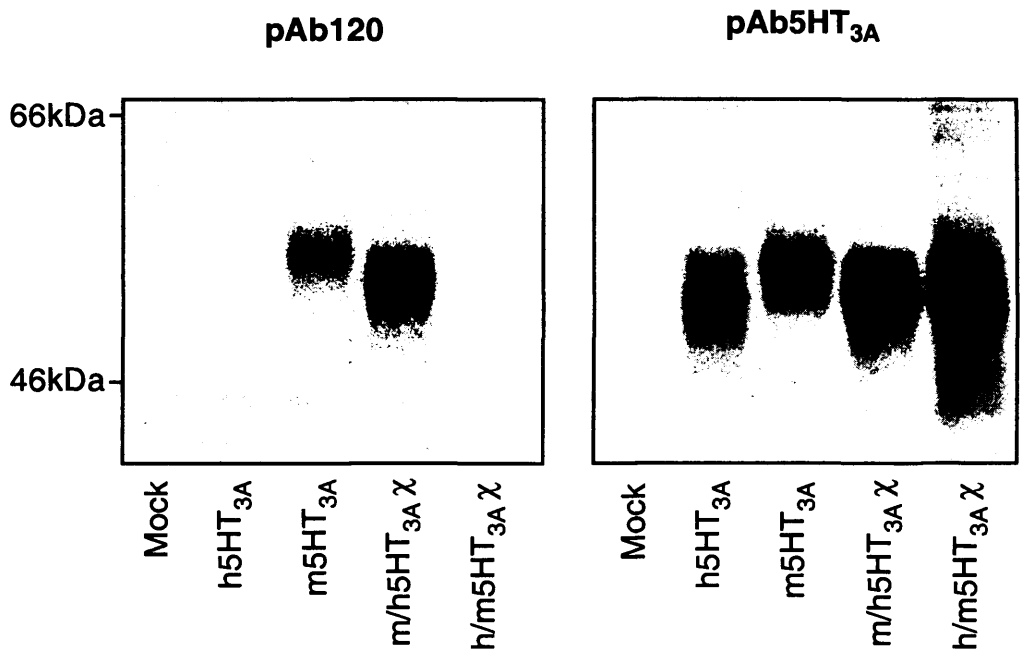

Figure 4.4 *Metabolic labelling and immunoprecipitation of $5HT_{3A}R$ chimeric subunits.* Heterologous expression of $5HT_{3A}R$ chimeric subunits transiently transfected in tsA201 cells. Cells were metabolically labelled, detergent-solubilised and the lysates immunoprecipitated with polyclonal antibodies against the extracellular domain of $5HT_{3A}$ (pAb120) and against a region within the intracellular loop between M3 and M4 ($pAb5HT_3$). Specific immunoreactive bands were detected for each wild type and chimeric subunit. Positions of molecular weight markers are indicated. This figure is representative of 3 similar experiements.

chimeric subunits were predicted to have an approximate molecular weight of 56 kDa. The bands detected were as the approximate predicted size.

4.4.3 Functional characterisation by intracellular calcium (FLIPR) assay

To confirm that the chimeric subunits were capable of forming functional receptors they were transiently transfected into tsA201 cells and assayed by an intracellular calcium (FLIPR) assay. Transfected cells were replated in a 96-well plate, loaded with the Ca^{2+}-sensitive dye, Fluo-4, and agonist-induced changes in intracellular calcium recorded. Both chimeric subunits showed agonist-induced (5-HT and CPBG) increases in intracellular Ca^{2+} indicating that they had formed functional receptors (Figure 4.5).

4.5 Effects of 5-HI examined by intracellular calcium (FLIPR) assay

4.5.1 Studying the effects of 5-HI on $5HT_{3A}$ in stably transfected HEK293 cells

The potentiating effect of 5-HI on the 5-HT-induced responses of the $m5HT_{3A}R$, and the lack of effect on the $h5HT_{3A}R$, were confirmed in HEK293 cells stably expressing the mouse or human $5HT_{3A}R$ subunit (Figure 4.6). The $m5HT_{3A}R$ responses, measured as agonist-induced changes in intracellular calcium using a FLIPR, were potentiated by approximately 100%.

4.5.2 Studying the effects of 5-HI on $5HT_{3A}$ in transiently transfected HEK293 cells

HEK293 cells were transiently transfected, using the FuGENE transfection reagent, with the human or mouse $5HT_{3A}R$. The effects of 5-HI on 5-HT-induced responses, recorded as agonist-induced changes in intracellular calcium, were studied using a FLIPR. Co-application or pre-incubation (5 minutes) of 1 mM 5-HI inhibited the 5-HT-induced responses of both the human and mouse $5HT_{3A}R$ (Figure 4.7). The lack of potentiation of the $m5HT_{3A}R$ by 5-HI was unexpected because (as described above, Sections 4.2 and 4.5.1) the responses of the $m5HT_{3A}R$, stably expressed in HEK293 cells, were potentiated by 5-HI.

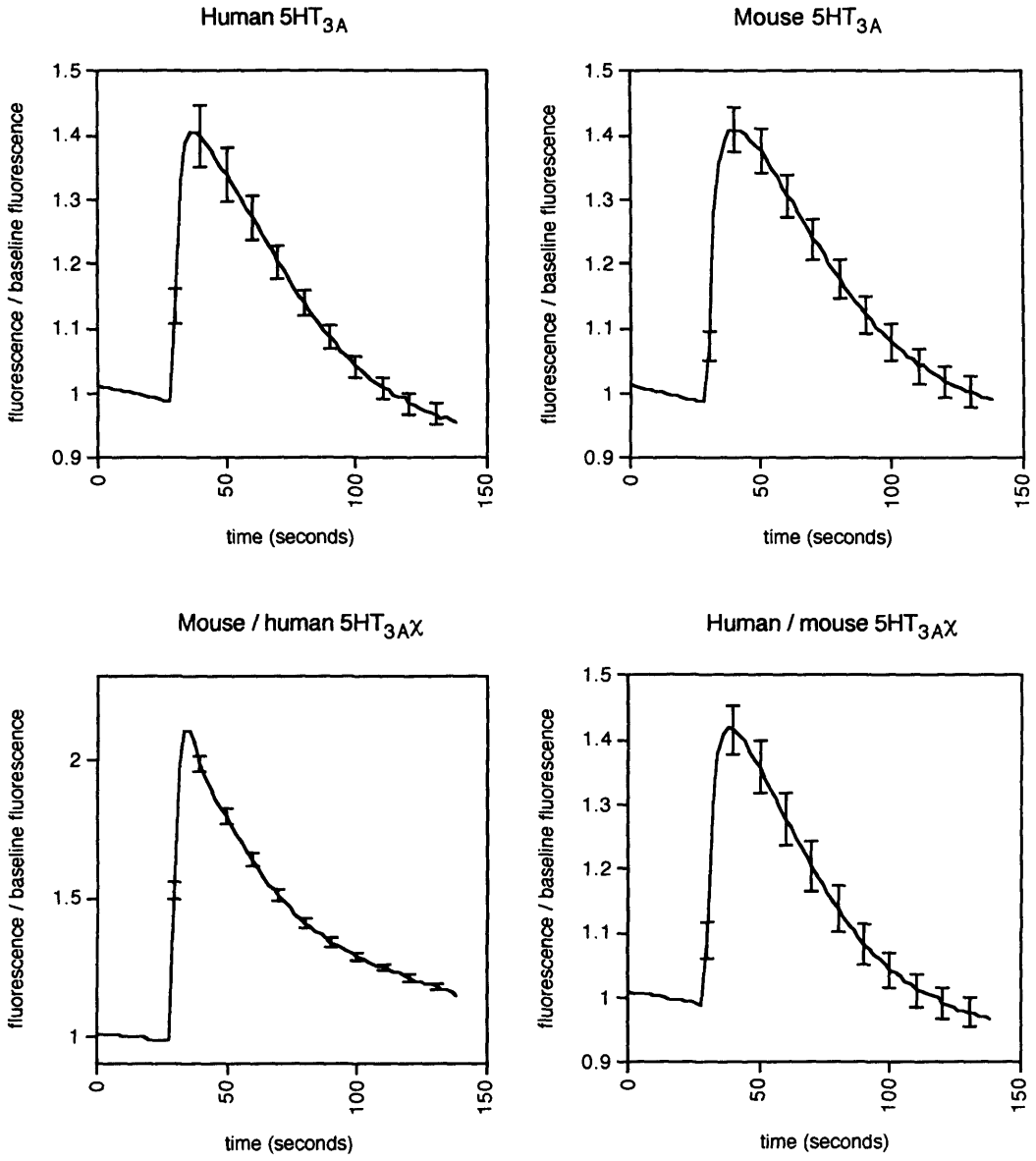

Figure 4.5 *Functional study of wild-type and chimeric $5HT_{3A}$ subunits, expressed in tsA201 cells, using a FLIPR.* Cells were transiently transfected with the wild-type mouse or human $5HT_{3A}$ subunits or the chimeric $5HT_{3A}$ subunits, and responses to 10 μM 5-HT assayed using a FLIPR. Traces are average changes in fluorescence/baseline fluorescence (± standard error every 10 seconds) from at least 6 wells, of cells loaded with the Ca^{2+}-sensitive dye, Fluo-4, from a representative experiment. Both the h/m$5HT_{3A}$ chimera and the m/h$5HT_{3A}$ chimera were observed to form functional homomeric receptors.

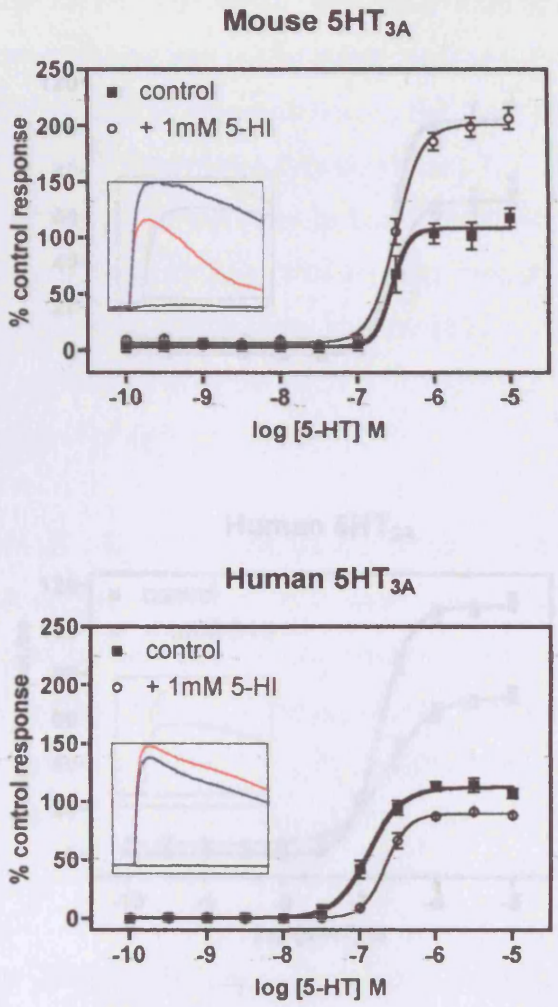

Figure 4.6 *Effect of 5-HI on $5HT_{3A}$ receptors stably expressed in HEK293 cells.* Concentration-response curves of 5-HT alone or with 5-HI obtained from recombinant mouse and human $5HT_{3A}$Rs stably expressed in HEK293 cells. Responses are expressed relative to maximal (30 μM) 5-HT control responses. Traces represent mean ± standard error of 8 experiments. 5-HI potentiated responses mediated by mouse $5HT_{3A}$Rs, but had no effect on human $5HT_{3A}$Rs stably transfected in HEK293 cells. Goodness of curve fits: Mouse (control, R^2=0.9930; +5-HI, R^2=0.9985); Human (control, R^2 = 0.9984; +5-HI, R^2 = 0.9996). Insets show example traces upon application of 10 μM 5HT in the presence (blue) or absence (red) of 1 mM 5-HI. Addition of buffer alone is shown by a black trace. Horizontal axis is time (72 seconds); Vertical axis is fluorescence units (7100 units for mouse and 15000 for human).

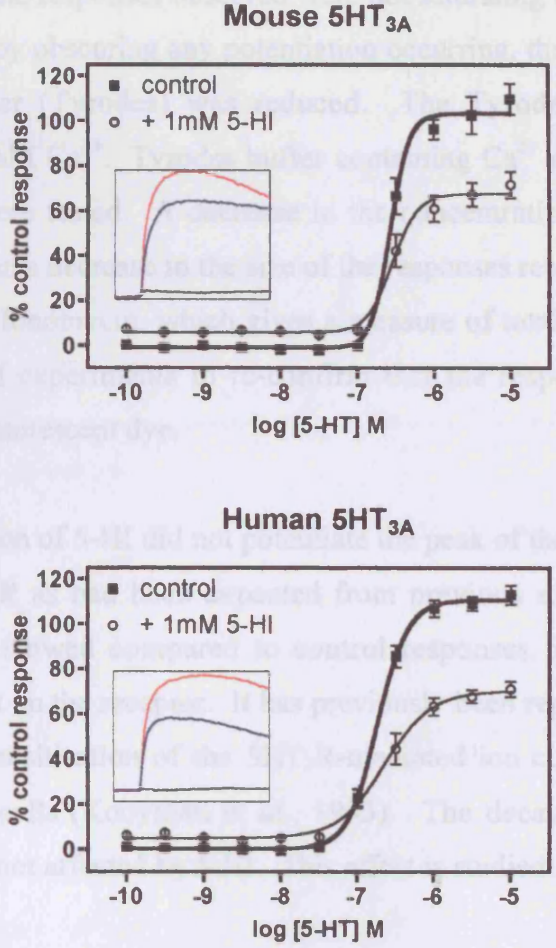

Figure 4.7 *Effect of 5-HI on $5HT_{3A}$ receptors transiently expressed in HEK293 cells.* Concentration-response curves of 5-HT alone or with 5-HI obtained from recombinant mouse and human $5HT_{3A}$Rs transiently transfected in HEK293 cells. Responses are expressed relative to maximal (30 μM) 5-HT control responses. Traces represent mean ± standard error of 10 experiments. 5-HI did not potentiate mouse or human $5HT_{3A}$ transiently transfected in HEK293 cells. Goodness of curve fits: Mouse (control, R^2=0.9963; +5-HI, R^2=0.9938); Human (control, R^2 = 0.9995; +5-HI, R^2 = 0.9968). Insets show example traces upon application of 10 μM 5HT in the presence (blue) or absence (red) of 1 mM 5-HI. Addition of buffer alone is shown by a black trace. Horizontal axis is time (60 seconds); Vertical axis is fluorescence units (6100 units for mouse and 12000 for human).

To ensure that the responses observed were not saturating the fluo-3 fluorescent dye used, and thereby obscuring any potentiation occurring, the concentration of Ca^{2+} in the assay buffer (Tyrodes) was reduced. The Tyrodes buffer routinely used contained 2.5 mM Ca^{2+}. Tyrodes buffer containing Ca^{2+} concentrations of 0.1 mM and 0.5 mM were tested. A decrease in the concentration of Ca^{2+} in the Tyrodes buffer resulted in a decrease in the size of the responses recorded, but no potentiation was observed. Ionomycin, which gives a measure of total cellular Ca^{2+}, was added near the end of experiments to re-confirm that the responses observed were not saturating the fluorescent dye.

Although addition of 5-HI did not potentiate the peak of the 5-HT induced responses of the m5HT$_{3A}$R as had been expected from previous studies, the 'decay' of the responses was slowed compared to control responses, indicating that 5-HI was having an effect on the receptor. It has previously been reported that 5-HI decreases the rate of desensitisation of the 5HT$_3$R-mediated ion current in N1E-115 mouse neuroblastoma cells (Kooyman *et al.*, 1993). The decay of the responses of the h5HT$_{3A}$R were not affected by 5-HI. This effect is studied further in Section 4.8.3.

4.6 Effects of 5-HI on 5HT$_{3A}$Rs expressed in *Xenopus* oocytes

The effects of 5-HI on 5HT$_{3A}$Rs expressed in oocytes were investigated to confirm the previously observed species-specific effects of 5-HI in an alternative assay.

4.6.1 Optimisation of experimental conditions

To examine the functional properties of 5HT$_3$Rs in *Xenopus* oocytes, cDNA (2 ng) encoding the human or mouse 5HT$_{3A}$R, resuspended in water, was injected per oocyte. Application of 5-HT induced large currents (about 40 μA) which were non-desensitising. Typical responses are illustrated in figure 4.8B. The amount of cDNA injected was varied; with 0.2 ng/oocyte, large responses with the same kinetics as with the higher DNA concentration were observed, with 0.04 ng/oocyte responses could not be detected. All further experiments were carried out using 0.2 ng DNA/oocyte. The concentration-response curves for 5-HT were independent of the amount of DNA injected. Initial recordings were carried out in a saline solution

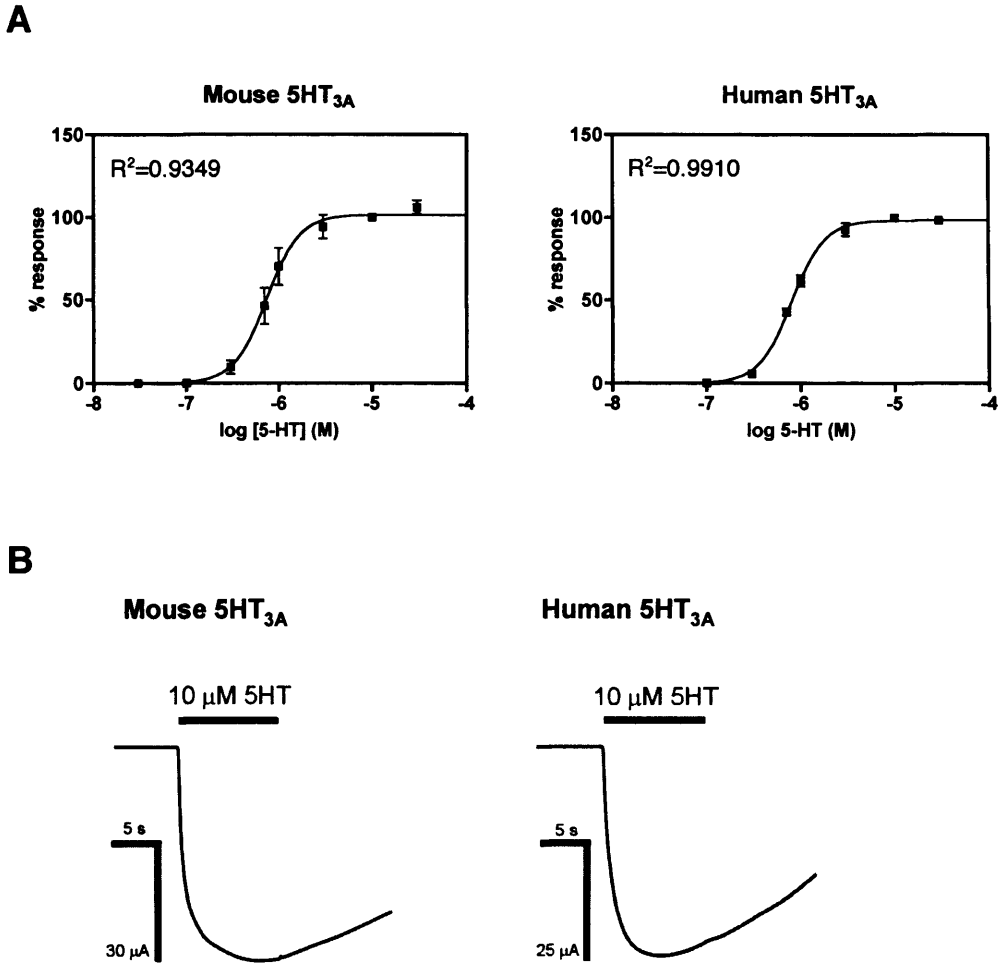

Figure 4.8 *Functional responses in Xenopus oocytes injected with $5HT_{3A}$ subunit cDNA.* **A**, Concentration-response curves of 5-HT obtained from oocytes expressing mouse and human $5HT_3AR$ yielding estimates of EC_{50} 0.74 ± 0.004 µM and 0.8 ± 0.002 µM respectively, and Hill coefficient (nH) 2.4 ± 0.5 and 2.4 ± 0.2. All current amplitudes are normalised to the 100 µM 5-HT response, ± standard error. Each set of data points was obtained from the same oocyte, repeated 4 times with different oocytes. Goodness of fit (R^2) is indicated. **B**, Examples of the currents obtained with application of 10 µM 5-HT in *Xenopus* oocytes expressing the human and mouse $5HT_3ARs$. Application of 5-HT induced large, non-desensitising currents.

containing barium. Replacing barium in the saline solution with calcium did not affect responses and so all further experiments were carried out using saline solution containing calcium. Barium is often used in preference to calcium to minimise the contribution of endogenous Ca^{2+}-activated chloride channels.

Concentration-response curves were measured for the mouse and human $5HT_{3A}R$ expressed in oocytes. The normalised data are shown in figure 4.8A. Fitting a concentration-response curve (Equation: i/imax = $1/\{1+(EC_{50}/[agonist])nH\}$) to the $m5HT_{3A}R$ data yielded estimates of EC_{50} and Hill coefficient (n_H) of 0.74 ± 0.004 μM and 2.4 ± 0.5 respectively, and the $h5HT_{3A}R$: 0.8 ± 0.002 μM and 2.4 ± 0.2 (Figure 4.8A).

4.6.2 Effects of 5-HI on human and mouse $5HT_{3A}$Rs expressed in Xenopus oocytes

Application of a 20% effective concentration (EC_{20}) of 5-HT (0.4 and 0.6 μM for mouse and human $5HT_{3A}$Rs respectively) to oocytes expressing the $5HT_{3A}$Rs evoked transient inward currents, whereas application of 1-10 mM 5-HI did not. Co-application of increasing concentrations of 5-HI with an EC_{20} of 5-HT had no potentiating effect on the peak amplitude of the 5-HT-induced ion currents of either the mouse or human $5HT_{3A}R$. Example traces illustrating currents obtained upon co-application of 1 mM 5-HI with an EC_{20} of 5-HT are shown for mouse and human $5HT_{3A}$ (Figure 4.9A). At higher concentrations of 5-HI the 5-HT-induced responses were inhibited. Fitting an inhibition curve to the data yielded IC_{50} estimates of 4.5 ± 0.09 mM for mouse and 1.8 ± 0.04 mM for human $5HT_{3A}R$ (Figure 4.10).

5-HI was also co-applied with 5-HT at an E_{max} concentration (10 μM) to oocytes expressing the $m5HT_{3A}R$. Example traces are shown (Figure 4.9B). 5-HI did not potentiate the 5-HT-induced ion currents. When 5-HT was used at E_{max}, the inhibition of 5-HT-induced currents by 5-HI occurred at higher concentrations compared to when 5-HI was used at EC_{20}. Fitting an inhibition curve to the data yielded an estimate for IC_{50} of 24 ± 1.01 mM (Figure 4.10). These results suggest that at higher concentrations 5-HI interacts in a competitive manner, as has been previously suggested (Kooyman *et al.*, 1994).

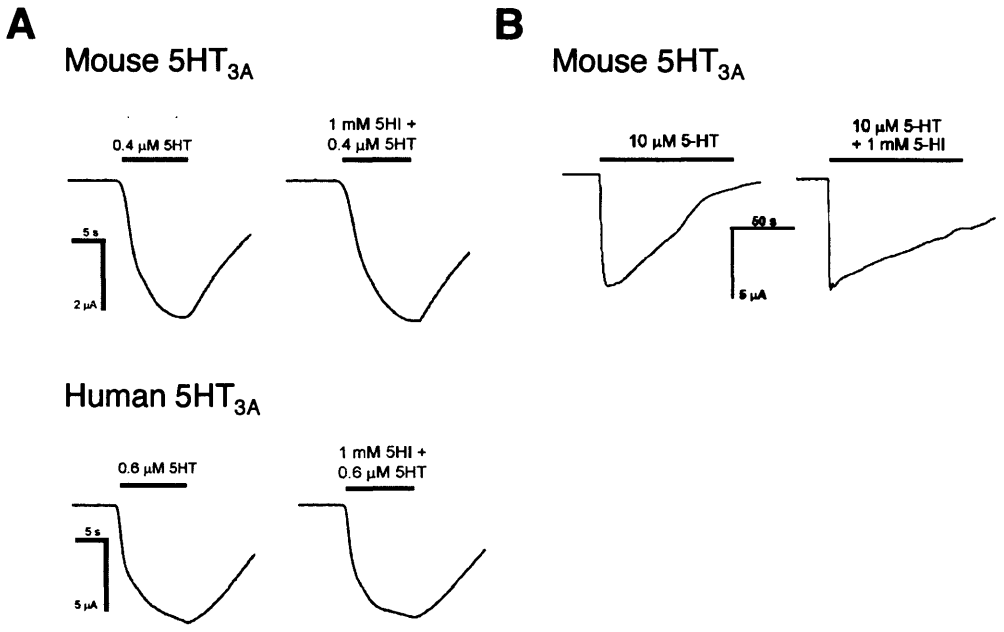

Figure 4.9 *Example traces showing the effects of 5-HI on $5HT_{3A}$ expressed in Xenopus oocytes.* **A**, Application of 5-HT at an EC_{20} induces ion currents in oocytes expressing either mouse or human $5HT_{3A}$. Co-application of 1 mM 5-HI with an EC_{20} of 5-HT has no effect on 5-HT-induced ion currents. **B**, Co-application of 1 mM 5-HI with an E_{max} of 5-HT. These traces are typical traces representative of several experiments.

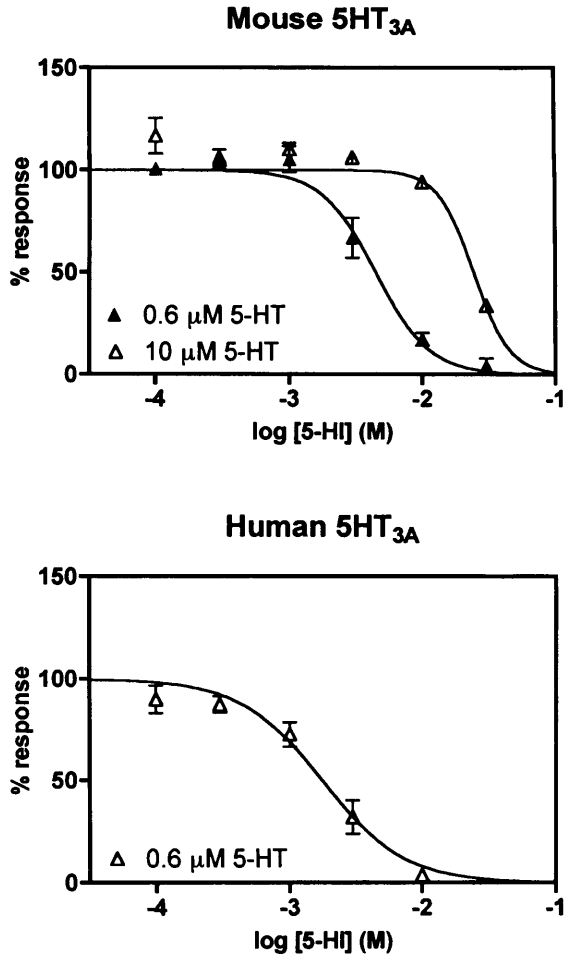

Figure 4.10 *Effect of 5-HI on $5HT_{3A}$ receptors expressed in Xenopus oocytes.* Concentration-response curves of 5-HI co-applied with a fixed concentration of 5-HT. Each set of data points was obtained from the same oocyte, repeated 3 times with different oocytes. Data are mean percentage of control response ± standard error. Co-application of 5-HI with an EC_{20} of 5-HT inhibits 5-HT-induced ion currents in oocytes expressing mouse or human $5HT_{3A}$, with IC_{50}s 4.5 ± 0.09 and 1.8 ± 0.04 mM respectively. When 5-HI is co-applied with an E_{max} concentration of 5-HT to oocytes expressing $m5HT_{3A}$, the inhibition by 5-HI occurs at a higher concentration (IC_{50} of 24 ± 1.01 mM). Goodness of curve fits: mouse (0.6 μM 5HT), R^2=0.9466; mouse (10 μM 5HT), R^2=0.6872; human, R^2=0.9227.

There were no significant effects of 5-HI on the decay kinetics of the $5HT_{3A}$Rs expressed in oocytes. The 5-HT application time was increased from 10 to 75 seconds to ensure that any differences could be measured, but no significant effects were observed (data not shown).

4.7 Splice variants of the mouse $5HT_{3A}$R subunit

The stable HEK293 cell line which showed potentiation in the presence of 5-HI expresses the short splice variant of the mouse $5HT_{3A}$ subunit ($m5HT_{3A(S)}$). Transiently transfected HEK293 cells and oocytes which were not potentiated by 5-HI express the long splice variant of the mouse $5HT_{3A}$ subunit ($m5HT_{3A(L)}$). The long $m5HT_{3A}$ splice variant differs from the short by an additional 6 amino acids in the large intracellular loop between transmembrane regions 3 and 4 (Figure 4.11). This difference is reported to have little effect on the pharmacological properties of the receptors, although differences in the efficacy of the agonist 2-Methyl-5-hydroxytryptamine have been reported (Niemeyer and Lummis, 1998). In the human genome only a single functional splice variant of the $5HT_{3A}$ subunit has been detected ($5HT_{3A(S)}$) (Miyake *et al.*, 1995). It was thought that the reason for contradictory results observed for the $m5HT_{3A}$R might be due to the use of different splice variants.

$5HT_{3A(S)}$	^{375}FQANKTDDCS_____AMGNHCSHVG
$5HT_{3A(L)}$	^{375}FQANKTDDCSGSDLLPAMGNHCSHVG

Figure 4.11 *Alignment of the partial amino acid sequence from the large intracellular loop of the mouse $5HT_{3A(S)}$ and $5HT_{3A(L)}$ subunits.*

To examine whether differences in the ability of 5-HI to potentiate the mouse $5HT_{3A}$R could be attributed to the differential splicing of the subunit, *Xenopus* oocytes were injected with $m5HT_{3A(S)}$ (obtained from Dr Sarah Lummis). Application of 5-HT to oocytes expressing the $m5HT_{3A(S)}$ subunit resulted in

transient desensitising inward currents. A concentration-response curve for 5-HT-induced ion currents with $m5HT_{3A(S)}$ was constructed yielding estimates of EC_{50} and n_H of 1.3 μM and 2.6, respectively (n=1). Various concentrations of 5-HI were co-applied with 5-HT at EC_{20} (0.8 μM). 5-HI did not potentiate the currents, but rather inhibited the 5-HT-induced ion currents with an IC_{50} of 1.3 mM, n_H of -1.5. When 5-HI was co-applied with an E_{max} concentration of 5-HT a slowing of the desensitisation kinetics was observed and there was no potentiation of the current peak. These results are consistent with those of Gunthorpe and Lummis, 1999 ($m5HT_{3A(S)}$ expressed in HEK293 cells), but differ from those of van Hooft *et al.*, 1997 (native $m5HT_3$Rs in N1E-115 cells). The experiments in this section were performed by Dr Ruud Zwart at Eli Lilly.

4.8 Comparison of the short and long mouse $5HT_{3A}$ and human $5HT_{3A}$ subunits in transiently transfected tsA201 and HEK293 cells using a FLIPR

4.8.1 Comparison of $m5HT_{3A(S)}$, $m5HT_{3A(L)}$ and $h5HT_{3A}$ receptors in tsA201 cells

The effects of 5-HI on the 5-HT-induced responses of the $m5HT_{3A(S)}$ receptor subunit were studied, alongside the $m5HT_{3A(L)}$ and $h5HT_{3A}$ receptors. The subunits were transiently transfected into tsA201 cells and assayed using a FLIPR. As previously observed, 1 mM 5-HI had no effects on the 5-HT-induced responses of the $h5HT_{3A}$R (Figure 4.12A(i)). However, the responses of both $m5HT_{3A(S)}$ and $m5HT_{3A(L)}$ were slightly potentiated in the presence of 1 mM 5-HI (Figure 4.12A(ii) and (iii)). The responses were potentiated most at the higher 5-HT concentrations. The size of the responses of $m5HT_{3A(L)}$ were significantly increased in the presence of 5-HI by approximately 20% at 5-HT concentrations of 10 μM and above. The increases in the responses of $m5HT_{3A(S)}$ in the presence of 5-HI were consistently, but not, significantly increased at 30 and 100 μM 5-HT, compared to controls. When assayed using a FLIPR, the responses of the $m5HT_{3A(S)}$ subunit were less robust than those of the $m5HT_{3A(L)}$, for example, the baseline fluorescence decreased significantly over the time course of the experiment; therefore accurate extraction of data such as 'maximum fluorescence – minimum fluorescence' was not possible.

Figure 4.12 *5-HT concentration-response curves showing the effects of 5-HI on $m5HT_{3A(S)}$, $m5HT_{3A(L)}$ and $h5HT_{3A}$ transiently transfected in tsA201 and HEK293 cells.* tsA201 (**A**) and HEK293 (**B**) cells were transiently transfected with the $m5HT_{3A(S)}$ (i), $m5HT_{3A(L)}$ (ii) and $h5HT_{3A}$ (iii) subunits. Responses to 5-HT in the presence or absence of 5-HI were assayed using a FLIPR. Responses are expressed relative to maximal 5-HT. Data is mean ± standard error for at least 3 independent experiments. Significance determined by Student's *t* test (*$p<0.05$; **$p<0.01$). Goodness of curve fits: A(i) control, $R^2=0.9974$; +5-HI, $R^2=0.9985$; A(ii) control, $R^2=0.9958$; +5-HI, $R^2=0.9977$; A(iii) control, $R^2=0.9975$; +5-HI, $R^2=0.9982$; B(i) control, $R^2=0.9857$; +5-HI, $R^2=0.9804$; B(ii) control, $R^2=0.9944$; +5-HI, $R^2=0.9960$; B(iii) control, $R^2=0.9721$; +5-HI, $R^2=0.9969$. Insets show example traces upon application of 10 μM 5HT in the presence (blue) or absence (red) of 1 mM 5-HI. Addition of buffer alone is shown by a black trace. Horizontal axis is time (160 seconds); Vertical axis is change in fluorescence/baseline fluorescence (0.8-2.1 units for A(i) and (ii); 0.8-1.5 units for A(iii) and B).

The effects of 1 mM 5-HI on the 5-HT-induced responses of $m5HT_{3A(L)}$ expressed in tsA201 cells (Figure 4.12A(ii)) differed from those of $m5HT_{3A(L)}$ previously observed in transiently transfected HEK293 cells (Section 4.5.2, Figure 4.7) in that a significant increase in response size in transiently transfected tsA201 cells was observed. Also, an increase in responses to 5-HT in the presence of 5-HI of $m5HT_{3A(S)}$ expressed in tsA201 cells was observed. To determine whether these differences were cell-type specific, the experiments were repeated using transiently transfected HEK293 cells.

4.8.2 Comparison of $m5HT_{3A(S)}$, $m5HT_{3A(L)}$ and $h5HT_{3A}$ receptors in HEK293 cells

HEK293 cells were transiently transfected with $m5HT_{3A(S)}$, $m5HT_{3A(L)}$ or $h5HT_{3A}$ and assayed using a FLIPR. Co-application of 1 mM 5-HI with 5-HT did not, as observed previously, potentiate responses when $h5HT_{3A}$ was expressed in HEK293 cells. The responses appeared to be slightly inhibited by 5-HI (Figure 4.12B(i)). The 5-HT-induced responses of mouse $5HT_{3A(L)}$ expressed in HEK293 cells were slightly and consistently increased when 1 mM 5-HI was co-applied with 5-HT, particularly at the higher 5-HT concentrations (Figure 4.12B(ii)). The increase was statistically significant at 5-HT concentrations of 10 μM and above. The 5-HT-induced responses of the mouse $5HT_{3A(S)}$ expressed in HEK293 cells were highly variable. Co-application of 1 mM 5-HI with 5-HT did not have any significant effect on the responses (Figure 4.12B(iii)), although the concentration-response curve could not be fit well.

Generally, the responses from transiently transfected HEK293 cells were not as consistent as responses from tsA201 cells. The amplitudes of the responses from HEK293 cells varied significantly between wells, and frequently the baseline fluorescence decreased over the time course of an experiment which led to inaccuracies when data such as 'maximum fluorescence – minimum fluorescence' were extracted using the FLIPR computer software. Usually, experiments were performed in HBSS. In an attempt to optimise experimental conditions for the HEK293 cells, Tyrodes buffer was used, as previously robust responses from $5HT_{3A}$ receptors expressed in HEK293 cells were recorded in this buffer. However, the stability of the responses did not improve.

4.8.3 *Analysis of the decay of the responses of the mouse and human $5HT_{3A}R$ in the presence and absence of 5-HI*

Although differences in potentiation of the peak responses between the $m5HT_{3A}$ splice variants were observed as well as differences between cell types, the decay of the responses of both $m5HT_{3A(S)}$ and $m5HT_{3A(L)}$ were quite clearly affected by 5-HI in both tsA201 and HEK293 cells. If control responses are compared to responses in the presence of 5-HI then a decrease in the rate of decay of the responses where 5-HI is present can clearly be seen. Typical time-sequence traces illustrate this (Figure 4.13A and 4.13B). The responses of $h5HT_{3A}$ were never potentiated by 5-HI and it did not affect the decay of the responses as illustrated (Figure 4.13C).

To further investigate the effects of 5-HI on the decay of the responses, particularly of the $m5HT_{3A}$Rs, the data from FLIPR assays was re-analysed. The sum of the area under the curve was extracted from the point of agonist addition to a point near the end of the experiment; the results are described below.

Analysis of the area under the curve of 5-HT-induced responses of $h5HT_{3A}$ transiently expressed in tsA201 cells showed that it was not significantly affected by 5-HI (Figure 4.14A(i)). The responses in the presence of 1 mM 5-HI were not significantly different from those in the absence of 5-HI. When $h5HT_{3A}$ was expressed in HEK293 cells, 5-HT responses were inhibited slightly by 1 mM 5-HI. 5-HI had no statistically significant effect on the responses (Figure 4.14A(ii)), but at 5-HT concentrations of 3 μM and below responses were more evidently inhibited than at 5-HT concentrations greater than 3 μM.

In tsA201 cells expressing mouse $5HT_{3A(L)}$, the area under the curve of responses at the higher 5-HT concentrations was clearly increased (35-60%; significant at some 5-HT concentrations) in the presence of 1 mM 5-HI (Figure 4.14B(i)). In HEK293 cells, there was a clear increase in the area under the curve (15-42%), but it was not statistically significant (Figure 4.14B(ii)).

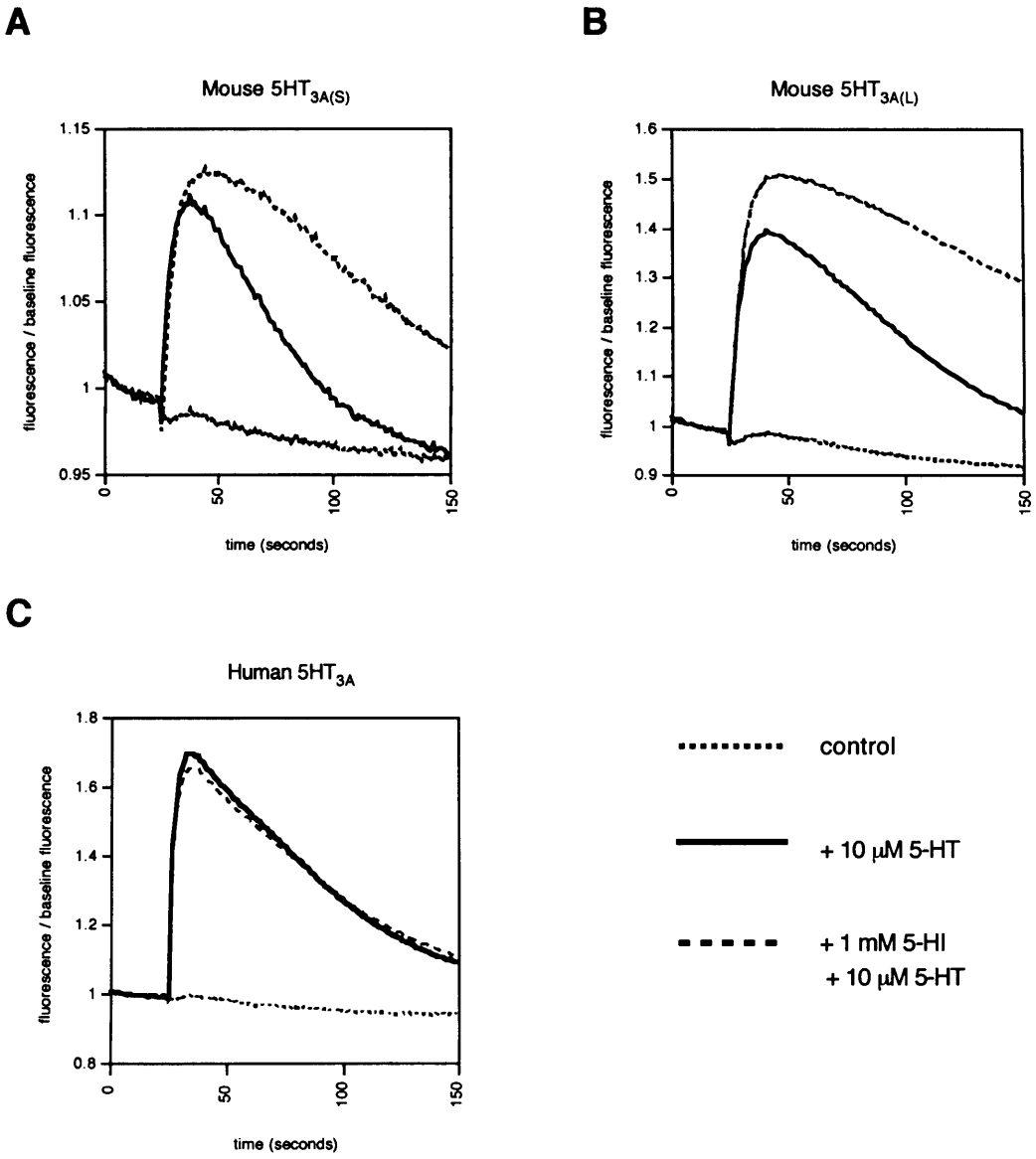

Figure 4.13 *Typical responses showing the effects of 5-HI on $5HT_{3A}$ receptors expressed in mammalian cells.* Cells (tsA201) were transiently transfected with the $m5HT_{3A(S)}$ (**A**), $m5HT_{3A(L)}$ (**B**) or $h5HT_{3A}$ (**C**) subunit. Responses shown are with the addition of buffer (control), with the addition of 10 µM 5-HT and with the addition of 1 mM 5-HI and 10 µM 5-HT, assayed using a FLIPR. Responses are averages of 2-6 wells from a typical experiment and are also representative of those observed in HEK293 cells.

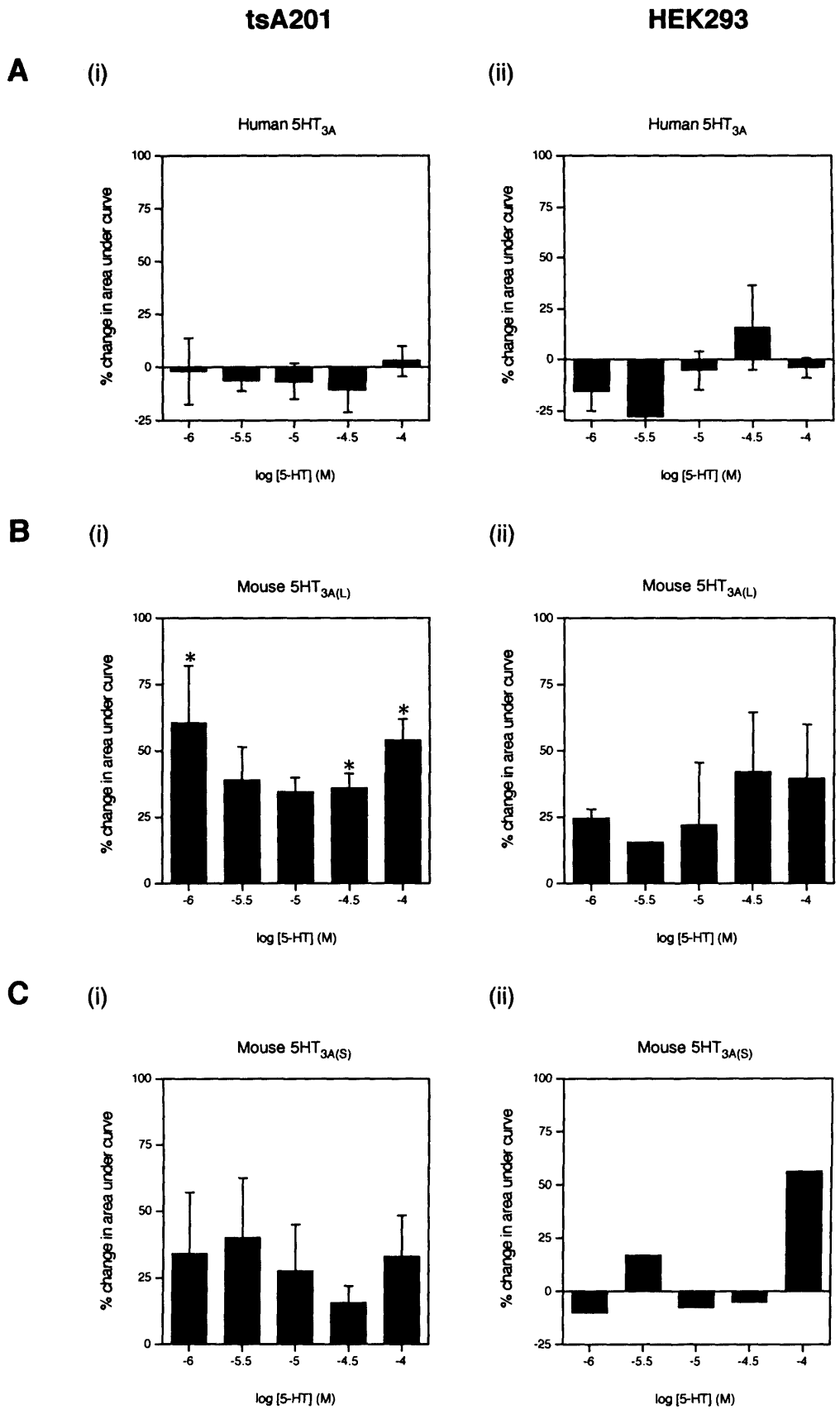
tsA201
HEK293
A
(i)
(ii)
Human 5HT3A
Human 5HT3A
% change in area under curve
log [5-HT] (M)
B
(i)
(ii)
Mouse 5HT3A(L)
Mouse 5HT3A(L)
C
(i)
(ii)
Mouse 5HT3A(S)
Mouse 5HT3A(S)

Figure 4.14 *Effects of 5-HI on 5-HT-induced responses of $5HT_{3A}$ receptors, expressed as area under the curve.* HEK293 cells (right panel, (ii)) and tsA201 cells (left panel, (i)) were transiently transfected with $h5HT_{3A}$ (**A**), $m5HT_{3A(L)}$, (**B**), or $m5HT_{3A(S)}$ (**C**) and the effects of 5-HI on 5-HT-induced responses assayed using a FLIPR. Data was extracted as area under curve. The average percentage change, in the presence of 5-HI, compared to control (5-HT alone) is plotted for several 5-HT concentrations. Data is mean ± standard error for at least 3 independent experiments, except for C(ii) where n = 1. Significance was determined by Student's *t* tests (*$p<0.05$); data at each 5-HT concentration was compared with control data (in the absence of 5-HI) of the same 5-HT concentration.

In tsA201 cells expressing $m5HT_{3A(S)}$ the area under the curve of responses was consistently increased (15-48%) in the presence of 1 mM 5-HI, but was not shown to be statistically significant (Figure 4.14C(i)). The responses of $m5HT_{3A(S)}$ in HEK293 cells were variable and it was difficult to extract the area under the curve data from many experiments (Figure 4.14C(ii)), so conclusions cannot be drawn.

4.9 Effects of 5-HI on the $5HT_{3A}$ chimeras assayed using a FLIPR

The $5HT_{3A}$ chimeras, described in Section 4.3, were studied using a FLIPR. The effects of 5-HI on the 5-HT-induced responses of the $m/h5HT_{3A}$ chimera and $h/m5HT_{3A}$ chimera transiently transfected in both tsA201 and HEK293 cells were examined.

4.9.1 Effects of 5-HI on the $5HT_{3A}$ chimeras transiently transfected in HEK293 cells

HEK293 cells were transiently transfected with the chimeric subunits using the FuGene transfection reagent. The effects of 5-HI on the 5-HT-induced responses of the chimeras were examined through the use of a FLIPR assay. Application of 5-HT evoked increases in intracellular Ca^{2+}, whereas application of 5-HI did not. Co-application of 1 mM 5-HI slightly inhibited the 5-HT responses (data not shown) as previously observed for the mouse $5HT_{3A(L)}$ and human $5HT_{3A}$ subunits assayed in this way (Section 4.5.2).

4.9.2 Effects of 5-HI on the $5HT_{3A}$ chimeras transiently transfected in tsA201 cells

Cells (tsA201) were transiently transfected with the chimeric subunits and the effects of 5-HI studied using a FLIPR. Responses to 5-HT of both chimeras were slightly increased in the presence of 5-HI (Figure 4.15). Selected traces illustrate that although 5-HI did not always potentiate the peak of responses it did have an effect on the 5-HT induced responses of the chimeras (Figure 4.16). A slowing of the decay of the responses for both chimeras was observed in the presence of 5-HI. Analysis of the area under the curve of the responses showed that 5-HI potentiated the responses of both the $m/h5HT_{3A}$ chimera and $h/m5HT_{3A}$ chimera (Figure 4.17). The $m/h5HT_{3A}$

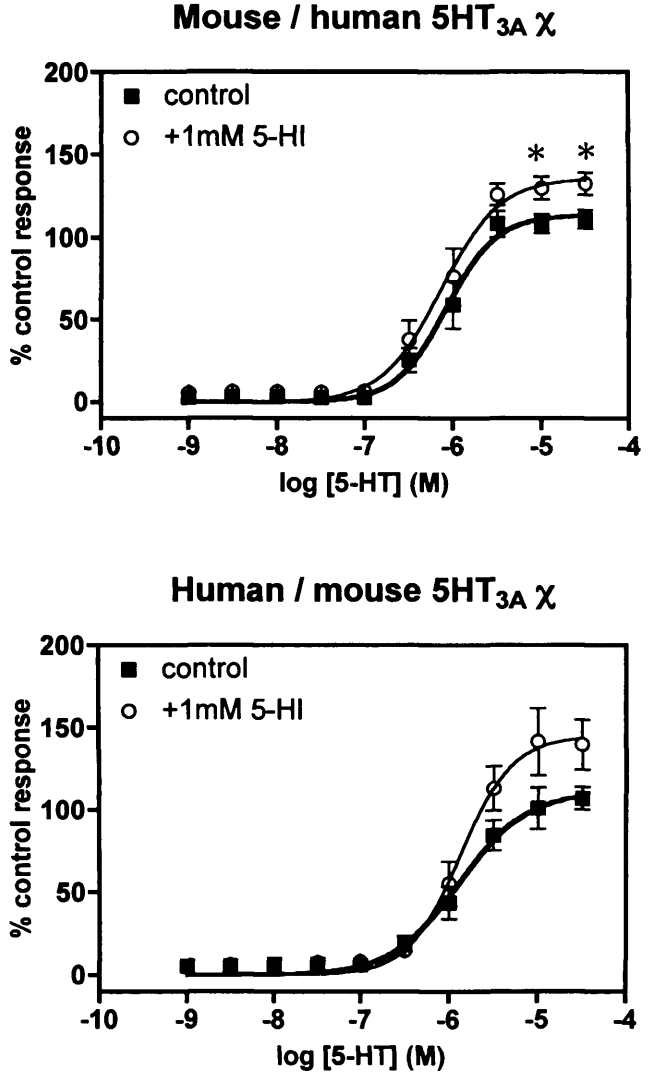

Figure 4.15 *Effects of 5-HI on the $5HT_{3A}$ chimeras expressed in tsA201 cells.* Concentration-response curves of 5-HT alone or with 5-HI obtained from recombinant m/h$5HT_{3A}$ chimera or h/m$5HT_{3A}$ chimera transiently transfected in tsA201 cells. Responses are expressed relative to maximal (30 μM) 5-HT control responses. Traces represent mean ± standard error of at least 3 experiments. Significance determined by Student's *t* test (*$p<0.05$). Goodness of curve fits: m/h5HT3A χ control, $R^2=0.9927$; +5-HI, $R^2=0.9921$; h/m5HT3A χ control, $R^2=0.9911$; +5-HI, $R^2=0.9931$.

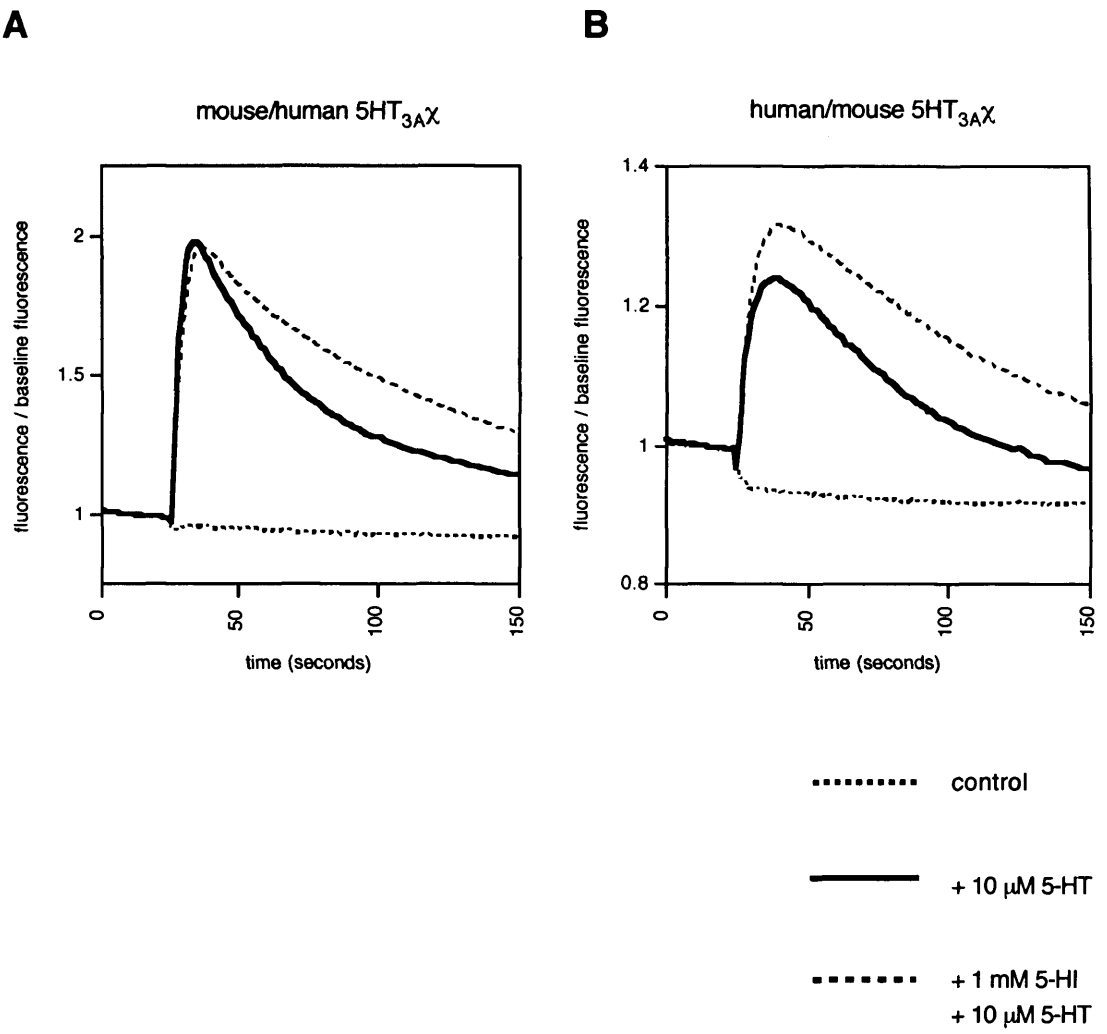

Figure 4.16 *Typical responses showing the effects of 5-HI on $5HT_{3A}$ chimeras expressed in mammalian cells.* Cells (tsA201) were transiently transfected with the m/h$5HT_{3A}$ (**A**) and h/m$5HT_{3A}$ (**B**) chimeric subunits. Responses shown are with the addition of buffer (control), with the addition of 10 μM 5-HT or with the addition of 1 mM 5-HI and 10 μM 5-HT, assayed using a FLIPR. Responses are averages of 4 wells. The trace in B shows potentiation of the peak response; this did not always occur, nor did the lack of potentiation illustrated in A.

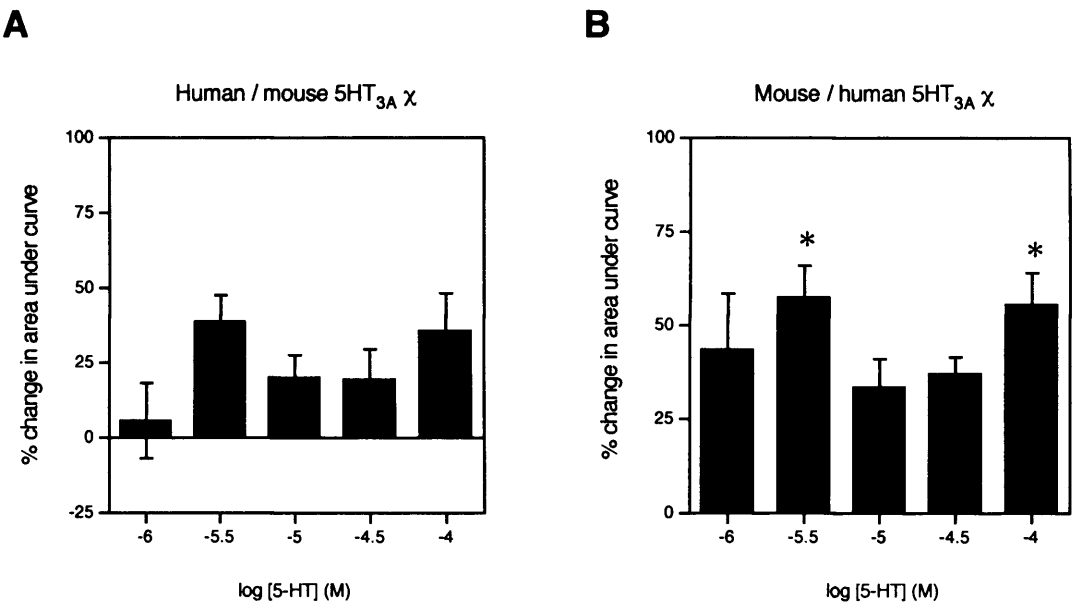

Figure 4.17 *Effects of 5-HI on the $5HT_{3A}$ chimeras, expressed as area under the curve.* Cells (tsA201) were transiently transfected with the h/m$5HT_{3A}$ chimera (A) or the m/h$5HT_{3A}$ chimera (B). Responses to 5-HT in the presence or absence of 5-HI were assayed using a FLIPR. Area under curve data was extracted and the average percentage change compared to control plotted. Data is mean ± standard error for at least 4 independent experiments. Significance determined by Student's *t* test (*$p<0.05$); data at each 5-HT concentration was compared with control data (in the absence of 5-HI) of the same 5-HT concentration.

chimera responses were potentiated slightly more than those of the h/m$5HT_{3A}$ chimera and at some 5-HT concentrations were shown to be significantly enhanced.

4.10 Discussion

In this study, the effects of 5-HI at the mouse and human $5HT_{3A}$Rs were investigated. 5-HI, the aromatic moiety of 5-HT, has been shown to potentiate the responses of the mouse $5HT_{3A}$R (Kooyman *et al.*, 1993; Kooyman *et al.*, 1994; van Hooft *et al.*, 1997) and is also reported to potentiate the α7 nAChR (Gurley *et al.*, 2000; Zwart *et al.*, 2002). The potentiation of the $5HT_3$R is accompanied by a slowing of the current decay (Kooyman *et al.*, 1994). 5-HI (at concentrations up to 10 mM) potentiates responses of $5HT_3$R, but at higher concentrations (greater than 10 mM) blocks 5-HT-evoked currents. The potentiating effects of 5-HI are thought to be mediated via a non-competitive interaction whereby the open state of the receptor is stabilised (Kooyman *et al.*, 1994; van Hooft *et al.*, 1997). The blocking action of 5-HI is thought to be mediated by a competitive interaction (Kooyman *et al.*, 1994).

The action of 5-HI on the mouse and human $5HT_{3A}$Rs was previously investigated at Eli Lilly. Mouse $5HT_{3A(S)}$ receptor cDNA stably expressed in the HEK293 cell line was potentiated by 5-HI, whilst human $5HT_{3A}$ stably expressed in the HEK293 cell line showed no evidence of potentiation. The aim of this project was to investigate the different activity of 5-HI on the different $5HT_{3A}$R species and in so doing identify regions or residues involved in 5-HI binding. The structural determinants of ligand binding at the $5HT_3$R are not yet fully characterised. Several regions and some specific residues involved in ligand binding to the $5HT_3$R have been identified. Evidence from studies with the nAChR, $GABA_A$ and glycine receptors suggest the extracellular N-terminal portion of the receptor to contain the ligand binding domain (Dunn *et al.*, 1994; Karlin and Akabas, 1995; Kuhse *et al.*, 1995). Further evidence has been provided by studies of a chimeric subunit consisting of the N-terminal region of α7 up to TM1, fused to the remainder of mouse $5HT_{3A}$ (α7/$5HT_{3A}$) (Eiselé *et al.*, 1993). The α7/$5HT_{3A}$ chimera displays the pharmacological properties of the nicotinic receptor, but ion channel properties of the $5HT_3$R. Further evidence of the

N-terminal domain of the $5HT_3R$ containing the ligand binding site was provided by human/mouse $5HT_{3A}$ chimeric constructs (Hope *et al.*, 1999). The $5HT_3R$ antagonist, *d*-tubocurarine (*d*-TC), is more potent at mouse than at human $5HT_{3A}$ receptors. Replacement of the entire extracellular N-terminal portion of the mouse $5HT_{3A}$ with that of the human, and vice versa, switches the differential potency of *d*-TC, indicating that the ligand binding site is contained within this region. A number of individual residues and groups of residues important in binding specific ligands have also been identified; for example glutamate 106 is found to be important in ligand recognition (Boess *et al.*, 1997).

Defining the binding site of 5-HI would be useful for the rationalisation of drug design, with the final aim of generating $\alpha 7$ nAChR selective potentiators which might be useful in the treatment of neurological disorders such as neurodegeneration (Maelicke and Albuquerque, 2000; Dani *et al.*, 2004). From previous studies (unpublished data, Eli Lilly), it was thought likely that 5-HI would act via the extracellular N-terminal domain of the $5HT_3R$. Through the use of human/mouse $5HT_{3A}$ chimeric subunits it was hoped that residues and/or regions implicated in the binding of this compound could be identified.

The potentiation of the mouse $5HT_{3A(S)}R$, stably expressed in the HEK293 cell line, by 5-HI was confirmed. Using a FLIPR, the 5-HT-induced elevations in intracellular calcium were enhanced in the presence of 1 mM 5-HI; the peaks of responses were significantly increased. Human $5HT_{3A}$, stably expressed in the HEK293 cell line, was not potentiated by 5-HI as had been seen in previous studies (unpublished data, Eli Lilly). However, when the experiments were repeated in HEK293 cells transiently expressing the subunits, the results were not consistent with those obtained with stably transfected cells. Surprisingly, the peaks of the 5-HT-evoked responses of mouse $5HT_{3A(L)}$ were not potentiated in the presence of 5-HI. The responses of both mouse $5HT_{3A(L)}$ and human $5HT_{3A}R$ were inhibited by 1 mM 5-HI. To ensure that the fluo-3 calcium-sensitive dye was not being saturated, and therefore obscuring any potentiation of the mouse $5HT_{3A(L)}R$, the calcium concentration of the assay buffer was reduced. Response size decreased with reduced calcium concentrations, yet no potentiation was observed. The presence of 1 mM 5-HI did however cause a slowing of response decay for the mouse $5HT_{3A(L)}R$.

This effect of 5-HI has previously been reported (Kooyman *et al.*, 1993; Kooyman *et al.*, 1994; van Hooft *et al.*, 1997; Gunthorpe and Lummis, 1999).

To investigate the effects of 5-HI on the 5-HT-evoked responses of the $5HT_{3A}R$ in an alternative expression system, *Xenopus* oocytes were utilised. 5-HI (1 mM) did not potentiate the amplitude of 5-HT-evoked currents of human $5HT_{3A}$, mouse $5HT_{3A(L)}$ or mouse $5HT_{3A(S)}$ expressed in *Xenopus* oocytes. At higher concentrations, 5-HI was seen to inhibit responses of both mouse and human $5HT_{3A}Rs$. The blocking effect of 5-HI was surmounted with increasing 5-HT concentrations suggesting that 5-HI was interacting in a competitive manner. The blocking effect of 5-HI has previously been reported to be mediated by a competitive interaction with the agonist/antagonist recognition sites of the $5HT_3R$ (Kooyman *et al.*, 1994). 5-HI (1 mM) did not appear to effect the decay kinetics of $m5HT_{3A(L)}$ or $h5HT_{3A}$. In order to examine a possible effect of 5-HI on the decay kinetics of 5-HT-evoked currents the application time of 5-HI was extended; no effects were observed. The current decay kinetics of $m5HT_{3A(S)}$ were slowed by 3 mM 5-HI which is consistent with some reports (Gunthorpe and Lummis, 1999). The 5-HT-evoked currents of $h5HT_{3A}$ and $m5HT_{3A(L)}$ expressed in *Xenopus* oocytes were non-desensitising, but those of $m5HT_{3A(S)}$ did desensitise. This difference may explain why a slowing of decay kinetics was observed in the presence of 5-HI for $m5HT_{3A(S)}$, but not for $m5HT_{3A(L)}$.

To eliminate the possibility that the differing effects of 5-HI on the $m5HT_{3A}R$, expressed in HEK293 cells, were due to differences between splice variants, both $m5HT_{3A(S)}$ and $m5HT_{3A(L)}$ (and $h5HT_{3A}$) were compared in parallel. Transiently transfected HEK293 cells and a subclone, the tsA201 cell line, were used. The responses in HEK293 and tsA201 cells were comparable, although generally the responses from HEK293 cells were less stable and less consistent than those from tsA201 cells. It was not the expression of $5HT_{3A}$ in HEK293 cells which caused this as untransfected cells behaved similarly.

The absence of an effect of 5-HI on the $h5HT_{3A}$ receptor was observed consistently. In HEK293 cells, 1 mM 5-HI slightly inhibited 5-HT-induced responses. This finding suggests that 5-HI is capable of interacting with the human $5HT_{3A}R$ in a competitive manner, thereby inhibiting binding of 5-HT. Although not always

statistically significant, 5-HI did have potentiating effects on both $m5HT_{3A(L)}$ and $m5HT_{3A(S)}$. Potentiation of the peaks of responses (up to 36% ($m5HT_{3A(L)}$) and up to 84% ($m5HT_{3A(S)}$)) was observed at the higher 5-HT concentrations (above 3 μM) in the presence of 5-HI. Increases in the area under the curve of responses for both $m5HT_{3A(L)}$ and $m5HT_{3A(S)}$ were observed. The results from $m5HT_{3A(S)}$ transiently expressed in HEK293 cells were very difficult to analyse, but there was evidence of 5-HI potentiating responses. Taken together, these further experiments provided evidence to reconfirm the original finding that $m5HT_{3A}$ is potentiated by 5-HI, whilst $h5HT_{3A}$ is not.

Through the use of mouse/human $5HT_{3A}$ chimeras it was originally hoped that the regions involved in 5-HI binding could be defined. The $m/h5HT_{3A}$ chimera consisted of the extracellular N-terminal domain of mouse $5HT_{3A(L)}$ fused to the remainder of human $5HT_{3A}$ from M1. The $h/m5HT_{3A}$ chimera consisted of the extracellular N-terminal domain of $h5HT_{3A}$ fused to the C-terminal of $m5HT_{3A(L)}$ from M1. Based on previous experimental data (Eiselé *et al.*, 1993; Hope *et al.*, 1999) suggesting that the N-terminal domain contained the ligand binding site it was predicted that the $m/h5HT_{3A}$ chimera would be potentiated by 5-HI and that the $h/m5HT_{3A}$ chimera would not. It was hoped that these chimeras would be the basis for creating further chimeric subunits and mutants to narrow down regions and residues involved in conferring 5-HI sensitivity to the $m5HT_{3A}R$.

The results obtained with the $5HT_{3A}$ chimeric subunits were not as expected. The peaks of 5-HT-induced responses of both chimeras were slightly potentiated in the presence of 5-HI. Analysis of the area under the curve of responses in the presence of 5-HI increased for both chimeras suggesting that 5-HI affected the decay kinetics of the responses. These results suggested that both the C- and N-terminal regions of $5HT_{3A}$ may be involved in mediating the effects of 5-HI. Evidence for both the C- and N-terminal regions mediating the actions of 5-HI is also provided by studies using $\alpha7/5HT_{3A}$ chimeras performed at Eli Lilly (see Section 4.2). Although both human $\alpha7$/mouse $5HT_{3A}$ and human $\alpha7$/human $5HT_{3A}$ chimeras were potentiated by 5-HI, the potentiation of the human $\alpha7$/human $5HT_{3A}$ chimera was less significant, suggesting the C-terminal region to be involved.

A recent study has identified a residue in the α7 nAChR subunit, mutation of which results in the loss of potentiation by 5-HI (Placzek *et al.*, 2004). The mutation (threonine to phenylalanine) is at the beginning of M2 (in the 6' position according to the numbering scheme proposed by Miller (1989)). These results suggest that the action of 5-HI could be mediated by a region outside of the extracellular N-terminal domain, although it was not shown whether this mutation abolishes 5-HI binding. The binding of 5-HI may induce a conformational change involving M2 which could result in an agonist remaining bound to a receptor for longer. This threonine residue is conserved in both mouse and human $5HT_{3A}$ and so cannot explain the species differences observed.

An alternative approach to identify residues important in 5-HI sensitivity has been used in studies performed by a research group at Eli Lilly. A sequence alignment of the mouse and human $5HT_{3A}$ receptor subunits and the human and rat α7 neuronal nAChR subunits was made. Three residues which were found to be conserved between the rat and human α7 nAChRs and $m5HT_{3A}R$, but not $h5HT_{3A}$ were identified in the extracellular N-terminal domain of the subunits. These residues were identified as possibly conferring 5-HI sensitivity. Molecular modelling studies using the predicted structure of the nAChR binding site deduced from the ACh binding protein (Smit *et al.*, 2001; Brejc *et al.*, 2001) suggested that the residues identified were likely to be involved in ligand binding. Mutant $h5HT_{3A}$ subunits were constructed where the differing residues were replaced by the conserved homologous mouse $5HT_{3A}$/α7 nAChR residues. Single, double and triple point mutations were made in $h5HT_{3A}$. The mutants were introduced by transient transfection into HEK293 cells and the effects of 5-HI on 5-HT responses studied using a FLIPR. All of the mutants tested were functional, but none were potentiated by 5-HI, suggesting that these residue differences were not responsible for sensitivity to 5-HI (unpublished results, Eli Lilly).

In summary, the species specific activity of 5-HI at the mouse and human $5HT_{3A}$Rs has been confirmed; 5-HI potentiates the 5-HT induced responses of the $m5HT_{3A(L)}$ and $m5HT_{3A(S)}$, but not of the $h5HT_{3A}$. Studies using human/mouse chimeric subunits have provided evidence for the involvement of regions other than the

extracellular N-terminal domain in conferring 5-HI sensitivity, possibly by an allosteric mechanism.

4.11 Future directions

The ligand binding site of the $5HT_3R$ requires extensive further characterisation. The binding site and mechanism of action for 5-HI are still to be characterised.

Studies, conducted by others at Eli Lilly, identified residues that were not conserved between mouse and human $5HT_{3A}$, but which were conserved between mouse $5HT_{3A}$ and rat and human $\alpha 7$ (which are all potentiated by 5-HI). None of the residues identified were shown to be responsible for conferring 5-HI sensitivity (unpublished data, Eli Lilly). There are a number of residues which are not conserved between mouse and human $5HT_{3A}$ (or $\alpha 7$) in the extracellular N-terminal domain. It would be interesting to study these residues further using site directed mutagenesis to determine whether they are responsible for conferring sensitivity to 5-HI and its analogues. By drawing analogies with the $\alpha 7$ nAChR many of these unconserved residues are predicted to be in 'loop 3', or 'C', of the principal binding component. This loop region has been identified as involved in the binding of several other $5HT_3R$ ligands (Lankewicz *et al.*, 1998; Hope *et al.*, 1996; Hope *et al.*, 1997; Hope *et al.*, 1999).

Human $5HT_{3A}$ differs from mouse $5HT_{3A}$ by a five amino acid deletion in the extracellular N-terminal domain. The homologous residues could be deleted in mouse $5HT_{3A}$ to determine whether these residues are important in ligand binding, particularly in conferring 5-HI sensitivity.

CHAPTER 5

Investigation of the effects of the RIC3 proteins on the α7 nAChR and $5HT_{3A}R$ expressed in mammalian cells

5.1 Introduction

The folding, assembly and cell-surface expression of ligand-gated ion channels is a complex and poorly understood process. The α7 nicotinic acetylcholine receptor (nAChR) subunit forms functional homomeric receptors when expressed in *Xenopus* oocytes (Couturier *et al.*, 1990) and in some cultured mammalian cells lines (Puchacz *et al.*, 1994; Gopalakrishnan *et al.*, 1995). However, the inefficient expression of the α7 subunit in a number of other mammalian cell lines has suggested cell-specific factors to be required for the folding, assembly and correct subcellular localisation of this protein (Cooper and Millar, 1997; Dineley and Patrick, 2000; Sweileh *et al.*, 2000).

Recent studies investigating proteins required for nAChR activity in *Caenorhabditis elegans* (*C. elegans)* identified the RIC3 protein (CeRIC3) (Halevi *et al.*, 2002). CeRIC3 and its human homologue (hRIC3) have been shown to enhance the currents of both *C. elegans* DEG-3/DES-2 and mammalian α7 nAChRs expressed in *Xenopus* oocytes (Halevi *et al.*, 2002; Halevi *et al.*, 2003). The RIC3 proteins have been shown to have no effect on the functional expression of the GABA, glutamate and glycine receptors (Halevi *et al.*, 2003). However, hRIC3 has been shown to reduce whole-cell current amplitudes of the α4β2 and α3β4 nAChR and $5HT_{3A}R$ expressed in *Xenopus* oocytes (Halevi *et al.*, 2003).

The CeRIC3 protein is encoded by the *ric-3* gene (resistant to inhibitors of cholinesterase). Mutations in the *ric-3* gene result in the intracellular accumulation of nAChRs suggesting that the CeRIC3 protein plays a role in the maturation of the nAChRs (Halevi *et al.*, 2002).

The RIC3 proteins are a family of conserved proteins, in vertebrates and invertebrates, and all members are predicted to have two transmembrane domains, separated by a proline-rich spacer, followed by at least one coiled-coil domain (Halevi *et al.*, 2003). According to these predictions the RIC3 proteins are located on membranes with their N-terminal domain and C-terminal coiled coil domain(s) in the cytoplasm (Figure 5.1) (Halevi *et al.*, 2003).

In this chapter the effects of the RIC3 proteins co-expressed with the α7 nAChR and $5HT_{3A}R$ in a mammalian cell line have been investigated.

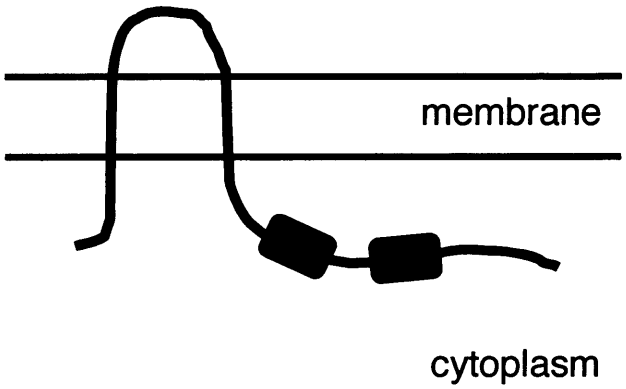

Figure 5.1 *Structure and topology of the RIC3 proteins* (predicted by Halevi *et al.*, 2002; Halevi *et al.*, 2003). Structure predictions suggest the RIC3 proteins to consist of two transmembrane domains separated by a proline-rich domain, followed by at least one coiled coil region (CC), with their N- and C-termini being cytoplasmic.

5.2 Co-expression of the RIC3 proteins with the α7 and α8 nAChRs

5.2.1 Co-expression of the RIC3 proteins with α7 examined by [^{125}I]-α-BTX binding

To investigate the effects of the RIC3 proteins on α7 nAChRs heterologously expressed in a mammalian cell line, rat or human α7 subunit cDNAs were transiently co-transfected into tsA201 cells with CeRIC3 or hRIC3 cDNA. Binding studies were performed on both intact cells and cell membrane preparations with iodinated α-bungarotoxin ([^{125}I]-α-BTX), a nAChR antagonist which binds with high affinity to nAChRs containing the α7 subunit. When expressed alone, neither rat α7 (rα7), human α7 (hα7), CeRIC3 or hRIC3 gave specific [^{125}I]-α-BTX binding. However, when α7 was co-expressed with either CeRIC3 or hRIC3, specific binding was detected, both to cell membrane preparations and to cell surface receptors on intact cells (Figure 5.2). In the absence of RIC3, α7 failed to form a high affinity binding site for α-BTX in this cell line (Cooper and Millar, 1997).

A number of hRIC3 splice variants have been identified, but their functions have not been defined (Halevi *et al.*, 2003). When hRIC3 was cloned, in this laboratory, an alternatively spliced variant was also identified and isolated. This partial hRIC3 clone consisted of the first transmembrane domain spliced to the C-terminal portion. A consequence of this was that this clone lacked a second transmembrane domain and coiled coil domain according to the structure predicted by Halevi *et al.*, 2003. The effects of co-expression of this partial hRIC3 with α7 were examined by performing [^{125}I]-α-BTX binding studies. Co-transfection of the partial hRIC3 clone with α7 did not result in any specific binding of [^{125}I]-α-BTX (n=3, data not shown).

5.2.2 Co-expression of the RIC3 proteins with α8 examined by [^{125}I]-α-BTX binding

The α7 nAChR shares a high sequence similarity with the chick α8 nAChR subunit (Schoepfer *et al.*, 1990). Similar difficulties in efficient heterologous expression of the α8 subunit are also observed (Cooper and Millar, 1998). Therefore, the effects of

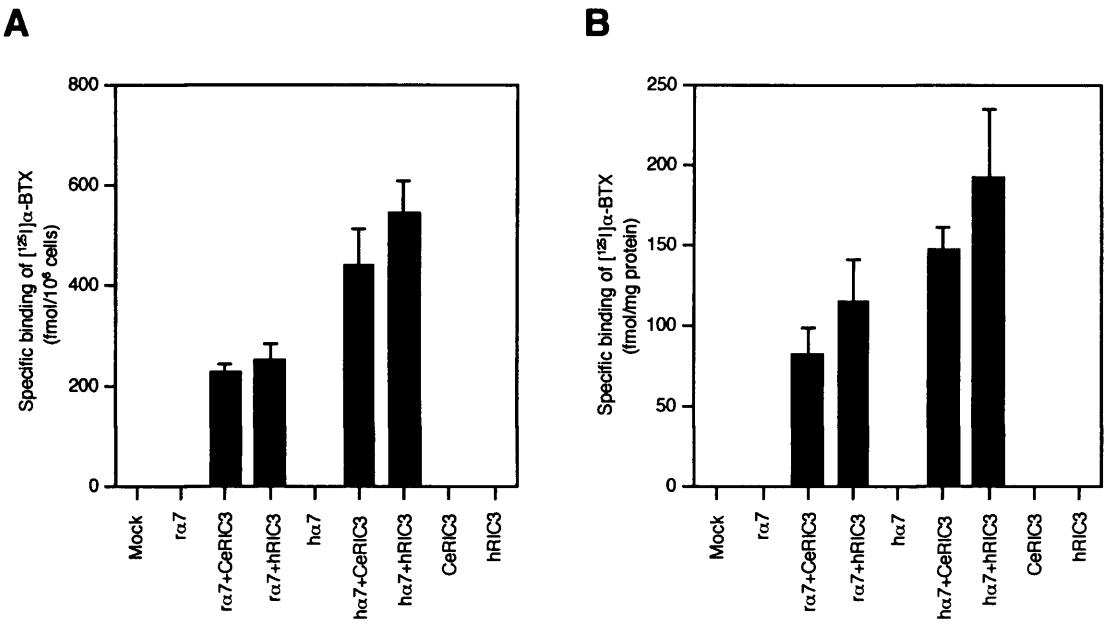

Figure 5.2 *Specific [^{125}I]-α-BTX binding to α7 nAChR subunits co-expressed with the RIC3 proteins.* Cells (tsA201) were transiently transfected with combinations of human or rat α7 with or without CeRIC3 or hRIC3, and binding performed using 10 nM [^{125}I]-α-BTX. **A**, Specific binding to intact cells and **B**, to cell membrane preparations are mean values ± standard error from 3 independent experiments performed in triplicate.

the RIC3 proteins on the α8 subunit were examined. Cells (tsA201) were co-transfected with α8 and the RIC3 proteins and [^{125}I]-α-BTX binding studies were performed. Specific cell-surface binding of [^{125}I]-α-BTX was detected in cells co-transfected with α8 and the RIC3 proteins (Figure 5.3). The experiment was only performed once.

5.2.3 Co-assembly studies of the RIC3 proteins with α7

To enable detection of the RIC3 proteins a FLAG epitope (Hopp *et al.*, 1988) was introduced in the C-terminal region of the proteins (CeRIC3^{FLAG-A} and hRIC3^{FLAG-A}; see Chapter 2, Section 2.4). To investigate whether the RIC3 proteins co-assemble with the α7 nAChR subunit, tsA201 cells were transiently transfected with combinations of α7 and RIC3 cDNAs and examined by immunoprecipitation. The α7-specific antibody mAb319 (raised against a linear intracellular epitope) and mAbFLAG-M2, which recognises the FLAG epitope, were used.

A single band of approximately 58 kDa, absent in untransfected cells, was detected using mAbFLAG-M2, in cells transfected with hRIC3^{FLAG-A}. This band was also detected in cells co-expressing hRIC3^{FLAG-A} with hα7 as well as a co-precipitating band the correct size for α7 (~50 kDa) (Figure 5.4A). Co-precipitation of hRIC3^{FLAGA} with hα7 was observed in cells co-transfected with hα7 and hRIC3^{FLAG-A} using mAb319. In cells co-transfected with untagged hRIC3 a band of approximately 55 kDa was found to co-precipitate with α7 (Figure 5.4B). The absence of cross-reactivity of mAbFLAG-M2 with hα7, and of mAb319 with hRIC3^{FLAG-A} was confirmed (Figure 5.4).

The FLAG-tagged RIC3 proteins appeared to have higher molecular masses than the wild-type proteins. The introduction of a FLAG epitope has previously been reported to lead to an apparent increase in the molecular weight of tagged proteins, such as nAChR subunits (Lansdell and Millar, 2002), and is discussed in Section 5.5.

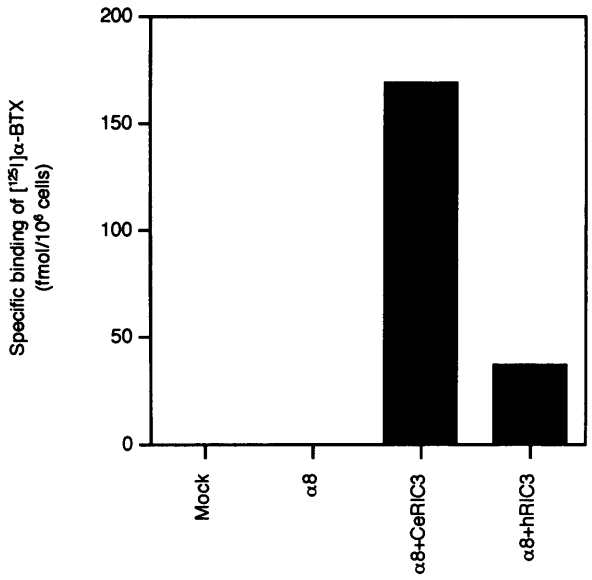

Figure 5.3 *Specific [^{125}I]-α-BTX binding to the chick α8 nAChR subunit co-expressed with the RIC3 proteins.* Cells (tsA201) were transiently transfected with chick α8 with or without CeRIC3 or hRIC3, and binding performed using 10 nM [^{125}I]-α-BTX. The mean value of specific binding to intact cells is shown from one experiment performed in triplicate.

A

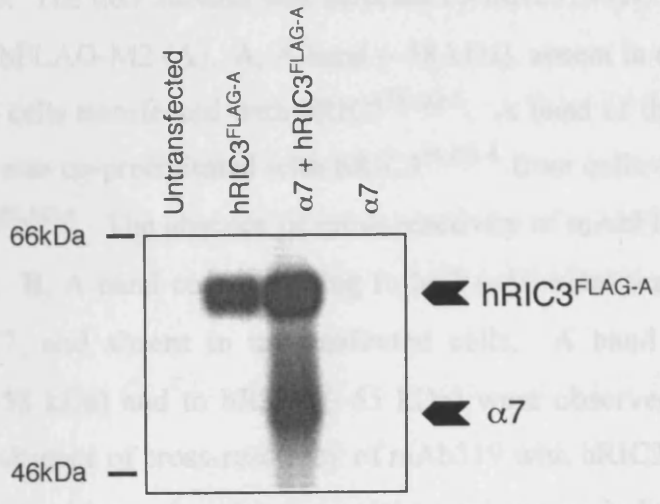
Untransfected
hRIC3FLAG-A
α7 + hRIC3FLAG-A
α7
66kDa
46kDa
hRIC3FLAG-A
α7

B

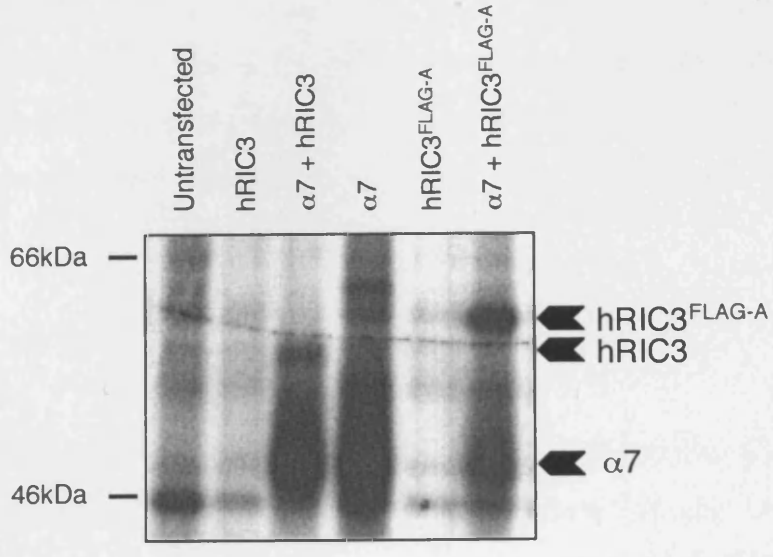
Untransfected
hRIC3
α7 + hRIC3
α7
hRIC3FLAG-A
α7 + hRIC3FLAG-A
66kDa
46kDa
hRIC3FLAG-A
hRIC3
α7

Figure 5.4 *Co-assembly of hRIC3 with the human α7 nAChR subunit demonstrated by co-immunoprecipitation.* Cells (tsA201) were transfected with combinations of hα7 and hRIC3/hRIC3^{FLAG-A}. Proteins were immunoprecipitated from metabolically labelled cells and analysed by SDS-PAGE, followed by autoradiography. The hα7 subunit was detected by mAb319 (B). hRIC3^{FLAG-A} was detected by mAbFLAG-M2 (A). **A**, A band (~58 kDa), absent in untransfected cells, was detected in cells transfected with hRIC3^{FLAG-A}. A band of the size expected of hα7 (~50 kDa) was co-precipitated with hRIC3^{FLAG-A} from cells co-transfected with hα7 and hRIC3^{FLAG-A}. The absence of cross-reactivity of mAbFLAG-M2 with hα7 was confirmed. **B**, A band corresponding to hα7 (~50 kDa) was detected in cells expressing hα7, and absent in untransfected cells. A band corresponding to hRIC3^{FLAG-A} (~58 kDa) and to hRIC3 (~55 kDa) were observed to co-precipitate with hα7. The absence of cross-reactivity of mAb319 with hRIC3/ hRIC3^{FLAG-A} was confirmed. The positions of molecular weight markers are indicated. The images are representative of at least 3 independent experiments.

Co-immunoprecipitation of rα7 with hRIC3 was not observed. Co-immunoprecipitation of CeRIC3 with rat or human α7 was not observed, but $CeRIC3^{FLAG\text{-}A}$ could be detected with mAbFLAG-M2. Results not shown (n=3).

5.3 Co-expression of the RIC3 proteins with the $5HT_{3A}R$

Previous studies have reported that the co-expression of hRIC3 with mouse $5HT_{3A}R$ in *Xenopus* oocytes leads to 5-HT-induced currents being abolished (Halevi *et al.*, 2003). In the present study, the effects of co-expression of the RIC3 proteins with the mouse and human $5HT_{3A}R$ in mammalian cells (tsA201) were investigated.

5.3.1 Co-expression of the RIC3 proteins with $5HT_{3A}$ examined by radioligand binding

Radioligand binding studies using [^{3}H]-GR65630, a $5HT_3R$ specific antagonist, were performed to investigate the effects of the RIC3 proteins on the $5HT_{3A}R$. Binding was performed on cell membrane preparations of tsA201 cells transiently transfected with mouse $5HT_{3A}$ ($m5HT_{3A}$) or human $5HT_{3A}$ ($h5HT_{3A}$) with or without CeRIC3 or hRIC3. Co-expression of the RIC3 proteins with both $m5HT_{3A}$ and $h5HT_{3A}$ significantly increased levels of specific binding (Figure 5.5). The increase in specific binding was greater when $5HT_{3A}$ was co-transfected with CeRIC3 than with hRIC3.

5.3.2 Effect of the RIC3 proteins on cell surface expression of $5HT_{3A}$

An enzyme-linked antibody binding assay was used to examine the effects of the RIC3 proteins on expression levels of the mouse and human $5HT_{3A}R$. The pAb120 antibody, which recognises a region in the extracellular domain of the $5HT_{3A}R$, was used to study the cell surface expression of the $m5HT_{3A}R$. CeRIC3 and hRIC3 had no significant effect on the cell surface levels of the $m5HT_{3A}R$ (Figure 5.6). Total levels of $m5HT_{3A}R$, using permeabilised cells, could not be measured because the pAb120 antibody gave too high a level of non-specific binding.

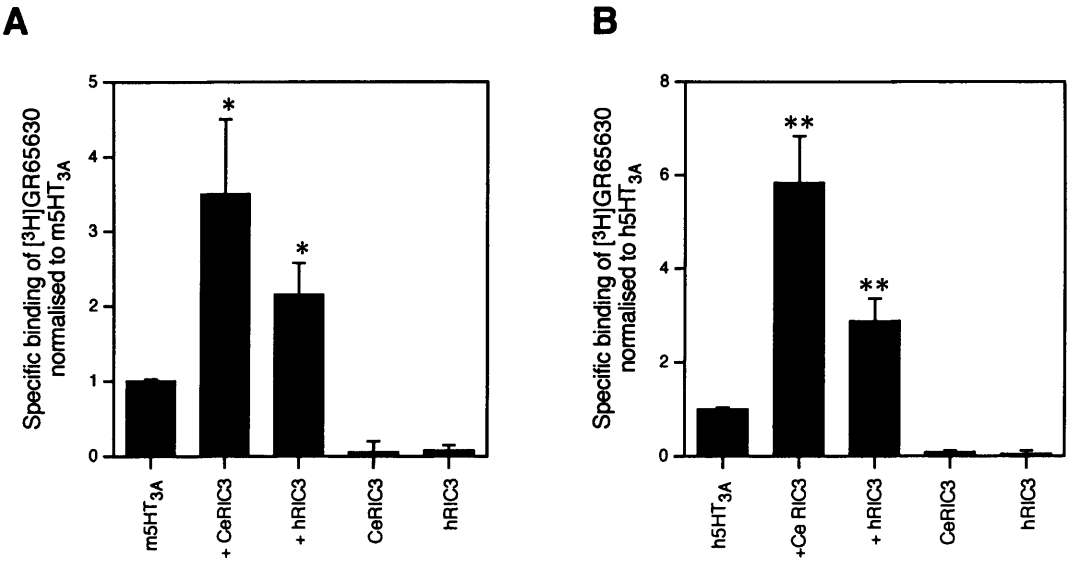

Figure 5.5 *Specific [^{3}H]GR65630 binding to 5HT$_{3A}$ co-expressed with the RIC3 proteins.* Cells (tsA201) were transiently transfected with combinations of mouse (**A**) or human (**B**) 5HT$_{3A}$ with or without the RIC3 proteins. Specific binding, using 12.5 nM [^{3}H]GR65630, to cell membrane preparations are mean values ± standard errors from 6 independent experiments performed in triplicate. Significance determined by Student's *t* test (*$p<0.05$; **$p<0.01$).

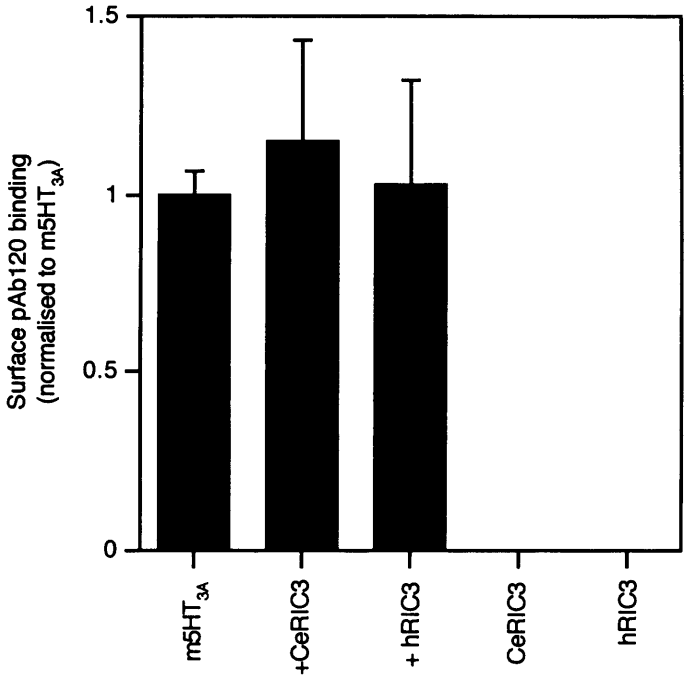

Figure 5.6 *Effects of the RIC3 proteins on the cell surface expression of the m5HT$_{3A}$R.* Cells (tsA201), grown on glass coverslips were transfected with the m5HT$_{3A}$ subunit alone or with CeRIC3 or hRIC3. Cells were labelled with pAb120, a polyclonal antibody raised against an extracellular epitope of the m5HT$_{3A}$R and levels of antibody binding determined through the use of an enzyme-linked assay. Data are means ± standard error of 4 independent experiments performed in triplicate. The background signal measured in mock-transfected cells has been subtracted.

To study the effects of the RIC3 proteins on the expression levels of the human $5HT_{3A}R$, cells were co-transfected with an HA-tagged $h5HT_{3A}$ subunit ($h5HT_{3A}$-HA) and CeRIC3 or hRIC3. The expression level of the $h5HT_{3A}$-HA construct was quantified through detection by an anti-HA antibody. CeRIC3 and hRIC3 were observed to increase both cell-surface and total levels of the $h5HT_{3A}$-HA receptor expression (Figure 5.7).

5.3.3 Effect of the RIC3 proteins on $5HT_{3A}R$ function assayed using a FLIPR

The effects of the RIC3 proteins on $5HT_{3A}R$ function were investigated by measurement of agonist-induced changes in intracellular Ca^{2+}, using a Fluorometric Imaging Plate Reader system (FLIPR). Cells (tsA201) were transiently transfected with $5HT_{3A}$ alone or together with CeRIC3 or hRIC3. Transfected cells were replated on to 96-well plates and grown for at least 24 hours. Cells were loaded with the Ca^{2+}-sensitive dye, fluo-4, and 5-HT-induced changes in intracellular Ca^{2+} recorded.

Co-expression of CeRIC3 with the $m5HT_{3A}R$ had no significant effect on the 5-HT-induced responses (Figure 5.8A). However, co-expression of hRIC3 with $m5HT_{3A}$ significantly decreased the size of the 5-HT-induced responses (Figure 5.8A). Co-expression of CeRIC3 with the $h5HT_{3A}R$ increased responses, but hRIC3 had no significant effect on the responses (Figure 5.8B).

5.3.4 Co-assembly studies of hRIC3 with $5HT_{3A}$

To investigate whether hRIC3 co-assembles with the $5HT_{3A}R$ subunit tsA201 cells were transiently transfected with combinations of mouse or human $5HT_{3A}$ and FLAG-tagged or untagged hRIC3 and examined by immunoprecipitation. An antibody to the putative intracellular loop between M3 and M4 of the $5HT_{3A}R$ ($pAb5HT_3$; Turton *et al.*, 1993), and mAbFLAG-M2 which recognises the FLAG epitope were used. A band of approximately 58 kDa, which was absent in untransfected cells, was detected using mAbFLAG-M2, in cells transfected with $hRIC3^{FLAG\text{-}A}$. This band was also detected in cells co-expressing $hRIC3^{FLAG\text{-}A}$ with mouse and human $5HT_{3A}$ as well as a faint co-precipitating band

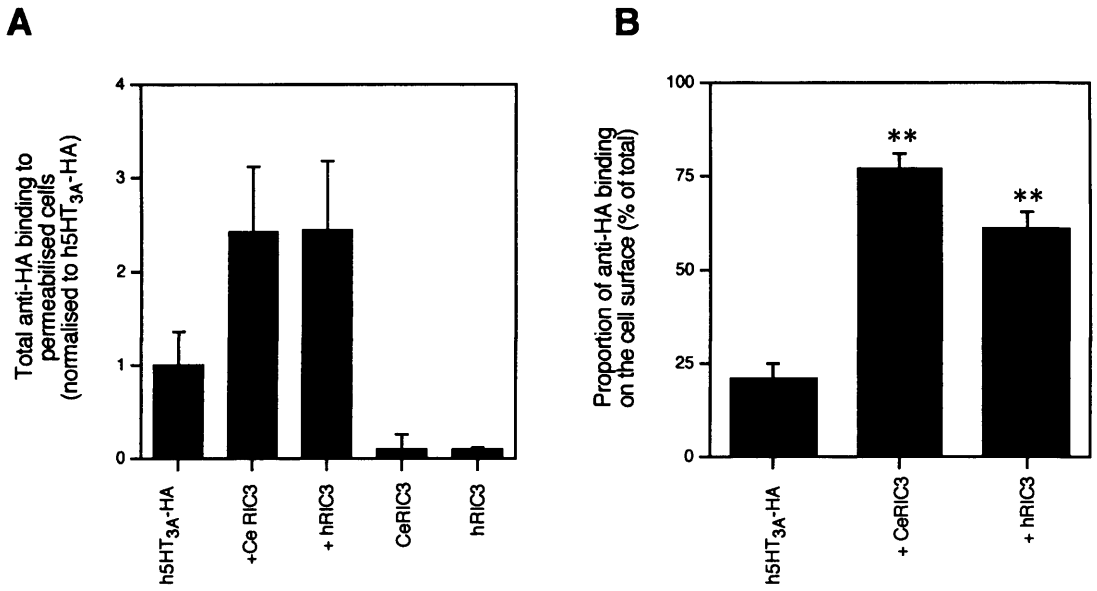

Figure 5.7 *Effects of the RIC3 proteins on the subcellular distribution of human 5HT$_{3A}$.* Cells (tsA201), grown on coverslips, were transfected with a human HA-tagged 5HT$_{3A}$ subunit alone or with CeRIC3 or hRIC3. Cells were labelled with an anti-HA antibody either after membrane permeabilisation or as intact cell monolayers. Data are presented as total antibody binding to permeabilised cells (**A**) and as the proportion of cell surface antibody binding sites (**B**). Data are means ± standard error of 3 independent experiments each carried out in triplicate. Significance determined by Student's *t* test (**$p<0.01$).

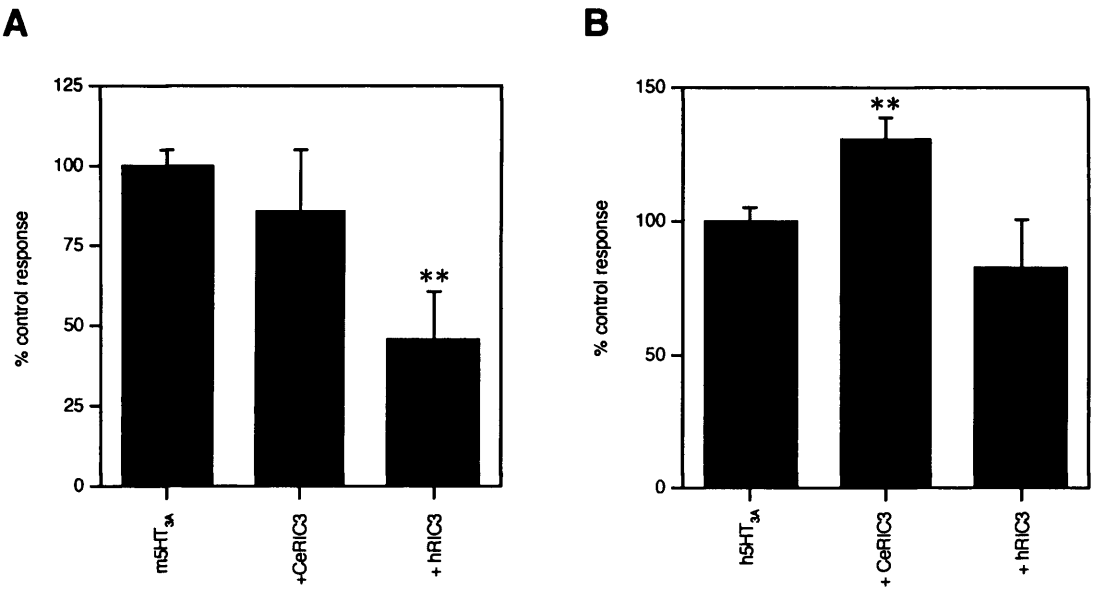

Figure 5.8 *Effects of the RIC3 proteins on $5HT_{3A}R$ function assayed using a FLIPR.* Transiently transfected cells (tsA201) plated on to poly-L-lysine-coated 96-well plates were loaded with the calcium-sensitive dye, fluo-4, and changes in fluorescence measured upon addition of 10 μM 5-HT. **A**, mouse $5HT_{3A}$ alone or with CeRIC3 or hRIC3 and **B**, human $5HT_{3A}$ alone or with CeRIC3 or hRIC3. Data are means (normalised to mouse (A) or human (B) $5HT_{3A}$) ± standard error, of the 'maximum fluorescence – minimum fluorescence', of 6 wells per experiment, from 5 independent experiments. Baseline fluorescence from addition of buffer to cells has been subtracted. Significance determined by Student's *t* test (**$p<0.01$).

the correct size for $5HT_{3A}$ (Figure 5.9A). Co-transfection of $hRIC3^{FLAG-A}$ with $5HT_{3A}$ and co-immunoprecipitation with $pAb5HT_3$ resulted in precipitation of a band corresponding to $hRIC3^{FLAG-A}$ and of another slightly unclear band of the correct size for mouse or human $5HT_{3A}$. In cells co-transfected with untagged hRIC3 a band of approximately 55 kDa was found to co-precipitate with both mouse and human $5HT_{3A}$ (Figure 5.9B). A band of approximately 55 kDa was also detected by $pAb5HT_3$ in untransfected cells. The absence of cross-reactivity of mAbFLAG-M2 with $5HT_{3A}$ and of $pAb5HT_3$ with hRIC3/$hRIC3^{FLAG-A}$ was confirmed (Figure 5.9).

5.4 Investigation into RIC3 topology through the use of epitope tags

A conserved membrane topology for the RIC3 family of proteins, consisting of two transmembrane domains followed by at least one coiled coil domain, has been proposed (Halevi *et al.*, 2002; Halevi *et al.*, 2003; see Figure 5.1). The proteins are predicted to be located on membranes with their N-terminal and C-terminal coiled coil domains in the cytoplasm, but no experimental evidence has been provided to support this prediction. Immunofluorescence studies using a GFP-tagged CeRIC3 construct suggested the protein to be localised to the endoplasmic reticulum (ER) (Halevi *et al.*, 2002). However, recently the presence of hRIC3 has been detected on the cell surface (Williams *et al.*, 2005). Also, use of a new 'combined transmembrane topology and signal peptide predictor' has suggested hRIC3 to possess only a single transmembrane domain with its N-terminal extracellular (Williams *et al.*, 2005). Evidence has been provided to support the idea that the C-terminal of hRIC3 is cytoplasmic (Williams *et al.*, 2005).

5.4.1 Epitope tagging of hRIC3

To investigate the transmembrane topology of the RIC3 proteins the FLAG epitope tag was introduced at several positions. For tagging purposes the topology of the RIC3 proteins was assumed as that predicted by Halevi *et al.*, 2002 and 2003 (Figure 5.1). The FLAG epitope was introduced into the C-terminal region (FLAG-A), in between the two predicted transmembrane domains (FLAG-B) and close to the N-

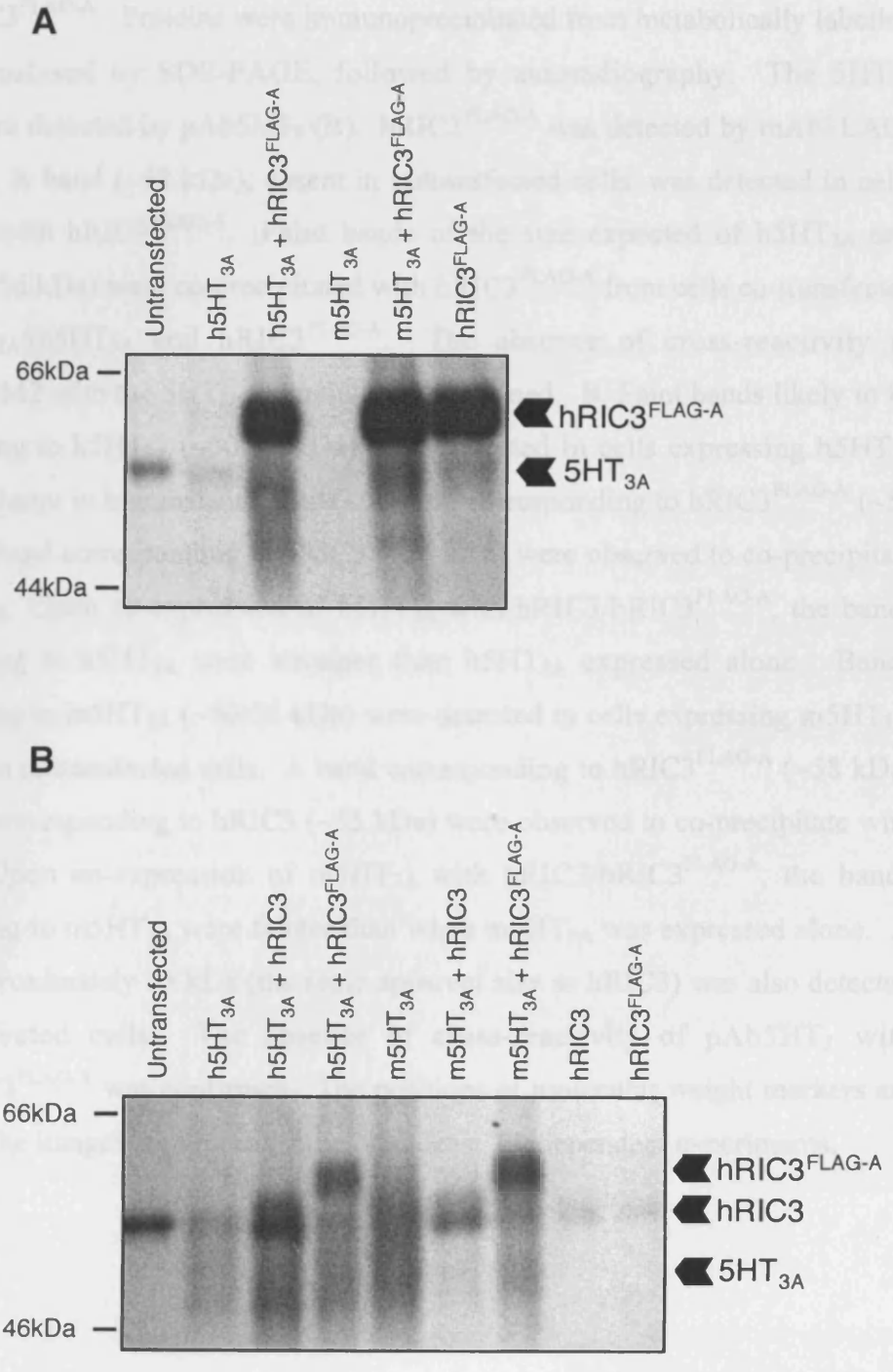
A
Untransfected
h5HT3A
h5HT3A + hRIC3FLAG-A
m5HT3A
m5HT3A + hRIC3FLAG-A
hRIC3FLAG-A
66kDa
44kDa
hRIC3FLAG-A
5HT3A
B
Untransfected
h5HT3A
h5HT3A + hRIC3
h5HT3A + hRIC3FLAG-A
m5HT3A
m5HT3A + hRIC3
m5HT3A + hRIC3FLAG-A
hRIC3
hRIC3FLAG-A
66kDa
46kDa
hRIC3FLAG-A
hRIC3
5HT3A

Figure 5.9 *Co-immunoprecipitation studies of hRIC3 co-expressed with $5HT_{3A}$.* Cells (tsA201) were transfected with combinations of $h5HT_{3A}$ or $m5HT_{3A}$ and hRIC3/$hRIC3^{FLAG\text{-}A}$. Proteins were immunoprecipitated from metabolically labelled cells and analysed by SDS-PAGE, followed by autoradiography. The $5HT_{3A}$ subunits were detected by $pAb5HT_3$ (B). $hRIC3^{FLAG\text{-}A}$ was detected by mAbFLAG-M2 (A). **A**, A band (~58 kDa), absent in untransfected cells, was detected in cells transfected with $hRIC3^{FLAG\text{-}A}$. Faint bands of the size expected of $h5HT_{3A}$ and $m5HT_{3A}$ (~ 56 kDa) were co-precipitated with $hRIC3^{FLAG\text{-}A}$ from cells co-transfected with $h5HT_{3A}$/$m5HT_{3A}$ and $hRIC3^{FLAG\text{-}A}$. The absence of cross-reactivity of mAbFLAG-M2 with the $5HT_{3A}$ subunits was confirmed. **B**, Faint bands likely to be corresponding to $h5HT_{3A}$ (~50-56 kDa) were detected in cells expressing $h5HT_{3A}$ alone, and absent in untransfected cells. A band corresponding to $hRIC3^{FLAG\text{-}A}$ (~58 kDa) and a band corresponding to hRIC3 (~55 kDa) were observed to co-precipitate with $h5HT_{3A}$. Upon co-expression of $h5HT_{3A}$ with hRIC3/$hRIC3^{FLAG\text{-}A}$, the bands corresponding to $h5HT_{3A}$ were stronger than $h5HT_{3A}$ expressed alone. Bands corresponding to $m5HT_{3A}$ (~50-56 kDa) were detected in cells expressing $m5HT_{3A}$, and absent in untransfected cells. A band corresponding to $hRIC3^{FLAG\text{-}A}$ (~58 kDa) and a band corresponding to hRIC3 (~55 kDa) were observed to co-precipitate with $m5HT_{3A}$. Upon co-expression of $m5HT_{3A}$ with hRIC3/$hRIC3^{FLAG\text{-}A}$, the bands corresponding to $m5HT_{3A}$ were fainter than when $m5HT_{3A}$ was expressed alone. A band of approximately 55 kDa (the same apparent size as hRIC3) was also detected in untransfected cells. The absence of cross-reactivity of $pAb5HT_3$ with hRIC3/$hRIC3^{FLAG\text{-}A}$ was confirmed. The positions of molecular weight markers are indicated. The images are representative of at least 3 independent experiments.

terminal (FLAG-C) of hRIC3. The construction of these FLAG-tagged proteins is detailed in Chapter 2, Section 2.4 and Figure 2.4.

5.4.2 Heterologous expression of the tagged hRIC3 constructs

To confirm that introduction of the FLAG epitope did not disrupt the function of hRIC3, in facilitation of cell surface expression of the α7 nAChR, the tagged constructs were co-transfected into tsA201 cells with α7 and the effects assayed by [^{125}I]-α-BTX binding. Co-expression of all FLAG-tagged hRIC3 constructs with hα7 gave specific [^{125}I]-α-BTX binding (Figure 5.10).

Co-expression of hα7 with hRIC3^{FLAG-A} or hRIC3^{FLAG-B} gave levels of specific cell surface [^{125}I]-α-BTX binding, performed on intact cells, not significantly different to that observed upon co-expression of wild type hRIC3 (Figure 5.10A). However, co-expression of hα7 with hRIC3^{FLAG-C} resulted in a significantly reduced level (~ 5-fold) of specific cell surface [^{125}I]-α-BTX binding compared to that observed upon co-expression of wild type hRIC3 (Figure 5.10A). Levels of [^{125}I]-α-BTX binding to membrane preparations of cells co-transfected with combinations of hα7 and FLAG-tagged hRIC3 constructs were also assayed. All hRIC3 FLAG-tagged constructs, when co-expressed with hα7, gave levels of specific [^{125}I]-α-BTX binding not significantly different to that observed upon co-expression of wild type hRIC3 (Figure 5.10B).

5.4.3 Investigation of subcellular location of hRIC3 using FLAG epitope tagged subunits

The expression of the FLAG-tagged hRIC3 constructs was investigated using an enzyme-linked antibody binding assay (Section 2.11). Cells (tsA201) grown on poly-L-lysine and collagen-coated glass coverslips, were transiently transfected with the FLAG-tagged hRIC3 constructs. Expression of the constructs was analysed using an anti-FLAG antibody, mAbFLAG-M2. Cell surface expression was assayed using intact cells and total cellular expression using permeabilised cells.

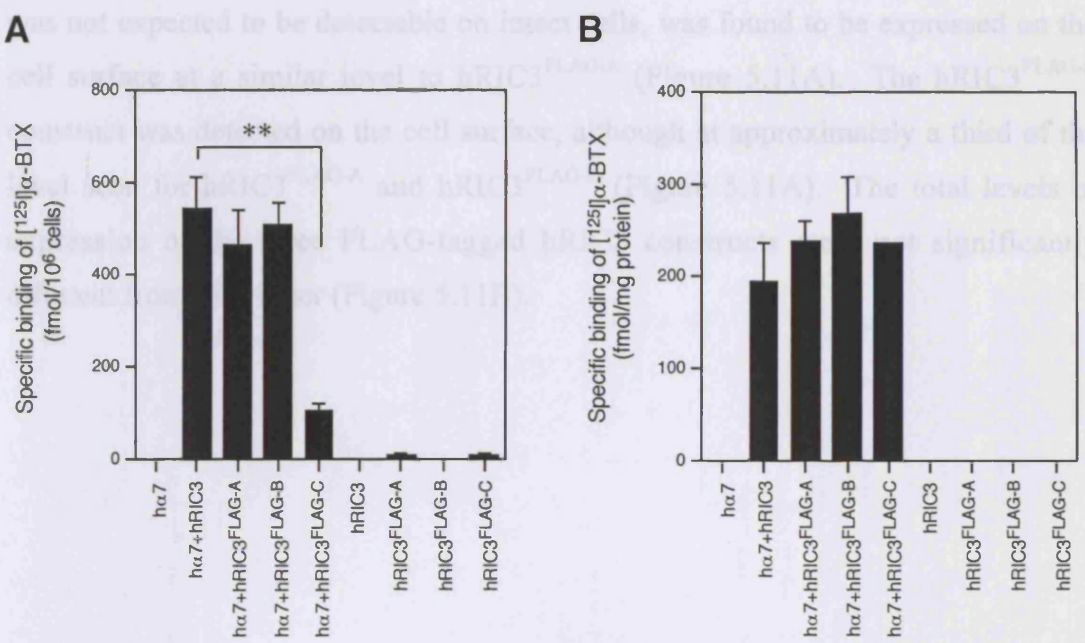

Figure 5.10 *Specific [^{125}I]-α-BTX binding to hα7 co-expressed with FLAG-tagged hRIC3 constructs.* Cells (tsA201) were transiently transfected with combinations of hα7 and FLAG-tagged hRIC3 and binding performed using 10 nM [^{125}I]-α-BTX. Specific binding to intact cells (A) and to cell membrane preparations (B) are mean ± standard error from at least 3 independent experiments each performed in triplicate. Significance determined by Student's *t* test (**$p<0.01$).

The hRIC3^{FLAG-A} construct was found to be expressed on the cell surface at a low level. This result was unexpected because the FLAG tag was presumed to be intracellular, based on the membrane topology predicted by Halevi *et al.*, 2002 and Halevi *et al.*, 2003 (Figure 5.11A). In addition, the hRIC3^{FLAG-C} construct, which was not expected to be detectable on intact cells, was found to be expressed on the cell surface at a similar level to hRIC3^{FLAG-A} (Figure 5.11A). The hRIC3^{FLAG-B} construct was detected on the cell surface, although at approximately a third of the level seen for hRIC3^{FLAG-A} and hRIC3^{FLAG-C} (Figure 5.11A). The total levels of expression of the three FLAG-tagged hRIC3 constructs were not significantly different from each other (Figure 5.11B).

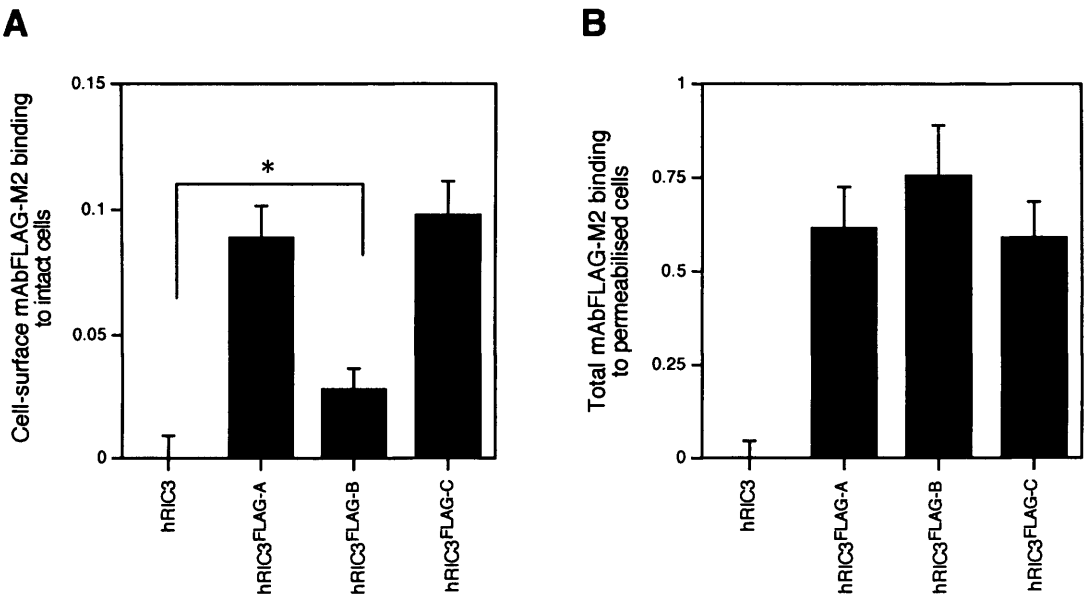

Figure 5.11 *Analysis of the subcellular location of hRIC3 using FLAG-tagged hRIC3 constructs.* Cells (tsA201) grown on glass coverslips were transfected with the various FLAG-tagged hRIC3 constructs. Cells were labelled with an anti-FLAG antibody (mAbFLAG-M2) as intact cell monolayers (**A**) or after membrane permeabilisation (**B**). Data are presented as means ± standard error, normalised to $\alpha 4\chi\beta 2^{FLAG}$ (data not shown), of at least 4 independent experiments each carried out in triplicate. Significance determined by Student's t test (*$p<0.05$).

5.5 Discussion

The expression of functional ligand-gated ion channels requires that the receptor subunits adopt an appropriate membrane topology, and associate with other subunits to form pentamers in the endoplasmic reticulum (ER) before export through the Golgi apparatus to the plasma membrane. This maturation process is slow and relatively inefficient (Merlie and Lindstrom, 1983). It has been suggested that the formation of pentameric complexes is a strict requirement before exit from the ER, but there is evidence for the occurrence of further folding events after exit from the ER (Green and Wanamaker, 1998; Green, 1999).

In contrast to most nAChR subunits, which form only heteromeric complexes, the α7 nAChR subunit has been shown to form homomeric assemblies (Chen and Patrick, 1997). The α7 nAChR subunit forms functional receptors when expressed in *Xenopus* oocytes (Couturier *et al.*, 1990b; Séguéla, 1993) and in some cultured mammalian cells lines (Puchacz *et al.*, 1994; Gopalakrishnan *et al.*, 1995). However, the inefficient expression of the α7 subunit has been observed for a number of other mammalian cell lines (Cooper and Millar, 1997; Kassner and Berg, 1997). The reason for the poor heterologous expression of the α7 nAChR is not well understood. In contrast, the $5HT_3R$, a closely related member of the ligand-gated ion channel family which is also capable of assembling as a homomeric receptor, efficiently forms functional receptors in several cell lines, for example HEK293 cells (Hope *et al.*, 1996). These data suggest that cell-specific factors are required for the correct and efficient folding, assembly and subcellular localisation of the α7 nAChR (Cooper and Millar, 1997; Dineley and Patrick, 2000; Sweileh *et al.*, 2000).

The recently identified *C. elegans* protein CeRIC3 has been shown to be important in the maturation of a number of nAChR subtypes (Halevi *et al.*, 2002). Co-expression of CeRIC3, and its human homologue, hRIC3, in *Xenopus* oocytes was shown to enhance the activity of the *C. elegans* DEG-3/DES-2 and rat and human α7 nAChRs (Halevi *et al.*, 2002; Halevi *et al.*, 2003). CeRIC3 was shown to have no effects on the function of GABA and glutamate receptors (Halevi *et al.*, 2002). hRIC3 reduced

human α4β2 and α3β4 nAChR current amplitudes, totally abolished those of mouse $5HT_{3A}$, but had little effect on α1 glycine receptor currents (Halevi *et al.*, 2003).

CeRIC3 was identified in a screen for suppression of a dominant mutation in the DEG-3 nAChR subunit. The DEG-3 mutation results in a non-desensitising nAChR channel which leads to cell death. Mutations in CeRIC3 were found to prevent this cell death and were characterised by an intracellular accumulation of DEG-3 protein suggesting a role for RIC3 proteins in maturation pathway of nAChRs (Halevi *et al.*, 2002).

5.5.1 RIC3 and α7 nAChR

The effects of the RIC3 proteins on the α7 nAChR expressed in the mammalian tsA201 cell line were investigated in this study. Co-expression of CeRIC3 or hRIC3 with both rat and human α7 enabled the α7 subunits to form a ligand-binding site as illustrated by specific [^{125}I]-α-BTX binding to cell membrane preparations of transiently transfected tsA201 cells. When [^{125}I]-α-BTX binding was performed on intact cells, specific binding was observed indicating that the α7 subunit was expressed as a ligand-binding pentamer on the cell surface of tsA201 cells. Previous studies had shown that the α7 subunit could be expressed in this cell line, but could not bind [^{125}I]-α-BTX (Cooper and Millar, 1997). Co-expression of the RIC3 proteins with the avian α8 subunit also resulted in this subunit forming a correctly folded receptor complex which was expressed on the cell surface.

Evidence for the co-assembly of human α7 with hRIC3/hRIC3^{FLAG-A} was obtained by co-immunoprecipitation. A band of approximately 58 kDa, absent in untransfected cells, was detected using the anti-FLAG antibody, mAbFLAG-M2, in cells transfected with hRIC3^{FLAG-A}. This band was also seen in cells co-expressing hRIC3^{FLAG-A} with hα7 as well as a co-precipitating band the correct size for α7. Further evidence for the co-assembly of hα7 and hRIC3 was provided using an antibody to α7 (mAb319). In cells co-transfected with hα7 and hRIC3^{FLAG-A} a band corresponding to hRIC3^{FLAG-A} was observed to co-precipitate with hα7. In cells co-

transfected with untagged hRIC3 a band of approximately 55 kDa was found to co-precipitate with α7.

The molecular weight of hRIC3^{FLAG-A} based on its primary amino acid sequence, is predicted to be approximately 42 kDa. However, the apparent molecular weight is greater (~58 kDa). The FLAG tag is predicted to add about 0.9 kDa, but the actual increase in apparent molecular weight observed is greater. The reason for this is not fully understood, but has been described before (Lansdell and Millar, 2002). However, it is not only the addition of the FLAG tag which is responsible for the increase as the apparent molecular weight of untagged hRIC3 (~55 kDa) is also much greater than predicted (41 kDa). In a recent study the hRIC3 protein is also reported to be of this apparent molecular weight in co-immunoprecipitation and Western blotting experiments (Williams *et al.*, 2005). The reason for this increase from predicted size is unclear, it is possible that hRIC3 is post-translationally modified. There are no potential *N*-linked glycosylation sites (N-X-S/T) in hRIC3, so the high apparent molecular weights cannot be attributed to this. hRIC3 contains five cysteine residues which could possibly be palmitoylated resulting in an increased molecular weight. Also, occasionally the hRIC3 proteins appear as a double band. This could be explained by the existence of two differently modified forms, both of which co-associate with α7.

Studies conducted by others in this laboratory indicate that co-expression of the RIC3 proteins with rat or human α7 in the mammalian tsA201 cell line results in the expression of functional receptors (Lansdell *et al.*, manuscript submitted). Cells co-expressing RIC3 and α7 were examined by whole-cell patch-clamp recording. Application of 200 μM acetylcholine evoked rapidly desensitising responses (Lansdell *et al.*, manuscript submitted). The responses were characteristic of native α7 nAChRs, for example those in areas such as the hippocampus (Jones and Yakel, 1997). Similar results for α7 expressed in HEK293 cells were also recently reported by Williams *et al.*, 2005.

A correlation between the endogenous expression of the RIC3 proteins and the ability to express functional α7 nAChR, either endogenously or by heterologous

expression of α7 cDNA has been observed (Lansdell *et al.*, manuscript submitted). In cell lines that endogenously express α7, or which are capable of expressing functional recombinant α7, for example the SH-SY5Y human neuroblastoma cell line (Lukas *et al.*, 1993, Cooper and Millar, 1997), RIC3 mRNA was detected using RT-PCR. No evidence of RIC-3 mRNA could be detected in the human embryonic kidney tsA201 cell line which has previously been shown to be incapable of expressing functional α7 receptors (Cooper and Millar, 1997; Lansdell *et al.*, manuscript submitted). Similar results were also recently reported by Williams *et al.*, 2005.

Many receptor-associated/chaperone proteins which mediate folding, assembly and trafficking of receptors have been identified (Nishimune *et al.*, 1996). However, there are relatively few specific for nAChR which is surprising as nAChRs are widely expressed and have numerous functions. The proteins reported to associate with nAChRs so far are chaperones such as calnexin, BiP and 14-3-3 (Blount and Merlie, 1991; Forsayeth *et al.*, 1992; Gelman *et al.*, 1995; Chang *et al.*, 1997, Jeanclos *et al.*, 2001), or regulatory proteins such as Lynx1 and VILIP which directly effect function (Miwa *et al.*, 1999; Ibanez-Tallon *et al.*, 2002; Lin *et al.*, 2002). Rapsyn (or 43K) causes clustering of nAChRs at the neuromuscular junction and in the electric organ of fish such as *Torpedo*, but is not thought to associate with neuronal nAChRs (Phillips *et al.*, 1991a). PDZ-containing proteins of the PSD-95 family have also been shown to associate with neuronal nAChRs (Conroy *et al.*, 2003). RIC3 is not an ubiquitously expressed protein and has varying effects on different subtypes of nAChRs, but appears not to effect other members of the ligand-gated ion channel family except for the closely related $5HT_{3A}R$ (Halevi *et al.*, 2002; Halevi *et al.*, 2003).

Another factor recently identified to be important in α7 expression has been the illustration of a correlation between palmitoylation of the α7 nAChR and expression of functional α7 nAChRs (Drisdel *et al.*, 2004). In cell lines such as HEK293 which are incapable of expressing functional, α-BTX-binding α7 nAChRs, receptors are not significantly palmitoylated. However, in cell lines such as PC12 where α7 is functionally expressed, the receptors are shown to be palmitoylated. Also, the

$5HT_{3A}R$ and $\alpha7/5HT_{3A}$ chimeric receptor is shown to be palmitoylated in HEK293 cells (Drisdel *et al.*, 2004). Palmitoylation of membrane proteins has been shown to be important in trafficking of proteins to the plasma membrane (reviewed in Smotrys and Linder, 2004). Perhaps α7 has to be folded/assembled to a certain extent, which requires association with RIC3, before palmitoylation and trafficking to the plasma membrane can occur. It would be interesting to determine whether the α7 nAChR is palmitoylated in the presence of RIC3 in cell lines such as HEK293.

In summary, it has been observed that the RIC3 proteins enable correct subunit assembly and cell surface expression of rat and human α7 (and chick α8) in the mammalian tsA201 cell line, which is not usually capable of functional α7 expression. Williams *et al.* (2005) reported that α7 could be detected on the cell surface of the HEK293 cell line in the absence of RIC3, but the receptors were incapable of binding α-bungarotoxin and not functional. However, co-expression with RIC3 enables functional expression of α7. The presence of α7 on the cell surface in the absence of RIC3 (Williams *et al.*, 2005) suggests that RIC3 does not play a direct role in regulating traffic of α7 receptors to the cell surface. Williams *et al.* (2005) also report that RIC3 does not alter α7 expression levels implicating that the increase in cell surface functional receptors is not due to a general increase in cell surface receptors. Together the results described suggest RIC3 to be an α7-associated protein which is necessary for the efficient folding and assembly of α7 nAChR into functional receptors.

5.5.2 RIC3 and $5HT_{3A}$

The effects of the RIC3 proteins on other members of the ligand-gated ion channel family were investigated by Halevi *et al.* (2003). Of particular interest was the observation that co-expression of hRIC3 with the mouse $5HT_{3A}R$ subunit in *Xenopus* oocytes led to the abolishment of agonist-induced currents. In this chapter the effects of hRIC3 and CeRIC3 on both human and mouse $5HT_{3A}$ expressed in the mammalian tsA201 cell line were investigated.

There was some evidence for the co-assembly of hRIC3 with both the mouse and human $5HT_{3A}$Rs, although the co-immunoprecipitation data was not particularly clear. This may be due to the interaction being transient or may be because RIC3 only interacts with a small proportion of $5HT_{3A}$R, for example, immature receptor subunits/complexes.

In contrast to the complete inhibition of hRIC3 on $m5HT_{3A}$R function (Halevi *et al.*, 2003) an approximately 50% reduction of 5-HT-induced elevations in intracellular calcium assayed using a FLIPR was observed in tsA201 cells. CeRIC3 had no significant effect on the function of $m5HT_{3A}$. However CeRIC3 significantly increased functional responses of $h5HT_{3A}$, whilst hRIC3 had no significant effect. Differences in the expression systems used (oocytes versus mammalian tsA201 cells) may explain the different result for co-expression of hRIC3 with $m5HT_{3A}$ compared to Halevi *et al.* (2003). A *Xenopus leavis* RIC3 homologue has recently been identified (Halevi *et al.*, 2003). Over-expression of the RIC3 protein could therefore be creating an inhibitory effect. There is no endogenous RIC3 in tsA201 cells (Lansdell *et al.*, manuscript submitted) and so the potential inhibitory effect of RIC3 would be reduced.

RIC3 increased levels of specific [^{3}H]-GR65630 binding to membrane preparations of tsA201 cells expressing mouse or human $5HT_{3A}$. Cell surface expression levels of $m5HT_{3A}$, assayed by antibody binding, were not affected by co-expression with RIC3. However, the cell surface expression of human $5HT_{3A}$, assayed by antibody binding, was increased by co-expression with RIC3 as was total expression. In the antibody binding assay, CeRIC3 and hRIC3 were seen to enhance the total level of $h5HT_{3A}$ to a similar extent. However, in radioligand binding studies, CeRIC3 increased $h5HT_{3A}$ levels significantly more than hRIC3. This suggests that not all of the additional $5HT_{3A}$Rs formed in the presence of hRIC3 are completely or correctly formed and therefore capable of ligand binding.

Unlike the α7 nAChR, co-expression of RIC3 is not required for functional cell-surface expression of either mouse or human $5HT_{3A}$ in the tsA201 cell line. The effects of CeRIC3 and hRIC3 on the level of protein expression, cell-surface expression and radioligand binding are conserved. There are species differences

between mouse and human $5HT_{3A}$ in the effects of the RIC3 proteins. Generally, the RIC3 proteins enhance the expression of the $5HT_{3A}R$ possibly by promoting subunit folding and assembly resulting in $5HT_{3A}R$ stabilisation. However, with the increased expression levels observed an increase in $5HT_{3A}R$ function was expected. Only CeRIC3 was observed to increase $h5HT_{3A}$ function, by an increase in 5-HT-induced responses.

Like the α7 nAChR, few $5HT_3R$ associated proteins have been identified. The chaperone proteins BiP and calnexin have been shown to interact with $5HT_{3A}R$ (Boyd *et al.*, 2002), but these are ubiquitously expressed and their action is not specific to $5HT_3R$.

5.5.3 Topology of RIC3

Halevi *et al.* (2002) identified CeRIC3 as a novel protein. Structure predictions (using programs on http://www.expasy.ch and http://psort.nibb.ac.jp) suggested that it contained no signal peptide and was composed of two transmembrane domains, separated by a proline-rich spacer, followed by coiled coil domains resulting in the N- and C-termini being cytosolic (Halevi *et al.*, 2002). Cloning of hRIC3 and homologues from a number of other species revealed that CeRIC3 belonged to a conserved gene family which shared the predicted structure and topology for CeRIC3 (Halevi *et al.*, 2003). Immunofluorescence studies using an N-terminal GFP-tagged CeRIC3 suggested CeRIC3 to be localised to the ER (Halevi *et al.*, 2002).

The methods used by Halevi *et al.* (2002) to predict the structure of the RIC3 proteins do not distinguish between a transmembrane domain and a signal peptide. Using more recent protein structure prediction programs, such as SignalP3.0 (http://www.cbs.dtu.dk/services/SignalP/), a signal peptide predictor, suggests that the first transmembrane domain of hRIC3 predicted by Halevi *et al.* (2002, 2003), to be a signal peptide. This implies that hRIC3 contains only a single transmembrane domain. Sequence analysis by Williams *et al.* (2005) using SignalP2.0, and Phobius, a combined transmembrane topology and signal peptide predictor (Kall *et al.*, 2004), also suggest that hRIC3 contains a signal peptide and a single transmembrane

domain. Using SignalP3.0, CeRIC3 is suggested not to contain a signal peptide. The use of an N-terminal GFP-tagged CeRIC3 construct supports this result (Halevi *et al.*, 2002).

The topology of hRIC3 was further investigated through the use of epitope tags. The FLAG epitope tag was introduced into hRIC3 at three positions based upon the topology predicted by Halevi *et al.* (2002). To determine whether the tags interfered with the function of RIC3, the constructs were co-expressed with human α7 and [^{125}I]-α-BTX binding studies performed. Co-expression of hα7 with hRIC3 tagged at the N-terminal (hRIC3$^{FLAG\text{-}C}$) resulted in a reduced level of specific cell surface [^{125}I]-α-BTX binding compared to that observed upon co-expression of wild type hRIC3. Total levels of binding did not differ. hRIC3$^{FLAG\text{-}C}$ was shown to be capable of facilitating α7 folding and assembly in tsA201 cells, but either less α7 reached the cell surface or fewer α7 receptors capable of ligand/α-BTX binding reached the cell surface resulting in the observed decrease in binding.

Using the FLAG tagged hRIC3 constructs, the presence of hRIC3 at the cell surface was detected. Unexpectedly, all of the tags appeared to be detected on the cell surface. Antibody binding to the constructs tagged at the N- and C- termini was greater than that to the construct tagged in between the two predicted transmembrane domains (hRIC3$^{FLAG\text{-}B}$). These results weakly suggested the topology of hRIC3 to be opposite to that predicted by Halevi *et al.* (2002) with the N- and C-termini extracellular. However, the presence of a coiled coil domain in the C-terminal domain would suggest this region to be intracellular as coiled coil domains are often seen to mediate intracellular protein-protein interactions (Stefancsik *et al.*, 1998). The weak presence of hRIC3$^{FLAG\text{-}B}$ on the cell surface could be explained if the cells had become slightly permeabilised. If the cells had become permeabilised then the detection of all three differently tagged subunits would be more likely. The level of antibody binding to hRIC3$^{FLAG\text{-}B}$ could be reduced compared to the other tagged constructs if the tag was obscured. The loop between the two transmembrane domains is rich in proline residues which may form a rigid structure that obscures the FLAG tag.

The detection of the N-terminal tag on the cell surface would suggest that there is no cleaved signal peptide which disagrees with the SignalP3.0 predictions and Williams *et al.* (2005). Williams *et al.* (2005) provide evidence for the expression of hRIC3 on the cell surface, but suggest that hRIC3 contains a single transmembrane domain with an extracellular N-terminus. Further studies are required before firm conclusions about the topology and the localisation of the RIC3 proteins can be made.

5.5.4 Summary

In summary, the RIC3 proteins have been shown to enable functional cell-surface expression of α7 nAChRs in a mammalian cell line (tsA201) in which α7 is not usually efficiently expressed. Correlation between expression of RIC3 and ability to express functional α7 nAChRs strongly suggests that the lack of RIC3 is the primary cause of inefficient functional expression. Although not essential for the functional cell surface expression of the $5HT_{3A}R$, the RIC3 proteins have been shown to enhance expression. These effects on both the α7 nAChR and the $5HT_{3A}R$ are suggested to be mediated by a promotion of folding and assembly resulting in the production of stable receptor complexes. The exact mechanisms by which ligand-gated ion channels fold, assemble and traffic are unknown. The precise role of RIC3, its mechanism of action, and location are still to be determined.

5.6 Future directions

Reports defining the cellular location of RIC3 have been contradictory and further investigations are required. Selective permeabilisation of cells expressing RIC3 could help to determine whether RIC3 is plasma membrane- or ER-localised. The compound Streptolysin O which selectively permeabilises the plasma membrane, but not Golgi or ER membranes (Crystal *et al.*, 2003), could be used. The use of techniques such as immunofluorescence with antibodies to RIC3 itself or to epitope tags, introduced into the RIC3 proteins, may prove useful in investigating RIC3 expression and distribution. Co-staining with ER markers, such as BiP and calnexin, may help in these studies.

Glycosylation scanning mutagenesis could be used to examine the topology of the RIC3 proteins. The method involves the introduction of glycosylation sites into proteins of interest by site-directed mutagenesis, followed by an analysis of the glycosylation state of the expressed proteins by methods such as Western blotting The method takes advantage of the fact that membrane proteins are glycosylated only on the lumenal side of the ER (Crystal *et al.*, 2003).

Site-directed mutagenesis could be used to determine residues and regions involved in interactions with RIC3. The yeast 2-hybrid system could be used to identify binding partners of RIC3 and to determine whether RIC3 interacts directly with the α7 nAChR and $5HT_{3A}R$.

To further characterise the role and function of the RIC3 proteins, it would be interesting to investigate the effects of RIC3 on other members of the nAChR and $5HT_3R$ families. RIC3 has been reported to inhibit the whole-cell currents of the α4β2 and α3β4 nAChRs expressed in *Xenopus* oocytes (Halevi *et al.*, 2003). It would therefore be of interest to examine the effects of the RIC3 proteins on these nAChR subtypes, and others, in mammalian cell lines.

CHAPTER 6

CONCLUSION

The neuronal nAChRs and $5HT_3$Rs play numerous roles in physiological processes such as neurotransmission and the modulation of neurotransmitter release. In addition, both have been implicated in several neurological disorders. Nicotinic receptors have also been implicated in mediating addiction to nicotine from tobacco smoking, and the $5HT_3$Rs are involved in mediating emesis. The nAChR and $5HT_3$R subunits assemble into pentameric structures, and form both heteromeric and homomeric complexes. The muscle-type nAChR has been studied extensively and many of its defined structural and functional characteristics serve as a model for other members of the ligand-gated ion channel family, including the neuronal nAChRs and $5HT_3$Rs.

In this study, aspects of nAChR and $5HT_3$R expression, assembly and function were investigated through heterologous expression of cloned receptor subunits in mammalian cell lines and *Xenopus* oocytes. Further knowledge of these receptors is important in understanding their functional roles as native receptors, and may provide insight into the function of other ligand gated ion channels. Also, gaining further insight into the function of these receptors will aid in understanding their potential as therapeutic targets.

The assembly of the nAChR or $5HT_3$R subunits leading to the expression of a functional receptor is a complex and poorly characterised process. Individual subunits must fold with the correct membrane topology, and assemble with other subunits, within the endoplasmic reticulum (ER), before functional expression at the cell surface (Green and Millar, 1995). Throughout the assembly process, the receptor subunits undergo several post-translational modifications, such as glycosylation and phosphorylation. A number of other factors are also required for receptor assembly, for example, chaperone proteins play a role in 'quality control' by interacting with folding receptor intermediates, and by preventing incorrectly and incompletely folded and assembled complexes from reaching the cell surface.

The efficient heterologous expression of the nAChRs has proved difficult. The α7 nAChR can be expressed as a functional homomeric receptor in some expression systems, such as *Xenopus* oocytes (Couturier *et al.*, 1990b), but there are relatively few reports of its functional expression in mammalian cell lines (Puchacz *et al.*,

1994; Gopalakrishnan *et al.*, 1995; Quik *et al.*, 1996). The functional expression of the α7 nAChR has been reported to be dependent upon host-cell specific factors (Cooper and Millar, 1997; Sweileh *et al.*, 2000). Several approaches have been used to attempt to overcome these difficulties in expression, for example, the use of chimeric subunits between the nAChR α7-subunit and $5HT_{3A}$ subunit (Eiselé *et al.*, 1993; Blumenthal *et al.*, 1997; Rangwala *et al.*, 1997; Cooper and Millar, 1998). The α7/$5HT_{3A}$ subunit chimera is able to generate a functional receptor efficiently in diverse cell types, and has proven to be a very useful tool in the pharmacological characterisation of the α7 receptor. However, the chimeric receptor is not native and its use in studies such as drug discovery are limited. Unlike the α7 nAChR, the ability of the $5HT_{3A}R$ to generate a functional receptor is independent of host-cell type. The reason for the difference in expression of nAChRs and $5HT_3Rs$ is unclear, but may be due to a requirement for interactions with different intracellular proteins to aid in folding and assembly.

The RIC3 family of proteins was recently identified and studies suggested its involvement in the maturation of several nAChR subtypes, when expressed in *Xenopus* oocytes (Halevi *et al.*, 2002; Halevi *et al.*, 2003). RIC3 has been observed to enhance the functional responses of the α7 nAChR expressed in *Xenopus* oocytes (Halevi *et al.*, 2002; Halevi *et al.*, 2003). In this study, the effects of RIC3 on α7 nAChR expression in a mammalian cell line (tsA201), which is not capable of functional α7 expression, were investigated. Co-expression of RIC3 with α7, in the tsA201 cell line, resulted in the cell-surface expression of an α7 nAChR capable of [^{125}I]-α-BTX binding. The α7 subunit protein was also shown to co-associate with RIC3. Studies by others in this laboratory have shown that co-expression of RIC3 with α7 results in the expression of functional α7 receptors. A correlation between the expression of RIC3 and the ability to express functional α7 nAChRs has also been shown. Together these data suggest that RIC3 may be a protein required for efficient α7 nAChR expression. Studies by Williams *et al.* (2005) reported the presence of the α7 nAChR on the cell surface of HEK293 cells in the absence of RIC3, but the receptors were non-functional and could not bind α-BTX. Upon co-expression with hRIC3 the same level of α7 was observed at the cell surface, but the receptors were reported to be functional and could bind α-BTX (Williams *et al.*,

2005). This data, together with the data in this study, suggests the RIC3 proteins to be involved in the efficient folding and assembly of the α7 nAChR, and not in the trafficking of the receptor to the cell surface. The ability to efficiently express a functional α7 nAChR, by co-expression with RIC3, in non-neuronal cultured cell lines will be extremely useful for high-throughput screening purposes as well as to enable further characterisation of the functional and pharmacological properties of the α7 nAChR.

The structure of the RIC3 proteins and their mechanism of action require further characterisation. Through the use of different structure prediction programs, various membrane topologies of the RIC3 proteins have been suggested (this study; Halevi *et al.*, 2002; Halevi *et al.*, 2003; Williams *et al.*, 2005). RIC3 contains at least one transmembrane domain. The location of the RIC3 proteins also requires further characterisation. One study suggests RIC3 to be localised to the ER (Halevi *et al.*, 2002), whilst others have reported its expression at the cell surface (this study; Williams *et al.*, 2005).

The effects of RIC3 are not limited to the nAChR family. The function of the $5HT_3R$ has also been observed to be effected by RIC3 (Halevi *et al.*, 2003). In *Xenopus* oocytes, co-expression of hRIC3 with the mouse $5HT_{3A}$ subunit resulted in an abolition of 5-HT-induced responses (Halevi *et al.*, 2002). The effects of the RIC3 proteins on the expression of the mouse and human $5HT_{3A}$Rs in mammalian cells were investigated in this study. There was some evidence for the co-assembly of the RIC3 proteins with $5HT_{3A}$, shown by immunoprecipitation. Levels of [^{3}H]-GR65630 binding to membrane preparations of cells expressing $5HT_{3A}$ were significantly enhanced in the presence of the RIC3 proteins. An enhancement of the levels of cell-surface and total expression of human $5HT_{3A}$ upon co-expression with RIC3 was shown through an enzyme-linked antibody binding assay. The level of cell-surface mouse $5HT_{3A}$ was not affected by RIC3. A decrease in the size of functional responses of mouse $5HT_{3A}$, when co-expressed with hRIC3 in tsA201 cells, was observed when assayed by FLIPR, but function was not totally abolished as reported for expression in *Xenopus* oocytes by Halevi *et al.* 2003. Response size was increased for human $5HT_{3A}$ in the presence of CeRIC3. From these studies the

RIC3 proteins are suggested to play a role in stabilising or promoting the efficient folding and assembly of the $5HT_{3A}R$, but further studies need to be performed to clarify the effects of the RIC3 proteins on $5HT_{3A}R$ expression and function.

Whilst the $5HT_{3A}$ subunit, when expressed alone, forms functional homomeric receptors, the $5HT_{3B}$ subunit, when expressed alone, does not form a functional receptor (Davies *et al.*, 1999; Dubin *et al.*, 1999; Hanna *et al.*, 2000; Spier and Lummis, 2000). The $5HT_{3B}$ subunit alone does not reach the cell surface, but is retained within the ER (Boyd *et al.*, 2002). Co-expression of $5HT_{3A}$ and $5HT_{3B}$ enables $5HT_{3B}$ to reach the cell surface (this study; Boyd *et al.*, 2002). In this study, the mechanism for the retention in the ER of the $5HT_{3B}$ subunit was investigated and an ER retention motif of the RXR type was identified in the $5HT_{3B}$ subunit, in between M1 and M2. The presence of ER retention/retrieval motifs such as the one identified here have been shown to play a role in regulating the expression of a number of receptors (Zerangue *et al.*, 1999; Bichet *et al.*, 2000; Margeta-Mitrovic *et al.*, 2000). When these motifs are exposed/unmasked, then the protein containing them is retained within the ER by an, as of yet, unknown mechanism. The motifs may be masked by assembly with another subunit, interactions with other proteins or other modifications, such as phosphorylation, resulting in release from the ER. When $5HT_{3B}$ is co-expressed with $5HT_{3A}$, it can be detected on the cell surface as part of a functional receptor complex. It appears therefore, that the $5HT_{3A}$ subunit masks the RXR motif within the $5HT_{3B}$ subunit, upon assembly, resulting in the generation of a functional heteromeric receptor. Although this motif is capable of retaining the $5HT_{3B}$ subunit within the ER, it has been shown not to be the only factor involved in the retention of the subunit. Further studies are required to identify other retention motifs in the $5HT_{3B}$ subunit and to identify regions or residues in the $5HT_{3A}$ subunit or other proteins/factors responsible for masking the RXR motif.

As described previously (Section 1.8; Chapter 4), the $\alpha 7$ nAChR and $5HT_{3A}R$ are structurally and functionally related proteins and share approximately 33% amino acid sequence identity in their N-terminal ligand binding domains. Cross-reactivity of some ligands is observed and this is thought to be due to similarities of the ligand binding sites. Many site-directed mutagenesis and affinity labelling studies have

identified residues and regions of the nAChR and $5HT_3R$ involved in ligand binding (see Section 1.3.3). The six loops, A-F, identified as important in forming the ligand binding site contain several residues which are conserved between the nAChR and $5HT_3R$ (see Section 1.3.3).

The aromatic moiety of 5-HT, 5-hydroxyindole (5-HI), has been shown to potentiate the responses of both the α7 nAChR and the mouse $5HT_{3A}R$ (Kooyman *et al.*, 1993; Kooyman *et al.*, 1994; van Hooft *et al.*, 1997; Gurley *et al.*, 2000; Zwart *et al.*, 2002). However, 5-HI does not potentiate the human $5HT_{3A}R$ (unpublished result, Eli Lilly). There is approximately 84% amino acid sequence identity between the human and mouse $5HT_{3A}$ receptors, but differences in their pharmacological properties are observed. For example, the $5HT_3R$ antagonist *d*-tubocurarine (*d* -TC) is significantly (1800-fold) more potent at mouse $5HT_{3A}$, than human $5HT_{3A}$. In this study the differing effects of 5-HI on mouse and human $5HT_{3A}$ were investigated, with the aim of determining the ligand binding site for this compound. Mammalian tsA201/HEK293 cells were transfected with mouse or human $5HT_{3A}$ and the effects of 5-HI assayed using a FLIPR. The responses of the mouse $5HT_{3A}$ were potentiated by 5-HI, whilst the responses of human $5HT_{3A}$ were unaffected by 5-HI. The effects of 5-HI on chimeric subunits (containing human and mouse $5HT_{3A}$ subunit domains) were investigated. It was hoped that these chimeras would be the basis for further chimeras to identify regions and residues conferring sensitivity to 5-HI. However, both the human/mouse and mouse/human $5HT_{3A}$ chimeras were potentiated slightly suggesting both the N- and C-terminal domains of the receptors to be important in binding or mediating the actions of 5-HI. Previous studies have suggested that there may be more than one binding site for 5-HI. At low concentrations, 5-HI potentiates the responses of the $5HT_3R$, but at higher concentrations 5-HI blocks 5-HT-evoked currents (Kooyman *et al.*, 1994; van Hooft *et al.*, 1997). The results in this study suggest that the actions of 5-HI may be mediated by regions in both the N- and C-terminal of the $5HT_3R$.

Defining the ligand binding site for 5-HI would be useful to enable the creation of receptor specific and subtype-specific compounds. Defining the binding site of 5-HI as a potentiator of the α7 nAChR would be useful for rationalisation of drug design

with the aim of generating α7 nAChR-selective potentiators for the treatment of neurological disorders such as neurodegeneration (Maelicke and Albequerque, 2000; Dani *et al.*, 2004). The cross-reactivity of ligands between $5HT_{3A}$ and α7 needs to be considered when designing potential receptor subtype-specific compounds, for example, the $5HT_3R$ antagonist tropisetron, which is used in the treatment of emesis, has also been reported to act as a partial agonist at the α7 nAChR, when expressed in *Xenopus* oocytes (Macor *et al.*, 2001).

Summary

The aim of this project was to gain a better understanding of the structural and functional properties of the nAChRs and $5HT_3Rs$. Through three different studies, aspects of the assembly, trafficking and pharmacological properties of these receptors have been investigated. Through co-expression of the α7 nAChR subunit with RIC3, the cell-surface expression of an α7 receptor, capable of α–BTX binding, in a non-neuronal mammalian cell line, has been demonstrated. The characterisation of the effects of the RIC3 proteins on α7 have identified RIC3 as a protein involved in the facilitation of efficient folding and assembly of the α7 nAChR. These results will allow further characterisation of a receptor which has previously been very difficult to express in heterologous expression systems. The observation that the RIC3 proteins also interact with the $5HT_{3A}R$ subunit and, to an extent, promote its expression suggest that they may have a conserved role in ligand gated ion channel assembly. Aspects of the assembly of the heteromeric $5HT_{3A}/5HT_{3B}$ receptor have been revealed in the identification of an ER retention motif in the $5HT_{3B}$ subunit. The RXR motif in $5HT_{3B}$ has been shown to require masking by $5HT_{3A}$ to achieve cell-surface expression. The differing effects of 5-HI at the human and mouse $5HT_{3A}$ receptors previously observed by Eli Lilly (unpublished results) have been confirmed in this study through expression in mammalian cell lines and *Xenopus* oocytes. The use of human/mouse $5HT_{3A}$ subunit chimeras suggest the effects of 5-HI to be mediated by both N- and C-terminal domains of $5HT_{3A}$. A number of residues observed to be present in mouse $5HT_{3A}$ and the α7 nAChR which are potentiated by 5-HI, but not in human $5HT_{3A}$ which is not potentiated by 5-HI, have been shown not to be responsible for conferring 5-HI sensitivity.

Further elucidation of the mechanisms by which the nAChRs and $5HT_3Rs$ assemble is not only important in understanding the native functions of these receptors, as well as their potential as therapeutic targets, but also in gaining insight into the assembly and function of other ligand gated ion channels. The identification of residues and regions involved in ligand binding is critical to enable development of receptor-specific and receptor subtype-specific compounds for the treatment of neurological disorders.

REFERENCES

Anand, R., Conroy, W. G., Schoepfer, R., Whiting, P. and Lindstrom, J. (1991). Neuronal nicotinic acetylcholine receptors expressed in *Xenopus* oocytes have a pentameric quaternary structure. *J. Biol. Chem.*, **266,** 11192-11198.

Anand, R., Peng, X., Ballesta, J. J. and Lindstrom, J. (1993b). Pharmacological characterization of α-bungarotoxin-sensitive acetylcholine receptors immunoisolated from chick retina: contrasting properties of α7 and α8 subunit-containing subtypes. *Molec. Pharmacol.*, **44,** 1046-1050.

Anand, R., Peng, X. and Lindstrom, J. (1993a). Homomeric and native α7 acetylcholine receptors exhibit remarkably similar but non-identical pharmacological properties, suggesting that the native receptor is a heteromeric protein complex. *FEBS Letts*, **327,** 241-246.

Barnard, E. A., Miledi, R. and Sumikawa, K. (1982). Translation of exogenous messenger RNA coding for nicotinic acetylcholine receptors produces functional receptors in *Xenopus* oocytes. *Proc. R. Soc. Lond. B.*, **215,** 241-246.

Barnes, N. M. and Sharp, T. (1999). A review of central 5-HT receptors and function. *Neuropharmacology*, **38,** 1083-1152.

Belelli, D., Balcarek, J. M., Hope, A. G., Peters, J. A., Lambert, J. J. and Blackburn, T. P. (1995). Cloning and functional expression of a human 5-hydroxytryptamine type 3AS receptor subunit. *Molec. Pharmacol.*, **48,** 1054-1062.

Benwell, M. E. M., Balfour, D. J. K. and Anderson, J. M. (1988). Evidence that tobacco smoking increases the density of (-)-[^{3}H]nicotine binding sites in human brain. *J. Neurochem.*, **50,** 1243-1247.

Bertrand, D., Bertrand, S. and Ballivet, M. (1992). Pharmacological properties of the homomeric alpha 7 receptor. *Neurosci. Lett.*, **146,** 87-90.

Bertrand, D., Galzi, J. L., Devillers-Thiery, A., Bertrand, S. and Changeux, J. P. (1993). Mutations at two distinct sites within the channel domain M2 alter calcium permeability of neuronal alpha 7 nicotinic receptor. *Proc. Natl. Acad. Sci. USA*, **90,** 6971-5.

Betz, H. and Pfeiffer, F. (1984). Monoclonal antibodies against the α-bungarotoxin-binding protein of chick optic lobe. *J. Neurosci.*, **4,** 2095-2105.

Bichet, D., Cornet, V., Geib, S., Carlier, E., Volsen, S., Hoshi, T., Mori, Y. and De Waard, M. (2000). The I-II loop of the Ca^{2+} channel α1 subunit contains an endoplasmic reticulum retention signal antagonized by the β subunit. *Neuron*, **25,** 177-190.

Blount, P. and Merlie, J. P. (1989). Molecular basis of the two nonequivalent ligand binding sites of the muscle nicotinic acetylcholine receptor. *Neuron*, **3,** 349-57.

Blount, P. and Merlie, J. P. (1990). Mutational analysis of muscle nicotinic acetylcholine receptor subunit assembly. *J. Cell Biol.*, **111,** 2613-2622.

Blount, P. and Merlie, J. P. (1991). BIP associates with newly synthesized subunits of the mouse muscle nicotinic receptor. *J. Cell Biol.*, **113,** 1125-32.

Blount, P., Smith, M. M. and Merlie, J. P. (1990). Assembly intermediates of the mouse muscle nicotinic acetylcholine receptor in stably transfected fibroblasts. *J. Cell Biol.*, **111,** 2601-2611.

Blumenthal, E. M., Conroy, W. G., Romano, S. J., Kassner, P. D. and Berg, D. K. (1997). Detection of functional nicotinic receptors blocked by α-bungarotoxin on PC12 cells and dependence of their expression on post-translational events. *J. Neurosci.*, **17,** 6094-6104.

Boess, F. G., Beroukhim, R. and Martin, I. L. (1995). Ultrastructure of the 5-hydroxytryptamine$_3$ receptor. *Journal of Neurochemistry*, **64,** 1401-1405.

Boess, F. G., Steward, L. J., Steele, J. A., Liu, D., Reid, J., Glencorse, T. A. and Martin, I. L. (1997). Analysis of the ligand binding site of the 5-HT_3 receptor using site directed mutagenesis: importance of glutamate 106. *Neuropharmacology*, **36,** 637-647.

Boorman, J. P. B., Groot-Kormelink, P. J. and Sivilotti, L. G. (2000). Stoichiometry of human recombinant neuronal nicotinic receptors containing the β3 subunit expressed in *Xenopus* oocytes. *J. Physiol.*, **529,** 565-577.

Boulter, J., Connolly, J., Deneris, E., Goldman, D., Heinemann, S. and Patrick, J. (1987). Functional expression of two neuronal nicotinic acetylcholine receptors from cDNA clones identifies a gene family. *Proc. Natl. Acad. Sci. USA*, **84,** 7763-7767.

Boulter, J., Evans, K., Goldman, D., Martin, G., Treco, D., Heinemann, S. and Patrick, J. (1986). Isolation of a cDNA clone coding for a possible neural nicotinic acetylcholine receptor α-subunit. *Nature*, **319,** 368-374.

Boulter, J., O'Shea-Greenfield, A., Duvoisin, R. M., Connolly, J. G., Wada, E., Jensen, A., Gardner, P. D., Ballivet, M., Deneris, E. S., McKinnon, D., Heinemann, S. and Patrick, J. (1990). α3, α5, and β4: three members of the rat neuronal nicotinic acetylcholine receptor-related gene family form a gene cluster. *J. Biol. Chem.*, **265,** 4472-82.

Boyd, G. W., Doward, A. I., Kirness, E. F., Millar, N. S. and Connolly, C. N. (2003). Cell surface expression of 5-hydroxytryptamine type 3 receptors is controlled by an endoplasmic reticulum retension signal. *J. Biol. Chem.*, **278,** 27681-27687.

Boyd, G. W., Low, P., Dunlop, J. I., Robertson, L. A., Vardy, A., Lambert, J. J., Peters, J. A. and Connolly, C. N. (2002). Assembly and cell surface expression of homomeric and heteromeric 5-HT3 receptors: the role of oligomerization and chaperone proteins. *Molecular and Cellular Neuroscience*, **21,** 38-50.

Brady, C. A., Stanford, I. M., Ali, I. L. L., Williams, J. M., Dubin, A. E., Hope, A. G. and Barnes, N. M. (2001). Pharmacological comparison of human homomeric 5-HT_{3A} receptors versus heteromeric 5-$HT_{3A/3B}$ receptors. *Neuropharmacology*, **41.**

Brejc, K., van Dijk, W. J., Klaassen, R. V., Schuurmans, M., van der Oost, J., Smit, A. B. and Sixma, T. K. (2001). Crystal structure of an ACh-binding protein reveals the ligand-binding domain of nicotinic receptors. *Nature*, **411,** 269-276.

Brisson, A. and Unwin, P. N. T. (1984). Tubular crystals of acetylcholine receptor. *J. Cell Biol.*, **99,** 1202-1211.

Broad, L. M., Felthouse, C., Zwart, R., McPhie, G., Pearson, K. H., Craig, P. J., Wallace, L., Broadmore, R. J., Boot, J. R., Keenan, M., Baker, S. R. and Sher, E. (2002). PSAB-OFP, a selective α7 nicotinic receptor agonist, is also a potent agonist of the 5-HT_3 receptor. *Eur. J. Pharmacol.*, **452,** 137-144.

Brown, A. M., Hope, A. G., Lambert, J. J. and Peters, J. A. (1998). Ion permeation and conduction in a human recombinant 5-HT3 receptor subunit (h5-HT3A). *J. Physiol.*, **507,** 653-665.

Brüss, M., Barann, M., Hayer-Zillgen, M., Eucker, T., Gothert, M. and Bonisch, H. (2000). Modified 5-HT_{3A} receptor function by co-expression of alternatively spliced human 5-HT_{3A} receptor isoforms. *Naunyn Schmiedebergs Archives of Pharmacology*, **362,** 392-401.

Chang, W., Gelman, M. S. and Prives, J. M. (1997). Calnexin-dependent enhancement of nicotinic acetylcholine receptor assembly and surface expression. *J. Biol. Chem.*, **272,** 28925-28932.

Changeux, J.-P., Bertrand, D., Corringer, P.-J., Dehaene, S., Edelstein, S., Lena, C., Le Novére, N., Marubio, L., Picciotto, M. and Zoli, M. (1998). Brain nicotinic receptors: structure and regulation, role in learning and reinforcement. *Brain Res. Rev.*, **26,** 198-216.

Changeux, J.-P., Kasai, M. and Lee, C. Y. (1970). Use of a snake venom toxin to characterise the cholinergic receptor protein. *Proc Natl Acad Sci U S A*, **67,** 1241-1247.

Chen, D. and Patrick, J. W. (1997). The α-bungarotoxin-binding nicotinic acetylcholine receptor from rat brain contains only the α7 subunit. *J. Biol. Chem.*, **272,** 24024-24029.

Chiara, D. C., Middleton, R. E. and Cohen, J. B. (1998). Identification of tryptophan 55 as the primary site of [^{3}H]nicotine photoincorporation in the γ-subunit of the *Torpedo* nicotinic acetylcholine receptor. *FEBS Lett.*, **423,** 223-226.

Chiara, D. C., Xie, Y. and Cohen, J. B. (1999). Structure of the agonist-binding sites of the *Torpedo* nicotinic acetylcholine receptor: affinity-labeling and mutational analyses identify γTyr-111/δArg-113 as antagonist affinity determinants. *Biochemistry*, **38,** 6689-6698.

Claudio, T., Paulson, H. L., Green, W., N., Ross, A. F., Hartman, D. S. and Hayden, D. (1989). Fibroblasts transfected with Torpedo acetylcholine receptor beta-, gamma-, and delta-subunit cDNAs express functional receptors when infected with a retroviral alpha recombinant. *J. Cell Biol.*, **108,** 2277-2290.

Conroy, W. G. and Berg, D. K. (1995). Neurons can maintain multiple classes of nicotinic acetylcholine receptors distinguished by different subunit compositions. *J. Biol. Chem.*, **270,** 4424-4431.

Conroy, W. G., Liu, Z., Nai, Q., Coggan, J. S. and Berg, D. K. (2003). PDZ-containing proteins provide a functional scaffold for nicotinic receptors in neurons. *Neuron*, **38,** 759-771.

Conroy, W. G., Vernallis, A. B. and Berg, D. K. (1992). The α5 gene product assembles with multiple acetylcholine receptor subunits to form distinctive receptor subtypes in brain. *Neuron*, **9,** 679-91.

Cooper, E., Couturier, S. and Ballivet, M. (1991). Pentameric structure and subunit stoichiometry of a neuronal nicotinic acetylcholine receptor. *Nature*, **350,** 235-238.

Cooper, S. T., Harkness, P. C., Baker, E. R. and Millar, N. S. (1999). Upregulation of cell-surface α4β2 neuronal nicotinic receptors by lower temperature and expression of chimeric subunits. *J. Biol. Chem.*, **274,** 27145-27152.

Cooper, S. T. and Millar, N. S. (1997). Host cell-specific folding and assembly of the neuronal nicotinic acetylcholine receptor α7 subunit. *J. Neurochem.*, **68,** 2140-2151.

Cooper, S. T. and Millar, N. S. (1998). Host cell-specific folding of the neuronal nicotinic receptor α8 subunit. *J. Neurochem.*, **70,** 2585-2593.

Cordero-Erausquin, M., Marubio, L. M., Klink, R. and Changeux, J.-P. (2000). Nicotinic receptor function: new perspectives from knockout mice. *Trends in Pharmacological Sciences*, **21,** 211-217.

Corringer, P.-J., Bertrand, S., Galzi, J.-L., Devillers-Thiéry, A., Changeux, J.-P. and Bertrand, D. (1999). Mutational analysis of the charge selectivity filter of the α7 nicotinic acetylcholine receptor. *Neuron*, **22,** 831-843.

Corringer, P.-J., Galzi, J.-L., Eliselé, J.-L., Bertrand, S., Changeux, J.-P. and Bertrand, D. (1995). Identification of a new component of the agonist binding site of the nicotinic α7 homooligomeric receptor. *J. Biol. Chem.*, **270,** 11749-11752.

Corringer, P.-J., Le Novére, N. and Changeux, J.-P. (2000). Nicotinic receptors at the amino acid level. *Ann. Rev. Pharmacol. Toxicol.*, **40,** 431-438.

Corriveau, R. A. and Berg, D. K. (1993). Coexpression of multiple acetylcholine receptor genes in neurons: quantification of transcripts during development. *J Neurosci*, **13,** 2662-71.

Couturier, S., Bertrand, D., Matter, J. M., Hernandez, M. C., Bertrand, S., Millar, N., Valera, S., Barkas, T. and Ballivet, M. (1990b). A neuronal nicotinic acetylcholine receptor subunit (α7) is developmentally regulated and forms a homo-oligomeric channel blocked by α-BTX. *Neuron*, **5,** 847-856.

Couturier, S., Erkman, L., Valera, S., Rungger, D., Bertrand, S., Boulter, J., Ballivet, M. and Bertrand, D. (1990a). α5, α3, and non-α3. Three clustered avian genes encoding neuronal nicotinic acetylcholine receptor-related subunits. *J. Biol. Chem.*, **265,** 17560-17567.

Cruz, H., Arrabit, C. and Slesinger, P. (2001). Structural features of the pore lining M2 transmembrane segment of the serotonin-gated ion channel. *Biophysical Journal*, **80,** 336A.

Crystal, A. S., Morais, V. A., Pierson, T., Pijak, D. S., Carlin, D., Lee, V. M.-Y. and Doms, R. W. (2003). Membrane topology of g-secretase component PEN-2. *J Biol Chem*, **278,** 43284-43291.

Dani, J. A., De Biasi, M., Liang, Y., Peterson, J., Zhang, L., Zhang, T. and Zhou, F. M. (2004). Potential applications of nicotinic ligands in the laboratory and clinic. *Bioorganic and Medicinal Chemistry Letters*, **14,** 1837-1839.

Davies, P. A., Pistis, M., Hanna, M. C., Peters, J. A., Lambert, J. J., Hales, T. G. and Kirkness, E. F. (1999). The 5-HT_{3B} subunit is a major determinant of serotonin-receptor function. *Nature*, **397,** 359-363.

Deneris, E. S., Connolly, J., Boulter, J., Wada, E., Wada, K., Swanson, L. W., Patrick, J. and Heinemann, S. (1988). Primary structure and expression of β2: a novel subunit of neuronal nicotinic acetylcholine receptors. *Neuron*, **1,** 45-54.

Derkach, V., Surprenant, A. and North, R. A. (1989). 5-HT_3 receptors are membrane ion channels. *Nature*, **339,** 706-709.

Dineley, K. T. and Patrick, J. W. (2000). Amino acid determinants of α7 nicotinic acetylcholine receptor surface expression. *J. Biol. Chem.*, **275,** 13974-13985.

DiPaola, M., Czajkowski, C., Karlin, A. (1989). The sidedness of the COOH terminus of the acetylcholine receptor δ subunit. *J Biol Chem*, **264,** 15457-15463.

Dominguez del Toro, E., Juiz, J. M., Smillie, F. I., Lindstrom, J. and Criado, M. (1997). Expression of alpha 7 neuronal nicotinic receptors during postnatal development of the rat cerebellum. *Brain Res Dev Brain Res*, **98,** 125-133.

Downie, D. L., Hope, A. G., Lambert, J. J., Peters, J. A., Blackburn, T. P. and Jones, B. J. (1994). Pharmacological characterization of the apparent splice variants of the murine 5-HT_3R-A subunit expressed in Xenopus leavis oocytes. *Neuropharmacology*, **33,** 473-482.

Drago, J., McColl, C. D., Horne, M. K., Finkelstein, D. I. and Ross, S. A. (2003). Neuronal nicotinic receptors: insights gained from gene knockout and knockin mutant mice. *Cell. Mol. Life Sci.*, **60,** 1267-1280.

Drisdel, R. C., Manzana, E. and Green, W. N. (2004). The role of palmitoylation in functional expression of nicotinic α7 receptors. *J. Neurosci.*, **24,** 10502-10510.

Dubin, A. E. (2001). *http://v3.espacenet.com; patent no. WO 01/16297.*

Dubin, A. E., Huvar, R., Dandrea, M. R., Pyati, J., Zhu, J. Y., Joy, K. C., Wilson, S. J., Galindo, J. E., Glass, C. A., Luo, L., Jackson, M. R., Lovenberg, T. W. and Erlander, M. G. (1999). The pharmacological and functional characteristics of the serotonin 5-HT_{3A} receptor are specifically modified by a 5-HT_{3B} receptor subunit. *J Biol Chem*, **274,** 30799-30810.

Dunn, S. M., Bateson, A. N. and Martin, I. L. (1994). Molecular neurobiology of the $GABA_A$ receptor. *Int. Rev. Neurobiol.*, **36,** 51-96.

Eiselé, J.-L., Bertrand, S., Galzi, J.-L., Devillers-Thiéry, A., Changeux, J.-P. and Bertrand, D. (1993). Chimaeric nicotinic-serotonergic receptor combines distinct ligand binding and channel specificities. *Nature*, **366,** 479-483.

Elgoyhen, A. B., Johnson, D. S., Boulter, J., Vetter, D. E. and Heinemann, S. (1994). α9: an acetylcholine receptor with novel pharmacological properties expressed in rat cochlear hair cells. *Cell*, **18,** 705-715.

Elgoyhen, A. B., Vetter, D. E., Katz, E., Rothlin, C. V., Heineman, S. F. and Boulter, J. (2001). α10: a determinant of nicotinic cholinergic receptor function in

mammakian vestibular and cochlear mechanosensory hair cells. *Proc. Natl. Acad. Sci. USA*, **98,** 3501-3506.

Ellgaard, L., Molinari, M. and Helenius, A. (1999). Setting the standards: Quality control in the secretory pathway. *Science*, **286,** 1882-1888.

Eusebi, F., Grassi, F., Nervi, C., Caporale, C., Adamo, S., Zani, B. M. and Molinaro, M. (1987). Acetylcholine may regulate its own nicotinic receptor-channel through the C-kinase system. *Proc. R. Soc. Lond. B. Biol. Sci.*, **230,** 355-365.

Fletcher, S. and Barnes, N. M. (1998). Desperately seeking subunits: are native 5-HT_3 receptors really homomeric complexes? *Trends in Pharmacological Sciences*, **16,** 212-215.

Fletcher, S., Lindstrom, J. M., McKernan, R. M. and Barnes, N. M. (1998). Evidence that porcine native 5-HT_3 receptors do not contain nicotinic acetylcholine receptor subunits. *Neuropharmacol.*, **37,** 397-399.

Flores, C. M., DeCamp, R. M., Kilo, S., Rogers, S. W. and Hargreaves, K. M. (1996). Neuronal nicotinic receptor expression in sensory neurons of the rat trigeminal ganglion: Demonstration of $\alpha 3\beta 4$, a novel subtype in the mammalian nervous system. *J. Neurosci.*, **16,** 7892-7901.

Flores, C. M., Rogers, S. W., Pabreza, L. A., Wolfe, B. B. and Kellar, K. J. (1992). A subtype of nicotinic cholinergic receptor in rat brain is composed of $\alpha 4$ and $\beta 2$ subunits and is up-regulated by chronic nicotine treatment. *Mol. Pharmacol.*, **41,** 31-37.

Forsayeth, J. R., Gu, Y. and Hall, Z. W. (1992). BiP forms stable complexes with unassembled subunits of the acetylcholine receptor in transfected COS cells and in C2 muscle cells. *J. Cell Biol.*, **117,** 841-847.

Forsayeth, J. R. and Kobrin, E. (1997). Formation of oligomers containing the $\beta 3$ and $\beta 4$ subunits of the rat nicotinic receptor. *J. Neurosci.*, **17,** 1531-1538.

Froehner, S. C. (1991). The submembrane machinery for nicotinic acetylcholine receptor clustering. *J Cell Biol*, **114,** 1-7.

Fu, D.-X. and Sine, S. M. (1994). Competitive antagonists bridge the α-γ interface of the acetylcholine receptor through quaternary ammonium-aromatic interactions. *J Biol Chem*, **269,** 26152-26157.

Fucile, S., Matter, J.-M., Erkman, L., Ragozzino, D., Barabino, B., Grassi, F., Alemà, S., Ballivet, M. and Eusebi, F. (1998). The neuronal $\alpha 6$ subunit forms

functional heteromeric acertylcholine receptors in human transfected cells. *Eur. J. Neurosci.*, **10,** 172-178.

Fucile, S., Palma, E., Eusebi, F. and Miledi, R. (2002). Serotonin antagonizes the human neuronal α7 nicotinic acetylcholine receptor and becomes an agonist after L248T α7 mutation. *Neuroscience*, **110,** 169-179.

Galzi, J.-L. and Changeux, J.-P. (1995). Neuronal nicotinic receptors: Molecular organization and regulations. *Neuropharmacology*, **34,** 563-582.

Galzi, J. L., Bertrand, D., Devillers-Thiery, A., Revah, F., Bertrand, S. and Changeux, J. P. (1991b). Functional significance of aromatic amino acids from three peptide loops of the alpha 7 neuronal nicotinic receptor site investigated by site-directed mutagenesis. *Febs Lett*, **294,** 198-202.

Galzi, J. L., Devillers-Thiery, A., Hussy, N., Bertrand, S., Changeux, J. P. and Bertrand, D. (1992). Mutations in the channel domain of a neuronal nicotinic receptor convert ion selectivity from cationic to anionic. *Nature*, **359,** 500-5.

Galzi, J. L., Revah, F., Black, D., Goeldner, M., Hirth, C. and Changeux, J. P. (1990). Identification of a novel amino acid alpha-tyrosine 93 within the cholinergic ligands-binding sites of the acetylcholine receptor by photoaffinity labeling. Additional evidence for a three-loop model of the cholinergic ligands-binding sites. *J Biol Chem*, **265,** 10430-7.

Galzi, J. L., Revah, F., Bouet, F., Menez, A., Goeldner, M., Hirth, C. and Changeux, J. P. (1991a). Allosteric transitions of the acetylcholine receptor probed at the amino acid level with a photolabile cholinergic ligand. *Proc Natl Acad Sci U S A*, **88,** 5051-5.

Gehle, V. M., Walcott, E. C., Nishizaki, T. and Sumikawa, K. (1997). *N*-glycosylation at the conserved sites ensures the expression of properly folded functional ACh receptors. *Mol. Brain Res.*, **45,** 219-229.

Gelman, M. S., Chang, W., Thomas, D. Y., Bergeron, J. J. M. and Prives, J. M. (1995). Role of the endoplasmic reticulum chaperone calnexin in subunit folding and assembly of nicotinic acetylcholine receptors. *J. Biol. Chem.*, **270,** 15085-15092.

Gerzanich, V., Anand, R. and Lindstrom, J. (1994). Homomers of α8 and α7 subunits of nicotinic receptors exhibit similar channels but contrasting binding site properties. *Mol. Pharmacol.*, **45,** 212-220.

Gilon, P. and Yakel, J. L. (1995). Activation of 5-HT_3 receptors expressed in *Xenopus* oocytes does not increase cytoplasmic Ca^{2+} levels. *Receptors and Channels*, **3,** 83-88.

Giraudat, J., Dennis, M., Heidmann, T., Chang, J.-Y. and Changeux, J.-P. (1986). Structure of the high-affinity binding site for noncompetitive blockers of the acetylcholine receptor: serine-262 of the δ subunit us labeled by [^{3}H]chlorpromazine. *Proc. Natl. Acad. Sci. U S A*, **83,** 2719-1723.

Glitsch, M., Wischmeyer, E. and Karschin, A. (1996). Functional characterisation of two 5-HT_3 receptor splice variants isolated from a mouse hippocampal cell line. *Pflugers Arch. - Eur. J. Phsyiol.*, **432,** 134-143.

Goldman, D., Deneris, E., Luyten, W., Kochhar, A., Patrick, J. and Heinemann, S. (1987). Members of a nicotinic acetylcholine receptor gene family are expressed in different regions of the mammalian central nervous system. *Cell*, **48,** 965-73.

Gopalakrishnan, M., Buisson, B., Touma, E., Giordano, T., Campbell, J. E., Hu, I. C., Donnelly-Roberts, D., Arneric, S. P., Bertrand, D. and Sullivan, J. P. (1995). Stable expression and pharmacological properties of the human α7 nicotinic acetylcholine receptor. *Eur. J. Pharmacol.*, **290,** 237-246.

Gotti, C., Hanke, W., Maury, K., Moretti, M., Ballivet, M., Clementi, F. and Bertrand, D. (1994). Pharmacology and biophysical properties of α7 and α7-α8 α-bungarotoxin receptor subtypes immunopurified from the chick optic lobe. *Eur. J. Neurosci.*, **6,** 1281-1291.

Gotti, C., Moretti, M., Maggi, R., Longhi, R., Hanke, W., Klinke, N. and Clementi, F. (1997). α7 and α8 nicotinic receptor subtypes immunopreceipitated from chick retina have different immunological, pharmacological and functional properties. *Eur. J. Neurosci.*, **9,** 1201-1211.

Green, T., Stauffer, K. A. and Lummis, C. R. (1995). Expression of recombinant homo-oligomeric 5-hydroxytryptamine$_3$ receptors provides new insights into their maturation and structure. *J. Biol. Chem.*, **270,** 6056-6061.

Green, W. N. (1999). Ion channel assembly: creating structures that function. *J. Gen Physiol.*, **113,** 163-169.

Green, W. N. and Claudio, T. (1993). Acetylcholine receptor assembly: subunit folding and oligomerization occur sequentially. *Cell*, **74,** 57-69.

Green, W. N. and Millar, N. S. (1995). Ion-channel assembly. *Trends Neurosci.*, **18,** 280-287.

Green, W. N. and Wanamaker, C. P. (1997). The role of the cystine loop in acetylcholine receptor assembly. *J. Biol. Chem.*, **272,** 20945-20953.

Green, W. N. and Wanamaker, C. P. (1998). Formation of the nicotinic acetylcholine receptor binding site. *J. Neurosci.*, **18,** 5555-5564.

Greene, L., Sytkowski, A., Vogel, A., Nirenberg, M. (1973). α-Bungarotoxin used as a probe for acetylcholine receptors of culture neurons. *Nature*, **243,** 163-166.

Greenshaw, A. J. and Silverstone, P. H. (1997). The non-antiemetic uses of serotonin 5-HT_3 receptor antagonists. *Drugs*, **53,** 20-39.

Gu, Y., Forsayeth, J. R., Verrall, S., Yu, X. M. and Hall, Z. W. (1991). Assembly of the mammalian muscle acetylcholine receptor in transfected COS cells. *J. Cell Biol.*, **114,** 799-807.

Gunthorpe, M. J. and Lummis, S. C. (1999). Diltiazem causes open channel block of recombinant 5-HT3 receptors. *J. Physiol.*, **519,** 713-722.

Gunthorpe, M. J. and Lummis, S. C. R. (2001). Conversion of the ion selectivity of the 5-HT_{3A} receptor from cationic to anionic reveals a conserved feature of the ligand-gated ion channel superfamily. *J Biol Chem*, **276,** 10977-10983.

Gurley, D. A., Harris, E. W., Li, C., Johnson, E. C. and Lanthorn, T. H. (2000). 5-hydroxyindole potentiates the nicotinic acetylcholine receptor α7 subtype. *Society for Neuroscience Abstracts*, **716.15**.

Gurley, D. A. and Lanthorn, T. H. (1998). Nicotinic agonists competitively antagonize serotonin at 5-HT_3 receptors expressed in *Xenopus* oocytes. *Neuroscience Letters*, **247,** 107-110.

Haas, I. G. and Wabl, M. (1983). Immunoglobulin heavy chain binding protein. *Nature*, **306,** 387-389.

Halevi, S., McKay, J., Palfreyman, M., Yassin, L., Eshel, M., Jorgensen, E. M. and Treinin, M. (2002). The *C.elegans ric-3* gene is required for maturation of nicotinic acertylcholine receptors. *EMBO Journal*, **21,** 1012-1020.

Halevi, S., Yassin, L., Eshel, M., Sala, F., Sala, S., Criado, M. and Treinin, M. (2003). Conservation within the RIC-3 gene family: effectors of mammalian nicotinic acetylcholine receptor expression. *J. Biol. Chem.*, **278,** 34411-34417.

Hamilton, S. L., McLaughlin, M. and Karlin, A. (1979). Formation of disulphide linked oligomers of acetylcholine receptor in membrane from Torpedo electric tissue. *Biochemistry*, **18,** 155-163.

Hanna, M. C., Davies, P. A., Hales, T. G. and Kirkness, E. F. (2000). Evidence for expression of heteromeric serotonin 5-HT_3 receptors in rodents. *Journal of Neurochemistry*, **75,** 240-247.

Hargreaves, A. C., Lummis, S. C. and Taylor, C. W. (1994). Ca^{2+} permeability of cloned and native 5-hydroxytryptamine type 3 receptors. *Molec. Pharmacol.*, **46,** 1120-1128.

Harkness, P. C. and Millar, N. S. (2001). Inefficient cell-surface expression of hybrid complexes formed by the co-assembly of neuronal nicotinic acetylcholine receptor and serotonin receptor subunits. *Neuropharmacol.*, **41,** 79-87.

Harkness, P. C. and Millar, N. S. (2002). Changes in conformation and sub-cellular distribution of $\alpha4\beta2$ nicotinic acetylcholine receptors revealed by chronic nicotine treatment and expression of subunit chimeras. *J. Neurosci.*, **22,** 10172-10181.

Helekar, S. A. and Patrick, J. (1997). Peptidyl prolyl cis-trans isomerase activity of cyclophilin A in functional homo-oligomeric receptor expression. *Proc. Natl. Acad. Sci. USA*, **94,** 5432-5437.

Helenius, A. and Aebi, M. (2001). Intracellular functions of N-linked glycans. *Science*, **291,** 2364-2369.

Hermosilla, R., Oueslati, M., Donalies, U., Schönenberger, E., Krause, E., Oksche, A., Rosenthal, W. and Schülein, R. (2003). Disease-causing V2 vasopressin receptors are retained in different compartments of the early secretory pathway. *Traffic*, **5,** 993-1005.

Hope, A. G., Belelli, D., Mair, I. D., Lambert, J. J. and Peters, J. A. (1999). Molecular determinants of (+)-tubocurarine binding at recombinant 5-hydroxytryptamine$_{3A}$ receptor subunits. *Molec. Pharmacol.*, **55,** 1037-1043.

Hope, A. G., Downie, D. L., Sutherland, L., Lambert, J. J., Peters, J. A. and Burchell, B. (1993). Cloning and functional expression of an apparent splice variant of the murine 5-HT_3 receptor A subunit. *European Journal of Pharmacology*, **245,** 187-192.

Hope, A. G., Peters, J. A., Brown, A. M., Lambert, J. J. and Blackburn, T. P. (1996). Characterization of a human 5-hydroxytryptamine$_3$ receptor type A (h5-

HT_3R-AS) subunit stably expressed in HEK 293 cells. *Br. J. Pharmacol.*, **118,** 1237-1245.

Hope, A. G., Sutherland, L. and Lambert, J. J. (1997). Recombinant 5-hydroxytryptamine$_3$ receptors. *In Recombinant cell surface receptors: focal point for therapeutic intervention. Ed. M. J. Browne Academic Press,* 119-154.

Hopp, T. P., Prickett, K. S., Price, V. L., Libby, R. T., March, C. J., Cerretti, D. P., Urdal, D. L. and Conlon, P. J. (1988). A short polypeptide marker sequence useful for recombinant protein identification and purification. *Biotechnology*, **6,** 1204-1210.

Hoyer, D. and Martin, G. (1997). 5-HT receptor classification and nomenclature: towards a harmonization with the human genome. *Neuropharmacology*, **34,** 419-428.

Hubbard, P. C., Thompson, A. J. and Lummis, S. C. R. (2000). Functional differences between splice variants of the murine 5-HT_{3A} receptor: possible role for phosphorylation. *Molecular Brain Research*, **81,** 101-108.

Hucho, F., Oberthür, W. and Lottspeich, F. (1986). The ion channel of the nicotinic acetylcholine receptor is formed by the homologous helices MII of the receptor subunits. *FEBS Lett.*, **205,** 137-142.

Huganir, R. L. and Greengard, P. (1983). cAMP-dependent protein kinase phosphorylates the nicotinic acetylcholine receptor. *Proc Natl Acad Sci U S A*, **80,** 1130-1134.

Huganir, R. L. and Greengard, P. (1990). Regulation of neurotransmitter receptor desensitization by protein phosphorylation. *Neuron*, **5,** 555-567.

Huganir, R. L., Miles, K. and Greengard, P. (1984). Phosphorylation of the nicotinic acetylcholine receptor by an endogenous tyrosine-specific kinase. *Proc Natl Acad Sci USA*, **81,** 6968-6972.

Hunt, S. and Schmidt, J. (1978). Some observations on the binding patterns of αbungarotoxin in the central nervous system of the rat. *Brain Res.*, **157,** 213-232.

Hussy, N., Lukas, W. and Jones, K. A. (1994). Functional properties of a cloned 5-hydroxytryptamine ionotropic receptor subunit: comparison with native mouse receptors. *J. Physiol.*, **481,** 311-323.

Ibañez-Tallon, I., Miwa, J. M., Wang, H.-L., Adams, N. C., Crabtree, G. W., Sine, S. M. and Heintz, N. (2002). Novel modulation of neuronal nicotinic acetylcholine receptors by association with the endogenous prototoxin lynx1. *Neuron*, **33,** 893-903.

Imoto, K., Busch, C., Sakmann, B., Mishina, M., Konno, T., Nakai, J., Bujo, H., Mori, Y., Fukuda, K. and Numa, S. (1988). Rings of negatively charged amino acids determine the acetylcholine receptor channel conductance. *Nature*, **335,** 645-8.

Imperato, A. and Angelucci, L. (1989). 5-HT3 receptors control dopamine release in the nucleus accumbens of freely moving rats. *Neuroscience Letters*, **101,** 214-217.

Isenberg, K. E., Ukhun, I. A., Holstad, S. G., Jafri, S., Uchida, U., Zorumski, C. F. and Yang, J. (1993). Partial cDNA cloning and NGF regulation of a rat 5-HT_3 receptor subunit. *Neuroreport*, **5,** 121-124.

Itier, V. and Bertrand, D. (2001). Neuronal nicotinic receptors: from protein structure to function. *FEBS Lett.*, **504,** 118-125.

Jackson, M. B. and Yakel, J. L. (1995). The 5-HT_3 receptor channel. *Ann. Rev. Physiol.*, **57,** 447-468.

Jaskolski, F., Coussen, F., Nagarajan, N., Normand, E., Rosenmund, C. and Mulle, C. (2004). Subunit composition and alternative splicing regulate membrane delivery of kainite receptors. *J. Neurosci.*, **24,** 2506-2515.

Jeanclos, E. M., Lin, L., Treuil, M. W., Rao, J., DeCoster, M. A. and Anand, R. (2001). The chaperone protein 14-3-3η interacts with the nicotinic acetylcholine receptor α4 subunit. *J. Biol. Chem.*, **276,** 28281-28290.

Johnson, D. S. and Heinemann, S. F. (1992). Cloning and expression of the rat 5-HT_3 receptor reveals species-specific sensitivity to curare antagonism. *Society for Neuroscience Abstracts*, **18,** 249.

Jones, B. J. and Blackburn, T. P. (2002). The medical benefit of 5-HT research. *Pharmacology, Biochemistry and Behaviour*, **71,** 555-568.

Jones, S., Sudweeks, S. and Yakel, J. L. (1999). Nicotinic receptors in the brain: correlating physiology with function. *Trends Neurosci.*, **22,** 555-561.

Jones, S. and Yakel, J. L. (1997). Functional nicotinic ACh receptors on interneurones in the rat hippocampus. *J. Physiol.*, **504,** 603-610.

Jones, S. and Yakel, J. L. (2003). Casein kinase II (protein kinase CK2) regulates serotonin 5-HT_3 receptor channel function in NG108-15 cells. *Neuroscience*, **119,** 629-634.

Kall, L., Krogh, A. and Sonnhammer, E. L. (2004). A combined transmembrane topology and signal peptide prediction method. *J. Mol. Biol.*, **338,** 1027-1036.

Kao, P. N., Dwork, A. J., Kaldany, R. R. J., Silver, M., Wideman, J., Stein, J. and Karlin, A. (1984). Identification of the alpha-subunit half cysteine specifically labeled by an affinity reagent for acetylcholine receptor binding site. *J. Biol. Chem.*, **259,** 11662-65.

Kao, P. N. and Karlin, A. (1986). Acetylcholine receptor binding site contains a disulfide cross-link between adjacent half-cystinyl residues. *J. Biol. Chem.*, **261,** 8085-8088.

Karlin, A. (2002). Emerging structure of the nicotinic acetylcholine receptors. *Nat Rev Neurosci*, **3,** 102-114.

Karlin, A. and Akabas, M. H. (1995). Towards a structural basis for the function of nicotinic acetylcholine receptors and their cousins. *Neuron*, **15,** 1231-1244.

Karlin, A., Holtzman, E., Yodh, N., Lobel, P., Wall, J. and Hainfeld, J. (1983). The arrangement of the subunits of the acetylcholine receptor of *Torpedo californica*. *J Biol Chem*, **258.**

Karnovsky, A. M., Gotow, L. F., McKinley, D. D., Piechan, J. L., Ruble, C. L., Mills, C. J., Schellin, K. A. B., Slightom, J. L., Fitzgerald, L. R., Benjamin, C. W. and Roberds, S. L. (2003). A cluster of novel serotonin receptor 3-like genes on human chromosome 3. *Gene*, **319,** 137-148.

Kassner, P. D. and Berg, D. K. (1997). Differences in the fate of neuronal acetylcholine receptor protein expressed in neurons and stably transfected cells. *J. Neurobiol.*, **33,** 968-982.

Keller, S. H., Lindstrom, J. and Taylor, P. (1996). Involvement of the chaperone protein calnexin and the acetylcholine receptor β-subunit in the assembly and cell surface expression of the receptor. *J Biol Chem*, **271,** 22871-22877.

Keller, S. T. and Taylor, P. (1999). Determinants responsible for assembly of the nicotinic acetylcholine receptor. *J. Gen. Physiol.*, **113,** 171-176.

Kelley, S. P., Dunlop, J. I., Kirkness, E. F., Lambert, J. J. and Peters, J. A. (2003). A cytoplasmic region determines single-channel conductance in 5-HT_3 receptors. *Nature*, **424,** 321-324.

Keyser, K. T., Britto, L. R., Schoepfer, R., Whiting, P., Cooper, J., Conroy, W., Brozozowska-Prechtl, A., Karten, H. J. and Lindstrom, J. (1993). Three subtypes of α-bungarotoxin-sensitive nicotinic acetylcholine receptors are expressed in chick retina. *J. Neurosci.*, **13,** 442-54.

Khiroug, S. S., Harkness, P. C., Lamb, P. W., Sudweeks, S. N., Khiroug, L., Millar, N. S. and Yakel, J. L. (2002). Rat nicotinic receptor α7 and β2 subunits co-assemble to form functional heteromeric nicotinic receptor channels. *J. Physiol.*, **540,** 425-434.

Kolodziej, P. A. and Young, R. A. (1991). Epitope tagging and protein surveillance. *Methods Enzymol.*, **194,** 508-519.

Kooyman, A. R., van Hooft, J. A., Vanderheijden, P. M. L. and Vijverberg, H. P. M. (1994). Competitive and non-competitive effects of 5-hydroxyindole on 5-HT_3 receptors in N1E-115 neuroblastoma cells. *Br. J. Pharmacol.*, **112,** 541-546.

Kooyman, A. R., van Hooft, J. A. and Vijverberg, H. P. M. (1993). 5-Hydroxyindole slows desensitisation of the 5-HT_3 receptor-mediated ion current in N1E-115 neuroblastoma cells. *Br. J. Pharmacol.*, **108,** 287-289.

Kriegler, S., Sudweeks, S. and Yakel, J. L. (1999). The nicotinic α4 receptor subunit contributes to the lining of the ion channel pore when expressed with the 5-HT_3 receptor subunit. *J. Biol. Chem.*, **274,** 3934-3936.

Kuhse, J., Betz, H. and Kirsch, J. (1995). The inhibitory glycine receptor: architecture, synaptic localization and molecular pathology of a postsynaptic ion-channel complex. *Curr. Opin. Neurobiol.*, **5,** 318-323.

Kuryatov, A., Olale, F., Cooper, J., Choi, C. and Lindstrom, J. (2000). Human α6 AChR subtypes: subunit composition, assembly, and pharmacological responses. *Neuropharmacol.*, **39,** 2570-2590.

Lambert, J. J., Belelli, D., Hill-Venning, C. and Peters, J. A. (1995). Neurosteroids and $GABA_A$ receptor function. *Trends Pharmacol Sci*, **16,** 295-303.

Lankiewicz, S., Huser, M. B., Heumann, R., Hatt, H. and Gisselmann, G. (2000). Phosphorylation of the 5-hydrotryptamine$_3$ (5-HT_3) receptor expressed in HEK293 cells. *Receptors and Channels*, **7,** 9-15.

Lankiewicz, S., Lobitz, N., Wetzel, C. H. R., Rupprecht, R., Gisselmann, G. and Hatt, H. (1998). Molecular cloning, functional expression, and

pharmacological characterization of 5-hydroxytryptamine$_3$ receptor cDNA and its splice variants from guinea pig. *Mol. Pharmacol.*, **53,** 202-212.

Lansdell, S. J., Gee, V. J., Harkness, P. C., Doward, A. I., Baker, E. R., Gibb, A. J. and Millar, N. S. RIC3 enhances functional expression of multiple nicotinic acetylcholine receptor subtypes in mammalian cells. *Manuscript submitted.*

Lansdell, S. J. and Millar, N. S. (2002). Dβ3, an atypical nicotinic acetylcholine receptor subunit from *Drosophila*: molecular cloning, heterologous expression and coassembly. *J. Neurochem.*, **80,** 1009-1018.

LaPolla, R. J., Mayne, K. M. and Davidson, N. (1984). Isolation and characterisation of a cDNA clone for the complete coding region of the δ subunit of the mouse acetylcholine receptor. *Proc Natl Acad Sci U S A*, **81,** 7970-7974.

Le Novère, N., Grutter, T. and Changeux, J.-P. (2002). Models of the extracellular domain of the nicotinic receptors and of agonist- and Ca^{2+}-binding sites. *Proc Natl Acad Sci U S A*, **99,** 3210-3215.

Le Novère, N., Zoli, M., Lena, C., Ferrari, R., Picciotto, M. R., Merlo Pich, E. and Changeux, J.-P. (1999). Involvement of alpha6 nicotinic receptor subunit in nicotine-elicited locomotion, demonstrated by in vivo antisense oligonucleotide infusion. *Neuroreport*, **10,** 2497-2501.

Lee, C. Y. and Chang, C. C. (1966). Modes of action of purified toxins from elapid venoms on neuromuscular transmission. *Mem. Inst. Butantan. Sao Paulo*, **33,** 555-572.

Lena, C. and Changeux, J.-P. (1998). Allosteric nicotinic receptors, human pathologies. *J. Physiol.*, **92,** 63-74.

Levin, E. D. and Simon, B. B. (1998). Nicotinic acetylcholine involvement in cognitive function in animals. *Psychopharmacology*, **138,** 217-230.

Lin, L., Jeanclos, E. M., Treuil, M. W., Braunewell, K.-H., Gundelfinger, E. D. and Anand, R. (2002). The calcium sensor protein visinin-like protein-1 modulates the surface expression and agonist-sensitivity of the α4β2 nicotinic acetylcholine receptor. *J. Biol. Chem.*, **277,** 41872-41878.

Lloyd, G. K. and Williams, M. (2000). Neuronal nicotinic acetylcholine receptors as novel drug targets. *J. Pharmacol. Exp. Ther.*, **292,** 461-467.

Lukas, R. J., Changeux, J.-P., Le Novère, N., Albuquerque, E. X., Balfour, D. J. K., Berg, D. K., Bertrand, D., Chiappinelli, A. A., Clarke, P. B. S., Collins, A. C.,

Dani, J. A., Grady, S. R., Kellar, K. J., Lindstrom, J. M., Marks, M. J., Quik, M., Taylor, P. W. and Wonnacott, S. (1999). International union of pharmacology. XX. current status of the nomenclature for nicotinic acetylcholine receptors and their subunits. *Pharmacol. Rev.*, **51,** 397-401.

Lustig, L. R., Peng, H., Hiel, H., Yamamoto, T. and Fuchs, P. A. (2001). Molecular cloning and mapping of the human nicotinic acetylcholine receptor α10 (CHRNA10). *Genomics*, **73,** 272-283.

Machu, T. K., Hamilton, M. E., Frye, T. F., Shanklin, C. L., Harris, M. C., Sun, H., Tenner, T. E. J., Soti, F. S. and Kem, W. R. (2001). Benzylidene analogs of anabaseine display partial agonist and antagonist properties at the mouse 5-hydroxytryptamine(3A) receptor. *J. Pharmacol. Exp. Ther.*, **299,** 1112-1119.

Macor, J. E., Gurley, D., Lanthorn, T., Loch, J., Mack, R. A., Mullen, G., Tran, O., Wright, N. and Gordon, J. C. (2001). The 5-HT_3 antagonist tropisetron (ICS 205-930) is a potent and selective α7 nicotinic receptor partial agonist. *Bioorganic and Medicinal Chemistry Letters*, **11,** 319-321.

Maelicke, A. and Albuquerque, E. X. (2000). Allosteric modulation of nicotinic acetylcholine receptors as a treatment strategy for Alzheimer's disease. *Eur. J. Pharmacol.*, **393,** 165-170.

Mandelzys, A., Pié, B., Deneris, E. S. and Cooper, E. (1994). The developmental increase in ACh current densities on rat sympathetic neurons correlates with changes in nicotinic ACh receptor a-subunit gene expression and occurs independent of innervation. *J. Neurosci.*, **14,** 2357-2364.

Mansvelder, H. D. and McGehee, D. S. (2000). Long-term potentiation of excitatory inputs to brain reward areas by nicotine. *Neuron*, **27,** 349-357.

Mansvelder, H. D. and McGehee, D. S. (2002). Cellular and synaptic mechanisms of nicotine addiction. *J. Neurobiol.*, **53,** 606-617.

Marazziti, D., Betti, L., Giannaccini, G., Rossi, A., Masala, I., Baroni, S., Cassano, G. B. and Lucacchini, A. (2001). Distribution of [^{3}H]GR65630 binding in human brain postmortem. *Neurochemical Research*, **26,** 187-190.

Margeta-Mitrovic, M., Jan, Y. N. and Jan, L. Y. (2000). A trafficking checkpoint controls $GABA_B$ receptor heterodimerization. *Neuron*, **27,** 97-106.

Maricq, A. V., Peterson, A. S., Brake, A. J., Myers, R. M. and Julius, D. (1991). Primary structure and functional expression of the $5HT_3$ receptor, a serotonin-gated ion channel. *Science*, **254,** 432-437.

Martin, M., Czajkowski, C. and Karlin, A. (1996). The contribution of aspartyl residues in the acetylcholine receptor γ and δ subunits to the binding of agonists and competitive antagonists. *J Biol Chem*, **271,** 13497-13503.

Marubio, L. M. and Changeux, J.-P. (2000). Nicotinic acetylcholine receptor knockout mice as animal models for studying receptor function. *Eur. J. Pharmacol.*, **393,** 113-121.

Marubio, L. M., del Mar Arroyo-Jimenez, M., Lena, C., Le Novére, N., Kerchove d'Exaerde, A., Huchet, M., Damaj, M. I. and Changeux, J.-P. (1999). Reduced antinociception in mice lacking neuronal nicotinic receptor subunits. *Nature*, **398,** 805-810.

McGehee, D. S. and Role, L. W. (1995). Physiological diversity of nicotinic acetylcholine receptors expressed by vertebrate neurons. *Annu. Rev. Physiol.*, **57,** 521-546.

McKernan, R. M. (1992). Biochemical properties of the $5\text{-}HT_3$ receptor. *Central and Peripheral 5-HT_3 receptors, M. Hamon, ed. (London: Academic Press)*, 89-102.

Mei, L. and Xiong, W. C. (2003). Two birds with one stone: a novel motif for ACh receptor assembly quality control. *Trends in Neurosciences*, **26,** 178-181.

Merlie, J. P. and Lindstrom, J. (1983). Assembly in vivo of mouse muscle acetylcholine receptor: identification of an alpha subunit species that may be an assembly intermediate. *Cell*, **34,** 747-757.

Millar, N. S. (2003). Assembly and subunit diversity of nicotinic acetylcholine receptors. *Biochem. Soc. Trans.*, **31,** 869-874.

Miller, C. (1989). Genetic manipulation of ion channels: a new approach to structure and mechanism. *Neuron*, **2,** 1195-1205.

Miquel, M. C., Emerit, M. B., Gingrich, J. A., Nosjean, A., Hamon, M. and El Mestikawy, S. (1995). Developmental changes in the differential expression of two serotonin $5\text{-}HT_3$ receptor splice variants in the rat. *Journal of Neurochemistry*, **65,** 475-483.

Mishina, M., Takai, T., Imoto, K., Noda, M., Takahashi, T., Numa, S., Methfessel, C. and Sakman, B. (1986). Molecular distinction between fetal and adult forms of muscle acetylcholine receptor. *Nature*, **313,** 364-369.

Mitra, M., Wanamaker, C. P. and Green, W. N. (2001). Rearrangement of nicotinic a subunits during formation of the ligand binding sites. *J. Neurosci.*, **21,** 3000-3008.

Miwa, J. M., Ibañez-Tallon, I., Crabtree, G. W., Sanchez, R., Sali, A., Role, L. W. and Heintz, N. (1999). lynx1, an endogenous toxin-like modulator of nicotinic acetylcholine receptors in the mammalian CNS. *Neuron*, **23,** 105-114.

Miyake, A., Mochizuki, S., Takemoto, Y. and Akuzawa, S. (1995). Molecular cloning of human 5-hydroxytryptamine$_3$ receptor: heterogeneity in distribution and function among species. *Molec. Pharmacol.*, **48,** 407-416.

Miyazawa, A., Fujiyoshi, Y., Stowell, M. and Unwin, N. (1999). Nicotinic acetylcholine receptor at 4.6A resolution: transverse tunnels in the channel wall. *J. Mol. Biol.*, **288,** 765-786.

Miyazawa, A., Fujiyoshi, Y. and Unwin, N. (2003). Structure and gating mechanism of the acetylcholine receptor pore. *Nature*, **423,** 949-955.

Mochizuki, S., Miyake, A. and Furuichi, K. (1999a). Identification of a domain affecting agonist potency of meta-chlorophenylbiguanide in 5-HT$_3$ receptors. *European Journal of Pharmacology*, **369,** 125-132.

Mochizuki, S., Miyake, A. and Furuichi, K. (1999b). Ion permeation properties of a cloned human 5-HT$_3$ receptor transiently expressed in HEK293 cells. *Amino Acids*, **17,** 243-255.

Mochizuki, S., Watanabe, T., Miyake, A., Saito, M. and Furuichi, K. (2000). Cloning, expression and characterization of ferret 5-HT$_3$ receptor subunit. *European Journal of Pharmacology*, **399,** 97-106.

Morales, M. and Wang, S.-D. (2002). Differential composition of 5-hydroxytryptamine$_3$ receptors synthesized in the rat CNS and peripheral nervous system. *J. Neurosci.*, **22,** 6732-6741.

Moransard, M., Borges, L. S., Willmann, R., Marangi, P. A., Brenner, H. R., Ferns, M. J. and Fuhrer, C. (2003). Agrin regulates rapsyn interaction with surface acetylcholine receptors, and this underlies cytoskeletal anchoring and clustering. *J Biol Chem*, **278,** 7350-7359.

Moss, S. J., McDonald, B. J., Rudhard, Y. and Schoepfer, R. (1996). Phosphorylation of the predicted major intracellular domains of rat and chick neuronal nicotinic acetylcholine receptor α7 subunit by cAMP-dependent protein kinase. *Neuropharmacol.*, **35,** 1023-1028.

Mukerji, J., Haghighi, A. and Séguéla, P. (1996). Immunological characterization and transmembrane topology of 5-hydroxytryptamine$_3$ receptors by functional epitope tagging. *Journal of Neurochemistry*, **66,** 1027-1032.

Nayak, S. V., Rondé, P., Spier, A. D., Lummis, S. C. R. and Nichols, R. A. (2000). Nicotinic receptors co-localize with 5-HT$_3$ serotonin receptors on striatal nerve terminals. *Neuropharmacol.*, **39,** 2681-2690.

Nef, P., Mauron, A., Stalder, R., Alliod, C. and Ballivet, M. (1984). Structure, linkage and sequence of the two genes encoding the δ and γ subunits of the nicotinic acetylcholine receptor. *Proc Natl Acad Sci U S A*, **81,** 7975-7979.

Nef, P., Oneyser, C., Alliod, C., Couturier, S. and Ballivet, M. (1988). Genes expressed in the brain define three distinct neuronal nicotinic acetylcholine receptors. *Embo J*, **7,** 595-601.

Nelson, M. E., Kuryatov, A., Choi, C. H., Zhou, Y. and Lindstrom, J. (2003). Alternate stoichiometries of a4b2 nicotinic acetylcholine receptors. *Molec. Pharmacol.*, **63,** 332-341.

Nichols, R. A. and Mollard, P. (1996). Direct observation of serotonin 5-HT$_3$ receptor-induced increases in calcium levels in individual brain nerve terminals. *Journal of Neurochemistry*, **67,** 581-592.

Niemeyer, M.-I. and Lummis, S. C. R. (1998). Different efficacy of specific agonists at 5-HT$_3$ receptor splice variants: the role of the extra six amino acid segment. *British Journal of Pharmacology*, **123,** 661-666.

Niesler, B., Frank, B., Kapeller, J. and Rappold, G. A. (2003). Cloning, physical mapping and expression analysis of the human 5-HT$_3$ serotonin receptor-like genes *HTR3C*, *HTR3D* and *HTR3E*. *Gene*, **310,** 101-111.

Nisell, M., Nomikos, G. G. and Svensson, T. H. (1994). Systemic nicotine-induced dopamine release in the rat nucleus accumbens is regulated by nicotinic receptors in the ventral tegmental area. *Synapse*, **16,** 36-44.

Nishimune, A., Nash, S. R., Nakanishi, S. and Henley, J. M. (1996). Detection of protein-protein interactions in the nervous system using the two-hybrid system. *Trends Neurosci.*, **19,** 261-266.

Noda, M., Takahashi, H., Tanabe, T., Toyosato, M., Kikyotani, S., Furutana, Y., Hirose, T., Takashima, H., Inayama, S., Miyata, T. and Numa, S. (1983). Stuctural homology of *Torpedo californica* acetylcholine receptor subunits. *Nature*, **302,** 528-532.

Nomoto, H., Takahashi, N., Nagaki, Y., Endo, S., Arata, Y. and Hayashi, K. (1986). Carbohydrate structures of acetylcholine receptor from Torpedo californica and distribution of oligosaccharides among the subunits. *Eur. J. Biochem.*, **157,** 133-142.

North, R. A. (1995). Ligand- and voltage-gated ion channels. *Handbook of receptors and channels, S. Peroutka, eds (Boca Raton: CRC Press)*, 1-349.

Olale, F., Gerzanich, V., Kuryatov, A., Wang, F. and Lindstrom, J. (1997). Chronic nicotine exposure differentially affects the function of human α3, α4, and α7 neuronal nicotinic receptor subtypes. *J. Pharm. Exp. Ther.*, **283,** 675-683.

Orr-Urtreger, A., Goldner, F. M., Saeki, M., Lorenzo, I., Goldberg, L., De Biasi, M., Dani, J. A., Patrick, J. W. and Beaudet, A. L. (1997). Mice deficient in the α7 neuronal nicotinic acetylcholine receptor lack α-bungarotoxin binding sites and hippocampal fast nicotinic currents. *J. Neurosci.*, **17,** 9165-9171.

Palma, E., Bertrand, S., Binzoni, T. and Bertrand, D. (1996). Neuronal nicotinic α7 receptor expressed in *Xenopus* oocytes presents five putative binding sites for methyllycaconitine. *J. Physiol.*, **491,** 151-161.

Palma, E., Maggi, L., Barabino, B., Eusebi, F. and Ballivet, M. (1999). Nicotinic acetylcholine receptors assembled from the α7 and β3 subunits. *J. Biol. Chem.*, **274,** 18335-18340.

Paterson, D. and Nordberg, A. (2000). Neuronal nicotinic receptors in the human brain. *Prog. Neurobiol.*, **61,** 75-111.

Paulson, H. L., Ross, A. F., Green, W. N. and Claudio, T. (1991). Analysis of early events in acetylcholine receptor assembly. *J. Cell Biol.*, **113,** 1371-84.

Pedersen, S. E. and Cohen, J. B. (1990). *d*-Tubocurarine binding sites are located at α-γ and α-δ subunit interfaces of the nicotinic acetylcholine receptor. *Proc Natl Acad Sci U S A*, **87,** 2785-2789.

Pelham, H. R. B. (1989). Control of protein exit from the endoplasmic reticulum. *Annu. Rev. Cell. Biol.*, **5,** 1-23.

Peng, X., Gerzanich, V., Anand, R., Wang, F. and Lindstrom, J. (1997). Chronic nicotine treatment up-regulates α3 and α7 acetylcholine receptor subtypes expressed by the human neuroblastoma cell line SH-SY5Y. *Mol. Pharmacol.*, **51,** 776-784.

Peng, X., Katz, M., Gerzanich, V., Anand, R. and Lindstrom, J. (1994). Human α7 acetylcholine receptor: cloning of the α7 subunit from the SH-SY5Y cell line and determination of pharmacological properties of native receptors and functional α7 homomers in *Xenopus* oocytes. *Mol. Pharmacol.*, **45,** 546-554.

Peters, J. A., Malone, H. M. and Lambert, J. J. (1992). Recent advances in the electrophysiological characterization of 5-HT_3 receptors. *Trends in Pharmacological Sciences*, **13,** 391-397.

Phillips, W. D., Kopta, C., Blount, P., Gardner, P. D., Steinbach, J. H. and Merlie, J. P. (1991a). ACh receptor-rich membrane domains organized in fibroblasts by recombinant 43-kildalton protein. *Science*, **251,** 568-70.

Phillips, W. D., Maimone, M. M. and Merlie, J. P. (1991b). Mutagenesis of the 43-kD postsynaptic protein defines domains involved in plasma membrane targeting and AChR clustering. *J Cell Biol*, **115,** 1713-23.

Picciotto, M. R. and Zoli, M. (2002). Nicotinic receptors in aging and dementia. *J. Neurobiol.*, **53,** 641-655.

Picciotto, M. R., Zoli, M., Lena, C., Bessis, A., Lallemand, Y., Le Novére, N., Vincent, P., Merlo Pich, E., Brulet, P. and Changeux, J.-P. (1995). Abnormal avoidance learning in mice lacking functional high-affinity nicotine receptor in the brain. *Nature*, **374,** 65-67.

Picciotto, M. R., Zoli, M., Rimondini, R., Lena, C., Marubio, L. M., Merlo Pich, E., Fuxe, K. and Changeux, J.-P. (1998). Acetylcholine receptors containing the β2 subunit are involved in the reinforcing properties of nicotine. *Nature*, **391,** 173-177.

Placzek, A. N., Grassi, F., Papke, T., Meyer, E. M. and Papke, R. L. (2004). A single point mutation confers properties of the muscle-type nicotinic acetylcholine receptor to homomeric alpha7 receptors. *Molec. Pharmacol.*, **66,** 169-177.

Price, K. L. and Lummis, S. C. (2004). The role of tyrosine residues in the extracellular domain of the 5-hydroxytryptamine$_3$ receptor. *J Biol Chem*, **279,** 23294-23301.

Prince, R. J. and Sine, S. M. (1996). Molecular dissection of subunit interfaces in the acetylcholine receptor. *J Biol Chem*, **271,** 25770-25777.

Puchacz, E., Buisson, B., Bertrand, D. and Lukas, R. L. (1994). Functional expression of nicotinic acetylcholine receptors containing rat α7 subunits in human SH-SY5Y neuroblastoma cells. *FEBS Letters*, **354,** 155-159.

Pugh, P. C., Corriveay, R. A., Conroy, W. G. and Berg, D. K. (1995). Novel subpopulation of neuronal acetylcholine receptors among those binding α-bungarotoxin. *Mol. Pharmacol.*, **47,** 717-725.

Qu, Z., Apel, E. D., Doherty, C. A., Hoffman, P. W., Merlie, J. P. and Huganir, R. L. (1996). The synapse-associated protein rapsyn regulates tyrosine phosphorylation of proteins colocalized at nicotinic acetylcholine receptor clusters. *Mol. Cell. Neurosci.*, **8,** 171-184.

Quik, M., Choremis, J., Komourian, J., Lukas, R. J. and Puchacz, E. (1996). Similarity between rat brain nicotinic α-bungarotoxin receptors and stably expressed α-bungarotoxin binding sites. *J. Neurochem.*, **67,** 145-154.

Quirk, P. and Siegel, R. (2000). N-Glycosylation is necessary for surface expression of the 5-HT$_3$ receptor. *Society for Neuroscience Abstracts*, **811.4.**

Quirk, P. L., Rao, S., Roth, B. L. and Siegel, R. E. (2004). Three putative N-glycosylation sites within the murine 5-HT$_{3A}$ receptor sequence affect plasma membrane targeting, ligand binding, and calcium influx in heterologous mammalian cells. *Journal of Neuroscience Research*, **77,** 498-506.

Raggenbass, M. and Bertrand, D. (2002). Nicotinic receptors in circuit excitability and epilepsy. *J. Neurobiol.*, **53,** 580-589.

Ragozzino, D., Fucile, S., Giovannelli, A., Grassi, F., Mileo, A. M., Ballivet, M., Alema, S. and Eusebi, F. (1997). Functional properties of neuronal nicotinic acetylcholine receptor channels expressed in transfected human cells. *Eur. J. Neurosci.*, **9,** 480-488.

Rakhilin, S., Drisdel, R. C., Sagher, D., McGehee, D. S., Vallejo, Y. and Green, W., N. (1999). α-bungarotoxin receptors contain α7 subunits in two different disulfide-bonded conformations. *J. Cell Biol.*, **146,** 203-217.

Rangwala, F., Drisdel, R. C., Rakhilin, S., Ko, E., Atluri, P., Harkins, A. B., Fox, A. P., Salman, S. B. and Green, W. N. (1997). Neuronal α-bungarotoxin receptors differ structurally from other nicotinic acetylcholine receptors. *J. Neurosci.*, **17,** 8201-8212.

Reeves, D. C., Goren, E. N., Akabas, M. H. and Lummis, S. C. R. (2001). Structural and electrostatic properties of the 5-HT_3 receptor pore revealed by substituted cysteine accessibility mutagenesis. *J Biol Chem*, **276,** 42035-42042.

Reeves, D. C. and Lummis, S. C. R. (2000). Mutation of an isoleucine residue M2 alters the Ca^{2+} permeability of 5-HT_{3A} receptors. *Br. J. Pharmacol.*, **129,** 39P.

Reeves, D. C., Sayed, M. F. R., Chau, P.-L., Price, K. L. and Lummis, S. C. R. (2003). Prediction of 5-HT_3 receptor agonist-binding residues using homology modeling. *Biophysical Journal*, **84,** 2238-2344.

Revah, F., Bertrand, D., Galzi, J. L., Devillers-Thiery, A., Mulle, C., Hussy, N., Bertrand, S., Ballivet, M. and Changeux, J. P. (1991). Mutations in the channel domain alter desensitization of a neuronal nicotinic receptor. *Nature*, **353,** 846-9.

Revah, F., Galzi, J. L., Giraudat, J., Haumont, P. Y., Lederer, F. and Changeux, J. P. (1990). The noncompetitive blocker [^{3}H]chlorpromazine labels three amino acids of the acetylcholine receptor γ subunit: implications for the α-helical organization of regions MII and for the structure of the ion channel. *Proc Natl Acad Sci U S A*, **87,** 4675-9.

Reynolds, J. A. and Karlin, A. (1978). Molecular weight in detergent solution of acetylcholine receptor from *Torpedo californica*. *Biochemistry*, **17,** 2035-2038.

Roerig, B., Nelson, D. A. and Katz, L. C. (1997). Fast synaptic signaling by nicotinic acetylcholine and serotonin 5-HT_3 receptors in developing visual cortex. *J. Neurosci.*, **17,** 8353-8362.

Role, L. W. and Berg, D. K. (1996). Nicotinic receptors in the development and modulation of CNS synapses. *Neuron*, **16,** 1077-1085.

Rust, G., Burgunder, J.-M., Lauterburg, T. E. and Cachelin, A. B. (1994). Expression of neuronal nicotinic acetylcholine receptor subunit genes in the rat autonomic nervous system. *Eur. J. Neurosci.*, **6,** 478-485.

Sargent, P. B. (1993). The diversity of neuronal nicotinic acetylcholine receptors. *Annu. Rev. Neurosci.*, **16,** 403-443.

Schapira, M., Abagyan, R. and Totrov, M. (2002). Structural model of nicotinic acetylcholine receptor isotypes bound to acetylcholine and nicotine. *BMC Structural Biology*, **2,** 1-8.

Schoepfer, R., Conroy, W. G., Whiting, P., Gore, M. and Lindstrom, J. (1990). Brain α-bungarotoxin binding protein cDNAs and mAbs reveal subtypes of this branch of the ligand-gated ion channel gene superfamily. *Neuron*, **5,** 35-48.

Schoepfer, R., Whiting, P., Esch, F., Blacher, R., Shimasaki, S. and Lindstrom, J. (1988). cDNA clones coding for the structural subunit of a chicken brain nicotinic acetylcholine receptor. *Neuron*, **1,** 241-8.

Schrag, J. D., Procopio, D. O., Cygler, M., Thomas, D. Y. and Bergeron, J. J. M. (2003). Lectin control of protein folding and sorting in the secretory pathway. *Trends in Biochemical Sciences*, **28,** 49-57.

Schutze, M.-P., Peterson, P. A. and Jackson, M. R. (1994). An N-terminal double-arginine motif maintains type II membrane proteins in the endoplasmic reticulum. *Embo J*, **13,** 1696-1705.

Scott, D. B., Blanpied, T. A. and Ehlers, M. D. (2003). Coordinated PKA and PKC phosphorylation suppresses RXR-mediated retention and regulates the surface delivery of NMDA receptors. *Neuropharmacology*, **45,** 755-767.

Scott, D. B., Blanpied, T. A., Swanson, G. T., Zhang, C. and Ehlers, M. D. (2001). An NMDA receptor ER retention signal regulated by phosphorylation and alternative splicing. *J. Neurosci.*, **21,** 3063-3072.

Sealock, R. (1982). Visualization at the mouse neuromuscular junction of a submembrane structure in common with *Torpedo* postsynaptic membranes. *J. Neurosci.*, **2,** 918-923.

Séguéla, P., Wadiche, J., Dineley-Miller, K., Dani, J. A. and Patrick, J. W. (1993). Molecular cloning, functional properties, and distribution of rat brain α7: a nicotinic cation channel highly permeable to calcium. *J. Neurosci.*, **13,** 596-604.

Sgard, F., Charpantier, E., Bertrand, S., Walker, N., Caput, D., Graham, D., Bertrand, D. and Besnard, F. (2002). A novel human nicotinic receptor

subunit, α10, that confers functionality to the α9-subunit. *Mol. Pharmacol.*, **61,** 150-159.

Shikano, S. and Li, M. (2003). Membrane receptor trafficking: Evidence of proximal and distal zones conferred by two independent endoplasmic reticulum signals. *Proc Natl Acad Sci U S A*, **100,** 5783-5788.

Sivilotti, L. G., Colquhoun, D. and Millar, N. S. (2000). Comparison of native and recombinant neuronal nicotinic receptors: problems of measurement and expression. *In* F. Clementi, D. Fornasari and C. Gotti (Eds.), *Handbook of Experimental Pharmacology, Vol. 144, Neuronal Nicotinic Receptors* (pp. 379-416). Berlin: Springer.

Sixma, T. K. and Smit, A. B. (2003). Acetylcholine binding protein (AChBP): A secreted glial protein that provides a high-resolution model for the extracellular domain of pentameric ligand-gated ion channels. *Ann. rev. Biophys. Biomol. Struct.*, **32,** 311-334.

Smit, A. B., Syed, N. I., Schaap, D., van Minnen, J., J., K., Kits, K. S., Lodder, H., van der Schors, R. C., van Elk, R., Sorgedrager, B., Brejc, K., Sixma, T. and Geraerts, W. P. M. (2001). A glial-derived acetylcholine-binding protein that modulates synaptic transmission. *Nature*, **411,** 261-268.

Smith, M. M., Lindstrom, J. and Merlie, J. P. (1987). Formation of the alpha-bungarotoxin binding site and assembly of the nicotinic acetylcholine receptor subunits occur in the endoplasmic reticulum [published erratum appears in J Biol Chem 1987 Jul 5;262(19):9428]. *J Biol Chem*, **262,** 4367-76.

Smotrys, J. E. and Linder, M. E. (2004). Palmitoylation of intracellular signaling proteins: Regulation and function. *Annu. Rev. Biochem.*, **73,** 559-587.

Spier, A. D. and Lummis, S. C. R. (2000). The role of tryptophan residues in 5-hydroxytryptamine(3) receptor ligand binding domain. *J Biol Chem*, **275,** 5620-5625.

Spier, A. D., Wotherspoon, G., Nayak, S. V., Nichols, R. A., Priestly, J. V. and Lummis, S. C. R. (1999). Antibodies against the extracellular domain of the 5-HT_3 receptor label both native and recombinant receptors. *Mol. Brain Res.*, **67,** 221-230.

Standley, S., Roche, K. W., McCallum, J., Sans, N. and Wenthold, R. (2000). PDZ domain suppression of an ER retention signal in NMDA receptor NR1 splice variants. *Neuron*, **28,** 887-898.

Stefancsik, R., Jha, P. K. and Sarkar, S. (1998). Identification and mutagenesis of a highly conserved domain in troponin T responsible for troponin I binding: potential role for coiled coil interaction. *Proc. Natl. Acad. Sci. USA.*, **95,** 957-962.

Steward, L. J., Boess, F. G., Steele, J. A., Liu, D., Wong, N. and Martin, I. L. (2000). Importance of phenylalanine 107 in agonist recognition by the 5-hydroxytryptamine(3A) receptor. *Molec. Pharmacol.*, **57,** 1249-1255.

Stewart, A., Davies, P. A., Kirkness, E. F., Safa, P. and Hales, T. G. (2003). Introduction of the 5-HT_{3B} subunit alters the functional properties of 5-HT_3 receptors native to neuroblastoma cells. *Neuropharmacology*, **44,** 214-223.

Stroud, R. M., McCarthy, M. P. and Shuster, M. (1990). Nicotinic acetylcholine receptor superfamily of ligand-gated ion channels. *Biochemistry*, **29,** 11009-11023.

Sudweeks, S. N., van Hooft, J. A. and akel, J. L. (2002). Serotonin 5-HT_3 receptors in rat CA1 hippocampal interneurons: functional and molecular characterisation. *J. Physiol.*, **544,** 715-726.

Sugita, S., Shen, K. Z. and North, R. A. (1992). 5-hydroxytryptamine is a fast excitatory transmitter at 5-HT_3 receptors in rat amygdala. *Neuron*, **8,** 199-203.

Sumikawa, K., Houghton, M., Emtage, J. S., Richards, B. M. and Barnard, E. A. (1981). Active multi-subunit ACh receptor assembly by translation of heterologous mRNA in *Xenopus* oocytes. *Nature*, **292,** 862-864.

Sweileh, W., Wenberg, K., Xu, J., Forsayeth, J., Hardy, S. and Loring, R. H. (2000). Multistep expression and assembly of neuronal nicotinic receptors is both host-cell- and receptor-subtype-dependent. *Mol. Brain Res.*, **75,** 293-302.

Takai, T., Noda, M., Mishina, M., Shimizu, S., Furutani, Y., Kayano, T., Ikeda, T., Kubo, T., Takahashi, H., Takahashi, T., Kuno, M. and Numa, S. (1985). Cloning, sequencing and expression of cDNA for a novel subunit of acetylcholine receptor from calf muscle. *Nature*, **315,** 761-764.

Taylor, P., Malany, S., Molles, B. E., Osaka, H. and Tsigelny, I. (2000). Subunit interface selective toxins as probes of nicotinic acetylcholine receptor struture. *Eur. J. Physiol.*, **440,** R115-117.

Teasdale, R. D. and Jackson, M. R. (1996). Signal-mediated sorting of membrane proteins between the endoplasmic reticulum and the golgi apparatus. *Ann. Rev. Cell Dev. Biol.*, **12,** 27-54.

Terzano, S., Court, J. A., Fornasari, D., Griffiths, M., Spurden, D. P., Lloyd, S., Perry, R. H., Perry, E. K. and Clementi, F. (1998). Expression of the alpha3 nicotinic receptor subunit mRNA in aging and Alzheimer's disease. *Brain Res Mol Brain Res*, **63,** 72-78.

Toyoshima, C. and Unwin, N. (1990). Three-dimensional structure of the acetylcholine receptor by cryoelectron microscopy and helical image reconstruction. *J Cell Biol*, **111,** 2623-35.

Turton, S., Gillard, N. P., Stephenson, F. A. and McKernan, R. M. (1993). Antibodies against the 5-HT_3-A receptor identify a 54 kDa protein affinity-purified from NCB20 cells. *Mol. Neuropharmacol.*, **3,** 167-171.

Unwin, N. (1993). Nicotinic acetylcholine receptor at 9 A resolution. *J. Mol. Biol.*, **229,** 1101-1124.

Unwin, N. (2003). Structure and action of the nicotinic acetylcholine receptor explored by electron microscopy. *Febs Lett*, **555,** 91-95.

Unwin, N. (2005). Refined structure of the nicotinic acetylcholine receptor at 4 Å resolution. *J. Mol. Biol.*, **346,** 967-989.

Unwin, N., Miyazawa, A., Li, J. and Fujiyoshi, Y. (2002). Activation of the nicotinic acetylcholine receptor involves a switch in conformation of the α subunits. *J. Mol. Biol.*, **319,** 1165-1176.

van Hooft, J. A., Spier, A. D., Yakel, J. L., Lummis, S. C. R. and Vijverberg, H. P. M. (1998). Promiscuous coassembly of serotonin 5-HT_3 and nicotinic α4 receptor subunits into Ca^{2+}-permeable ion channels. *Proc. Natl. Acad. Sci. USA.*, **95,** 11456-11461.

van Hooft, J. A., van der Haar, E. and Vijverberg, H. P. M. (1997). Allosteric potentiation of the 5-HT_3 receptor-mediated ion current in N1E-115 neuroblastoma cells by 5-hydroxyindole and analogues. *Neuropharmacology*, **36,** 649-653.

van Hooft, J. A. and Vijverberg, H. P. (1995). Phosphorylation controls conductance of 5-HT_3 receptor ligand-gated ion channels. *Receptors and Channels*, **3,** 7-12.

van Hooft, J. A. and Vijverberg, H. P. M. (2000). 5-HT_3 receptors and neurotransmitter release in the CNS: a nerve ending story? *Trends in Neurosciences*, **23,** 605-610.

van Hooft, J. A. and Yakel, J. L. (2003). 5-HT_3 receptors in the CNS: 3B or not 3B? *Trends in Pharmacological Sciences*, **24,** 157-160.

Vernallis, A. B., Conroy, W. G. and Berg, D. K. (1993). Neurons assemble acetylcholine receptors with as many as three kinds of subunits while maintaining subunit segregation among receptor subtypes. *Neuron*, **10,** 451-64.

Verrall, S. and Hall, Z. W. (1992). The N-terminal domains of acetylcholine receptor subunits contain recognition signals for the initial steps of receptor assembly. *Cell*, **68,** 23-31.

Virginio, C., Giacometti, A., Aldegheri, L., Rimland, J. M. and Terstappen, G. C. (2002). Pharmacological properties of rat α7 nicotinic receptors expressed in native and recombinant cell systems. *Eur. J. Pharmacol.*, **445,** 153-161.

Wada, E., Wada, K., Boulter, J., Deneris, E., Heinemann, S., Patrick, J. and Swanson, L. W. (1989). Distribution of alpha 2, alpha 3, alpha 4, and beta 2 neuronal nicotinic receptor subunit mRNAs in the central nervous system: a hybridization histochemical study in the rat. *J. Comp. Neurol.*, **284,** 314-335.

Wang, J.-M., Zhang, L., Yao, Y., Viroonchatapan, N., Rothe, E. and Wang, Z.-Z. (2002). A transmembrane motif governs the surface trafficking of nicotinic acetylcholine receptors. *Nature Neuroscience*, **5,** 963-970.

Weiland, S., Witzemann, V., Villarroel, A., Propping, P. and Steinlein, O. K. (1996). An amino acid exchange in the second transmembrane segment of a neuronal nicotinic receptor causes partial epilepsy by altering its desensitization kinetics. *FEBS Lett.*, **398,** 91-96.

Werner, P., Kawashima, E., Reid, J., Hussy, N., Lundström, K., Buell, G., Humbert, Y. and Jones, K. A. (1994). Organization of the mouse 5-HT_3 receptor gene and functional expression of two splice variants. *Mol. Brain Res.*, **26,** 233-241.

Whiting, P., Esch, F., Shimasaki, S. and Lindstrom, J. (1987a). Neuronal nicotinic acetylcholine receptor beta-subunit is coded for by the cDNA clone alpha 4. *FEBS Lett.*, **219,** 459-63.

Whiting, P. J. and Lindstrom, J. M. (1986). Purification and characterization of a nicotinic acetylcholine receptor from chick brain. *Biochemistry*, **25,** 2082-2093.

Whiting, P. J., Liu, R., Morley, B. J. and Lindstrom, J. M. (1987b). Structurally different neuronal nicotinic acetylcholine receptor subtypes purified and characterized using monoclonal antibodies. *J. Neurosci.*, **7,** 4005-16.

Whiting, P. J., Schoepfer, R., Swanson, L. W., Simmons, D. M. and Lindstrom, J. M. (1987c). Functional acetylcholine receptor in PC12 cells reacts with a monoclonal antibody to brain nicotinic receptors. *Nature*, **327,** 515-8.

Williams, M. E., Burton, B., Urrutia, A., Shcherbatko, A., Chavez-Noriega, L. E., Cohen, C. J. and Aiyar, J. (2005). RIC-3 promotes functional expression of the nicotinic acetylcholine receptor a7 subunit in mammalian cells. *J Biol Chem*, **280,** 1257-1263.

Wonnacott, S. (1997). Presynaptic nicotinic ACh receptors. *Trends Neurosci.*, **20,** 92-98.

Wonnacott, S., Kaiser, S., Mogg, A., Soliakov, L. and Jones, A. W. (2000). Presynaptic nicotinic receptors modulating dopamine release in the rat striatum. *Eur. J. Pharmacol.*, **393,** 51-58.

Yakel, J. L., Lagrutta, A., Adelman, J. P. and North, R. A. (1993). Single amino acid substitution affects desensitization of the 5-hydroxytryptamine type 3 receptor expressed in *Xenopus* oocytes. *Proc Natl Acad Sci U S A*, **90,** 5030-5033.

Yan, D., Schulte, M. K., Bloom, K. E. and White, M. M. (1999). Structural features of the ligand-binding domain of the serotonin $5HT_3$ receptor. *J Biol Chem*, **274,** 5537-5541.

Yang, J. (1990). Ion permeation through 5-hydroxytryptamine-gated channels in neuroblastoma N18 cells. *J. Gen Physiol.*, **96,** 1177-1198.

Yang, J., Mathie, A. and Hille, B. (1992). $5\text{-}HT_3$ receptor channels in dissociated rat superior cervical ganglion neurons. *J. Physiol.*, **448,** 237-256.

Yu, C. R. and Role, L. W. (1998a). Functional contribution of the α5 subunit to neuronal nicotinic channels expressed by chick sympathetic ganglion neurones. *J. Physiol.*, **509,** 667-681.

Yu, C. R. and Role, L. W. (1998b). Functional contribution of the α7 subunit to multiple subtypes of nicotinic receptors in embryonic chick sympathetic neurones. *J. Physiol.*, **509,** 651-665.

Yuan, H., Michelsen, K. and Schwappach, B. (2003). 14-3-3 dimers probe the assembly status of multimeric membrane proteins. *Current Biology*, **13,** 638-646.

Zerangue, N., Schwappach, B., Jan, Y. N. and Jan, L. Y. (1999). A new ER trafficking signal regulates the subunit stoichiometry of plasma membrane K_{ATP} channels. *Neuron*, **22,** 537-548.

Zoli, M., Le Novére, N., Hill, J. A. and Changeux, J.-P. (1995). Developmental regulation of nicotinic ACh receptor subunit mRNAs in the rat central and peripheral nervous systems. *J. Neurosci.*, **15,** 1912-1939.

Zoli, M., Lena, C., Picciotto, M. R. and Changeux, J.-P. (1998). Identification of four classes of brain nicotinic receptors using β2 mutant mice. *J. Neurosci.*, **18,** 4461-4472.

Zwart, R., De Filippi, G., Broad, L. M., McPhie, G. I., Pearson, K. H., Baldwinson, T. and Sher, E. (2002). 5-Hydroxyindole potentiates human α7 nicotinic receptor-mediated responses and enhances acetylcholine-induced glutamate release in cerebellar slices. *Neuropharmacology*, **43,** 374-84.

Zwart, R. and Vijverberg, H. P. M. (1998). Four pharmacologically distinct subtypes of α4β2 nicotinic acetylcholine receptor expressed in *Xenopus laevis* oocytes. *Mol. Pharmacol.*, **54,** 1124-1131.